UNIVERSITAT DE BARCELONA

Characterization of the *in vivo* immunomodulatory properties of CD5 and CD6

Inês Tadeu dos Anjos Simões

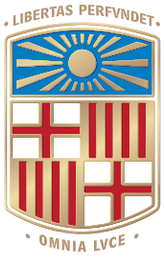

UNIVERSITAT DE BARCELONA

DEPARTMENT OF BIOMEDICINE
SCHOOL OF MEDICINE
UNIVERSITY OF BARCELONA

CHARACTERIZATION OF THE *IN VIVO* IMMUNOMODULATORY PROPERTIES OF CD5 AND CD6

A THESIS TO BE SUBMITTED BY:

INÊS TADEU DOS ANJOS SIMÕES

FOR THE AWARD OF THE DEGREE OF:

DOCTOR OF PHILOSOPHY IN BIOMEDICINE BY THE UNIVERSITY OF BARCELONA

CO-ADVISOR: VANESA GABRIELA MARTINEZ, PHD **SUPERVISOR:** FRANCISCO LOZANO SOTO, MD PHD

BARCELONA, SEPTEMBER 2017

To my family (blood and non-blood related),

that supported me during these years!

"Somewhere, something incredible is waiting to be known."

Carl Sagan

"Não tenhamos pressa, mas não percamos tempo."

José Saramago

INDEX

ABBREVIATIONS

aa	Amino acid
Ab	Antibody
Ag	Antigen
AICD	Activation-induced cell death
ALCAM	Activated leukocyte cell adhesion molecule
APC	Antigen presenting cell
B10	IL-10 producing regulatory B cell
B_{reg}	Regulatory B cell
CD5KO/CD6KO	CD5/CD6 Knockout mice
CLL	Chronic lymphocytic leukemia
BCR	B cell receptor
BM	Bone Marrow
bp	Base pair
BSA	Bovine serum albumin
CD	Cluster of differentiation
CFA	Complete Freund adjuvant
CFSE	Carboxyfluorescein succinimidyl ester
CIA	Collagen-induced arthritis
CK II	Casein kinase II
Da	Dalton
DAMP	Damage-associated molecular pattern
DC	Dendritic cell
DN	Double negative
DP	Double positive
DSS	Dextran sulfate sodium
EAE	Experimental autoimmune encephalomyelitis
FBS	Fetal bovine serum
h	hour
HRP	Horseradish peroxidase
HSA	Human serum albumin
IFA	Incomplete Freund's adjuvant
IFN	Interferon
Ig	Immunoglobulin
IL	Interleukin
i.p.	Intraperitoneal
IS	Immunological/Immune synapsis
i.v.	Intravenous
KLH	Keyhole limpet hemocyanin
KO	Knock-out
LN	Lymph node
LPS	Lipopolysaccharide

LSCL	Lymphosarcoma cell leukemia
mAb	Monoclonal antibodies
MAPK	Mitogen-activated protein kinase
MHC	Major histocompatibility complex
min	Minutes
MOG	Myelin Oligodendrocyte Glycoprotein
MS	Multiple sclerosis
NK	Natural killer cell
NKT	Natural killer T cell
nm	nanometers
Non-Tg	Non-transgenic mice
OD	Optic density
o.n.	Overnight
OVA	Ovalbumin
PAMP	Pathogen-associated molecular pattern
PBS	Phosphate buffered saline solution
PBS-T	PBS-Tween 20 solution
PCR	Polymerase chain reaction
PKC	Protein kinase C
PMA	Phorbol myristate acetate
PRR	Pattern-recognition receptor
p.t.	Peritumoral
RA	Rheumatoid arthritis
RNA	Ribonucleic acid
rpm	Revolutions per minute
rshCD5	Recombinant soluble human CD5
shCD5EμTg/ shCD5LckEμTg	Transgenic mice for soluble human CD5
rshCD6	Recombinant soluble human CD6
shCD6LckEμTg	Transgenic mice for soluble human CD6
RT	Room temperature
RTA	Ricin toxin A chain
s.c.	Subcutaneous
sec	Seconds
sCD5	soluble CD5 (human)
sCD6	soluble CD6 (human)
SEM	Standard error of the mean
SIRS	Systemic Inflammatory Response Syndrome
SNP	Single Nucleotide Polymorphism
SP	Single positive
SR	Scavenger receptor
SRCR	Scavenger receptor cysteine-rich

TCR	T cell receptor
TD	T-dependent (humoral response)
TdLN	Tumor draining lymph node
TEM	T effector/memory cell
TGF	Tumor growth factor
Th	T helper cell
TI	T-independent (humoral response)
TIL	Tumor infiltrating lymphocytes
TLR	Toll-like receptor
TNF	Tumor necrosis factor
TNP	Trinitrophenyl
$\mathbf{T_{reg}}$	Regulatory T cell
WT	Wild-type mice

I. INTRODUCTION

THE IMMUNE SYSTEM

The immune system is responsible for the integrity of the individual against foreign and/or self menaces. In almost every moment the human body, like all organisms, is challenged by external (e.g., microbes) or internal (e.g, altered self-cells) pathogenic agents. For this reason, our body has to be prepared to answer against these stimuli in a controlled way so as not to endanger its own survival. In this way, stimuli cause the organism to send warning signals that begin a response from the Immune System in order to eliminate this threat. To this purpose, two types of immune responses are available: innate and adaptive.

The innate responses (also named natural or nonspecific) are phylogenetically the oldest and constitute the first line of host defense for multicellular organisms. It is a very fast response (available in a few seconds or minutes) that does not require prior exposure to the pathogenic agent and has similar characteristics to different kinds of pathogens since it is driven by a relative short group of non-polymorphic receptors (generically named PRRs, for pattern-recognition receptors) recognizing common structures shared by different pathogens but absent from the host – the so-called pathogen-associated molecular patterns (PAMPs). These responses do not keep memory of the encounter and will respond in an identical manner in future recurring challenges.

On the other hand, the adaptive responses (also named acquired or specific) take a few days or weeks to assemble after pathogen exposure since they are not constitutively available. They give protection only against specific pathogens since they target specific structures not shared by different pathogens or the host. They also generate memory so that in future encounters with the same pathogen the response is quicker and better both quantitatively and qualitatively.

This simplified breakdown of the immune response helps to understand this complex system, but in reality it is very difficult to establish defined boundaries between those two response types. Indeed, there is a close interplay between them, since innate responses not only quickly react against pathogenic agents but also put into operation adaptive responses. Once operative, the later ones further support and potentiate innate responses.

1. THE INNATE IMMUNE SYSTEM

This first line of defense is composed of cellular and humoral components, which in the event of infection are activated through recognition of PAMPs by PRRs and release chemical mediators, cytokines and other factors that promote inflammatory responses to contain host aggression and repair tissue damage.

The cellular component is composed of sessile cells from endothelia as well as

from epithelia of the skin and the mucosal surfaces of the respiratory, genitourinary and digestive tracts, as well as several mobile cell types of hematopoietic origin. The endothelial and epithelial cells are the first obstacle to the entrance of microbes not only by providing **physical barriers** (e.g., through tight intercellular junctions, sweat, desquamation, mucus production, or cilia and peristalsis movements), but by actively participating through production of antimicrobial peptides (e.g., defensins), proteolytic enzymes (e.g., lysozyme, pepsin), cytokines and chemokines, among others. The latter mobilize **innate immune cells** of hematopoietic origin (e.g., neutrophils, basophils, eosinophils, mast cells, macrophages, dendritic cells, and innate-like lymphoid cells) that, in case the microbes pass the epithelial barriers, phagocytose and/or kill them or the infected cells. To do this, they express membrane PRRs that can recognize and remove the pathogens and cellular debris. In the next section, we will elaborate into this theme.

Regarding the **humoral component**, we can enumerate four main intervenients: the complement system, the natural antibodies, the contact system, and the soluble PRRs. The complement system can be activated by three different pathways but all lead to the formation of the membrane attack complex, a pore in the cellular membrane of the microbes or altered self cells promoting their lysis/clearing (Shishido et al. 2012). Moreover, proteolytic products from some components of this system can also improve pathogen opsonization, recruit adaptive immune components, increase Ab production, and improve tissue regeneration. This is a highly regulated proteolytic cascade with several soluble and membrane bound inhibitors to prevent host damage (Shishido et al. 2012). Another humoral component is the natural antibodies which have restricted repertoires of antigenic specificities. As the name implies there is no need of external stimuli for their production by innate-like B lymphocytes (B1a cells). These natural antibodies are usually of IgM isotype (but also IgA and IgG isotypes may be found) and recognize a wide range of pathogens and intervene in clearance of cellular debris, pathogen opsonization, complement activation, and promotion of adaptive immune responses through interaction with B, T and dendritic cells (Shishido et al. 2012). The contact system is composed of those plasma components that activate the coagulation cascade leading to clot formation, vasodilatation and vascular permeability, neutrophil chemotaxis, complement activation, and adaptive response modulation. As for the soluble PRRs, we will focus on them on the next section, but as for the previous components they also help with inflammatory cell recruitment, pathogen surface opsonization and clearance/destruction of external microorganisms.

1.1. RECOGNITION IN THE INNATE IMMUNE SYSTEM

As mentioned above, innate immune cells (macrophages, DCs, neutrophils, endothelial cells, lymphocytes, and epithelial cells) express PRRs. Interestingly, these

receptors are expressed in different cell locations (cell membrane, endosomes and cytoplasm, or even in soluble forms) so that they can intervene at different points of the response to pathogen challenge. They, contrary to adaptive immune receptors, do not present genetic rearrange variability but are germline-encoded; do not present antigen specificity but recognize broad conserved molecular patterns; are non-clonally distributed, being identical in the same cell class; and they are already available at the beginning of a threat, not generating memory (Janeway and Medzhitov 2002). Once the pathogen is recognized, they opsonize the threat and/or phagocytose it, activate the complement and coagulation cascades, as well as intracellular signaling that leads to inflammation and pathogen elimination (Janeway and Medzhitov 2002).

Here, we briefly describe some families of structurally diverse PRRs.

1.1.1. Toll-like Receptors

The TLR gene was firstly described as relevant in embryonic development of *Drosophilla*, its role in antimicrobial responses being later identified (Lemaitre et al. 1996). To date, 10 human (TLR1-10) and 12 murine (TLR1-9 and TLR11-13) TLR genes have been described (Lee, Avalos, and Ploegh 2012). All TLRs are type I transmembrane proteins, both in the cellular membrane or intracellular vesicles. Their extracellular domains are composed by multiple leucine-rich repeats (LRRs), which are required for PAMP recognition, while the intracytoplasmic Toll/IL-1 receptor (TIR) domains (Jeannin et al. 2005) are implicated in signal transduction and lead to activation of immune response genes (Kumar, Kawai, and Akira 2011). The only exception to the latter is TLR10, which is a negative regulator of signaling by other TLRs (Jiang et al. 2016). TLRs can be divided in subfamilies depending on the PAMPs they recognize: lipoproteins, viral proteins, glucans, lipopolysaccharide, lipoteichoic acid, among others (Mogensen 2009). The fact that different TLRs recognize different ligands and interact with different adaptor proteins allows for a greater variability in the type of immune response stimulated by the diverse microbial products to which we are exposed.

1.1.2. Rig-like Receptors

This family of cytoplasmic PRRs is composed of three members, which recognize viral RNA. They are found expressed by several cell types with innate immune functions: myeloid cells, epithelial cells, central nervous system cells, DCs among others (Loo and Gale 2011; Takeuchi et al. 2010). In response to the virus infection, these receptors activate transcription factors that in turn stimulate the expression of anti-viral type I IFN (Kumar, Kawai, and Akira 2011; Takeuchi et al. 2010; Loo and Gale 2011). Another feature is their capacity to recruit and activate caspases leading to pro-inflammatory cytokine expression which in turn can lead to apoptosis (Loo and Gale 2011).

1.1.3. Nod-like Receptors

This family of cytoplasmic sensors for intracellular bacteria is composed of 23 members in humans and approximately 34 in mice (Kumar, Kawai, and Akira 2011). They are composed of a C-terminal domain implicated in ligand recognition; an intermediate domain involved in oligomerization induction; and a N-terminal domain responsible for the downstream signaling activation for the inflammatory response (Mogensen 2009; Takeuchi et al. 2010). Most of the ligands recognized by this family are the same as those of the TLRs (such as peptidoglycan), and for that reason synergy in the response of both families leading to enhanced proinflammatory cytokine production can be observed (Mogensen 2009; Takeuchi et al. 2010).

The interesting feature of this family, involving the oligomerization of different proteins, leads to the activation of a multiprotein-complex known as inflammasome. Various different types of inflammasomes have been described, which recognize different ligands, either PAMPs or Damage-Associated Molecular Patterns (DAMPs) leading to caspase activation and inflammatory cytokine (IL-1β and IL-18) production or cell death (Mogensen 2009; Kumar, Kawai, and Akira 2011).

1.1.4. C-type Lectin Receptors

The C-type lectin receptors (CLRs) are transmembrane proteins expressed on macrophages, DCs and leucocytes (Takeuchi et al. 2010). They are divided into different classes with different specificity but they all are characterized by the presence of carbohydrate-binding domains that recognize carbohydrates from the cell membrane of microorganisms (viruses, bacteria, and fungi) such as β-glucans and mannan. More recently, they have been implicated in the regulation of immune homeostasis, autoimmunity and allergy, as well as the anti-tumor response (Dambuza and Brown 2015). Examples of receptors from this family are Dectin-1 (the first non-Toll-like receptor that recognize microbial components to be described), Dectin-2, and Mincle. All three recognize mycobacterial components and promote induction of T_H17 responses. Dectin-1 and Dectin-2 also recognize β-glucans and mannan, respectively, inducing activation signals through ITAM/ITAM-like motifs, which in turn regulate phagocytosis, autophagy, cytokine and chemokine production among other cellular responses. Interestingly, a correlation between Dectin-1 polymorphisms and fungal infection susceptibility in humans was established (Dambuza and Brown 2015).

1.1.5. Pentraxins

Pentraxins (e.g., C Reactive Protein and Serum Amyloidal Protein) are an evolutionary conserved family that serve as markers in case of infections, inflammation,

and tissue damage since they are rapidly synthesized in those cases (Shishido et al. 2012). Primarily, they are produced and secreted by hepatocytes, but also by different cell types *in situ*, in particular, dendritic cells, macrophages, fibroblasts, activated endothelial cells, and neutrophils (Bassi et al. 2009). These receptors recognize several pathogens as well as apoptotic cells and extracellular matrix components. On the other hand, pentraxins can bind to macrophages, as well as other innate immune cells, facilitating the clearance of the before mentioned pathogens and cell debris. Pentraxins interact with several humoral innate immune components, such as the complement. Their non-redundant and versatile properties make them a fundamental element in the humoral response (Shishido et al. 2012).

1.1.6. Scavenger Receptors

Finally, I will describe a little more in detail the scavenger receptor (SR) family since two of its members are of major importance in this thesis.

In 2014, 15 experts in this family gathered in an attempt to standardize the mammalian scavenger receptor nomenclature (PrabhuDas et al. 2014). In that meeting, they defined the SRs as "*cell surface receptors that typically bind multiple ligands and promote the removal of non-self or altered-self targets. They often function by mechanisms that include endocytosis, phagocytosis, adhesion, and signaling that ultimately lead to the elimination of degraded or harmful substances*". Instead of the eight previously defined classes of SR, they proposed the establishment of ten classes (PrabhuDas et al. 2014). Early this year, it was updated to 12 classes after new discussion with participants of three new meetings (PrabhuDas et al. 2017). This revised classification was necessary since this is a family with many members differing structurally and functionally (**Fig. I.1**).

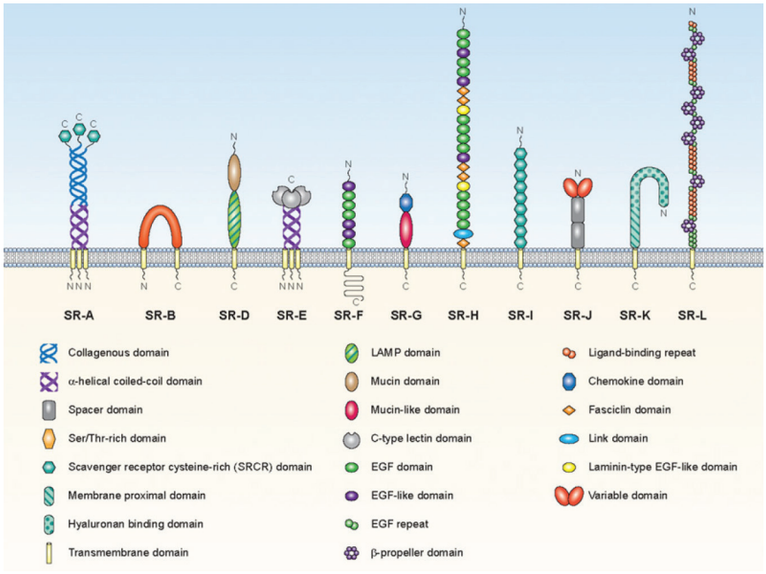

Fig. I.1 – Schematic representation of 11 mammalian SR classes. Adopted from (PrabhuDas et al. 2017).

Historically, the SRs were described as membrane receptors in macrophages (Brown et al. 1979; Brown and Goldstein 1979), where their function was to recognize and internalize oxidized low-density lipoproteins (LDL). In recent years, it was reported that they also recognize a high spectrum of modified self-molecules (DAMPs) but also a wide number of PAMPs, as well as playing a role in the transport of lipids, clearance of apoptotic cells, function as chaperons, modulation of lymphocyte signaling, and stabilization of cell-cell contacts (Zani et al. 2015). It can be said that this is a family of receptors which are highly promiscuous and that they are responsible for maintaining immune homeostasis. They can be found expressed in several cell populations of both hematopoietic (e.g, myeloid cells or lymphocytes) and non-hematopoietic (e.g. epithelial or endothelial) origin. Structurally, as well as functionally, there is a high diversity among their members and they can be divided into twelve classes according to their structure (PrabhuDas et al. 2017), as described in **Table I.1**.

Table I.1 – Summary of current Scavenger Receptor classes.

Class	Structural features	New nomenclature	Alternative names
A	Transmembrane proteins with α-helical coil domain, collagenous domain, and a C-terminal cysteine-rich domain (SRCR).	SR-A1 SR-A3 SR-A4 SR-A5 SR-A6	MSR1/SCARA1 MSRL1/SCARA3 SCARA4 SCARA5 MARCO/SCARA2
B	Transmembrane proteins with two transmembrane domains with an extracellular loop but with both the amino and carboxyl termini located in the cytoplasm.	SR-B1 SR-B2 SR-B3	SR-BI CD36 LIMP2
C	There is no mammalian SR of this class; it was only described in *Drosophila*.		
D	Type I transmembrane glycoprotein with lysosome-associated membrane glycoprotein, a 300-aa extracellular region rich in threonine and serine, and a short cytoplasmic tail.	SR-D1	CD68
E	Type 2 transmembrane proteins with C-type lectin-like domain.	SR-E1 SR-E2	Lox1 Dectin-1
F	Transmembrane proteins with extracellular epidermal growth factor-like domains and long cytoplasmic tails.	SR-F1 SR-F2 SR-F3	SREC-I/SCARF1 SREC-II/SCARF2 MEGF10
G	The only member of this class is a type 1 transmembrane glycoprotein with a CXC chemokine motif and a mucin stalk, and is also found as soluble protein.	SR-G1	SR-PSOX/CXCL16
H	Transmembrane proteins with large extracellular domains consisting in Fasciclin, EGF-like and lamin type EGF-like (FEEL) domains.	SR-H1 SR-H2	FEEL-1/CLEVER-1/ Stabilin-1 FEEL-2/Stabilin-2
I	Type I transmembrane glycoproteins with the extracellular region composed of several SRCR domains and short cytoplasmic tails.	SR-I1 SR-I2	CD163 CD163M CD5 CD6
J	The only member of this class is composed of a single transmembrane domain, a short cytoplasmic domain and an extracellular domain composed of three Ig-like regions.	SR-J1	RAGE
K	The only member of this class, a single-chain molecule, is composed of a distal extracellular domain, a membrane-proximal region, a transmembrane-spanning domain and a modest cytoplasmic tail.	SR-K1	CD44
L	Transmembrane glycoproteins with the extracellular region composed of ligand-binding domains and short cytoplasmic tails.	SR-L1 SR-L2	LRP1/APOER/CD91 Megalin/LRP2/gp330

1.1.6.1. Scavenger Receptor Cysteine-Rich Superfamily

Within the SRs there is a group of functionally diverse receptors all of them sharing a common structural feature: the presence of one or several repeats of an ancient and highly conserved protein domain named SRCR (for scavenger receptor cysteine-rich domain). They have been grouped apart and constitute the so named SRCR superfamily (SRCR-SF), which is currently composed by more than 30 different members, with representatives in all animal phyla (from low invertebrates to higher vertebrates) and plants (algae) (Martinez et al. 2011). As some members of the SRCR-SF behave as SRs (e.g., SR-AI and CD163), there is sometimes confusion between these two innate immune receptor families.

The SRCR domains are approximately 90 to 110aa in size and can be subdivided into two types: Group A domains contain six cysteines and are encoded by two exons; Group B members contain eight cysteine residues encoded by one single exon. The position of these cysteines is well conserved and they form disulfide bonds following a highly defined pattern (C1-C4 (absent in group A), C2-C7, C3-C8 and C5-C6) (Sarrias et al. 2004a). In the context of this thesis, the group B of this superfamily is of interest since it includes the lymphocyte surface receptors CD5 and CD6 (**Fig. I.2**). For a more detailed description of the SRCR-SF and the group A and B members, we refer to previous reviews from our group (Sarrias et al. 2004a; Martinez et al. 2011).

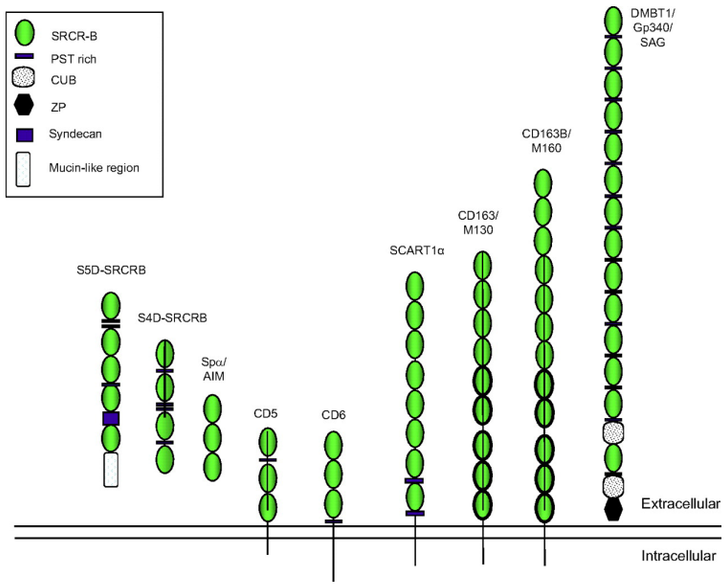

Fig. I.2 – Representation of human group B SRCR members. Adopted from (Martinez et al 2011).

2. THE ADAPTIVE IMMUNE SYSTEM

After the first line of defense is engaged to fight off an exogenous/endogenous challenging agent, a second line of defense intervenes – the **Adaptive Immune System**. This second line of defense is only present in vertebrates and is constituted by humoral and cellular arms. The latter is composed by T lymphocytes, which have cytotoxic and/or cytokine-producing capacities, and are specialized in the fight against intracellular pathogens. The humoral arm is mediated by antibodies, the soluble protein products of B lymphocytes specialized in binding to and neutralizing extracellular antigens. Both T and B lymphocytes are cell types of hematopoietic origin and characterized by the expression of unique and exclusive antigen-specific receptors (TCR and BCR, respectively).

The adaptive T and B immune response is **specific**, i.e. for each antigen there is a specific lymphocyte receptor capable of recognizing it. This means that there is a high **diversity** of receptors capable of recognizing a wide variety of antigens. After recognizing an antigen, the T and B lymphocytes with the same antigen specificity undergo **clonal expansion**, that meaning selective proliferation in order to keep up with the rapid spreading of the challenging agent. Another characteristic is that the adaptive system keeps **memory** of the first encounter with an antigen. This means that, when re-exposed, the response will be faster and of higher magnitude and quality (affinity). In order to be effective, the immune response has to be **specialized** for each type of different challenges (infectious, tumoral).

Another important aspect of the immune system in general and the adaptive one in particular is the lack of host response to self-components (tolerance), which is achieved by physical deletion or functional inactivation of auto-reactive lymphocytes. The latter is in part due to the existence of suppressor or regulatory T cells (T_{reg}), which are also important in the return to its basal equilibrium state (**homeostasis**), once the menace is neutralized by the immune system.

Even with mechanisms for controlling the immune response and maintaining the individual integrity, several factors can cause an exacerbated response or a response against host tissues that can lead to autoimmune disorders. Further on we will explore this theme a bit more in the context of our proteins of interest and their implications in autoimmunity (2.4.1.4 F and 2.4.2.4 F). On the other hand, there are situations of lack of response by anergy or non-recognition of the antigen as in tumors. We will also explore this theme later in the context of our proteins of interest (2.4.1.4 G and 2.4.2.4 G).

At this point, a brief synopsis of B and T cell development and maturation will be made, which is a stochastic process aiming at succeeding with the expression of fully functional TCR or BCR by undifferentiated committed lymphoid cells.

2.1. B-CELL DEVELOPMENT

Curiously, the discovery of the importance of the bursa of Fabricius in Aves (birds) for antibody production was reported in a peculiar journal instead of a more "mainstream" one, causing it to be unknown by immunologists for a long time (Cooper 2015; Glick, Chang, and G. 1956). The original study observed that although bursectomized birds developed normally, their antibody production was disrupted. The B cell designation came from this anatomical structure (bursa). In mammals, as is the case of humans, B cell development takes place in the bone marrow (BM). Years later, in 1962, the importance of the thymus for T cell development and maturation was reported (Miller 1962; Miller 2002). In 1965, it was established that B and T cells were two different lymphocyte lineages (Cooper, Peterson, and Good 1965).

As referred previously, B cells develop from hematopoietic precursors in BM after birth (liver in fetal life) passing through three different maturative stages that depend of the functional rearrangement process of the heavy and later the light immunoglobulin chain genes. The first phase is characterized by the rearrangement of the D_H and J_H segments of the heavy chain – which takes place in pro-B cells-, followed by V_H segment rearrangement of the heavy chain with the rearranged D_HJ_H segments– which takes place in pre-B cells. At this point, new V_L and J_L segment rearrangements take place in the light chains (κ and λ, in this stochastic order) leading to the expression of IgMκ (or IgMλ) molecule at the cell membrane – a marker of immature B cells. At different times along this process, the immune system has several checkpoints where the autoreactive B cells are purged (negative selection) in order to avoid self-reactivity phenomena. The surviving cells migrate then from the BM to the spleen, where they continue their developmental maturation process to transitional (T1/T2), marginal zone (MZ), follicular (FO), and plasma (PC) B cells, each one having different phenotypical and functional characteristics (Pieper, Grimbacher, and Eibel 2013). Later, depending on their selection process, some will migrate to lymph nodes and develop into memory or long-lived plasma B cells (**Fig. I.3**).

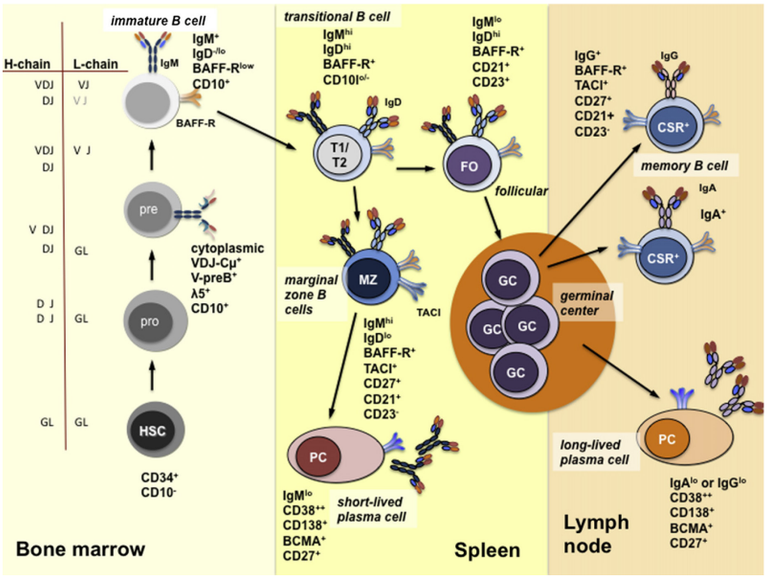

Fig. I.3 – B cell development and B-cell subsets. Adopted from (Pieper, Grimbacher, and Eibel 2013).

2.2. T-CELL DEVELOPMENT

Regarding conventional αβT cells, hematopoietic stem cells from BM (common lymphocyte precursor, CLP) migrate to the thymus in order to begin the T cell developmental process. The committed T-cell precursor is characterized as $CD4^{-}CD8^{-}$ double negative (DN), which can be further subdivided into four stages (DN1-DN4) depending on their CD44 and CD25 surface expression (**Fig. I.4**). When cells reach the DN4 stage, they express an incomplete and non-functional pre-TCR thanks to the successful rearrangement of coding segments (first Dβ-Jβ and then Vβ-DβJβ) from the TCRβ gene and their association with the invariable preTα chain.

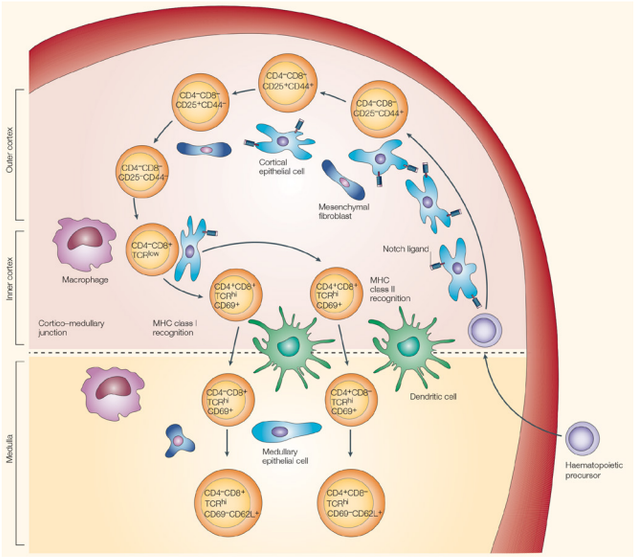

Fig. I.4 – T cell development and subsets. Adopted from (Zúñiga-Pflücker 2004).

At that point they proliferate and give rise to $CD4^+CD8^+$ double positive (DP) thymocytes with a complete and functional αβTCR (Zúñiga-Pflücker 2004; Germain 2002). These cells interact with cortical epithelial cells that present self-peptides allocated in the groove of class I or class II molecules of the Major Histocompatibility Complex (MHC). Depending on the signaling that TCR recognition of these self-peptides induce in the DP cells, they will undergo different fates: very low/null intensity TCR signaling will result in apoptosis (**death by neglect**); very strong TCR signaling will result in apoptosis (**negative selection**) or generation of natural regulatory T cells (nT_{reg}); and intermediate TCR signaling will result in maturation to simple positive (SP) thymocytes (**positive selection**) (Germain 2002). The type of MHC class I or II presenting the self-peptide that DP thymocytes recognize with intermediate affinity will determine the co-receptor that they will lose, giving rise to $CD8^+(CD4^-)$ SP or $CD4^+(CD8^-)$ SP mature thymocytes, respectively, which will migrate to the periphery and establish the T-cell repertoire.

Some developing T cells at the DN2-DN3 stage would instead rearrange the TCRγ and TCRδ genes giving rise to unconventional innate-like γδT cells, which recognize non-MHC I/II-restricted antigens of non-peptidic nature (phospho/lipidic). Similarly, some DP thymocytes with αβTCRs recognizing non-peptidic (phospho/lipidic) antigens presented by the MHC-like CD1 molecules will develop into innate-like NKT cells.

2.3. ANTIGEN-SPECIFIC ACTIVATION OF T- AND B-CELLS

In order for B and T lymphocytes to be activated, it is necessary that they recognize and bind to the antigen (Ag) through their respective antigen-specific BCR and TCR receptors. In some cases, the Ag alone can activate the B cell (T-independent antigens of non-peptidic nature such as lipopolisaccharide from Gram-negative bacteria), but mostly simultaneous activation by T cells (termed T helper cells) is necessary (T-dependent antigens of peptidic nature). When B lymphocytes are activated by both types of antigens, they generate immunoglobulins or antibodies (Ab), which are the soluble or secreted form of the Ag-specific B cell receptor (BCR or IgM/IgD). However, only TD antigens will efficiently give rise to important phenomena such as isotype class switching (to IgG, IgA or IgE), somatic hypermutation and affinity maturation, as well as long-lived plasma and memory B cells.

Regarding T cells, there are many subpopulations with different functions and characteristics, but these cells are generally divided for their study into two main subsets: T helper ($CD4^+$, which recognize Ag peptides via MHC class II and then promote T-cell responses and Ab production) and T cytotoxic cells ($CD8^+$, which recognize Ag peptides presented via MHC class I and lyse them). In order to be activated, a naïve $CD8^+$ or $CD4^+$ T cell has to establish contact with a professional Antigen-Presenting Cell (APC) such as DCs, macrophages or B cells to recognize the Ag presented via MHC class I or II, respectively.

Once the contact is established clonal expansion and differentiation into effector/memory cells take place. Both T cell subtypes need co-stimulation to be activated, which in the case of $CD4^+$ cells is afforded by the APC costimulators, and in the case of the $CD8^+$ by second contacts with APC costimulators or helper T cell signals. These contacts are made through formation of a key signaling complex, known as supramolecular activation complex (SMAC) or immunological synapse (IS). Such a complex is formed thanks to actin cytoskeleton reorganization following T-cell activation by the APC. This structure stabilizes and maintains the contact between the APC-T cell, as well as the receptor-ligand interactions mediated by other co-stimulator and accessory molecules important for the TCR activation. In fact, these contacts can last for hours (Huppa and Davis 2003).

The Ag recognition during these contacts can lead to activation of a naïve cell and consequent differentiation or polarization of the cell to a different effector T cell type: $CD4^+$ T-helper type 1, 2, 17, 9, 22; follicular (T_{FH}); or inducible T_{reg} cell (**Fig. I.5, top**); or $CD8^+$ cytotoxic T lymphocytes (T_c) 1, 2, 9, 17 or T_{reg} (Mittrücker, Visekruna, and Huber 2014) (**Fig. I.5, bottom**). This will depend on the quality of the TCR signals and the cytokine predominance in the microenvironment where the T cell is being activated.

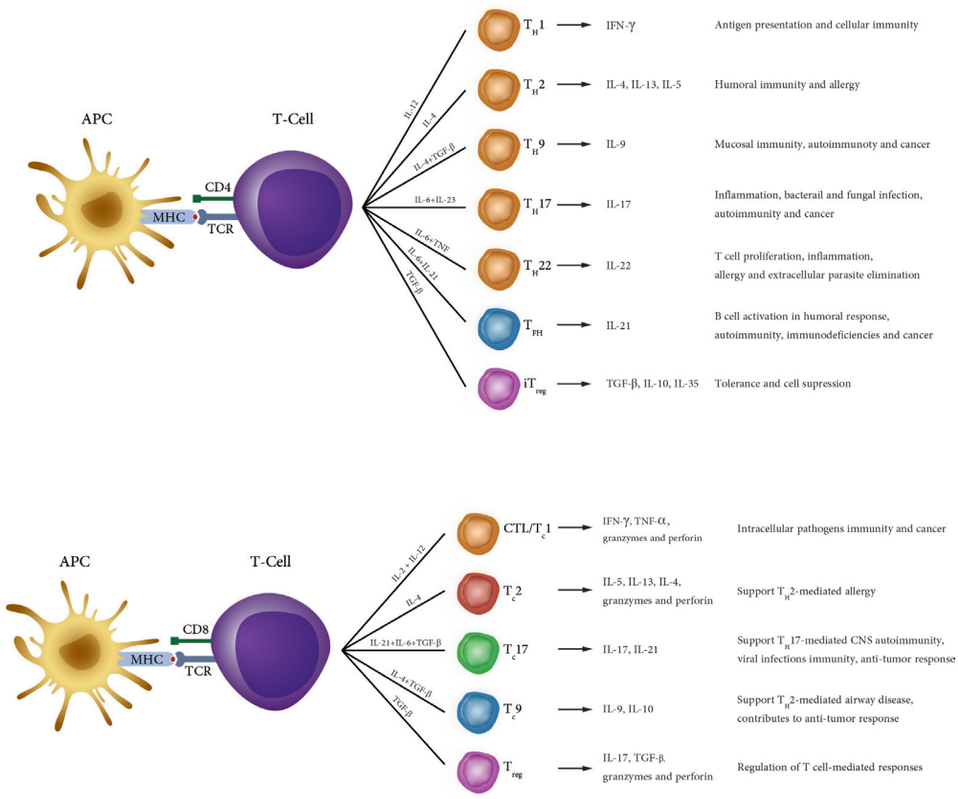

Fig. I.5 - Schematic representation of APC-T cell receptor interaction and subsequent $CD4^+$ T (top) and $CD8^+$ T (bottom) differentiation into different functional effector cell subsets.

2.4. ACCESSORY MOLECULES OF THE ANTIGEN-SPECIFIC T-CELL RECEPTOR

Structurally, the TCR is a dimer of covalently bound αβ (or γδ) chains (the Ag-recognition module), which is non-covalently bound to the CD3εδγξ complex (the signaling module responsible for lymphocyte activation following Ag recognition). CD3 signaling is highly regulated and for that there are several molecules with different functions helping that system, known as accessory molecules. Although they are called accessory, they perform important functions such as: identify their interlocutor (adhesive functions, such as molecules from the integrin superfamily: CD11a, CD18, VLA-4, CD29, CD49d), define the type of response (induction of a regulatory, helper, memory, cytotoxic, proliferative or anergic/apoptotic phenotype), and establish the signal intensity of that response (signaling functions).

The classical T-cell co-receptors are CD4 and CD8, all from the Immunoglobulin superfamily, which help stabilize and signal Ag recognition. However, signaling by accessory molecules can be co-stimulatory or inhibitory, and it is the competition between these signals that leads to a balanced response. Otherwise it would lead to aberrant immune cell activation or absence of response. These signal modulating molecules are known as stimulatory/inhibitory **immune checkpoints** depending on their function. Some examples of stimulatory immune checkpoints are CD27, which stimulates expansion of naïve T cells and generates memory through binding with its ligand CD70 expressed on lymphocytes and DCs (Hendriks et al. 2000); CD28, which recognizes CD80/B7.1 and CD86/B7.2 promoting T cell expansion (Boomer and Green 2010); OX40, which leads to effector and memory T cell expansion in addition to suppressing regulatory activity (Croft et al. 2009), among several other such as GITR (Glucocorticoid-Induced TNF-related gene), CD40L, and CD278/ICOS (Inducible T-cell Costimulatory). There are also several examples of inhibitory immune checkpoints: CTLA-4, which competes with CD28 for CD80/B7.1 and CD86/B7.2 ligands to control T-cell proliferation; PD-1 (Programmed cell Death protein 1), which also inhibits the activation, expansion and effector function of T cells; and many more such as TIM-3 (T cell immunoglobulin and mucin domain 3, LAIR1 (Leukocyte-associated immunoglobulin-like receptor 1), CD160, or LAG3 (Lymphocyte Activation Gene-3) (**Fig. I.6**). Interestingly, aside from accessory molecules, there are also other molecules that can act as inhibitory immune checkpoints, such as indoleamine 2,3-dioxygenase (IDO) enzyme, which suppresses NK and T cell function and promotes T_{reg} activity by tryptophan depletion.

Since regulation of TCR signaling is a very complex and still incompletely understood phenomenon, it is not unlikely that other lymphocyte receptors would also contribute to a lesser or greater extent. This could be the case of the CD5 and CD6 cell surface receptors which this thesis deals with. Their function as immune checkpoints has not been studied

in depth, but more and more it seems that they have a relevant role in this mechanism.

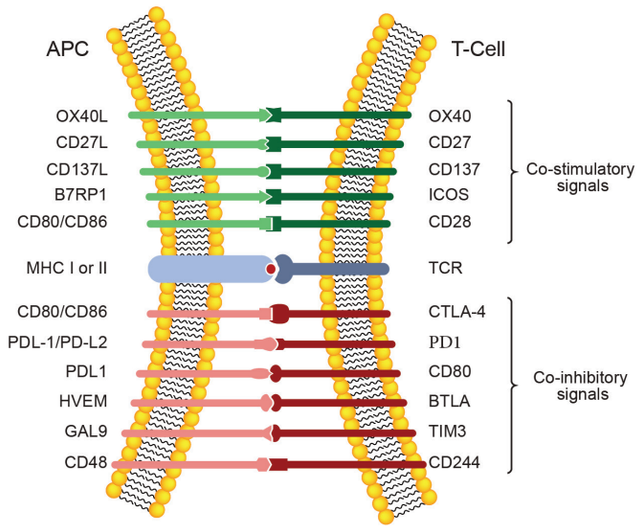

Fig. I.6 – Representation of co-stimulatory and co-inhibitory immune-checkpoint molecules that regulate T cell signaling responses.

2.4.1. The CD5 Receptor

CD5 was one of the first described lymphocyte receptors in mouse (Lyt-1), which allowed defining different T-cell subsets (Ledbetter et al. 1980). Later it was reported that it was also expressed in mouse B-cell lymphomas and leukemias (Lanier et al. 1981) and that its homologous receptor in humans was the Leu-1 molecule (Ledbetter et al. 1981).

2.4.1.1. CD5 Gene And Protein Structure

The human *CD5* gene is located in the 11q12.2 chromosome (Lecomte et al. 1996; Padilla et al. 2000), 82 kb downstream from the human *CD6* gene (described later in 2.4.2.1 section). The mouse gene is localized in the orthologue chromosome 19 (Lecomte et al. 1996). CD5 occupies 24.5Kb and has 11 exons: exons 3, 5 and 6 encode the extracellular region; exon 7 encodes the transmembrane region (31 aa), and exons 8, 9 and 10 codify the intracellular region (92 aa) (Padilla et al. 2000).

CD5 codes for a 67 kDa type I membrane glycoprotein with an extracellular domain exclusively composed by three SRCR domains, the first and second separated by a short interspersed PST-rich sequence (Sarrias et al. 2004a). The most N-terminal SRCR domain (D1) is the least conserved of the three domains and likely responsible for some receptor-ligand interactions (Sarrias et al. 2004a). Its cytoplasmic tail lacks intrinsic enzymatic activity but is well adapted for intracellular signaling. Indeed, when T cells are activated by specific Ag recognition, 4 tyrosines (three of them embedded into putative immunoreceptor tyrosine-based activation (ITAM) or inhibition (ITIM) motifs), 11 serines, and 4 threonines are available to phosphorylation by several intracellular kinases

(e.g., casein kinase II, protein kinase C, Ca^{2+}/calmodulin dependent kinase) and to further modulation of TCR signaling thanks to their interaction with several intracellular signal transducing proteins (e.g., ras-GAP, c-Cbl) (Martinez et al. 2011; Consuegra-Fernández et al. 2015) (**Fig. I.7**).

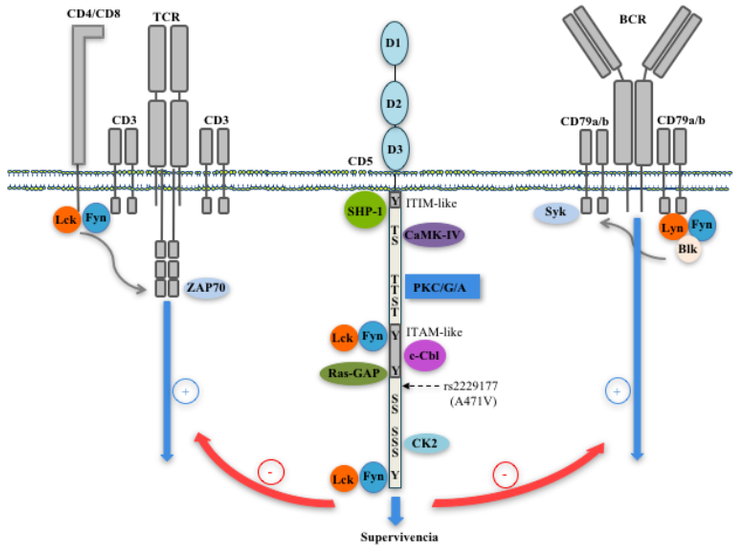

Fig. I.7 – Schematic representation of intracellular interactions mediated by CD5. Adopted from (Consuegra-Fernández et al. 2015).

2.4.1.2. CD5 Tissue Expression

It was demonstrated for the first time in the late 1970s that CD5 was expressed in 95-100% of human peripheral blood T cells, a subset of thymocytes, and also in T chronic lymphocytic leukemia cells (Reinherz et al. 1979). However, CD5 expression was not detected in normal B cells or in T acute lymphoblastic leukemia cells. A year later, CD5 expression was also described in B chronic lymphatic leukemia cells (Wang et al. 1980). For all this, CD5 was defined as a mature T cell differentiation antigen that appears in late intrathymic T cell development and persists in the periphery, thus being a good T cell marker (Reinherz et al. 1979).

In the late 1990s, it was established that CD5 levels correlate with thymocyte maturation, with low CD5 expression in immature double negative (DN) lymphocytes that increases around ten-fold in positively selected mature SP thymocytes. This expression pattern follows the TCR expression level and is influenced by TCR affinity (Suzuki et al. 1997; Azzam et al. 1998). Interestingly, CD5 was initially considered a marker to distinguish the T_{reg} cell subpopulation ($CD5^{hi}$) (Sakaguchi et al. 1985) before FoxP3 expression, which is the currently used marker. A recent study also reported that T_{reg} cells expressed higher levels of CD5 than their conventional T cell counterparts (Ordoñez-Rueda et al. 2009).

Although, as said before, normal B cells do not express CD5, there are some exceptions. CD5 expression was detected in a small B cell subpopulation (2-3% B cells) in normal human lymphoid tissue (Caligaris-Cappio et al. 1982; Antin et al. 1987). These $CD5^+$ B cells are named B1a cells ($IgM^{hi}IgD^{lo}CD23^-CD5^+$) and are typically localized at the mice peritoneum and human bone marrow, present low BCR variability (unlike conventional B cells), and are the major producers of polyreactive IgM natural antibodies (Berland and Wortis 2002). The other exception are the regulatory B cells (B_{reg}) that also express high levels of CD5 (Yanaba et al. 2008; Matsushita et al. 2008). It is believed that CD5, a negative regulator of T/B cell receptor signaling (as will be explained in section 2.4.1.4.), prevents non-desirable autoreactive cell activation (Berland and Wortis 2002).

Still, in the context of CD5 expression in B cells, a truncated isoform of CD5 expressed in B cells was described which used an alternative exon 1 located 20 kb from exon 2 (Renaudineau et al. 2005). This isoform is retained in the cytoplasm and competes with the expression of the complete CD5 protein, regulating in this way the expression and availability of full-length CD5 in B cell membrane.

In addition to the membrane-bound CD5, a circulating soluble form is also detected at picomolar range in sera from healthy individuals, as the result of proteolytic cleavage following lymphocyte activation (Calvo, Places, Espinosa, et al. 1999a). Furthermore, increased levels of soluble CD5 are detected in the serum of patients with lymphocyte hyperactivation diseases, such as Sjögren syndrome (Ramos-Casals et al. 2001) and Systemic Inflammatory Response Syndrome (SIRS) (Aibar et al. 2015). The function of this soluble form is still unknown but one hypothesis is that it may compete with membrane-bound CD5 for interaction with its ligand/s, as we will try to demonstrate with the work developed in this thesis.

2.4.1.3. CD5 Ligands

The ultimate nature of the endogenous CD5 ligand/s is still a controversial matter. There are several reported CD5 ligands, nevertheless the inability of independent research groups to validate results have made them dubious. That list includes counter-receptors expressed by B cells such as CD72 (Van de Velde et al. 1991), the framework region of IgV_H (Pospisil et al. 2000), and gp200 (Haas and Estes 2001); by B and T cells such as gp40-80 (Biancone et al. 1996; Bikah et al. 1998), and CD5 itself (Brown and Lacey 2010); by lymphoid, myelomonocytic and epithelial cells such as gp150 (Calvo, Places, Padilla, et al. 1999b); and soluble components such as IL-6 (Zhang et al. 2016; Masuda and Kishimoto 2016). Only some of these interactions have been mapped and they involve the most amino-terminal domains; D1 for CD5, D2 for the framework region of IgV_H, and D1-D2 for gp150.

Recent studies show that exogenous ligands can also interact with the extracellular region of CD5. This is the case of β-D-glucans, a broadly distributed constitutive component of fungal cell walls (Vera et al. 2009). The affinity of this interaction has been calculated (K_D, 3.7 ± 0.2 nM) and is in the same range of that reported for Dectin-1, the main known receptor of β-D-glucans in mammalian myeloid cells (Adams et al. 2008). All three individual extracellular domains of CD5 can bind to β-D-glucans, and the interaction seems to be specific since little or no binding is observed to other conserved fungal (mannan) and bacterial (lipopolysaccharide, peptidoglycan) cell wall constituents. Furthermore, exposure of CD5-transfectants to zymosan (a β-D-glucan-rich fungal particle) was shown to induce MAPK pathway activation and IL-8 secretion in CD5 cell transfectants, which was dependent on the integrity of the CD5 cytoplasmic region. Interestingly, CD5-deficient mice are hypersensitive to zymosan-induced septic shock-like syndrome as deduced from higher clinical scores and serum cytokine levels (Carreras E., Orta-Mascaró M., Simões I., Velasco M., Zaragoza O., Lozano F.; manuscript in preparation).

It has also been reported that CD5 is a relevant receptor for Hepatitis C virus (HCV) entry into both primary and leukemic human T cells (Sarhan et al. 2012). This explains the lymphoid reservoir reported for HCV and opens the possibility that CD5 may act as a receptor for other related and unrelated viruses. This is not surprising since viral recognition has been reported for other related members of the SRCR-SF such as Salivary Agglutinin/DMBT1/gp340 (gp120 HIV-1, influenza A virus) (Wu et al. 2006; White et al. 2005) and CD163 (PRRSV, porcine reproductive and respiratory syndrome virus; SHFV, Simian hemorrhagic fever virus) (Gorp et al. 2010; Caì et al. 2015).

2.4.1.4. CD5 Function

A. CD5 MODULATION OF T AND B CELL ACTIVATION

CD5 is physically associated to the TCR/BCR and a part of the macromolecular complex in the central area of the mature IS of T cells (Beyers, Spruyt, and Williams 1992; Brossard et al. 2003; Gimferrer et al. 2003). Therefore, it is well positioned for modulating the lymphocyte activation and/or death signals that follow Ag-specific recognition. However, the nature of its signaling was discrepant with studies demonstrating its role as either a positive or negative regulator of lymphocyte activation (Lozano et al. 2000).

The first *in vitro* studies performed with anti-CD5 mAbs, alone or in combination with anti-CD3 or anti-CD28 mAbs, pointed out a role for CD5 as a co-stimulatory molecule. Human T cells challenged with anti-CD5 mAbs presented higher levels of proliferation, cytokine secretion, activation of PKC and other tyrosine-kinases, and intracellular calcium release. Furthermore, CD5 would behave as a second signal with CD3 to activate

resting cells (Alberola-Ila et al. 1992; Ceuppens and Baroja 1986; Hollander, Pillemer, and Weissman 1981; Verwilghen et al. 1993; Imboden et al. 1990).

Later, the CD5 co-stimulatory role was questioned by *in vivo* studies performed in a new CD5-knockout (CD5KO) mouse model (Tarakhovsky et al. 1995). The authors reported that the CD5KO thymocytes stimulated through CD3 alone or in combination with CD4 showed higher release of intracellular calcium, higher phospholipase C gamma 1 (PLC-γ1) activity, and higher phosphorylation of TCR signaling pathway proteins (such as Vav, LAT and TCRζ). The same was described a year later for B1a cells; B1 cells from CD5KO mice stimulated with anti-IgM presented higher levels of proliferation and calcium mobilization (Bikah et al. 1996). In 2003 another *in vitro* evidence in this direction was reported; CD5 co-localizes with the TCR/CD3 complex in the center of the IS, in humans as well as in mice, and its expression levels correlate with higher inhibition of phosphorylation and calcium release but do not affect CD3 expression, T-APC contact or IS stabilization (Brossard et al. 2003). Altogether, these results highlight an inhibitory role of CD5 in T and B cell signaling.

B. CD5 ROLE IN THYMIC DEVELOPMENT

Thymic selection depends on TCR signal intensity (Jameson and Bevan 1995). As described in the previous section, CD5 acts as a negative modulator of the TCR signaling, so it was hypothesized that CD5 may influence the thymocyte selection process.

Indeed, the CD5KO mouse studies demonstrated that although the CD5KO thymic populations (CD3, CD4, CD8, CD69) were unaffected, when crossed with TCR transgenic mice, the SP populations were diminished, indicating that CD5 expression prevented their apoptosis, likely through modulation of thymocyte activation signals (Tarakhovsky et al. 1995). It thus appeared that thymocytes rely on CD5 signaling in the transition from DP to SP stages, precisely when CD5 expression increases, in parallel with other markers. Later, it was demonstrated that CD5 negatively modulates the development of CD4 SP T cells (Peña-Rossi and Zuckerman 1999) and that CD5 expression parallels TCR signaling intensity and avidity, playing a key role in the fine-tuning of TCR signaling (Azzam et al. 1998, 2001). Thus, CD5-mediated signal inhibition during thymocyte selection increases when the avidity of the positively selecting TCR–ligand interaction (and TCR signal strength) is relatively high. Conversely, CD5-mediated signal inhibition decreases when the avidity of the positively selecting TCR–ligand interaction (and TCR signal strength) is relatively low (Azzam et al. 2001).

In this context, CD5 is recognized as a marker of T cell reactivity - $CD5^{hi}$ cells are more reactive than their $CD5^{lo}$ counterparts. When challenged with foreign Ag, the naïve $CD8^{+}CD5^{hi}$ cells respond more efficiently by a higher proliferative response and cytokine

secretion than $CD8^+CD5^{lo}$ cells (Fulton et al. 2015). This appears to be due to the fact that $CD8^+CD5^{hi}$ cells expressed a higher proportion of genes linked to cell cycle preparation and division, providing an advantage in an immune challenge. CD5 expression levels also correlate with TCR avidity (in thymus and periphery), validated by the higher levels of Nur-77 in $CD8^+CD5^{hi}$ cells compared to $CD8^+CD5^{lo}$ cells (Fulton et al. 2015).

C. CD5 ROLE IN T AND B CELL SURVIVAL

The first evidence of CD5 implication in T/B cell survival came from CD5 regulation of the Ras/ERK signaling pathway in TCR activation. When DP thymocytes where co-crosslinked with anti-CD5 and CD3 antibodies, ERK activation increased leading to induction of the Bcl-2 anti-apoptotic protein (Zhou et al. 2000).

Axtell et al. studied an autoimmune-disease model – Experimental Autoimmune Encephalomyelitis (EAE), similar to Multiple Sclerosis in humans - in CD5KO mice. Surprisingly, they saw that the CD5KO mice showed an ameliorated disease despite their hyperactive thymocytes (Axtell et al. 2004). They explained this result by a higher Activation Induced Cell Death (AICD) and CKII activity. Years later, anti-tumoral response was also evaluated in the same mouse model and the authors reported slower tumor growth in the first days post-implantation of tumor cells in the CD5KO mice; however, the tumor growth rate soon after matched that of control mice (Tabbekh et al. 2011). Also in this case observations were explained by higher AICD, which led to enhanced activation – hence the slower tumor growth at first – but also increased cell death. CD5 modulates several signaling pathways inducing pro-survival proteins (Bcl-2, CK2, Akt) and/or inhibiting pro-apoptotic ones (FasL, caspases, Bid) (Soldevila, Raman, and Lozano 2011). Recently, another study reported an important role of Tyr429, located at ITAM-like domain, in survival induction (Mier-Aguilar et al. 2015).

Relative to B cells, the B1a population has a longer half-life than B2 cells *in vitro* and also *in vivo* (Hardy et al. 2000; Hayakawa and Hardy 2000). It seems that B cell survival depends on CD5 expression after BCR activation leading to IL-10 production and inhibition of Ca^{2+} mobilization (Gary-Gouy et al. 2002). In addition, it has been described that CD5 is expressed in B-cell chronic lymphocytic leukemia (B-CLL) – patients display an accumulation of $CD5^+CD23^+$ B cells, probably caused by deregulation of proliferation, apoptosis, or AICD (Salin et al. 2009). It can be caused by PKC activity or constitutive tyrosine phosphorylation in general (Nishimura, Bierer, and Burakoff 1988; Van de Velde et al. 1991). A single nucleotide polymorphism (SNP) in V447A, located in ITAM-like domain was also associated with an improvement in B cell survival (Sellick et al. 2008).

D. CD5 ROLE IN T AND B CELL TOLERANCE

In the early 2000s, taking advantage of a transgenic mouse that chronically expressed a self Ag (a nucleoprotein) in peripheral organs, it was reported that their CD8 T cells expressed higher levels of CD5 correlating with their resistance to activation through the Ag. Once the stimuli were removed, cells returned to their normal CD5 levels. This was the first evidence of CD5 preventing autoreactive processes (Stamou et al. 2003). A year later, in an EAE model to study the role of DCs in tolerance induction, it was found that while T cells pre-sensitized with MOG did not respond to *in vivo* re-stimulation, this tolerance was not observed in CD5-deficient T cells. The results suggested that DCs induced peripheral CD5 expression in T cells that in turn led to acquired tolerance and Ag unresponsiveness (Hawiger et al. 2004). Later, using the same EAE model, deletion of the CD5 domain of interaction with CK2 showed that the CD5-CK2 interaction was necessary for tolerance induction (Sestero et al. 2012).

Another interesting subpopulation to study the effect of CD5 on tolerance induction are the T_{reg} cells, which as previously mentioned express high levels of CD5. Dasu and collaborators demonstrated that T_{reg} cells from CD5KO mice were more suppressive *in vitro* than those of control mice, and although their FoxP3 intracellular levels were similar, CD5KO nT_{reg} showed higher calcium mobilization after CD3 stimulation (Dasu et al. 2008). Later studies showed that blockade of mTOR-dependent signaling, induced by effector-differentiating cytokines, through CD5 permits the induction of T_{reg} from T cells with high affinity for self-MHC in thymus or to tolerizing Ag in periphery (**Fig. I.8**) (Henderson and Hawiger 2015; Henderson et al. 2015). These results show a clear connection between CD5 and regulatory function in T cells.

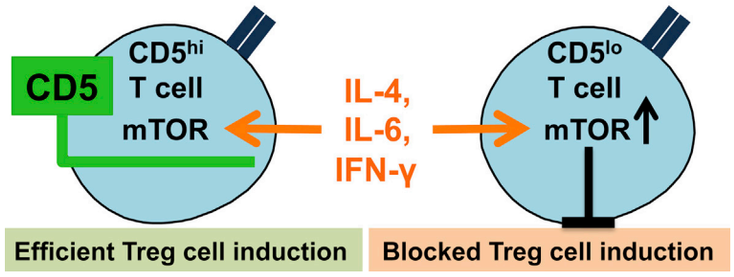

Fig. I.8 – Schematic representation of CD5 involvement in extrathymic T_{reg} development. Adopted from (Henderson et al. 2015).

In the case of B cells a similar situation applies; CD5 negatively regulates Ig receptor signaling inhibiting autoimmune B cell response (Hippen, Tze, and Behrens 2000). This study reported that anergic B cells from CD5KO mice mobilized more intracellular Ca^{2+}, were hyperproliferative and led to more autoreactivity. Finally, a recent study demonstrated that IL-10–producing $CD5^{+}$B cells inhibit IgE-mediated mast cell activation

and anaphylaxis in mice, in an IL-10–and cell-to-cell contact-dependent manner (H. S. Kim et al. 2015).

E. CD5 ROLE IN PATHOGEN RECOGNITION

As described in section 2.4.1.3, CD5 is able to recognize pathogen-associated structures present in fungi (β-glucans) and viruses. Its putative physiological relevance is currently under study. Increasing evidence demonstrates that the binding of microbial components to PRRs expressed by lymphocytes modulates lymphocyte function (Jeannin et al. 2005; Caramalho et al. 2003; Krupnick et al. 2005; Liu et al. 2006; Sutmuller et al. 2006). CD5-PAMP interaction stimulates intracellular signaling cascades (Vera et al. 2009; Carnero-Montoro et al. 2012), and it has been hypothesized that CD5 sensing of external microbial products is beneficial for the prevention of autoimmune responses triggered by infectious agents (microbial binding to CD5 provides inhibitory signals to low-affinity T/B-cell clones that could otherwise become autoreactive during infection) and antimicrobial immune response optimization (CD5 inhibitory signals would increase the threshold for activation of microbe-specific lymphocytes, allowing expansion of high- but not low-affinity T/B clones) (Lenz 2009). Another hypothesis is that CD5 may be expressed by non-lymphoid cell types and thus exert its pathogen-related effects through activation of innate immune responses. In line with this is the detection of CD5 expression on certain endothelial cells, macrophages, and peripheral blood and vaginal DC subsets (Gogolin-Ewens et al. 1989; Moreau et al. 1999; Borrello, Palis, and Phipps 2001; Wood and Freudenthal 1992; De Bernardis et al. 2006).

Our group demonstrated that as well as binding to pathogens, CD5 can also aggregate pathogenic fungi such as *Candida albicans* and *Cryptococcus neoformans*, and saprophytic fungi such as *Saccharomyces pombe* (Vera et al. 2009). Interestingly, recognition of these pathogens by CD5 was accompanied by MAPK activation and cytokine expression. Moreover, administration of recombinant soluble human CD5 significantly improved CD1 mice survival in a septic shock-like syndrome induced by zymosan (a fungal particle rich in β-glucans) (Vera et al. 2009), demonstrating its therapeutic potential.

A recent study analyzed the correlation between soluble CD5 levels in a cohort of critically ill patients with infectious and non-infectious systemic inflammatory response syndrome and their association with different clinical features and outcome (Aibar et al. 2015). Despite a high variation, there was no association between CD5 and risk of mortality in the analyzed conditions.

F. CD5 ROLE IN AUTOIMMUNITY

Due to the immunomodulatory properties of CD5, its implication in autoimmune disorders was extensively studied. Although controversial, some studies of Systemic Lupus Erythematosus (SLE) reported a correlation between $CD5^+$ circulating B cells and autoantibody secretion levels (Dauphinée, Tovar, and Talal 1988; Markeljevic et al. 1994; Böhm 2004) caused by uncontrolled Ig VDJ recombination as a result of their expression of recombination activation genes – RAG 1 and 2 (Morbach et al. 2006; Hillion et al. 2007). On the other hand, $CD5^+$ cells with immunosuppressive features involving IL-21 mediated secretion of Granzyme B have been shown to play a relevant role in SLE (Hagn et al. 2010). Interestingly, another study demonstrated that the reduction of membrane-bound CD5 in circulating $CD5^+$ B cells of SLE patients is caused by the increment of a truncated CD5 isoform (CD5-E1B) that is retained at the cytoplasm (Garaud et al. 2008), and that this isoform expression is induced by IL-6 (Garaud et al. 2009). This reduction of membrane-bound CD5 leads to limitation of the negative regulatory effects of CD5 on BCR-mediated signaling, which in turn reduces the BCR-mediated response threshold. Thus, the maintenance of anergy in autoreactive B cells by CD5 is deregulated. Moreover, preliminary clinical trials with blocking anti-IL-6 receptor mAb showed a reduction in lymphocyte activation and improvement in B- and T-cell homeostasis (Illei et al. 2010; Shirota et al. 2013). Few pilot studies with SLE patients were carried out using an immunoconjugate composed of a murine anti-CD5 mAb bound to ricin toxin A chain (zolimomab aritox), with the objective of inducing $CD5^+$ T cell depletion. Although modest T-cell depletion, which persisted for months, and a transient decrease in $CD5^+$ B cells without persistent depletion of total B-cell numbers was observed (Wacholtz and Lipsky 1992; Stafford et al. 1994), it led to powerful cytotoxic effects and multiple adverse reactions.

The importance of CD5 expression has also been reported in Multiple Sclerosis (MS) and also in this case there is a lot of controversy both in human and mice studies (Hawiger et al. 2004; Begum-Haque et al. 2011; Ochoa-Repáraz et al. 2010; Axtell et al. 2004; Strigård et al. 1988; Engelmann et al. 2014). On the one hand, an increased percentage of $CD5^+$ B cells in cerebrospinal fluid (Hardy and Hayakawa 2001; Mix et al. 1990; Correale et al. 1991) and blood (Villar et al. 2011) has been associated with higher MS risk and early conversion to the disease. A correlation between CD5 expression levels in B cells and occurrence/duration of relapsing-remitting MS has also been described (Bongioanni et al. 1996; Scott et al. 1994; Seidi, Semra, and Sharief 2002). On the other hand, other studies reported reduction of CD5 expression in B cells from patients with secondary progressive MS (a stage following relapsing-remitting MS) (Niino et al. 2012), and association of $CD5^+$ B cells with a lower prevalence of anti-myelin antibody production (Sellebjerg et al. 2002). In the case of mouse models, evidence pointed to a protective role for CD5 or $CD5^+$ B

cells in the EAE model (Hawiger et al. 2004; Begum-Haque et al. 2011; Ochoa-Repáraz et al. 2010). However, when this disease model was studied in CD5KO mice, they exhibited significantly delayed EAE onset and decreased severity (Axtell et al. 2004). The researchers proposed that this was due to the prosurvival activity of CD5 in T cells via engagement of the serine/kinase CK2 that binds to the receptor. Indeed, transgenic mice lacking the site of interaction between intracytoplasmic CD5 and CK2 were also resistant to EAE, which was attributed to increased AICD and decreased populations of cells co-expressing IFN-γ and IL-17 (Axtell et al. 2006). Later it was shown that the CK2-CD5 pathway is necessary for efficient differentiation of naïve $CD4^+$ T cells to T_H2 and T_H17, and for induction of T cell anergy (Sestero et al. 2012). Studies with mAbs were also performed; a mouse anti-CD5 mAb (OX19, IgG_1) given at the time of immunization partly prevented clinical signs of experimental autoimmune neuritis; however, when given shortly before the expected onset of the disease or during its height, OX19 drastically exaggerated disease symptoms (Strigård et al. 1988). Interestingly, results from another study that infected mice with adenovirus expressing CD5-immunoglobulin fusion protein (CD5-Fc) resulted in recovery from EAE (Axtell et al. 2004). It seems that the CD5-targeting outcome depends on the phase of disease.

Rheumatoid arthritis (RA) is a genetic disease involving a long list of risk loci shared with other autoimmune disorders (Stahl et al. 2010). Interestingly, *CD5* was identified among 14 new susceptibility loci for RA in populations of European ancestry (Eyre et al. 2012), with the non-synonymous SNP rs229177 (Ala471Val) being a strong candidate for the causal variant. The contribution of $CD5^+$ B cells to RA pathogenesis has been known for many years. Several studies reported increased $CD5^+$ B cells in peripheral blood of RA patients (Hara et al. 1988), and that these cells could be responsible for autoantibody production as seen for SLE (Smith and Olson 1990; Burastero et al. 1993; Cantaert et al. 2012; Burastero et al. 1990). Once again, there are also studies that failed to show that correlation (Sowden, Roberts-Thomson, and Zola 1987). Recent studies support a negative correlation between B_{reg} cells and RA, but also suggest this cell subset as potential target in future therapeutic strategies (Cui et al. 2014; Ma et al. 2014; Daien et al. 2014). Clinical studies performed with an anti-CD5 mAb linked to ricin toxin A chain (RTA) revealed inhibition of IL-2–induced proliferation of synovial-fluid T cells in some patients treated with this immunotoxin (Cannon et al. 1995; Fishwild and Strand 1994; Strand et al. 1993; Olsen, Teal, and Strand 1993; Verwilghen et al. 1992). Despite positive initial results, presumably mediated by the elimination of pathogenic B cells that contribute to inflammation, the use of depleting anti-CD5 mAbs was stopped when a wide double-blind placebo-controlled multicenter trial demonstrated no clinical benefits or significant differences between groups (Lorenz and Kalden 1998; Olsen et al. 1996). In a collagen-induced arthritis (CIA) mice model, similar to rheumatoid arthritis in humans, a non-

depleting anti-CD5 mAb (TIB104, rat IgG_{2a}) lead to significant disease severity decrease in 60% of the mice (Plater-Zyberk et al. 1994). It was reported that the levels of circulating antibodies to native collagen II were the same and the amelioration of the disease became visible six days after mAb treatment, supporting a T-cell mediated mechanism. This suggests that blockade of $CD5^+$ cells rather than depletion is a potential therapeutic strategy for RA treatment.

An increased proportion of $CD5^+$ B cells has also been reported for insulin-dependent diabetes mellitus (IDDM) (Muñoz et al. 1991; Lorini et al. 1993). In this case, one clinical study was performed with recent-onset IDDM patients that underwent anti-T-cell therapy with immunoconjugate anti-CD5 mAb bound to ricin toxin A chain (Skyler et al. 1993). The treatment was tolerated well and resulted in reversible T cell depletion with a dose-dependent preservation of pancreatic β-cell function. One study with a mouse model was also reported, using anti-Ly1 mAb linked to RTA (Vallera et al. 1992). In a similar way to the clinical study, treated mice were protected against diabetes onset in a dose-dependent manner. The underlying mechanism of this approach remains unclear but both studies show the usefulness of anti-CD5 immunotoxins for *in vivo* treatment of diabetes.

Regarding the involvement of $CD5^+$ B cells in autoimmune nephropathy, an inverse correlation was established between $CD5^+$ B cell number and response to treatment (Nagatani et al. 2013; Y. L. Kim et al. 2011; G. Wu et al. 2011; Y.-Y. Wang et al. 2014). Administration of anti-CD5 mAb (OX19) was studied in a rat model, as a pan-T cell-depleting treatment (alone or in combination with anti-CD4 and anti-CD8 mAbs) and proteinuria reduction and amelioration of glomerular lesions were observed (Tipping et al. 1996; Huang et al. 1997; Ikezumi et al. 2000, 2004). Similar results were observed with a CD5-Fc chimera in a mouse model (Biancone et al. 1996) by interfering with the CD5-CD5 ligand interaction.

For inflammatory bowel diseases, several mouse model studies were performed, including a model of ulcerative colitis (UC) caused by treatment with dextran sulfate sodium (DSS). Adoptive transfer of wild-type $CD1d^{hi}CD5^+IL\text{-}10^+$ cells into CD19-deficient mice showed reduced DSS-induced intestinal injury: this effect was mediated by the IL-10 produced by these cells (Yanaba et al. 2011). Also in CD5KO mice, DSS-induced colitis was less severe due to increased levels of FoxP3 mRNA in the mouse colon and enhanced suppressive activity of T_{reg} cells (Dasu et al. 2008). The use of CD5 antagonists may be crucial to delay or attenuate human UC; more studies must be carried out.

Lastly, it is fundamental to deepen our knowledge of the role of $CD5^+$ cells in different autoimmune disorders to clarify the conflicting results obtained so far. The design of target-specific treatments to down-modulate self-reactive cells or boost regulatory cell functions seems necessary.

G. CD5 ROLE IN CANCER

The role of CD5 in cancer immunotherapy has been investigated for many years. Seminal work showed that passive administration of a non-depleting mAb against Lyt-1 antigen induced rejection of transplanted lymphoid (EL-4 leukemia) and non-lymphoid (Lewis Lung Carcinoma) mouse tumors (Hollander 1985). It was later reported that CD5 was also expressed in certain mouse B-cell lymphomas and leukemias (Lanier et al. 1981). These discoveries led to two phase-I studies in patients with chronic lymphocyte leukemia or cutaneous T-cell lymphomas with the mouse anti-human CD5 mAb T101 (Dillman et al. 1984; Foss et al. 1998). The first one showed limited clinical benefit due to down-regulation of target antigen in leukemia cells and anti-mouse antibody production (Dillman et al. 1984). The second one was performed with a radioimmunoconjugate (^{90}Y-T101) and obtained a similar partial and transient response, together with modest toxicity (Foss et al. 1998).

Later on, it was reported that T cell clones from tumor-infiltrating lymphocytes (TILs) and peripheral blood lymphocytes (PBL) from a lung cancer patient with identical TCR specificity and similar lytic potential differed in their antitumor activity, which inversely correlated with CD5 expression (Dorothée et al. 2005). A second report by the same group showed an inverse correlation between CD5 expression and tumor-mediated AICD, wherein CD5low cells survived less since they underwent more AICD (Friedlein et al. 2007). This was due to higher FasL expression levels on CD5^{low} cells and consequent higher caspase-8 activity. Similar results were observed when studying the anti-tumor response to B16-F10 melanoma cells in CD5KO mice (Tabbekh et al. 2011). Such mice exhibited slow tumor growth coupled with an increment in the expression of T cell activation markers (e.g., CD25 and CD69) in TILs. Interestingly, concordant with the high levels of AICD observed, the tumor escaped the immune control, which could be reverted by FasL blockade (**Fig. I.9**).

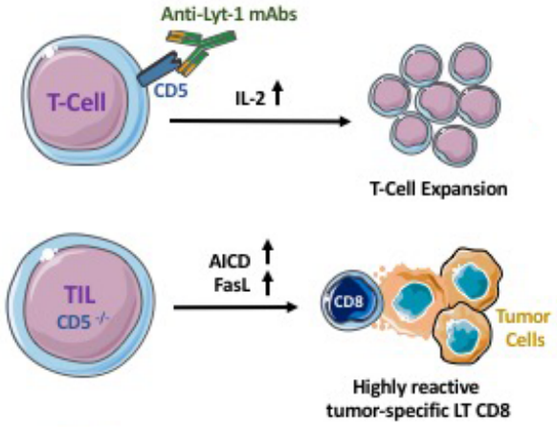

Fig. I.9 – Schematic representation of reported CD5 modulating involvement in anti-tumor immune response. Adapted from (Vasquez et al. 2017).

Last year, IL-6 was identified as a new CD5 ligand (Zhang et al. 2016); furthermore, it was shown that this interaction led to STAT3 activation via gp130 in B cells. The up-regulation of STAT3 increases CD5 expression, leading to a positive feedback loop. Moreover, the authors showed in murine tumor models that $CD5^+$ B cells promoted tumor growth and in several human tumor tissues $CD5^+$ B cells also had higher levels of phosphorylated STAT3.

From another point of view, genetic variants of immune checkpoint regulators may influence the outcome of cancer patients (Yoon et al. 2016; S. Y. Lee et al. 2016). Very recently, two retrospective studies have reported the relevance of non-synonymous *CD5* SNP (rs2241002 C>T, P224>L; rs2229177 C>T, A471>V) in the outcome of solid and non-solid tumors. The first study reported that patients with chronic lymphocytic leukemia carrying the ancestral P224-A471 haplotype had significantly prolonged progression-free survival rates (Delgado et al. 2016). This finding was in agreement with previous work (Cenit et al. 2014) showing that the ancestral A471 variant translated into lymphocyte hyper-responsiveness after TCR/CD3 crosslinking, reflecting a worse autoimmune prognosis. The second study evaluated two cohorts of melanoma patients and again showed a higher survival rate in those carrying the ancestral haplotype in homozygosis (Potrony et al. 2016).

Altogether, the available evidence supports CD5 as an immune checkpoint regulator and, consequently, as a target for novel immunomodulatory strategies aimed at potentiating the antitumor response (**Fig. I.10**). This could be achieved by adoptive transfer of tumor-reactive T cells expressing low to zero CD5 surface levels (e.g., through CRISPR technologies). Another strategy could involve the impairment of receptor-ligand interactions mediated by CD5 by means of blocking mAbs or recombinant sCD5 protein ("decoy receptor" effect). Finally, genetically-determined functional CD5 variants may pave the way for better identification of cancer patients responsive to conventional or forthcoming immunotherapy treatments.

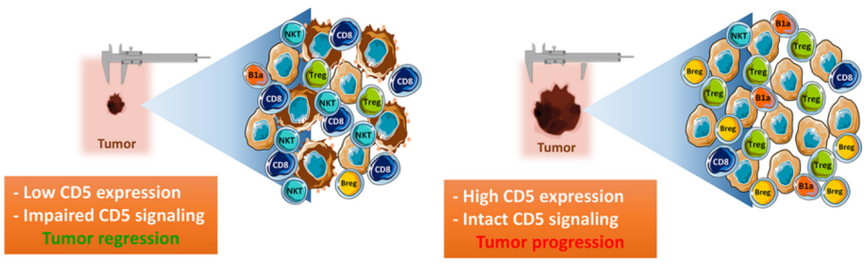

Fig. I.10 – Schematic representation of CD5 modulating consequences in anti-tumor immune response. Adapted from (Vasquez et al. 2017).

2.4.2. The CD6 Receptor

CD6 is a lymphocyte surface receptor highly homologue to CD5 in structure, function and also cell expression pattern. It is believed that both receptors derive from duplication of a common ancestral gene (Lecomte et al. 1996; Padilla et al. 2000). The functional role of this protein has not been as well studied as CD5, partly because a CD6-deficient mouse model was not developed until very recently (Orta-Mascaró et al. 2016; Enyindah-Asonye et al. 2017b; Li et al. 2017), which allowed to complement the *in vitro* studies previously performed.

2.4.2.1. CD6 Genetic And Protein Structure

Human *CD6* is located in 11q13 chromosome, in mice in chromosome 19, and is composed of at least 13 exons: exons 1 to 6 code for the extracellular region, in particular exons 3 to 5 encode the three SRCR domains; exon 7 codes for the transmembrane region, and exons 8 to 13 encode the cytoplasmic tail (Bowen et al. 1997). The human *CD6* gene expression is under RUNX and Ets transcriptional regulation (Arman et al. 2009).

CD6 is a type I membrane glycoprotein of 100-130 KDa, depending on its cytoplasmic tail phosphorylation condition (Sarrias et al. 2004a). The extracellular domain, highly homologue to CD5, is composed of three SRCR domains. In humans, the cytoplasmic tail can present five different lengths (from 24 to 244 aa) because of alternative splicing (Robinson et al. 1995; M A Bowen et al. 1997). The mouse cytoplasmic tail is 243 aa long. CD6, like CD5, also has several tyrosine, serine and threonine residues susceptible of being phosphorylated. In the early 1990s it was found that stimulation of T cells with anti-CD3 or by co-crosslinking with anti-CD2 or anti-CD4 led to CD6 cytoplasmic tail phosphorylation on tyrosine residues (Wee et al. 1993), and stimulation of T cells with anti-CD3 plus anti-CD6 resulted in increased induction of cell proliferation (Osorio et al. 1994), with similar results with anti-CD28 plus anti-CD6 (Osorio et al. 1998). A decade later, the association of CD6 with Lck, Itk, Fyn, and ZAP- 70 kinases was demonstrated by co-immunoprecipitation assays (Castro et al. 2003). Moreover, anti-CD6 mAbs - or even its natural ligand ALCAM - plus anti-CD3 (developed in section 2.4.2.3) induced a specific and dose-dependent activation of Erk1/2, p38 and JNK by CD6 ligation (Ibáñez et al. 2006). Besides tyrosine residue phosphorylation, it has also been reported that serine/threonine residue phosphorylation in CD6 is mandatory for MAPK activation (Bonet et al. 2013). This can lead to recruitment of several other proteins such as Syntenin-1 (Gimferrer et al. 2005), T cell-specific adaptor protein (TSAd) (Hem et al. 2017) and SLP-76, which in turn interact with other signaling proteins such as ZAP-70, LAT, PLCγ and GADS (Breuning and Brown 2017) and forming activation complexes (Roncagalli et al. 2014) (**Fig. I.11**).

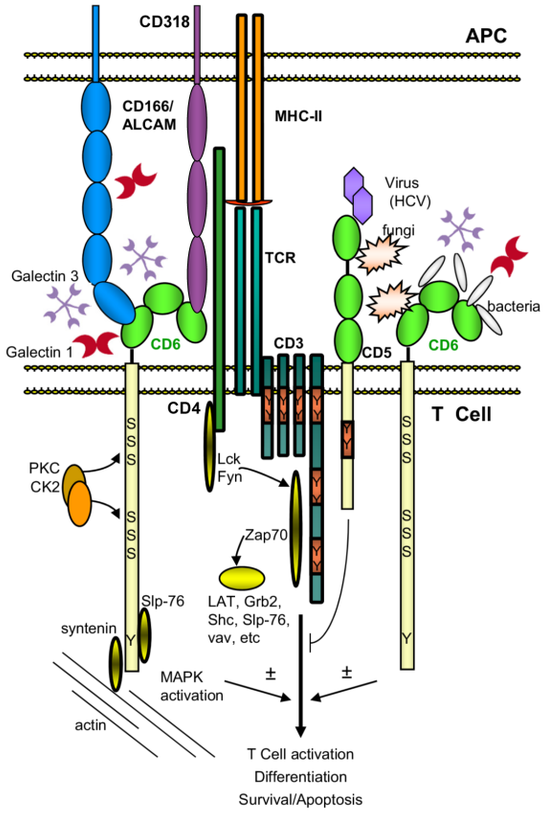

Fig. I.11 – Schematic representation of intracellular interactions mediated by CD6. Adapted from (Sarukhan et al. 2016).

2.4.2.2. CD6 Tissue Expression

CD6 is expressed on all mature T cells, a subset of B cells (B1a) (Kamoun et al. 1981) and NK cells (Braun et al. 2011), as well as some hematopoietic precursors (Cortés et al. 1999) and certain brain regions (Konno et al. 2001; Mayer et al. 1990). In thymus, CD6 is a marker of positive selection, like CD69, and survival (Singer et al. 2002; Orta-Mascaró et al. 2016).

Contrary to what is seen with CD5, human CD6 is not expressed in cells with regulatory functions such as T_{reg} cells (Garcia Santana, Tung, and Gulnik 2014).

As said before, there are five different CD6 isoforms described in humans (and two in mice) with various lengths caused by alternative splicing of exons 8 to 13 coding for different cytoplasmic regions (Kobarg et al. 1997) (**Fig. I.12**). This process leads to changes in the cytoplasmic tail and in turn reflects the differences in phosphorylation patterns between them (Kobarg et al. 1997). It is worth mentioning that an isoform lacking exon 5 and, consequently, the third extracellular SRCR domain (D3), the domain that recognizes ALCAM and is necessary for IS formation, is induced when cells are stimulated via CD3 plus CD6 crosslinking and not when stimulated only with anti-CD3 mAbs (Castro et

al. 2007). It is theorized that CD6 is necessary for the first T cell-APC contacts, and after T cell activation a negative feedback mechanism starts and the isoform lacking the SRCR domain 3 is expressed maintaining its cytoplasmic tail function but disrupting the ALCAM recognition at the membrane cell (Oliveira et al. 2012).

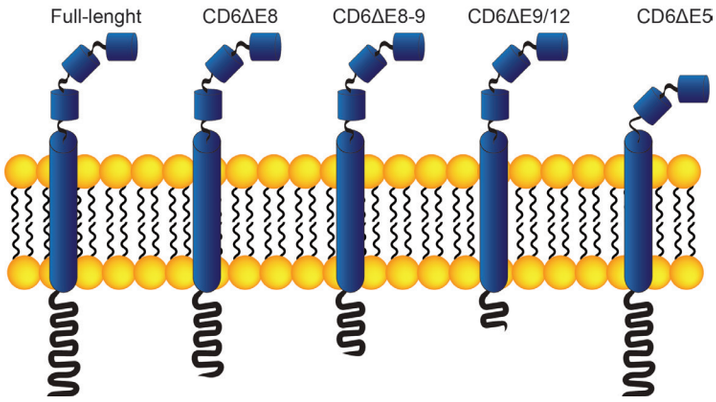

Fig. I.12 – Schematic representation of CD6 isoforms caused by alternative splicing. Full-length CD6, followed by three cytoplasmic truncated isoforms (exon 8, exon 8 and 9, and exon 9 and 12) and domain 3 absence isoform, respectively.

As mentioned above for CD5, a circulating soluble form of CD6 has been detected in serum at very low concentrations, but higher levels (ng/mL) have been found in Sjögren's syndrome patients (Ramos-Casals et al. 2001) and SIRS (Aibar et al. 2015) suggesting they may be an indicator of chronic or exacerbated T cell activation. The release mechanism has been recently elucidated (Carrasco et al. 2017) but its physiological relevance is yet to be defined.

2.4.2.3. CD6 Ligands

Unlike CD5, in the case of CD6 one well characterized ligand has been described, which has been validated by different groups – Activated Leukocyte Adhesion Molecule protein (CD166/ALCAM). ALCAM is an adhesion molecule belonging to the Ig superfamily and is broadly expressed in spleen, lymph node and amygdala mononuclear cells; hepatocytes, different organs such as thymus epithelial cells; bone marrow, neurons, microglia, macrophages, DCs, endothelial cells, activated T and B cells, and melanoma among others (Michael A Bowen et al. 1995; Konno et al. 2001; Whitney et al. 1995; Patel et al. 1995). As explained in the previous section, CD6 and ALCAM interact through the membrane-proximal SRCR domain (D3) of CD6 and the N-terminal Ig domain (D1) of CD166/ALCAM (Whitney et al. 1995), more specifically by the residues 43-364 in human, mouse and rat (Chappell et al. 2015) (**Fig. I.13** and **Fig. I.14**). Aside from this heterotypic CD6-ALCAM interactions, cis- and trans-acting homotypic ALCAM-ALCAM interactions also exist which are of lower affinity and mediated by the N-terminal D1 domain (**Fig. I.14**).

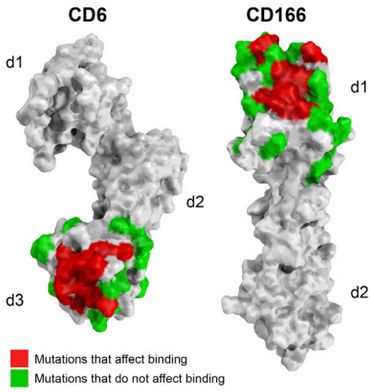

Fig. I.13 – Schematic representation of tridimensional CD6 and ALCAM structure and positions that affect the interaction. Adopted from (Chappell et al. 2015).

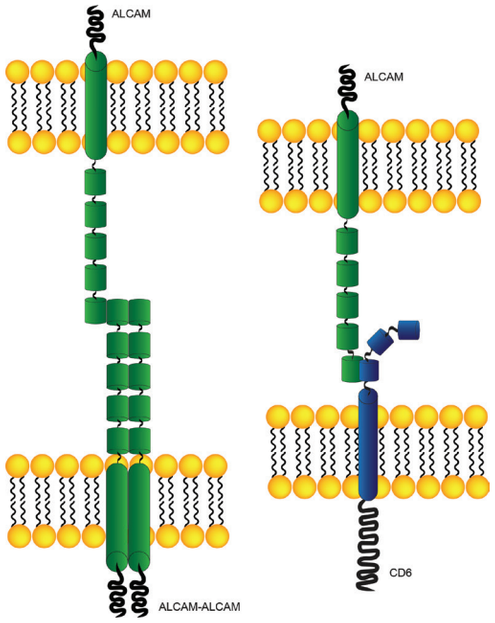

Fig. I.14 – Schematic representation of (left) cis- and trans-acting homotypic ALCAM-ALCAM interactions and (right) heterotypic CD6-ALCAM interactions.

Studies in human epithelial and synovial cells reported a different ligand of CD6, the 3A11 protein (recognized by the 3A11 mAb), that interacts with CD6 through different binding sites than ALCAM (Saifullah et al. 2004). Another group identified this ligand as being CD318, a cell surface protein expressed in several epithelial cells, some hematopoietic cells, mesenchymal stem cells, and many tumor cells (Enyindah-Asonye et al., 2017a). Indeed, the levels of CD318 in synovial tissues from Rheumatoid Arthritis patients were higher than those of healthy controls (Enyindah-Asonye et al., 2017a). A recent publication from our group identifies galectin-1 and galectin-3 as new ligands of CD6 and ALCAM, showing that both galectins can compete with ALCAM and PAMPs for binding to CD6 (Escoda-Ferran et al. 2014).

Exogenous ligands have also been described to interact with CD6. Thus, CD6 interacts with LPS from Gram-negative bacteria and with LTA and peptidoglycan from Gram-positive bacteria, though the responsible binding region/s has not been located yet. Besides binding, CD6 in soluble form is also able to aggregate bacteria, which could facilitate their clearing from circulation (Sarrias et al. 2007). The binding affinity of CD6 with LPS is similar to that of CD14, the main LPS receptor in mammalian myeloid cells; its relevance will be discussed later. Moreover, our laboratory has preliminary data demonstrating interaction between CD6 and surface structures present in clinically relevant viruses such as HIV (see Abstract HIV World Congress, Johannesburg) and CMV (unpublished observations).

2.4.2.4. CD6 Function

A. CD6 MODULATION OF T CELL ACTIVATION

As happened with CD5, CD6 was also initially defined as a positive modulator (co-stimulatory) of TCR signaling, but recently this has been challenged by different groups as will be described below.

In the late 80s/early 90s, studies with CD3 crosslinking plus CD2 or CD4 co-crosslinking resulted in CD6 tyrosine residues phosphorylation and also increased induction of T cell activation and proliferation in the event of co-crosslinking with anti-CD6 mAbs (Gangemi et al. 1989; Wee et al. 1993; L M Osorio et al. 1998; Ibáñez et al. 2006). Work from our group also demonstrated that CD6 co-precipitated with TCR/CD3 and co-localized with it at the center of the IS during T cell activation, as well as with ALCAM (Gimferrer et al. 2004). Interestingly, in the presence of sCD6, the early cell-cell interactions needed for IS maturation did not occur (**Fig. I.15**). Since the correct maturation of the IS is inhibited, the optimal conditions for T-cell proliferation are not present. This indicates that CD6-ALCAM interactions are fundamental to T cell activation. This effect was also observed in another report when T cell proliferation induced by APCs with superantigen was inhibited in the presence of galectin-1 and -3 (as they both interact with CD6 and ALCAM) (Escoda-Ferran et al. 2014).

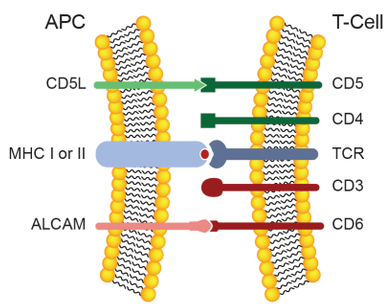

Fig. I.15 – Schematic representation of CD5 and CD6 implication in the IS.

Studies from other laboratories also reported the same effect; anti-CD6 mAbs or ALCAM-Fc protein inhibited T-cell proliferation induced by DCs plus superantigen (Zimmerman et al. 2006). They also showed that CD6-ALCAM interaction is important not only on the first cell-cell contacts but for several days afterwards, supporting the co-stimulatory role of CD6.

The controversy concerning the role of CD6 began around the same time as the aforementioned works (Hassan et al. 2006). Hassan *et al* reported that the co-stimulatory effect of CD6 was mediated by binding to SLP-76 through phosphorylation of the tyrosine residue 662Y. However, they also reported that 2B4 hybridoma cells expressing cytoplasmic mutants of CD6 produced less IL-2 than the ones expressing WT CD6, but these also expressed less IL-2 than untransfected 2B4 cells in response to APC contacts. In the case of the mutants, this can be explained by the absence of the docking site of SLP-76, but until 2012 the second observation remained unanswered. It was when the first evidence of the negative modulator role of CD6 were published (Oliveira et al. 2012). In this case, using human primary or Jurkat T cells expressing WT human or rat CD6, the intracellular Ca^{2+} release and IL-2 production in activated $CD6^{hi}$ cells were shown to be lower than in $CD6^{neg}$ cells. Moreover, it was also shown that the inhibitory effect was independent of CD6 presence at the IS and also of its interaction with ALCAM (using a CD6 variant without domain 3, the domain to which ALCAM binds).

Even more recent available data from CD6KO mice in C57BL/6 background indicate that CD6 is a negative modulator of TCR signaling during negative selection of immature thymocytes, and influences the generation and/or function of peripheral effector/memory (T_{EM}) and regulatory (T_{reg}) T cells (Orta-Mascaró et al. 2016). Another CD6KO mouse model in DBA-1 background showed that CD6 also acts as a negative regulator of activation and AICD in peripheral T cells (Li et al. 2017); more precisely, CD6KO T cells show higher expression of activation markers, less proliferation, a greater propensity to die by apoptosis and impaired transmigration across endothelial layers.

B. CD6 ROLE IN CELL SURVIVAL

Several studies have been uncovering the role of CD6 in cell survival, as will now be discussed. The first study showed that $CD6^+$ B-CLL cells stimulated with anti-IgM in the presence of anti-CD6 mAbs protected them against apoptosis by down regulating bax (pro-apoptotic gene) and consequently increasing the *bcl-2/bax* ratio (Osorio et al. 1997). Another *in vitro* study, in this case with thymocytes, showed that CD6 expression levels were higher in those thymocytes more resistant to apoptosis (Singer et al. 2002). Later, our group also described that the CD6-ALCAM interaction led to activation of three MAPK cascades, inducing p38 and JNK activity, likely influencing cell survival (Ibáñez et al. 2006). Indeed, the mechanisms by which CD6 regulates anti-apoptotic proteins is still

unknown but more work by our laboratory led to hypothesize that, as happens with CD5, CD6 has serine/threonine residues in its cytoplasmic tail susceptible to be phosphorylated by CK2, an anti-apoptotic protein that acts through caspase inhibition (Axtell et al. 2006; Bonet et al. 2013). In the same line, we also described that expression of membrane-bound CD6 can protect T-cells from apoptosis induced by galectin-1 and -3 (Escoda-Ferran et al. 2014).

C. CD6 ROLE IN CELL TOLERANCE

The first evidence of CD6 implication in tolerance came from a clinical study of bone marrow transplantation patients that received allogeneic bone marrow depleted with anti-CD6 mAb (anti-T12), to remove T cells from the donor (Soiffer et al. 1992). They reported that *in vitro* T cell depletion reduced acute and chronic graft-versus-host incidence without compromising the engraftment. In addition, the majority of patients that received the CD6-T cell depleted bone marrow did not need administration of immune suppressive medication. Indeed, later works reported that freshly isolated $CD6^-$ T cells had reduced alloreactivity in mixed lymphocyte reaction (Rasmussen et al. 1994), and that T cell autoreactive response can be inhibited by anti-CD6 mAbs (Singer et al. 1996). Recent work by our laboratory with T cells from CD6-KO mice shows that when challenged *in vitro* or *in vivo* with allogeneic cells these mice show reduced proliferative responses as well as a higher induction of T_{reg}, although with reduced functionality (Consuegra-Fernandez et al. 2017).

D. CD6 ROLE IN THYMIC DEVELOPMENT

The first evidence that CD6 could play a role in thymic development was a report from the late 80s where a slight inhibition of thymocyte binding to thymic epithelial cells was found in the presence of anti-CD6 mAbs (Vollger et al. 1987). Years later, another study showed up-regulation of CD6 in thymocytes in the presence of CD2 co-stimulation, but not in mature T cells (Bott et al. 1994). As CD2 triggered PKC activation which in turn up-regulated CD6, the authors hypothesized that this could lead to additional signaling essential for T cell activation and differentiation.

Indeed, in the early 2000s, another study demonstrated an increment in CD6 expression during human and murine thymocyte development, from DN (minimal expression) to $CD4^+$SP (maximum expression) (Singer et al. 2002). In the periphery, however, CD6 expression levels decreased. Moreover, CD6 expression correlated with $CD69^+$ expression, a positive selection marker, which could also be thought of as a differentiation marker. Further analysis showed that thymocytes resistant to apoptosis had elevated CD6 expression levels. Taken together, CD6 seems to play a role in thymocyte survival and functional avidity of selection.

It is worth noting that the interaction of CD6 with its ligands ALCAM, galectin-1 and galectin-3 - all of them expressed by thymic epithelial cells - may also have an impact in thymic development (Perillo et al. 1997; Villa-Verde et al. 2002).

Last year, a study from our group analyzing CD6-deficient mice reported that the thymus from these mice had a lower proportion of mature $CD4^+$SP and $CD8^+$SP cells (coupled with an increment of immature $CD8^+$SP cells) (Orta-Mascaró et al. 2016). Moreover, an increment of double positive cell frequency and a reduction of recently selected $CD69^+CD4^+$SP and $CD69^+CD8^+$SP was also observed in CD6KO mice. Another interesting observation was the higher Ca^{2+} mobilization by CD6KO DP thymocytes after *in vitro* TCR cross-linking. Similar results (lower number of thymic $CD4^+$SP and $CD8^+$SP) were obtained when CD6KO mice were crossed with either OT-I TCR mice (which produce MHC class I–restricted, OVA-specific $CD8^+$ T cells) or with Marilyn mice (which produce MHC class–II restricted $CD4^+$ T cells), suggesting that, rather than a defect in positive selection per se, CD6 deficiency triggers an increase in the negative selection of $CD4^+$ and $CD8^+$SP cells, the final product of the DP to SP transition (Orta-Mascaró et al. 2016).

E. CD6 ROLE IN INFECTION

Aside from the relevance of CD6 in the modulation of T cell activation and differentiation, a relatively new role is its capacity to bind PAMPs as well as DAMPs–functioning as a PRR (Sarukhan et al. 2016). A study from our group discovered that a recombinant soluble form corresponding to the human CD6 ectodomain (rshCD6) binds and aggregates Gram positive (*S. aureus*) and Gram negative (*E. coli*) bacteria, and interestingly their binding region was independent and non-overlapping (Sarrias et al. 2007). The study also confirmed that the membrane-bound form of human CD6 also binds to LPS (a component of *E. coli* outer membrane) and induces intracellular signals leading to MAPK activation through Erk1/2 phosphorylation, although this required an intact cytoplasmic tail. The affinity constant of the CD6-LPS interaction is in the same range as that of CD14, the main LPS receptor in mammalian myeloid cells. The therapeutic potential of this interaction was assessed *in vivo* and a single administration of rshCD6 was shown to significantly improve survival of mice undergoing LPS-induced septic shock concomitantly with reducing the levels of pro-inflammatory cytokines in serum.

Later, another study from our group described that similarly to LPS, CD6 also binds to lipoteichoic acid (LTA) and peptidoglycan (PGN) with an affinity constant in the same range as that of CD14 (Martínez-Florensa et al. 2014). *In vitro* cell culture assays demonstrated that rshCD6 blocked PGN+LTA- and LPS-induced cytokine production by TLR2- and TLR4-expressing cells in a dose-dependent manner. As performed previously for LPS, the therapeutic effect of rshCD6 was observed for PGN+LTA-induced septic shock as well as for lethal peritoneal infection with live Gram-positive (*S. aureus*) and Gram-

negative (*E. coli* and *A. baumanii*) bacteria. We hypothesized that bacteria aggregation would facilitate their clearance from circulation and reduce consequent inflammatory processes preventing mice death. When leukopenic mice were challenged with bacteria, the therapeutic effect of rshCD6 was affected. Surprisingly, the direct interaction between CD6 and both toxic shock syndrome toxin 1 and Staphylococcal enterotoxin B (exotoxins) also lead to survival improvement and cytokine release inhibition after toxic shock induction.

As described previously, CD6 can interact with Galectine-1 and Galectine-3, and it was reported that these two proteins can interfere with the ligand-binding properties of CD6, competing with LPS, PGN and LTA for CD6 binding (Escoda-Ferran et al. 2014).

More recently, another study showed the protective effect of rshCD6 (both prophylactic and therapeutic), and also of the murine isoform, in a lethal model of polymicrobial sepsis in mice – cecal ligation and puncture (Martínez-Florensa et al. 2017), together with proinflammatory cytokine modulation.

Altogether, these results suggest that rsCD6 could be a viable alternative for the current and growing problem of antibiotic resistance.

F. CD6 ROLE IN AUTOIMMUNITY

In the same way as CD5, due to its immunomodulatory potential, CD6 was expected to play a role in autoimmune disorders. Indeed, the interaction between CD6 and ALCAM has been shown to be important in human MS and murine EAE (Cayrol et al. 2008). ALCAM is expressed in the blood brain barrier and is crucial for leukocyte transmigration, since blockade of ALCAM restricted $CD4^+$ T cell recruitment. However, this notion has been recently challenged by the fact that ALCAM-KO mice develop a more severe form of EAE, which was associated with a significant increase in the number of CNS-infiltrating proinflammatory leukocytes compared with WT controls (Lécuyer et al. 2017). Recent reports also identified *CD6* as a significant susceptibility locus for MS in a cohort of 2624 patients and 7220 control subjects (De Jager et al. 2009; Kofler et al. 2016). The risk-associated allele, rs17824933, consists of an exchange of a C to a G in intron 1 (Kofler et al. 2011). This results in decreased expression of full-length CD6 in T cells which in turn is reflected in decreased $CD4^+$ T cell proliferation. This is caused by an alternative splicing involving exclusion of exon 5, which codes for SRCR domain 3 of CD6, the ALCAM-binding domain. Cells expressing this truncated isoform (CD6ΔD3) proliferate less when stimulated with anti-CD3 and anti-CD28 mAbs. Two years later, another study with a Spanish-Basque cohort identified an association between two non-synonymous SNPs (rs11230563 - R225W and rs2074225 - A257V) and MS (Swaminathan et al. 2013). The authors reported that this haplotype resulted in altered CD6 expression

patterns, specifically the protective haplotype showed higher expression of CD6 in $CD4^+$ and $CD8^+$ naïve T cells, $CD4^+$ and $CD8^+$ T central memory cells and NKT cells. Also, these CD6 polymorphisms correlated with clinical features and severity of MS (Kofler et al. 2016). It was also reported that, aside from polymorphism associations with disease, MS patients have lower CD6 mRNA levels than healthy controls (Wagner et al. 2014). This fact is interesting because CD6 - like ALCAM - seems to participate in leukocyte transmigration across the blood-brain barrier, but we also have to consider its role as a negative T cell modulator. Recent data from CD6KO mice of DBA background showed attenuation of disease severity in an EAE model by decreased pathogenic T cell response and T cell infiltration (Li et al. 2017). On the other hand, an exacerbated EAE response was reported in ALCAM-deficient mice (in a C57BL/6 background), as above mentioned (Lécuyer et al. 2017).

Interestingly, in the early 80s an anti-human CD6 mAb (anti-T12) was used for the first time to prevent GvHD in one severe combined immunodeficiency patient lacking a matched donor, and provided apparently good results (E L Reinherz et al. 1982). A year later, the same antibody was used to prevent acute renal transplant rejection with good responses (Kirkman et al. 1983). Later on, 12 MS patients treated with anti-T12 mAb showed reduction of $CD6^+$ T cells on the first days of treatment, though $CD6^-$ T cell activity and reappearance of $CD6^+$ T cells led to inconclusive results (Hafler et al. 1986).

The relevance of CD6 in RA has also been studied. As mentioned in previous sections, sCD6 was detected in the serum of patients affected of Sjögren syndrome (Ramos-Casals et al. 2001). An association between *CD6* and response to treatment with TNF-α inhibitors in RA patients was also shown (Krintel et al. 2012). The authors demonstrated that the presence of a 19 bp segment in the last intron of *CD6* correlates with a better response to treatment in the Danish cohort studied (Krintel et al. 2012). They hypothesize that this insertion can lead to a different splicing pattern of the gene.

Recently, a number of clinical studies have been testing a new humanized anti-human CD6 mAb (T1h - Itolizumab) against CD6 domain 1 (Hernández et al. 2016). *In vitro* studies demonstrated reduction of lymphocyte proliferation and production of pro-inflammatory cytokines. A phase I clinical study with five cohorts of RA patients showed that mAb treatment lead to no severe adverse effects, and positive and sustained clinical response was observed in more than 80% of the patients (Rodriguez et al. 2012). A phase III study was carried out in India with this mAb in a cohort of 225 moderate to severe psoriasis patients (Krupashankar et al. 2014). The authors observed improvement in the treatment groups over the placebo ones and no adverse side effects, proving previously proposed therapeutic benefits of Itolizumab for other autoimmune diseases such as Sjögren syndrome (Le Dantec et al. 2013). A year later, a new phase II study was performed

to analyze the safety and efficacy of combined therapy of Itolizumab with methotrexate in RA patients who did not respond to methotrexate alone (Chopra et al. 2016). Treatment was in general well tolerated, with some mild to moderated side effects and a few severe events. All mAb doses tested showed evidence of efficacy. Intriguingly, a study from our group with CD6KO mice in a C57BL/6 background reported an exacerbated autoimmune response in a CIA model, probably caused by impaired T_{reg} cell function (Orta-Mascaró et al. 2016).

G. CD6 ROLE IN CANCER

Contrary to what happens for autoimmune diseases, little has been studied regarding the role of CD6 in the antitumor response. Aside from T cells, CD6 expression was detected also in chronic lymphocytic leukemia (CLL) and in some lymphosarcoma cell leukemia (LSCL) cells (Kamoun et al. 1981). Currently, CD6 is used as a marker for CLL and LSCL cells, except for those cases with 11q deletion (Sembries et al. 1999), but its expression does not correlate with disease progression. As previously discussed, CD6 protects CLL cells from apoptosis induced by activation with anti-IgM in the presence of anti-CD6 mAbs (Osorio et al. 1997). In line with this data, recent work by our group shows that CD6 transfection protects leukaemic T cells from apoptosis induced by genotoxic drugs (Doxorubicin and Puromycin) (Carrasco et al. 2017). Moreover, a preliminary clinical trial with Itolizumab (12 doses of anti-CD6 mAb weekly) in patients with CLL showed some clinical and hematological improvement coupled with light secondary effects linked to the first mAb infusion (Izquierdo Cano et al. 2014).

II. WORK HYPOTHESIS AND OBJECTIVES

The ultimate goal of this thesis is the generation of proof-of-concept evidence on CD5 and CD6 as new targets for immunomodulatory therapies in immune-based disorders, namely autoimmunity and cancer –two opposite sides of the same coin. Both are intracellular signal transducing molecules associated to the TCR and BCR, and well positioned to modulate (more precisely, attenuate) antigen specific-driven differentiation/ activation signals in lymphocytes.

Accordingly, we intend to study the *in vivo* and *in vitro* biological consequences of blocking the molecular interactions established by these two receptors with their respective ligands (whether endogenous and/or exogenous), in normal and disease-induced experimental mouse models (**Fig. II.1**). For this purpose, our group has generated three different genetically modified mouse lines – two for CD5 and one for CD6. These three mouse models have been designed to constitutively express the human soluble form of the receptors (either CD5 or CD6) in lymphoid tissues, and they are expected to work as "decoy receptors", thus resulting in a "functional" knockdown effect. This kind of strategy has been successfully used in the past (e.g., CTLA-4, TNF-α, CD14, IL-6, etc) to understand whether soluble forms could be exploited to manipulate *in vivo* immune responses (Ronchese et al. 1994; Peters et al. 1996; Hunger et al. 1997; Tamura et al. 1999; Mäkinen et al. 2001; Bao et al. 2002). It is worth mention that this is possible because of the interspecies (mouse-human) conservation of the receptor-ligand interactions mediated by this receptors (Wee et al. 1994). Indeed, a great advantage of this strategy is that the results can be easily translated to clinical practice by means of already suitable protein delivery systems whether exogenously or endogenously.

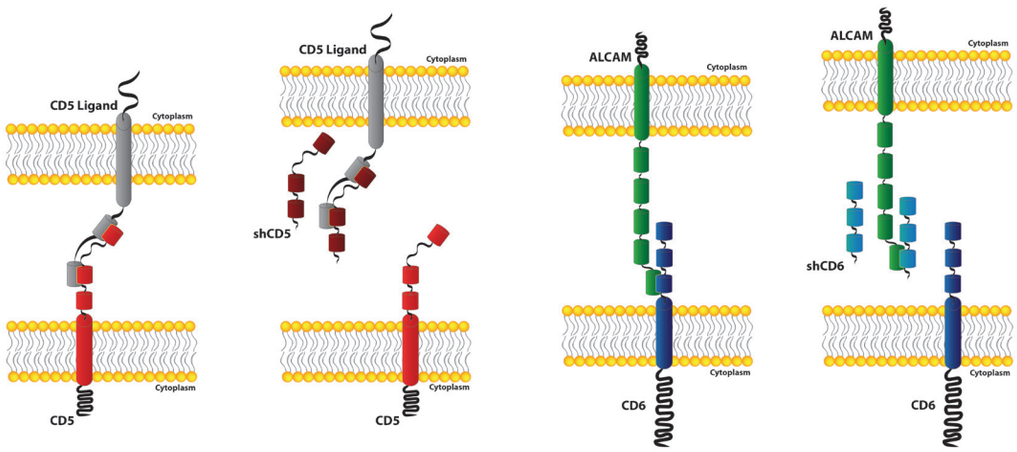

Fig. II.1 - Schematic representation of shCD5 and shCD6 interference of receptor/ligand/s interactions mediated by membrane-bound CD5 and CD6 receptors.

Based on the above-mentioned premises, the specific objectives of this thesis are the following:

- Evaluate the immunomodulatory effects and the underlying mechanism of transgenic shCD5 expression or purified rshCD5 protein infusion in experimental models of cancer and autoimmunity.
- Evaluate the immunomodulatory effects and the underlying mechanisms of transgenic shCD6 expression or purified rshCD6 protein infusion in normal conditions as well as in experimental disease-induced conditions (infection, cancer and autoimmunity).

III. MATERIALS AND METHODS

1. MICE

Animals were kept in individual ventilated cages under specific pathogen-free (SPF) conditions unless otherwise indicated, and utilized in agreement with the protocols approved by the Ethics Committee for Animal Research of the University of Barcelona and Generalitat de Catalunya (permits number 740/14, 741/14, 742/14, and 54/16). All efforts were made to minimize animal suffering.

For some purposes WT C57BL/6 mice purchased from Charles River were acclimatized for one week after their arrival prior to experimental manipulation. Regarding the transgenic mice studies, in all experiments we used transgenic and non-transgenic (control group) mice from each different colony. In all studies presented in this thesis, the mice were 7-12 weeks old, unless otherwise stated.

1.1. shCD5Eμ TRANSGENIC MICE GENERATION AND GENOTYPING

Generation of shCD5EμTg mice was carried out under service contract by Afigen (Cantoblanco, Spain). To this end, the cDNA sequence coding for the whole extracellular region of CD5 was amplified from the pHbAPRI-neo-CD5.P346stop construct (Calvo et al., 1999b) and subcloned into XhoI-ApaI restricted pIgHSV40s vector which contained the SV40 promoter and the immunoglobulin μ heavy chain enhancer (Eμ). The resulting pIgHSV40shCD5 vector was digested with ScaI and ApaLI and the transgene injected into fertilized eggs from a CBAxC57BL/6 mixed background. Founder mice were backcrossed for 10 generations into the C57BL/6 background. Transgenic mice were identified by PCR analysis of genomic DNA samples from ear punch specimens (50 μL of lysis buffer (1 M Tris pH = 8, 0.5 M EDTA, 5 M NaCl and 10 % SDS) plus 1 μL of proteinase K (Roche, Germany), followed by the PCR reaction: 200 μM of each dNTP, 300 nM of each primer, 1x of Expand High Fidelity buffer (1.5 mM $MgCl_2$), 2.6 U of Expand High Fidelity enzyme mix and 1 μL of DNA solution previously described) in a GeneAmp PCR System 2700 termocycler (Applied Biosystems, USA). The cycling conditions were: 1 cycle of 5 min at 94 °C; 30 cycles of 1 min at 92 °C, 1 min at 53 °C, and 8 min at 72 °C. The forward (5'-GCT GTC CCA GTG CCA CGA ACT T-3') and reverse (5'-GAA GCT CCT CTG TGT CCT CAT-3') primers to detect the transgene were specific for the extracellular region of human CD5. Internal control amplification primers (forward, 5'-TCA CTC AAG GCA ACC TTC CTG C-3'; reverse, 5'-CGA CCT CAT CTC TAA CCA TGA ACA G-3') specific for the invariant chain Ii of MHC class II (LIEX) were also included. The resulting PCR products (450 and 150 bp, respectively) were separated in a 2 % agarose gel and visualized in a G:Box system (SynGene, UK).

Complementary DNA was obtained using the High capacity cDNA kit (Life Technologies) retrotranscriptase according to the following conditions: 1 cycle of 10

min at 25.5 °C and 2 consecutive cycles of 60 min at 37 °C. Gene expression of hCD5 was determined with specific Taqman probe Hs00204397_m1 (Life Technologies/ ThermoFisher). For this, 2 µL of cDNA, 2.5 µL of distilled water, 5 µL of Master Mix (Taqman Fast universal PCR master Mix, Life Technologies) and 0.5 µL of primer/ probe for each gene analyzed were mixed. To determine the gene expression, we used Ct values inferior or equal to 30 cycles. The results were normalized with the expression values of the non-inducible gene Glyceraldehyde-3-phosphate dehydrogenase (GAPDH, Mm99999915_g1, Life Technologies/ThermoFisher), using the 2ΔCt formula, where ΔCt=Ct (desired gene)-Ct (GAPDH). The results are represented as relative quantity.

1.2. shCD5LckEµ TRANSGENIC MICE GENERATION AND GENOTYPING

The cDNA sequence coding for the whole extracellular region of CD5 was synthesized at Gen Script (New Jersey, USA) from the initiation Methionine to Asp345 and subcloned into the BamHI site of the p1026x vector (kindly provided by Roger Perlmutter), just downstream of the Lck proximal promoter and the immunoglobulin heavy chain enhancer (Eµ) (Iritani BM et al, EMBO J 1997). Transgenic mice were generated at PolyGene facilities (Rümlang, Switzerland) by injecting the purified NotI-NotI fragment into zygotes from superovulated C57BL/6N female mice mated to C57BL/6N breeder males (Charles River). Injected zygotes were cultured overnight and transferred into pseudopregnant B6xCBA F_1 females (Charles River). Born pups (n = 20) were biopsied at weaning and analyzed for transgene integration by PCR, of which four females and one male were positive for the transgene and mated to establish the colony in our mouse facility (School of Medicine, University of Barcelona). Genomic DNA was extracted from an ear punch by the KAPA Mouse Genotyping Kit (Kapa Biosystems, USA) and subjected to PCR (GeneAmp PCR System 2700, Applied Biosystems, USA) with primer pairs specific for the extracellular region of CD5 (Fw 5'-CTC ACC CGT TCC AAC TCG AAG-3' and Rv 5'-TCG CGC TGT AGA ACT CCA C-3') and the invariant Li chain of MHC class II (Fw 5'-TCA CTC AAG GCA ACC TTC CTG C-3' and Rv 5'-CGA CCT CAT CTC TAA CCA TGA ACA G-3'), resulting in 429 bp and 150 bp fragments, respectively. The cycling conditions were: 1 cycle, 5 min at 94 °C; 35 cycles, 15 sec at 94 °C, 15 sec at 58 °C, and 15sec at 72 °C; and 1 cycle, 10 min at 72 °C. The PCR products were separated on a 2 % agarose gel in 1x TBE buffer (89 mM Tris-HCl, 89 mM Boric Acid, 2 mM EDTA pH = 8, to a final volume of 1 L distilled water) containing a 10,000x dilution of SYBR Safe (Invitrogen, USA) and visualized in a G:Box appliance (SynGene, UK), and images obtained using GeneSnap.

To demonstrate that the 429 bp band corresponded to shCD5, the remaining PCR genotyping product was treated with ExoSap-IT (Affymetrix, USA) and sequenced with the Big Dye v3.1 Cycle Sequencing Kit (Life Technologies, USA). This was performed twice in a total of five samples from each phenotype.

To verify that the hCD5 is only expressed in the shCD5LckEμTg mice and in which lymphoid and non-lymphoid organs, a RT-qPCR was performed in kidney, lung, thymus, lymph node and spleen. Messenger RNA was extracted adding 1 mL of TRIzol (Invitrogen) and homogenizing the tissue with a sterile pipette tip in order to lyse the cells. Then 200 μL of chloroform (AnalaR NORMAPUR) were added and incubated at RT for 3 min. The samples were centrifuged 15 min at 4 °C and 12,000 g and the upper phase formed (containing RNA) transferred to a new eppendorf that contained the same volume of 70 % ethanol (Panreac), stirring to dissolve precipitates (35 % final concentration of ethanol). To purify the extracted RNA, the PureLink RNA Mini Kit (Ambion, Life technologies) was used according to manufacturer's instructions. The purified RNA was quantified with an Epoch (Gen5 1.09, BioTek) at a wavelength of 260 nm and 280 nm. RNA purity was calculated with the 260/280 nm quotient, with samples being studied only when the purity quotient was close to 2.

To determine the hCD5 gene expression, we performed the same protocol as described previously in 1.1. section.

1.3. shCD6LckEμ TRANSGENIC MICE GENERATION AND GENOTYPING

The codon-optimized cDNA sequence coding for the whole extracellular region of human CD6 (GenBank X60992.1) (Aruffo, Melnick, Linsley, & Seed, 1991), from the initiation Methionine to Arg373, was synthesized at Gen Script (New Jersey, USA) and cloned into the BamHI site of the p1026x vector (kindly provided by Roger Perlmutter), just downstream of the Lck proximal promoter and the immunoglobulin heavy chain enhancer (Eμ) (Iritani, Forbush, Farrar, & Perlmutter, 1997). Transgenic mice were generated at PolyGene facilities (Rümlang, Switzerland) by injecting the purified NotI-NotI fragment into zygotes from superovulated C57BL/6N female mice mated to C57BL/6N breeder males (Charles River). Injected zygotes were cultured overnight and transferred into pseudopregnant B6xCBA F1 females (Charles River). Born pups (n = 14) were biopsied at weaning and analyzed for transgene integration by PCR, of which one male and one female were positive for the transgene and mated to establish the colony in our mouse facility. Genomic DNA was extracted from an ear punch by the KAPA Mouse Genotyping Kit (Kapa Biosystems, USA) and subjected to PCR (GeneAmp PCR System 2700, Applied Biosystems, USA) with primer pairs specific for the extracellular region of CD6 (Fw 5'-ACC TGA CCA GCT CAA CAC-3' and Rv 5'-GTC ATC GCA CAC TGA TCC-3') and the invariant Li chain of MHC class II (Fw 5'-TCA CTC AAG GCA ACC TTC CTG C-3' and Rv 5'-CGA CCT CAT CTC TAA CCA TGA ACA G-3'), resulting in 495 bp and 150 bp fragments, respectively. The cycling conditions were: 1 cycle, 5 min at 94 °C; 35 cycles, 15 sec at 94 °C, 15 sec at 58 °C, and 15 sec at 72 °C; and 1 cycle, 10 min at 72 °C. The PCR products were separated on a 2 % agarose gel in 1X TBE buffer (89 mM

Tris-HCl, 89 mM Boric Acid, 2 mM EDTA pH = 8, to a final volume of 1 L distilled water) containing a 10,000x dilution of SYBR Safe (Invitrogen, USA) and visualized in a G:Box appliance (SynGene, UK), and images obtained using GeneSnap.

To demonstrate that the 495 bp band corresponded to shCD6, the remaining PCR genotyping product was treated with ExoSap-IT (Affymetrix, USA) and sequenced with the Big Dye v3.1 Cycle Sequencing Kit (Life Technologies, USA). This was performed once with two samples from each phenotype.

1.4. BREEDING STRATEGY TO OBTAIN HOMOZYGOUS MICE

All three colonies were initiated from intercrossing heterozygous mice at the mouse facility of the School of Medicine, University of Barcelona. Thus, the first litter rendered hetero- or homo-zygous transgenic mice as well as homozygous non-transgenic mice (referred hereafter as Non-Tg). Homozygous Tg animals were identified by crossing them with Non-Tg mice and analyzing the respective offspring; if all the offspring (at least two different litters) was positive for the transgene, we considered the progenitor homozygous. Once we obtained homozygous males and females for the transgene we bred them in order to obtain only homozygous offspring. Along with this, we also bred Non-Tg littermates to obtain the respective controls.

Once the homozygous were obtained, we proceeded to freeze embryos from the three colonies, needing for this one 3 month-old homozygous male and around 50 4-5 week-old homozygous females. The *in vitro* fertilization procedure was performed by the mouse facility veterinarian and about 300 embryos from each colony were frozen.

2. PRODUCTION AND PURIFICATION OF RECOMBINANT shCD5 AND shCD6 PROTEINS

Production of purified rshCD5 (R25-D345) and rshCD6 (D25-R397) proteins (PBS with 10 % glycerol, pH = 7.4) was performed based on previously reported methods (Sarrias et al., 2004) but using SURE CHO-M Cell line™ clones from the Selexis SUREtechnology Platform™ (Geneva, Switzerland) and subjecting serum-free supernatants to size-exclusion chromatography protocols developed at PX´Therapeutics (Grenoble, France). Recombinant Human Serum Albumin (HSA) from Sigma-Aldrich was prepared at the same working concentrations as rshCD5/rshCD6 with 10 % glycerol.

3. PHENOTYPICAL CHARACTERIZATION OF TRANSGENIC MICE

3.1. DETECTION OF HUMAN PROTEIN IN THE SERUM OF TRANSGENIC MICE BY SANDWICH ELISA

In order to confirm the presence of shCD6 and shCD5 in mouse serum, two different assays were performed: a specific Sandwich ELISA and a tolerance immunization test.

Before performing the ELISAs, blood was obtained by cardiac puncture (around 1 mL) from male and female mice. The blood was stored on ice until centrifuged at 4 °C at 5000 rpm for 15 min. The serum was recovered and stored at -80 °C until used.

The shCD6 protein present in the mice serum was detected and quantified with Human soluble CD6 PicoKine™ ELISA Kit sandwich (Boster Bio, USA) following manufacturer´s instructions and absorbance measured at 450 nm with a Gen5 1.09 (Epoch, BioTek).

Mouse serum shCD5 was detected and quantified with a home-made sandwich ELISA. A 96-well flat-bottom plate (F16 Maxisorp Nunc-Immunoplate, Thermo Fisher Scientific Inc.) was coated with 5 µg/mL of anti-human CD5 mAb (CRIS-1) as capture antibody in 100 µL of carbonate/bicarbonate buffer pH 9.5 (0.1 M sodium carbonate) overnight at 4 °C. After washing the plate three times with PBS-0.05 % Tween 20 (PBS-T), it was blocked for 1 h at room temperature (RT) with 100 µL of PBS plus 5 % inactivated FBS (PBS-FCS). The plate was washed a second time as described above and 100 µL of the sample and known concentrations of rshCD5 (serial dilutions from 0 - 30 ng/µL in blocking solution) were added in duplicate and incubated for 2 h at RT. The plate was then washed five times and incubated with 100 µL of biotinylated mouse anti-human CD5 mAb (LEU-1, 5 µg/mL) for 1 h at RT. The plate was then washed six times and incubated for 1 h at RT with 100 µL of a 1:5000 dilution of Streptavidin-Peroxidase (POD) Conjugate (Roche Diagnostics) in blocking solution. After another seven washes, 100 µL of TMB Substrate Reagent Set (BDOptEIA, BD Bioscience) were added to each well and incubated 15 min at RT in the dark. At this point, 100 µL 2 N sulfuric acid were added to each well to stop the reaction and the optical density (OD) was measured in an ELISA-plate reader (Gen5 1.09, Epoch, BioTek) at a wavelength of 450 nm and 620 nm. All the necessary ELISA controls were included (standard curve, negative control - without capture antibody – and negative control - without antigen). The ELISA standard curves were performed in Microsoft Office Excel.

3.2. IMMUNOGENICITY OF HUMAN sCD5 AND sCD6 PROTEINS TO TRANSGENIC AND NON-TRANSGENIC MICE

To verify the anti-human CD5 or CD6 antibody production by shCD6LckEμTg, shCD5LckEμTg mice, and shCD5EμTg mice, female mice were primed *i.p.* with 2 μg of rshCD5 or rshCD6, in the case of shCD6LckEμTg and shCD5LckEμTg mice, or 25 μg of rshCD5 or rshCD6, in the case of shCD5EμTg mice, in a total volume of 100 μL in complete Freund's adjuvant (CFA, Sigma-Aldrich) and boosted three weeks later with 1 μg of protein (in the case of shCD6LckEμTg and shCD5LckEμTg mice) and the same amount of the first boost in the case of the shCD5EμTg mice in 100 μL incomplete Freund's adjuvant (IFA, Sigma-Aldrich). In the case of the immunization with rshCD5 in shCD5LckEμTg mice and corresponding Non-Tg controls, a third boost (same as the second boost) was also administrated. The emulsion was prepared with two plastic syringes connected to a three-way valve. Sera obtained before the immunization (day 0) by submandibular vein and thirteen days after the second/third immunization by cardiac puncture were kept at -80 °C until analysis by ELISA for antibodies against rshCD6 (sCD6), rshCD5 (sCD5) or BSA (bovine serum albumin).

To evaluate the response to exogenous administration of rshCD6 and/or rshCD5, the detection of anti-human CD6 and CD5 mouse antibodies was performed with an ELISA assay. 96-well plates were coated overnight (o.n.) at 4 °C with 2 μg/mL of rshCD5, rshCD6 or BSA, respectively. After blocking with PBS plus 5 % BSA, mouse serum samples were added to the wells at increasing dilutions (100 μL each by duplicate) and incubated for 2 h at RT. After extensive washing with PBS-T, wells were incubated for 30 min at RT with Horseradish peroxidase (HRP)-labeled anti-mouse immunoglobulin antiserum (Sigma) (1:1000). Color was developed in the plate by addition of TMB substrate. The values represent mean absorbance (OD 450 nm – 620 nm) and standard deviation of total IgG levels for each group of mice analyzed.

3.3. IMMUNOPHENOTYPING OF LYMPHOID CELL POPULATIONS FROM TRANSGENIC MICE BY FLOW CYTOMETRY

For the studies of lymphocyte populations in basal conditions by flow cytometry, mice were euthanized with excess Isoflurane (Laboratoris Esteve) and the extracted tissues (spleen, thymus, lymph node (LN), bone marrow (BM)) or peritoneal lavage from Tg and Non-Tg mice preserved at 4 °C until the samples were processed.

Firstly, cell suspensions were obtained by mechanical tissue dissociation through a 40 μM nylon cell strainer (Biologix), except for peritoneal lavage, in PBS 2 % FBS. Erythrocytes were then lysed by 3 min incubation at RT with 1x RBC lysis buffer (eBioscience), when applicable. Total cells were counted and 1 x 10^6 cells per mouse collected and blocked with

PBS-10 % FBS plus Fc Block (anti-CD16/32, clone 2.4G2, TONBO Bioscience) for 15 min at 4 °C. Then the samples were stained for 30 min at 4 °C with the appropriate antibody panels (see below) for each study (**Table III.1**). Finally, after the appropriate washes cells were analyzed in a FACS Canto II flow cytometer (BD Biosciences) and the data analyzed with Flow Jo software (Tree Star).

B10 and T_{reg} cell analysis required intracellular staining with Cytofix/Cytoperm kit (BD Pharmingen, USA) and PE anti-mouse/rat FoxP3 Staining Set (eBioscience, USA), respectively, following the manufacturer's instructions.

3.3.1. Antibody Panels

Briefly, the below indicated panels were used:

- panel 1: B cell precursors in bone marrow;
- panel 2: B peritoneal cavity cells;
- panel 3: IL-10-producing B cells in spleen and peritoneal cavity;
- panel 4: T_{reg} subset in thymus, spleen and lymph node;
- panel 5: T memory cell subtypes in spleen and lymph node;
- panel 6: B cell subtypes in spleen and lymph node;
- panel 7: dendritic cells in spleen and lymph node;
- panel 8: NK and NKT subtypes in thymus, spleen and lymph node;
- panel 9: T maturation subsets in thymus;
- panel 10: NK and NKT cell activation markers in spleen and lymph node;
- panel 11: T cell activation and exhaustion markers in spleen and lymph node;
- panel 12: Double negative subsets in thymus and memory subsets in spleen and lymph node.

Table III.1. Antibody panels used in the flow cytometry characterization of lymphocyte subpopulations.

Surface Marker				**Violet Laser (405nm)**	**Blue Laser (488nm)**		**Green Laser (532nm) Yellow-green laser (561nm)**	**Red Laser (640nm)**	
				452	519	695	578	660	785
Panel	MAb name	Company	Clone	Pacific Blue	FITC	PerCP Cy5.5	PE	APC	APC Cy7
1	BP-1	eBioscience	6C3			X			
	CD43	BD Pharmingen	S7				X		
	CD24	BD Pharmingen	M1/69					X	
	B220	TONBO Bioscience	RA3-6B2	X					

2	IgD	SouthernBiotech	11-26						
	IgM	eBioscience	II/41					X	
	CD5	eBioscience	53-7.3			X			
	B220	TONBO Bioscience	Ra3-6B2		X				
3	B220	TONBO Bioscience	Ra3-6B2		X				
	CD5	eBioscience	53-7.3			X			
	CD1d	BioLegend	1B1					X	
	IL-10	BioLegend	JES5-16E3				X		
4	CD4	TONBO Bioscience	RM4-5		X				
	CD8	TONBO Bioscience	53-6.7	X					
	CD25	eBioscience	PC61.5					X	
	FoxP3	TONBO Bioscience	3G3				X		
5	CD4	BioLegend	GK1.5	X					
	CD8	TONBO Bioscience	53-6.7			X			
	CD44	BD Biosciences	IM7		X				
	CD62L	TONBO Bioscience	MEL-14					X	
	CD19	TONBO Bioscience	1D3				X		
6	IgD	SouthernBiotech	11-26				X		
	IgM	eBioscience	II/41					X	
	CD23	eBioscience	B3B4	X					
	CD93	eBioscience	AA 4.1			X			
	CD21/35	BD Biosciences	7G6		X				
7	CD11c	eBioscience	N418	X					
	MHC II	BioLegend	M5/114.15.2						
	CD3	TONBO Bioscience	145-2C11			X			
	B220	TONBO Bioscience	Ra3-6B2		X				
	CD8	BioLegend	53-6.7				X		
	CD80	BioLegend	16-10A1					X	
8	CD4	TONBO Bioscience	RM4-5		X				
	CD8	TONBO Bioscience	53-6.7						
	CD3	TONBO Bioscience	145-2C11					X	
	NK1.1	BD Biosciences	PK136				X		
9	CD4	BioLegend	GK1.5					X	
	CD8	BioLegend	53-6.7				X		
	CD69	eBioscience	H1.2F3	X					
	CD24	BD Pharmingen	M1/69		X				
	TCRβ	TONBO Bioscience	H57-597			X			
10	CD3	TONBO Bioscience	145-2C11			X			
	NK1.1	BD Biosciences	PK136				X		
	CD69	eBioscience	H1.2F3	X					
11	CD4	TONBO Bioscience	RM4-5		X				
	CD8	TONBO Bioscience	53-6.7					X	
	CD3	TONBO Bioscience	145-2C11			X			
	CD69	eBioscience	H1.2F3	X					
	PD-1	TONBO Bioscience	J43.1				X		

12	CD4	TONBO Bioscience	RM4-5		X				
	CD8	TONBO Bioscience	53-6.7	X					
	CD44	TONBO Bioscience	IM7			X			
	CD62L	TONBO Bioscience	MEL-14					X	
	PD-1	TONBO Bioscience	J43.1				X		
	CD25	BD Pharmingen	PC61						X

4. IMMUNOMODULATION OF WILD-TYPE MICE BY INFUSION OF EXOGENOUS RSHCD5 OR RSHCD6 PROTEINS

To confirm that the results obtained in the characterization of lymphocyte populations from Tg mice were not due to artifacts of random insertion of the shCD5 and rshCD6 transgenes, 1.25 mg/Kg per mouse of exogenous rshCD6, rshCD5 or vehicle were administered by *i.p.* injection to C57BL/6 WT mice for 15 days, on alternate days (**Fig. III.1**). The lymphocyte analysis was performed as described above (see section 3.3).

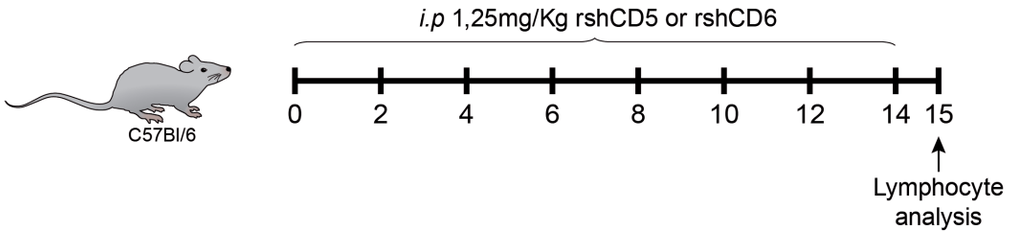

Fig. III.1 – Schematic representation of the protein administration schedule.

5. FUNCTIONAL CHARACTERIZATION OF TRANSGENIC AND PROTEIN INFUSED MICE

5.1. T CELL PROLIFERATION ASSAYS

For these studies, the spleen and/or lymph nodes (LNs) from WT or genetically modified mice were extracted under sterile conditions in a mouse facility laminar flow hood and maintained in RPMI (Lonza) 10 % FBS, 10 mM HEPES, 1 mM Sodium pyruvate, 50 mM β-Mercaptoethanol, Penicillin/Streptomycin, and Glutamine at 4 °C (from now on referred as complete RPMI). The cell suspension was also obtained with the previously described protocol, but in a laminar flow hood.

In order to analyze cell proliferation, cells were stained with Carboxyfluorescein Succinimidyl Esther (CFSE) following manufacturer´s instructions (**Fig. III.2**). Briefly, cells were washed with ice-cold PBS and then re-suspended in PBS-FBS at a concentration of 1 x 10^6 cells/mL, and the CFSE added at 1-2 µM (CFSE, Life Technologies). The tube was repeatedly inverted and incubated 15 min at 37 °C protected from light. After that time the cells were washed with PBS-FBS and complete RPMI adjusting the cells to the desired concentration depending on the experiment.

5.1.1. Total Spleen Cells Suspensions

CFSE-stained total spleen cell suspensions were seeded in triplicate in a 96-well U-bottom plate at a final concentration of 2.5 x 10^5 cells in 200 µL with 1 µg/mL hamster anti-mouse CD3 mAb (145-2C11; TONBO Bioscience) alone or in combination with 1 µg/mL soluble hamster anti-mouse CD28 mAb (37.51; TONBO Bioscience) for 72 h at 37 °C and 5 % CO_2. After this time, the cells were stained with labeled rat FITC anti-mouse CD4 (RM4-5, TONBO Bioscience) and PE anti-mouse CD8 mAb (53-6.7, BioLegend) and analyzed in a BD FACSCanto II flow cytometer. To distinguish the non-proliferative cells we had control non-stimulated cells that had the maximum CFSE intensity. The cells with lower CFSE intensity are the ones that have proliferated. In parallel, to analyze activation, splenocytes without CFSE stain were cultured as previously explained and approximately 18 h later stained with labeled anti-mouse CD4, CD8, CD69 (H1.2F3, BioLegend), and CD25 (PC61.5, TONBO Bioscience) mAbs and analyzed in a BD FACSCanto II flow cytometer.

We also analyzed the IFN-γ production in the supernatants of these cell cultures with a commercial DuoSet ELISA Kit (R&D Systems) following manufacturer´s instructions.

Activation with PMA (50 ng/mL) plus Ionomycin (500 ng/mL) in X-vivo medium (Lonza) was also tested in whole spleen cell supensions (2 x 10^5 and 6 x 10^5 cells) for 72 h at 37 °C and 5 % CO_2. Supernatants were tested for IFN-γ and TNF-α production (DuoSet ELISA Kit, R&D Systems) according to manufacturer´s instructions.

The ELISA standard curves were performed in Microsoft Office Excel.

5.1.2. Isolated Spleen T Cells

$CD4^+$ and $CD8^+$ T cells from Tg and Non-Tg mouse spleens were electronically sorted by flow cytometry with a BD FACSAria cytometer using specific antibodies (FITC-labeled CD4, RM4-5 clone, TONBO Bioscience and eFluor 450-labeled CD8, 53-6.7 clone, TONBO Bioscience) and CFSE stained as described previously. Then, 8 x 10^4 cells were cultured in a 96-well flat-bottom plate pre-sensitized o.n. with sterile 1 µg/mL hamster anti-mouse CD3 mAb (145-2C11; TONBO Bioscience) or isotype control (Armenian hamster IgG isotype, BioLegend) and 1 µg/mL soluble hamster anti-mouse CD28 mAb (37.51; TONBO Bioscience) for 72 h at 37 °C and 5 % CO_2. Proliferation was determined as described above in a BD FACSCanto II flow cytometer.

The effect of rshCD6 addition to the cell culture was also studied in isolated spleen T lymphocytes from WT mice at different concentrations (1 – 10 µg/mL).

We also analyzed TGF-β (eBioscience), IL-2 and IFN-γ (R&D Systems) production

in the cell culture supernatants with commercial DuoSet ELISA Kits according to manufacturer´s instructions. The ELISA standard curves were performed in Microsoft Office Excel.

5.2. REGULATORY T CELL SUPRESSION ASSAY

For T_{reg} cell suppression assays, spleen $CD4^+CD25^-$ (T_{conv} cells) and $CD4^+CD25^+$ (T_{reg} cells) T cells were electronically sorted by flow cytometry and, upon CFSE-labeling of the former, co-cultured for 72 h at different effector:suppressor ratios in 96-well flat-bottom plates pre-coated with hamster anti-mouse CD3 mAb (145-2C11; TONBO Bioscience) or isotype control (Armenian hamster IgG isotype, BioLegend) plus soluble anti-mouse CD28 (37.51; TONBO Bioscience). T effector cell proliferation was analyzed by determining the percentage of CFSElow cells in a BD FACSCanto II flow cytometer.

For the cell sorting, the following antibodies were used: FITC-labeled CD4, RM4-5 clone (TONBO Bioscience); eFluor 450-labeled CD8, 53-6.7 clone (TONBO Bioscience); APC-labeled CD25, PC61.5 clone (eBioscience); and PeCy7-labeled CD19, 1D3 clone (TONBO Bioscience).

The effect of rshCD6 addition (1 – 10 μg/mL) to the cell co-cultures of T effector and T_{reg} lymphocytes from WT mice was also studied.

We also analyzed TGF-β (eBioscience), IL-2 and IFN-γ (R&D Systems) production in the cell culture supernatants with commercial DuoSet ELISA Kits according to manufacturer´s instructions. The ELISA standard curves were performed in Microsoft Office Excel.

5.3. B CELL PROLIFERATION ASSAYS

These experiments were performed in parallel with the above mentioned T cell studies. The B cells were electronically sorted by flow cytometry with a PeCy7-labeled CD19 (1D3 clone, TONBO Bioscience) and then stained with CFSE. B cells were cultured under two different conditions: the first included treatment with 10 μg/mL anti-IgM (AffiniPure $F(ab')_2$ fragment goat anti-mouse IgM, Jackson ImmunoResearch) alone or in combination with 5 μg/mL anti-CD40 (LEAF Purified anti-mouse CD40, 1C10 clone, BioLegend) or 31.5 ng/mL recombinant mouse IL-4 (ImmunoTools); the second included treatment with 20 μg/mL LPS (L-2630 lot, Sigma) alone or in combination with 31.5 ng/mL IL-4, for 72 h at 37 °C and 5 % CO_2 in a 96-well flat-bottom plate. Proliferative responses were analyzed by determining the percentage of CFSElow cells with a BD FACSCanto II flow cytometer.

IL-6 and IL-10 production was also analyzed in cell culture supernatants with

commercial DuoSet ELISA Kits (R&D Systems) according to manufacturer´s instructions. The ELISA standard curves were performed in Microsoft Office Excel.

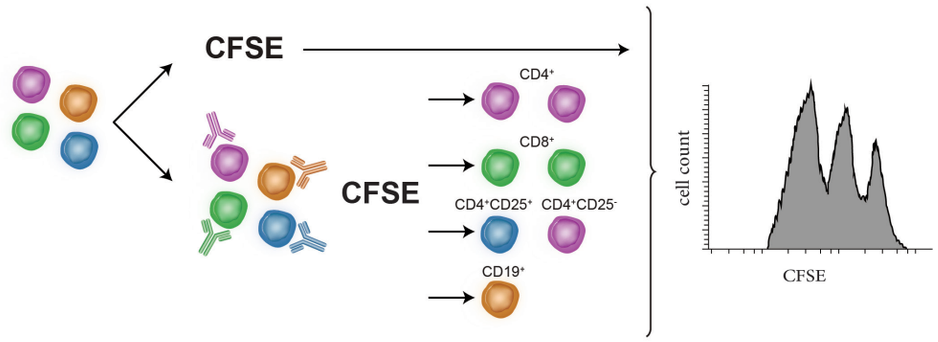

Fig. III.2 – Schematic representation of the *in vitro* proliferation assay studies.

5.4. BrdU INCORPORATION *IN VIVO*

For the detection of *in vivo* proliferating cells, shCD6LckEμTg and Non-Tg littermate mice were administered *i.p.* with 1 mg BrdU (FITC BrdU Flow Kit, BD Pharmingen). After approximately 16 h the spleen and LNs were harvested and cell suspensions obtained for FACS analysis as described in the BrdU assay kit, following the manufacturer's instructions. The antibodies used were: anti-CD4 APC, anti-CD8 eFluor450, anti-CD19 PE-Cy7, anti-BrdU FITC, 7AAD, anti-Foxp3 PE, and anti-CD25 APC-Cy7 (clone and commercial house described in **Table III.1**). The $BrdU^+$ cells were considered the ones that proliferated.

5.5. APOPTOSIS DETECTION ASSAYS

Apoptosis in spleen and LNs was measured with the Annexin/7AAD Kit (Immunostep) following manufacturer's indications. Once the cells were stained for flow cytometry, they were resuspended in 400 μL of Annexin buffer, 10 μL of Annexin and 10 μL of 7AAD. After incubating for 15 min at RT they were analyzed in the flow cytometer. The $Annexin^+/7AAD^+$ and $Annexin^+/7AAD^-$ cells were considered as apoptotic.

5.6. ANALYSIS OF T-DEPENDENT (TD) ANTIBODY RESPONSE

To study the antibody response to TD antigens (**Fig. III.3**), Tg and Non Tg mice from each colony were immunized *i.p.* with 50 μg of TNP_5-KLH (TD antigen, Biosearch Technologies, Inc. USA) in 400 μL of PBS in CFA at day 0 and of PBS alone at day 14. Serum from immunized mice was collected at days 0, 7, 14, and 21 (by submandibular vein puncture for the first time points and cardiac puncture at the endpoint) after the primary immunization and stored at -20 °C until analysis. The TNP_5-KLH-CFA emulsion was prepared as explained previously for protein immunization.

Levels of TNP-specific antibodies were determined by ELISA. Briefly, plates were sensitized o.n. with 3 µg/mL TNP_{18}-BSA (Biosearch Technologies, Inc. USA) diluted in PBS, washed with PBS 0.05 % Tween 20 and blocked with PBS 2 % BSA for 1 h at 37 °C. After performing a titration curve of serum for each antibody to select the best dilution (1:500), 100 µL of serum was added to the plate and incubated for 1 h at RT. To determine the levels of different isotypes of TNP-specific antibodies in the serum of immunized mice, biotinylated sheep anti-mouse IgM (1:200000 dilution), IgG_1 (1:400000 dilution), IgG_{2b} (1:20000 dilution), IgG_{2c} (1:50000 dilution), or IgG_3 (1:20000 dilution) antibodies (Jackson ImmunoResearch Laboratories, USA) were incubated for 1 h at RT. After 3 washes, Streptavidin-POD Conjugate (Roche Diagnostics) was added for 30 min at RT. The assay was developed with 100 µL of TMB (Tetramethylbenzidine, BD Biosciences, USA) for 30 min at RT in the dark. The reaction was stopped by adding 100 µL of 2 N sulfuric acid to each well. Subsequently, the absorbance was measured in an ELISA reader (Gen5 1.09, Epoch, BioTek) at a wavelength of 450 nm and 620 nm.

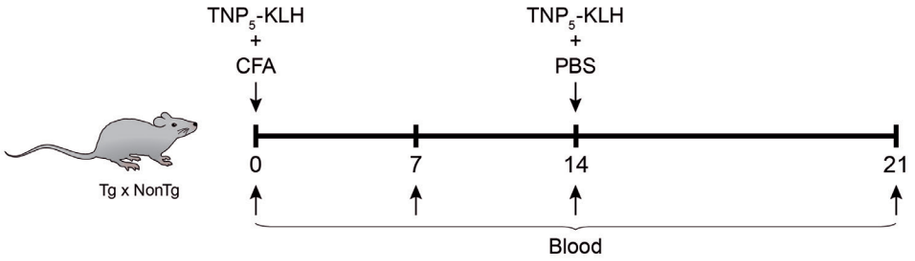

Fig. III.3 – Schematic representation of the TD antigen immunization protocol.

5.7. ANALYSIS OF T-INDEPENDENT TYPE 1 (TI-1) AND 2 (TI-2) ANTIBODY RESPONSES

To study the antibody response to TI type 1 and 2 antigens (**Fig. III.4**), Tg and Non-Tg mice from each colony were immunized *i.p.* with 50 µg of $TNP_{0,3}$-LPS (TI-1 antigen) and TNP_{65}-Ficoll (TI-2 antigen) in 400 µL of PBS (Biosearch Technologies, Inc. USA). Serum from immunized mice was collected at days 0, 7 and 14 after the immunization and stored at -20 °C until analysis.

ELISA assays as described for TD antigens were also performed for both TI antigens under the same conditions.

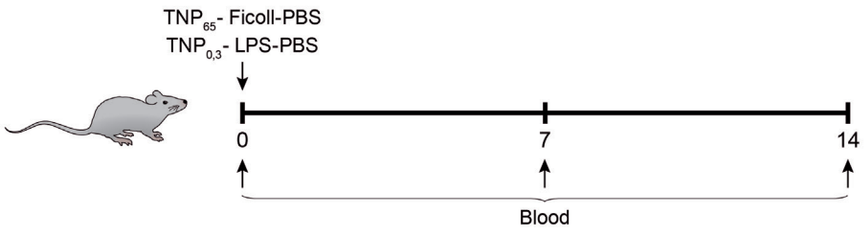

Fig. III.4 – Schematic representation of the TI antigens immunization protocol.

6. EXPERIMENTAL MOUSE MODELS OF DISEASE

6.1. LPS-INDUCED SEPTIC SHOCK

We performed a model of LPS-induced septic shock in shCD6LckEμTg and Non-Tg control mice (n = 7). The mice were weighed the day before induction in order to adjust the dosis of LPS injected. A solution of 1 mg/Kg of LPS was prepared in saline solution and injected *i.p.*. Blood was collected before and 3 h after the induction for analysis of IL-6, IL-1β, IL-10 and TNF-α serum cytokine levels (Duo-Set ELISA Kits, R&D Systems). Survival rate and clinical score were followed up (fur grooming, diarrhea, lachrymal secretions, and lethargy). Score of 1 or 0 was assigned denoting the presence or absence of the clinical signs, respectively.

The ELISA standard curves were performed in Microsoft Office Excel.

6.2. EXPERIMENTAL AUTOIMMUNE ENCEPHALOMYELITIS (EAE) MODEL

The EAE model was performed in 8-10 week old female Tg and Non-Tg control mice under conventional (non SPF) animal facility conditions as reported elsewhere (Martinez-Pasamar et al., 2013). To this end, mice were anesthetized by inhalation with 4 % Isoflurane 2.5-3 L/min in oxygen. Both hind paws were shaved in order to immunize *s.c.* with a previously prepared emulsion containing a mix of 7.5 mg/Kg Myelin Oligodendrocyte Glycoprotein (MOG_{35-55}) peptide (MEVGWYRSPFSRVVHLYRNGK; ESPIKEM ref. EPK1), 50 mg/Kg Mycobacterium tuberculosis (DIFCO), CFA and PBS in a total volume of 200 μL/mice (100 μL per paw). Subsequently, 25 mg/Kg Pertussis toxin (Sigma) was injected *i.p.* and the mouse weight registered. Two days later, the mice received a second 25 mg/Kg Pertussis toxin dose *i.p.*.

For the study of the effect of rshCD6 administration female C57BL/6N WT mice were *i.p.* administrated with 1.25 mg/Kg of protein per mice every other day starting on the day of EAE induction (day 0) until the end of the model (day 30) (**Fig. III.5**).

In the study performed with shCD5EμTg mice, mouse brains were snap frozen and sectioned (10 μm) at peak disease scores (determined empirically for each mouse as the fifth day after initial disease signs - score higher than 0) for histology study. Tissue was stained with hematoxylin and eosin to detect CNS inflammatory infiltrates, or solochrome cyanin to assess myelination.

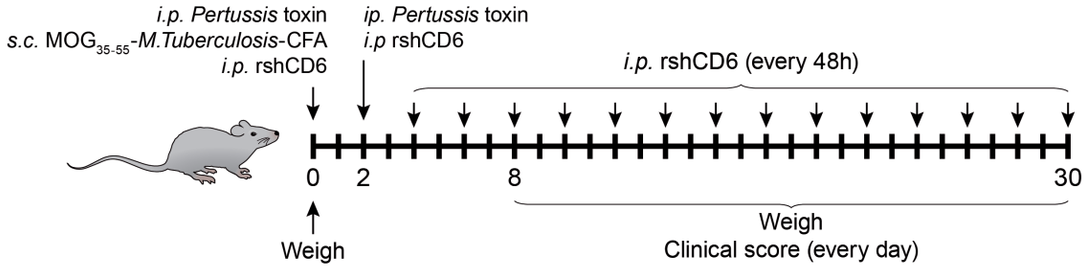

Fig. III.5 – Schematic representation of the EAE model induction protocol in WT rshCD6-treated mice.

The weight and the clinical score were determined daily based on the following scale:

Table III.2. Common clinical signs of EAE and respective clinical score.

Clinical signs	Score
Normal behavior Tail moves and raises, wraps around a round object if mouse is held at the base of the tail.	0
Decreased distal tail tone Tail does not respond to touch, tip of the tail droops.	0,5
Paralyzed tail The first noticeable clinical sign in ascending paralysis, tail totally droops.	1
Hind limb paresis, uncoordinated movement Difficulty in holding on the grid with hind legs.	1,5
Hind limb paresis Failure in holding on the grid with hind legs	2
Mild Ataxia Uncoordinated gait with one hind limb dragging.	2,5
Hind limb paraplegia Inability to move hind limbs, but maintains its capacity to move.	3
Partial Paralysis Drags hind limbs and loses the ability to move. Paralyzed lumbar spine.	3,5
Total Paralysis Entire posterior region paralyzed. Hind limbs retracted and sideways. Weakness in forelimbs.	4
Total Paralysis Mouse can not move, both forelimbs and hind limbs paralyzed.	4,5
Moribund No movement, altered breathing.	5
Dead	6

6.3. COLLAGEN-INDUCED ARTHRITIS (CIA) MODEL

The study of the CIA model in Tg and Non-Tg mice was performed in collaboration with the research group of Dr. Jesús Merino and Dr. Ramón Merino (Instituto de Biomedicina y Biotecnolgía de Cantabria, CSIC-UC-SODERCAN, Santander) as described previously (Postigo, et al., 2012). Two different protocols were performed, one for the study in shCD5EμTg mice and another one in the shCD6LckEμTg mice.

In the case of shCD5EμTg mice, type II bovine collagen (provided by Dr. M. Griffiths, University of Utah, Salt Lake City, USA) was dissolved at a concentration of 2 mg/mL in 0.05 M acetic acid and emulsified with CFA containing 4 mg/mL Mycobacterium tuberculosis (Chondrex, USA). For the induction of CIA, 8- to 10-week-old female non-transgenic and shCD5EμTg x (DBA _ B6) F_1 hybrid mice were immunized once at the base of the tail with 150 μg of collagen II in a final volume of 150 ml. Clinical evaluation of arthritis severity was performed as previously described in (López-Hoyos et al., 2003). For radiological studies, mice were anesthetized by *i.p.* injection of a mixture containing: 50 mg/Kg ketamine (Ketolar; Parke-Davis), 200 mg/Kg atropine sulfate (Braun Medical, Spain), and 4 mg/Kg diazepam (Roche, Spain). X-ray pictures were obtained using a CCX Rx ray source of 70 Kw with an exposure of 90 ms (Trophy Irix X-Ray System; Kodak, Spain). The radiological signal was digitalized with a Trophy RVG Digital Imagining system and analyzed using the Trophy Windows software. The severity of CIA was quantified radiologically with a graded scale according to the presence of five different radiological lesions (soft tissue swelling, juxtaarticular osteopenia due to alterations in bone density, joint space narrowing or disappearance, marginal erosions, and periosteal new bone formation). The extension of every individual lesion (local: affecting one digit or one joint in the carpus; diffuse: affecting two or more digits and/or two or more joints in the carpus) was graded from 0 to 1 as follows: 0, absence; 1/2, local; 1, diffuse. To clearly establish the radiological score in each paw, plain radiographs were assessed using a magnifying glass. Then, each paw was graded from 0 to 5, giving a maximum possible score of 20 for each mouse.

For shCD6LckEμTg mice evaluation, male mice at 8-12 weeks old were immunized once with 150 μg chicken collagen type II (CII; Chondrex) dissolved at a concentration of 2 mg/mL in 50 mM acetic acid and emulsified with CFA containing 4 mg/mL of Mycobacterium tuberculosis (Chondrex) in a final volume of 150 μL. The clinical score was determined weekly based on the following scale (**Table III.3**) evaluating each paw separately with a total value per mice of 12.

Table III.3. Common clinical signs of CIA and respective clinical score.

Clinical signals	Score
Non inflammation/Normal articulation	0
Detectable inflammation and/or erythema	1
>1 articulation inflamed	2
Paw inflamed and/or anchylosis	3

6.3.1. Anti-Collagen Type II Antibodies Analisis - Elisa

The levels of serum anti-collagen type II antibodies were evaluated by ELISA. To this end, ELISA plates (Maxisorb, Nunc) were sensitized o.n. at 4 °C with 1 µg/mL collagen type II (Immunization Grade Bovine Type II Collagen Solution, Chondrex, Inc) diluted in Tris-HCl 0.05 M pH 7.5 NaCl 0.2 M. After washing, the plate was blocked for 2 h. Again, the plate was washed and then 1:1000 serum dilutions were incubated for 3 h in duplicate. After washing the plate again, anti-mouse IgG_1 antibodies conjugated with alkaline phosphatase (Sigma) were incubated for 3 h. Then, the p-nitrophenyl phosphate (pNPP, ThermoFisher scientific) was added as substrate of the alkaline phosphatase and read at 405 nm wavelength with a Multiskan Fc equipment.

6.3.2. Cytokine mRNA Expression Analisis By RT-qPCR

When the mice were sacrificed, 8 weeks after collagen II immunization, the paws were stored at -80 °C to perform real time quantitative PCR (RT-qPCR). Total RNA was obtained by Trizol extraction method (Invitrogen, ThermoFisher Scientific) following the manufacturer's instructions. The concentration of RNA was determined by OD 260 nm with a Nanodrop 2000 (Thermo Scientific) spectrophotometer. For cDNA synthesis, the Super Script II reverse transcriptase kit (Invitrogen) was used starting from 5 µg of isolated RNA in a VERITI thermocycler (Applied Biosystems). From the cDNA obtained, RT-qPCR was performed using fluorescent TaqMan probes specific for *il-1β* (Mm00434228_m1), *il-6* (Mm00446190_m1), *il-17α* (Mm00439619_m1), *ifn-γ* (Mm00801778_m1), *tnf-α* (Mm00443258_m1), *tgf-β* (Mm00441724_m1), *il-10* (Mm01288386_m1), *il-2* (Mm00434256_m1) cytokines, and *tbet* (Mm00450960_m) and *foxp3* (Mm00475162_m1) transcription factors (Applied Biosystems). The TaqMan probe specific for GAPDH (Eurogentec) was used as control gene. The reaction mix had 1-2 µL of 250-500 ng cDNA, 11 µL of Premix Ex Taq (TAKARA), 1.1 µL of specific probe (Applied Biosystems), and 0.6 µL of *gapdh* plus sterile water to achieve a total volume of 22 µL. This mix was divided into duplicates of 10 µL in 96-well plates and sealed (Absolute QPCR Seal, Thermo Scientific). The reaction was performed in a MX3005P appliance (Stratagene) using the standardized

TaqMan amplification protocol. The results were analyzed with MxPro-3005P software using the ΔΔCt method, representing the relative gene expression of each protein normalized by the GAPDH expression.

6.4. ORTHOTOPIC AND NON-ORTHOTOPIC CANCER MODELS

We studied tumor growth induced by injection of isogenic cancer cell lines of different lineage origins.

6.4.1. Tumor Cell Lines

The B16-F0 melanoma tumor line comes from a solid tumor that arose spontaneously in C57BL/6 mice. B16-F0 cells were grown in DMEM media (Gibco Life Sciences) supplemented with 10 % inactivated FBS (Walkersville) and 100 IU/mL penicillin, 100 µg/mL streptomycin in a 5 % CO_2 atmosphere. The cells were kindly provided by Dr. Ramón Alemany (Institut Català d'Oncologia, L'Hospitalet de Llobregat, Spain).

The lymphoma RMA-S, sarcoma MCA-205 and thymoma EG7-OVA cell lines were grown in RPMI 1640 (Lonza, Switzerland) supplemented with 10 mM HEPES, 2 mM Glutamine, 10 % inactivated FBS, 0.05 mM β-mercaptoethanol, 1 mM sodium pyruvate and 100 IU/mL penicillin, 100 µg/mL streptomycin.

NK-sensitive YAC-1 cells were also used for some *in vitro* studies and were cultured in the RPMI medium described above.

Stocks from these cell lines were kept at -80 °C in inactivated FBS plus 10 % DMSO. To thaw them, warm culture medium was rapidly added to the cells in the cryotube in order to dilute the DMSO in contact with them. Then cells were centrifuged for 5 min at 1000 rpm and resuspended in the appropriate culture medium and conditions.

After the cells reached confluence, the adherent cells were trypsinized with a 1x trypsin (GIBCO, ThermoFisher) solution in PBS for 2 min at 37 °C; when cells detached, medium was added to neutralize trypsin and cells were centrifuged and resuspended in complete media. Non-adherent cells were counted, centrifuged, and diluted accordingly.

6.4.2. Induction Of Tumors By Subcutaneous Injection

To evaluate tumor growth differences between the different animal models studied, after optimizing the appropriate cell number for each model, cells were injected *s.c.* on the dorsum of mice anesthetized with Isoflurane (Esteve, Spain) using a 23G needle. Every other day the tumor growth *in vivo* was assessed with a Vernier caliper (Sigma-Aldrich, Scienceware) and its diameter or area calculated (measuring the largest and smallest diameter and calculating the mean diameter or multiplying the two measurements

obtaining the area). Upon reaching a certain area (200-400 mm^2) the mice were euthanized with Isoflurane and the tumors extracted, weighed (WNT-500, Coventry Scale) and kept at -80 °C for further studies (cytokine analyses) or processed for flow cytometry analysis. In some studies, the tumor draining (TdLN) and contralateral (cLN) lymph nodes were also extracted for further analysis.

To validate the results obtained with Tg mice, WT mice were treated with rshCD5 or rshCD6 protein (PX'Therapeutics, France). To do so, two groups of WT mice were injected *s.c.* or *i.p.* with 1.25 mg/Kg of protein or vehicle per mouse in 200 µL every 48 h from day 0 of B16-F0 *s.c.* cell injection. Alternatively, different protein doses were administrated *i.p.* or *s.c.* (peritumoraly, *p.t.*) when the tumor was palpable (around day 10 after cell injection) every 48 h until the end of the experiment.

In the cases we had to move the mice from a SPF facility (where they were breed) to a conventional facility, to analyze the tumor growth, the mice stayed between 1 and 2 weeks acclimatizing before start any manipulation.

6.4.3. NK Cell Depletion

Depletion of NK cells was achieved by *i.p.* administration of one 200 µg dose of rat NK1.1-PK136 mAb (BioXCell) when tumors reached approximately 2 mm^2, then two consecutive doses 100 µg the following two days and next 100 µg every 48 h. Control mice were administered with the same doses of rat IgG_{2a} isotype control. Protein treatment began on the third day post-NK depletion. Tumor tissue was dissected to determine the tumor weight (**Fig. III.6**).

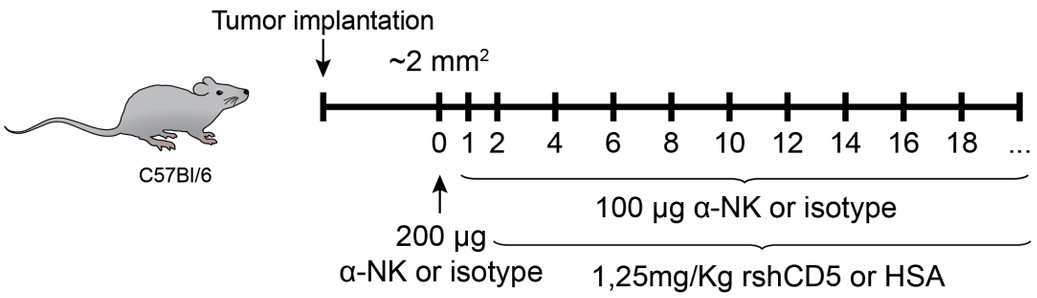

Fig. III.6 – Schematic representation of the NK depletion protocol in WT-bearing tumor rshCD5-treated mice.

In the case of Tg and Non-Tg mice, the first dose of 200 µg NK1.1-PK136 was administered two days before the tumor cell injection, followed by 100 µg NK1.1-PK136 mAb administration the two following days and then every 48 h until the end of the experiment (**Fig. III.7**).

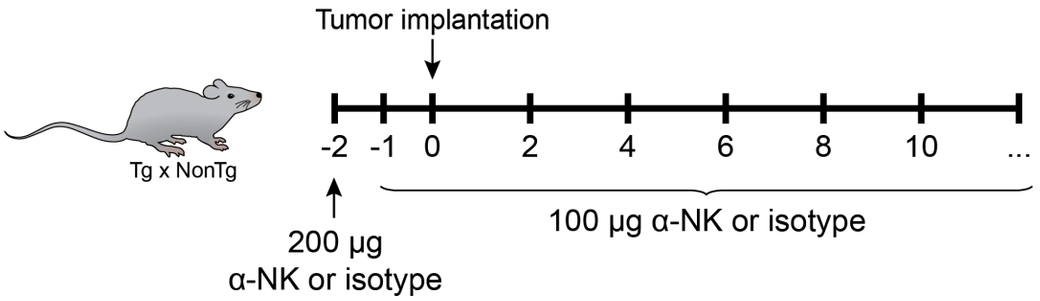

Fig. III.7 – Schematic representation of the NK depletion protocol in rshCD5Tg-tumor bearing mice.

6.4.4. Tumor Metastasis Induction By Intravenous Injection

To analyze the differences between the Tg and Non-Tg mice in an experimental metastasis assay, 1 x 10^5 B16-F0 cells were injected intravenously (*i.v.*) in the tail. After 15 days the mice were sacrificed and the lungs harvested in order to count the visible metastasis in the surface of the organ.

6.4.5. Effect Of rshCD5 And rshCD6 Injection As An Adjuvant To Immunotherapy Or Chemotherapy

To evaluate the combined treatment of rshCD5 with anti-mouse CTLA-4, mice were injected *s.c.* at day 0 with 5 x 10^4 B16-F0 tumor cells. Two days later, hamster anti-mouse CTLA-4 (9H10, Bio X Cell) treatment begun; 75 µg per mice were injected *i.p.* four times with 72 h interval between each time. The same amount of isotype control was injected in the control group (IgG_1, Bio X Cell). When tumors reached approximately 3 mm^2, rshCD5 protein treatment begun and was administered every 48 h until the end of the experiment. The tumor growth was monitored and at the final point the mice euthanized.

To evaluate the effect of rshCD5 and rshCD6 as an adjuvant to chemotherapy, two groups of WT mice were injected *s.c.* at day 0 with tumor cells and, from this day until the end of the experiment, injected *i.p.* with 1.25 mg/Kg of protein in 200 µL or vehicle per mouse every 48 h. On the third day they also received a single dose of Vincristine (1 mg/Kg; Pfizer, USA) plus Doxorubicin 3.3 mg/Kg (Pfizer, USA) or Doxorubicin (3.3 mg/Kg) alone, depending on the tumor type. The tumor growth was monitored and at the final point the mice euthanized and samples stored for further studies.

6.4.6. Measurement Of Cytokine Levels In Tumor Extracts By Elisa

As described before, tumor samples were preserved at -80 °C in order to analyze their cytokine profile. The protocol used was based on a previously reported method (Matalka, Tutunji, Abu-Baker, & Abu Baker, 2005). Murine IL-1β, IL-6, IL-10, IFN-γ and TNF-α were analyzed for each sample. The tumors were homogenized with a tissue

disrupter (1 mL Dounce Tissue Grinder, Wheaton, USA) in a solution of PBS-0.1 % NP40 plus 1x protease inhibitors (Complete, Roche). After centrifugation at 5000 rpm for 15 min at 4 °C, 100 µL of undiluted supernatant samples were analyzed according to the manufacturer's instructions (Mouse ELISA Set, BDOptEIA, BD Biosciences). The ELISA standard curves were performed in Microsoft Office Excel.

6.4.7. Intratumoral And LN Cytokyne Measurement By RT-qPCR

Messenger RNA was extracted from tumor and lymph node samples stored at -80 °C by adding 1 mL of TRIzol (Invitrogen) and homogenizing the tissue with a sterile pipette tip in order to lyse the cells. Then 200 µL of chloroform (AnalaR NORMAPUR) were added and incubated at RT for 3 min. The samples were centrifuged 15 min at 4 °C and 12,000 g and the upper phase formed (containing RNA) transferred to a new eppendorf that contained the same volume of 70 % ethanol (Panreac), stirring to dissolve precipitates (35 % final concentration of ethanol). To purify the extracted RNA, the PureLink RNA Mini Kit (Ambion, Life technologies) was used according to manufacturer's instructions. The purified RNA was quantified with an Epoch (Gen5 1.09, BioTek) at a wavelength of 260 nm and 280 nm. RNA purity was calculated with the 260/280 nm quotient, with samples being studied only when the purity quotient was close to 2.

Complementary DNA was obtained using the High capacity cDNA kit (Life technologies) retrotranscriptase according to the following conditions: 1 cycle of 10 min at 25.5 °C and 2 consecutive cycles of 60 min at 37 °C, storing the samples at 4 °C or -20 °C if stored for more than 1 week until performing the quantitative real-time PCR (qPCR). Gene expression of *il-6* (Mm01210733_m1), *il-22* (Mm01226722_g1), *il-10* (Mm01288386_m1), *ifn-γ* (Mm01168134_m1) and *foxp3* (Mm00475162_m1) were determined with specific Taqman probes (Life Technologies/ThermoFisher). For this, 2 µL of cDNA, 2.5 µL of distilled water, 5 µL of Master Mix (Taqman Fast universal PCR master Mix, Life Technologies) and 0.5 µL of primer/probe for each gene analyzed were mixed. To determine the gene expression, we used Ct values inferior or equal to 30 cycles. The results were normalized with the expression values of the non-inducible gene Glyceraldehyde-3-phosphate dehydrogenase (*gapdh*, Mm99999915_g1, Life Technologies/ThermoFisher), using the 2ΔCt formula, where ΔCt=Ct (desired gene)-Ct (GAPDH). The results are represented as percentage or relative quantity.

6.4.8. NK Cytotoxicity Assays

Total splenocytes were obtained in suspension and erythrocytes lysed with Red Blood cell lysis buffer (eBioscience). Tumor cells (B16-F0, EG7-OVA and RMA-S) were irradiated (2,000 gamma radiation, Hematology Unit of Clínic Hospital, Barcelona) and seeded in a round bottom 96-well plate (5 x 10^4 cells per well) in RPMI 1640 supplemented with

antibiotics but no FBS. Splenocytes from tumor-bearing mice were then seeded on top of the tumor cells at 50:1, 25:1 and 12.5:1 ratios and incubated for 5 h. Cell lysis was measured using the CytoTox-ONE™ Homogeneous Membrane Integrity Assay (Promega) according to manufacturer's instructions. Plates were read with a microplate luminometry reader (Bio-TEK). Percentage of relative lysis was calculated as follows: % specific cytotoxicity = [experimental lysis - spontaneous lysis]/[maximal lysis - spontaneous lysis] × 100.

6.4.9. *In Vitro* IFN-γ Measurement In Re-Stimulation Assays

To evaluate *in vitro* IFN-γ production, we co-cultured 2 x 10^5 tumor draining lymph node or contra-lateral lymph node cells from a single cell suspension with 2 x 10^4 EG7-OVA or YAC-1 irradiated cells, 10 µg of OVA protein (Endograde) or 5 µg of SIINFEKL ($OVA_{257-264}$ peptide: H-Ser - Ile - Ile - Asn - Phe - Glu - Lys - Leu – OH, Sigma) specific peptide 37 °C and 5 % CO_2. The supernatant was recovered after 48 h of incubation and IFN-γ was detected by ELISA kit as described previously.

6.4.10. Microbiome Study: Next-Generation Sequencing

Fecal samples from shCD5EµTg (n = 5) and Non-Tg (n = 4), and shCD6LckEµTg (n = 4) and Non-Tg (n = 4) mice, respectively, were collected immediately upon defecation from each mouse at baseline and stored at −80 °C. The first samples were collected when the mice were in the SPF facility. In the case of the shCD5EµTg, samples were also collected at different time points (2, 7, 14, and 30 days) after being moved to the conventional facility. Fecal DNA was extracted by using the E.Z.N.A Soil DNA Kit (Omega Bio-tek, Norcross, U.S.) according to the manufacturer's protocols. In collaboration with Dr. Jose González and Dr. Eduardo Huarte (South Dakota State University), the fecal samples were sequenced and analyzed. A 16S rRNA sequencing library was constructed according to the 16S metagenomics sequencing library preparation protocol (Illumina, San Diego, CA, USA) targeting the V3 and V4 hypervariable regions of the 16S rRNA gene. 16S ribosomal RNA (rRNA) sequencing is an amplicon-based sequencing method that targets a genetic marker found in all bacteria. It is commonly used to identify bacteria present within a given sample down to the genus and/or species level. 16S rRNA gene sequencing is a well-established method for studying phylogeny and taxonomy of samples from complex microbiomes or environments that can be difficult to study. Microbial genomic data were analyzed with CLC Genomics Workbench version 10.1, Microbial Genomics Module (QIAGEN Bioinformatics).

7. RETROSPECTIVE ANALYSIS OF DATA FROM THE CANCER GENOME ATLAS DATABASE

A retrospective analysis was carried out in human cancer data from "The Cancer Genome Atlas" (TCGA) database already pre-selected by the group of Dr. Yvonne Saenger (Hematology/Oncology, New York-Presbyterian - Columbia University Medical Center, New York). The database consisted of 409 melanoma tumor samples (biopsies) with the following information for each sample: gender, age, dead/alive status, days from diagnostic, submitted tumor site (distant metastasis, primary tumor, regional cutaneous or subcutaneous tumor, regional lymph node), presence/absence of tumor on last medical appointment, and gene expression data of 626 genes.

From these data, we defined two groups:

- Alive – being alive for more than 4 years (1,460 days) from day of diagnosis (n = 74);
- Dead – being dead less than 2 years (730 days) from diagnosis (n = 49).

From the previous "Alive" group, we obtained two other groups:

- With tumor: information from last follow-up (n = 16);
- Without tumor: information from last follow-up (n = 58).

In all groups, we analyzed the expression levels of the following genes: *CD3δ, CD3ε, CD4, CD8α, CD8β, CD19, CD6, CD5,* and *ALCAM*.

8. STATISTICAL ANALYSES

In this thesis the graphs and statistical analysis were performed using GraphPad PRISM 5.03 software. To compare the different groups studied the unpaired *T-student, Mann-Whitney* or the *A-NOVA* test were used as appropriate. Results are expressed as mean ± SD or mean ± SEM, always indicating in the graph which one is represented. Statistical significance was set at $p \leq 0.05$ and is represented as *-$p<0.05$; **-$p<0.01$ and ***-$p<0.001$.

IV. RESULTS

1. ANALYSIS OF THE IMMUNOMODULATORY PROPERTIES OF SOLUBLE HUMAN CD5 EXPRESSION

1.1. PHENOTYPICAL CHARACTERIZATION OF HETEROZYGOUS MICE FOR TRANSGENIC EXPRESSION OF SOLUBLE HUMAN CD5 (shCD5EμTg)

In an attempt to investigate the *in vivo* relevance of the receptor-ligand interactions mediated by CD5, our group generated a transgenic mouse line (shCD5EμTg) expressing a soluble form of human CD5 (shCD5, from initiation Met1 to Pro346) under the transcriptional control of the ubiquitous SV40 promoter and the B-cell specific immunoglobulin μ heavy chain enhancer (Eμ) (**Fig.IV.1a**). The transgene was injected into fertilized eggs of CBAxC57BL/6 mixed background and the founder mice were backcrossed into the C57BL/6 background for more than 10 generations. These mice showed no physical (weight, size, temperature), nor behavior (mobility, mating, cycles) abnormality. Mice housing was performed in a SPF facility and experiments in a conventional facility, after 1 to 2 weeks of acclimation.

To identify transgene carriage in each new litter, genomic DNA was extracted from the tail or ear tissue samples and amplified by PCR using specific primers (described in the Materials and Methods section). A fragment of 450 bp, for the extracellular region of human CD5, and another of 150 bp, PCR internal control (MHC class II-associated invariant chain) were amplified in the screening (**Fig.IV.1b**). In the case of Non-Tg mice, only the internal control was amplified. To confirm that the rshCD5EμTg mice produced shCD5 and that the protein could be found in serum, two different analyses were performed. First, sandwich ELISA assay showed that serum levels of shCD5 expressed by shCD5EμTg mice were in the 10–80 ng/mL range (**Fig.IV.1c**). Further confirmation on the transgenic expression of shCD5 was obtained from the demonstration that shCD5EμTg mice were poorly reactive (tolerant) to specific immunization with purified rshCD5 protein, but not to rshCD6 (a highly homologous protein) compared with non-transgenic (Non-Tg) mice, which were equally highly responsive to immunization with rshCD5 or rshCD6 (**Fig.IV.1d**).

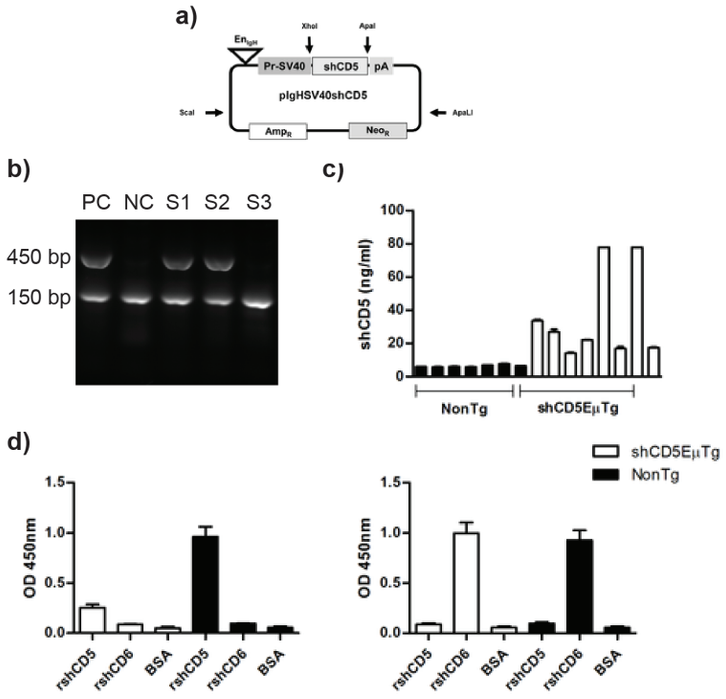

Fig.IV.1 - Generation of shCD5EμTg mice. **a)** Schematic representation of the transgene coding for shCD5 expression under the transcriptional control of the SV40 promoter and the immunoglobulin μ heavy chain enhancer (Eμ). **b)** Identification of shCD5EμTg mice by PCR from tail/ear DNA. A 450 bp PCR product was detected in transgenic mice. A fragment of 150 bp corresponding to the LIEX gene was also amplified as an internal control for the PCR (PC – positive control, NC – negative control, S1-3 – sample 1 to 3). **c)** ELISA detection of rshCD5 in sera from shCD5EμTg mice (shCD5EμTg, white) and Non-Tg mice (Non-Tg, black) mice by sandwich ELISA using Cris-1 and biotin-labeled Leu-1 as capture and developing mAbs, respectively. A standard rshCD5 curve was also analyzed in parallel to quantify results. **d)** shCD5EμTg mice and Non-Tg mice were immunized twice with 25 μg of rshCD5 (**left panel**) or rshCD6 (**right panel**) in Freund's adjuvant (complete and incomplete, sequentially) within a 3-week interval. Mouse sera were collected 2 weeks after the boosting and added to ELISA plates coated with purified rshCD5, rshCD6 or BSA, then developed with a HRP-labeled anti-mouse IgG. Values represent the mean OD 450 nm values ± SD obtained in triplicate determinations for each sample (5 mice per group).

Next, phenotypical studies on the main immune cell populations in central and peripheral lymphoid organs were performed. No differences were observed between shCD5EμTg and Non-Tg mice regarding total cell numbers in spleen, thymus, bone marrow (BM), and lymph nodes (LN). By contrast, significantly higher total cell numbers were detected in peritoneal cavity from shCD5EμTg (**Fig.IV.2a**). Further analysis of different T cell developmental stages (DN1 to DN4, DP, $CD4^+$SP, $CD8^+$SP) from thymus did not show any gross differences in percentages compared to Non-Tg mice (**Fig.IV.2b**). A similar scenario was observed with the major T cell subsets ($CD4^+$ and $CD8^+$) from secondary lymphoid organs (LN and spleen) (**Fig.IV.2c**).

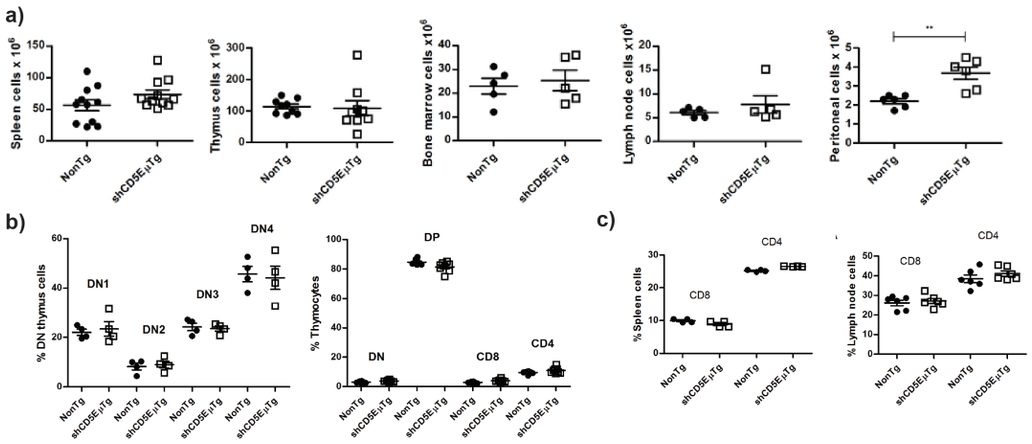

Fig.IV.2 - Analysis of total cell number and percentages of T-cell subsets from central and peripheral lymphoid organs of shCD5EμTg and Non-Tg mice. **a)** Total number of mononuclear cells in spleen (n = 11 mice per group), thymus (n = 8 mice per group), BM (n = 5 mice per group), LN (n = 5 mice per group) and peritoneal lavage (n = 6 mice per group). **b)** Percentage of DN1 ($CD44^+CD25^-$), DN2 ($CD44^+CD25^+$), DN3 ($CD44^-CD25^+$) and DN4 ($CD44^-CD25^-$) thymocytes (n = 4 mice per group) (**left panel**). Percentage of DN, DP, $CD4^+$SP and $CD8^+$SP thymocytes (n = 5 mice per group) (**right panel**). **c)** Spleen (n = 4 mice per group) (left) and LN (n = 5 mice per group) (**right panel**) $CD4^+$SP and $CD8^+$SP cells. Values are represented as mean ± SEM. **p<0.01 by unpaired *t*-test.

Regarding B-cell developmental stages in the BM (Pro/pre-B, early pro-B, pro-B and pre-B cells), also no significant differences were found between shCD5EμTg and Non-Tg mice (**Fig.IV.3a**). In spleen, a significant decrease in the percentage of the transitional 1 (T1, $IgM^{hi}IgD^{lo}CD93/AA4^+CD23^-$) and 2 (T2, $IgM^{hi}IgD^{lo}CD93/AA4^+CD23^+$) cells as well as an increase in marginal zone (MZ, $IgM^{hi}IgD^{lo}CD93/AA4^{lo}CD23^-$) B cells in shCD5EμTg mice compared with Non-Tg mice was detected (**Fig.IV.3b**). No significant differences were observed between shCD5EμTg and Non-Tg mice regarding the transitional 3 (T3, $IgM^{lo}IgD^{hi}CD93/AA4^+CD21^+$), follicular I (FOLI, $IgM^{lo}IgD^{hi}CD93/AA4^{lo}CD21^+$), follicular II (FOLII, $IgM^{hi}IgD^{hi}CD93/AA4^+CD21/35^{lo}$) and MZ precursor (MZP, $IgM^{hi}IgD^{hi}CD93/AA4^+CD21/35^{hi}$) cells (**Fig.IV.3c**).

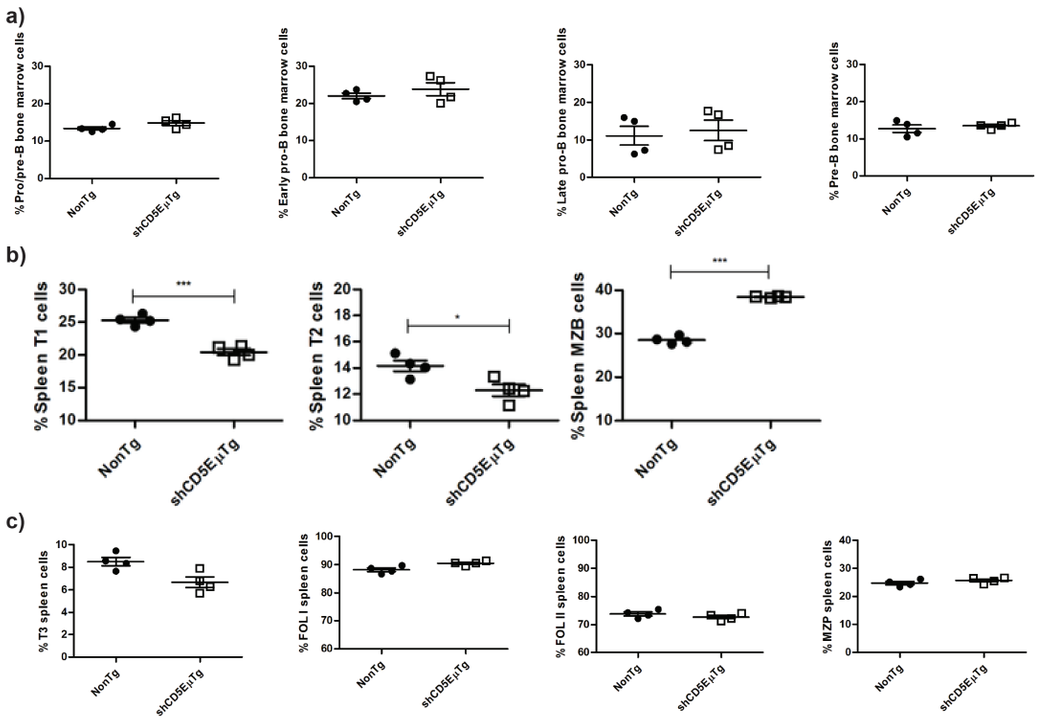

Fig.IV.3 - Analysis of B-cell subsets from central and peripheral lymphoid organs of shCD5EμTg and Non-Tg mice. **a)** BM cell subpopulations within $CD43^{+}B220^{+}$ subpopulation: pre-pro-B cells ($CD24^{lo}BP\text{-}1^{-}$), early pro-B cells ($CD24^{+}BP\text{-}1^{-}$), late pro-B cells ($CD24^{+}BP\text{-}1^{+}$) and pre-B cells ($CD24^{hi}BP\text{-}1^{+}$). **b)** Percentage of T1, T2 and MZ B-cell subsets from spleen. **c)** Percentage of T3, FOLI, FOLII, and MZP B-cell subsets from spleen. Values (n = 4 mice per group) are represented as mean ± SEM. *p<0.05; ***p<0.001 by unpaired *t*-test.

In the case of peritoneal cavity, a significant decrease in the percentage of B1a cells ($B220^{+}IgM^{hi}IgD^{lo}CD5^{+}$) and a smaller, albeit significant, increase in the percentage of B1b cells ($B220^{+}IgM^{hi}IgD^{lo}CD5^{-}$) and no differences in mature B2 cells ($B220^{+}IgM^{hi}IgD^{hi}CD5^{-}$) were observed (**Fig.IV.4**).

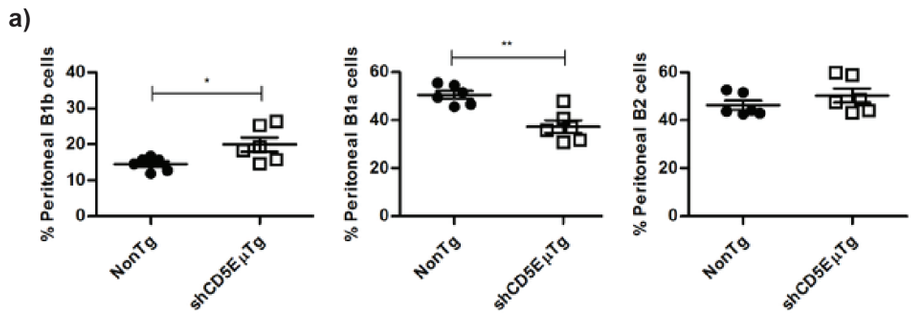

Fig.IV.4 - Analysis of B-cell subsets from peritoneal cavity of shCD5EμTg and Non-Tg mice. Percentage of B1a, B1b and B2 cells (n = 6 mice per group). Values are represented as mean ± SEM. *p<0.05; **p<0.01 by unpaired *t*-test.

The analysis of regulatory/suppressor B (B10 or B_{reg}) and T (T_{reg}) cell subsets showed that B_{reg} cells ($B220^{+}CD1d^{hi}CD5^{+}IL10^{+}$) were reduced both in peritoneal cavity and spleen (**Fig.IV.5a**) from shCD5EμTg mice compared with Non-Tg ones. In the T_{reg} case ($CD4^{+}CD25^{+}FoxP3^{+}$), no differences were observed in the thymus, while a significant reduction in their percentage was observed in LN from shCD5EμTg mice (**Fig.IV.5b**).

Interestingly, the percentage of NKT ($NK1.1^{+}CD3^{+}$) cells was increased in the spleen of shCD5EμTg mice (**Fig.IV.5c**). Overall, the data indicate that shCD5EμTg mice present alterations in different regulatory cell subpopulations, which could have important functional consequences for the immune response of these mice.

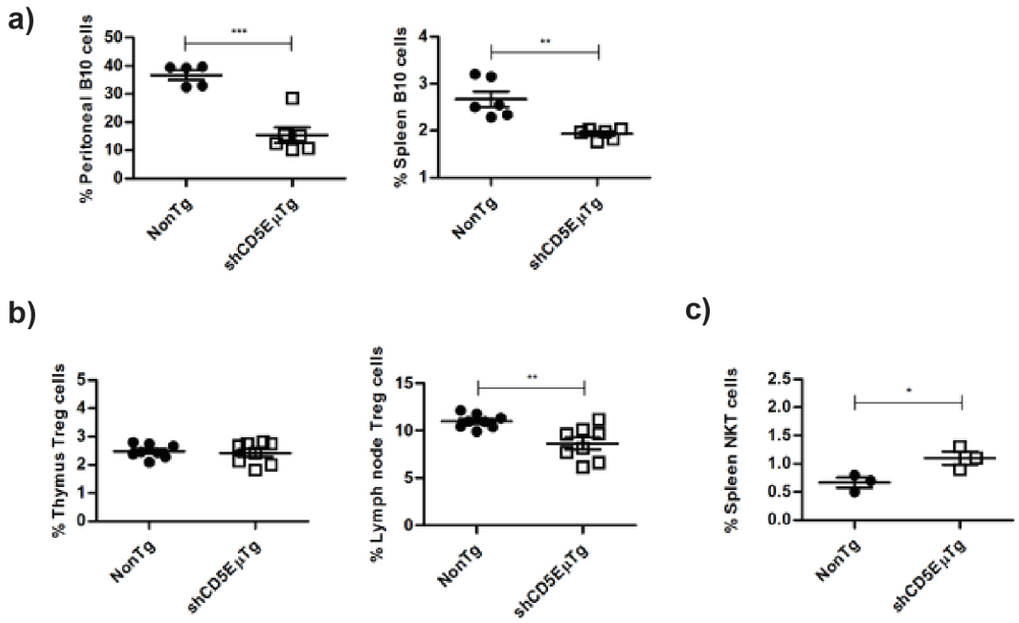

Fig.IV.5 – Analysis of regulatory T- and B-cell subsets from central and peripheral lymphoid organs of shCD5EμTg and Non-Tg mice. **a)** Percentage of peritoneal cavity and spleen B_{reg} cells (n = 6 mice per group). **b)** Percentage of thymus and LN T_{reg} cells (n = 8 mice per group). **c)** Percentage of spleen NKT cells (n = 3 mice per group). Values are represented as mean ± SEM. *p<0.05; **p<0.01; ***p<0.001 by unpaired *t*-test.

1.2. CHARACTERIZATION OF IMMUNOPHENOTYPICAL CHANGES INDUCED BY SUSTAINED INFUSION OF EXOGENOUS RSHCD5 PROTEIN TO WT MICE

At this point, the possibility that the phenotypical changes found in the shCD5EμTg mice were due to increased circulating levels of shCD5 rather than to random transgenesis events needed to be ruled out. To do so, similar cell analyses were performed on wild-type (WT) C57BL/6 mice treated with repeated *i.p.* infusions of purified rshCD5 or BSA protein (1.25 mg/kg, every other day for 2 weeks). As shown in **Fig.IV.6a**, B1a and B_{reg} cells were significantly reduced in the peritoneum, but not in the spleen of rshCD5-treated mice compared with BSA-treated control mice. In addition, T_{reg} cells were found significantly reduced in the spleen but not in LN of WT mice injected with rshCD5 (**Fig.IV.6b**). Finally,

spleen NKT cells were significantly increased in rshCD5-treated mice (**Fig.IV.6c**). These data indicate that repeated infusion of WT mice with exogenous rshCD5 can induce similar phenotypical changes to those observed in shCD5EμTg mice, unequivocally ascribing the effects of transgenesis to the presence of circulating rshCD5.

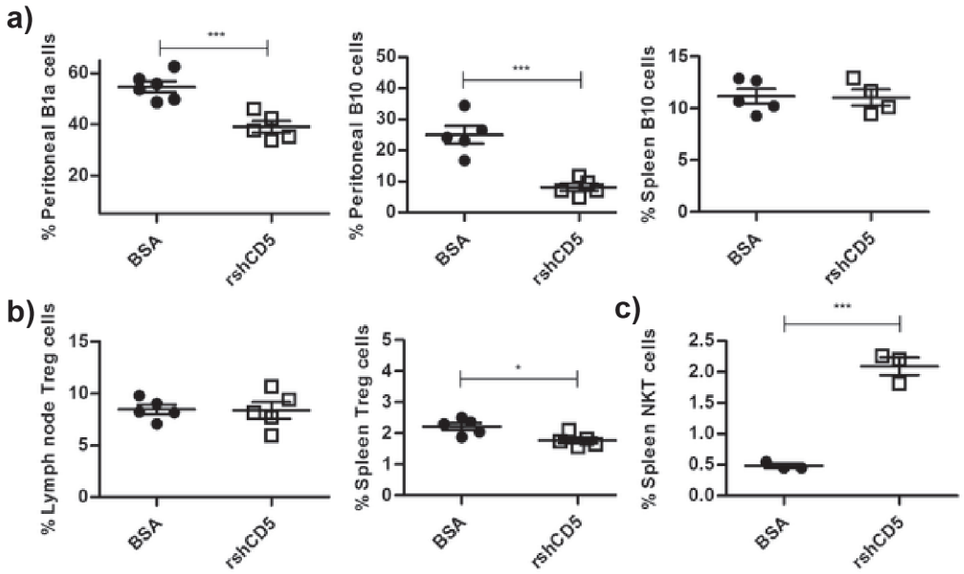

Fig.IV.6 - Analysis of different T and B cell subsets from peripheral lymphoid organs of WT C57BL/6 mice treated with exogenous rshCD5 or BSA proteins. **a)** Percentage of B1a and B_{reg} cells from peritoneal lavage and spleen of WT mice (n = 5 mice per group) *i.p.* treated with exogenous rshCD5 or BSA (25 μg every 48 h for 14 days). **b)** Percentage of LN and spleen T_{reg} cells from the same mice groups as in a). **c)** Percentage of spleen NKT cells (n = 3 mice per group) from the same mice groups as in a). Values are represented as mean ± SEM. *p<0.05; ***p<0.001 by unpaired *t*-test.

1.3. FUNCTIONAL CHARACTERIZATION OF HETEROZYGOUS shCD5EμTg MICE

In order to further explore the *in vivo* functional consequences of the immune-phenotypical changes observed in shCD5EμTg mice, they were subjected to different experimental immune-challenge models.

1.3.1. Humoral Response To TD And TI Antigens

To further evaluate the *in vivo* functional consequences of the lymphocyte subset alterations observed in shCD5EμTg mice the humoral responses to different T-dependent (TD) and –independent (TI) antigens were first analyzed. To this end, shCD5EμTg and Non-Tg mice were immunized *i.p.* with the trinitrophenol (TNP) hapten conjugated to TD (keyhole limpet hemocyanin; TNP_5-KLH), TI type 1 (TI-1; $TNP_{0,3}$-LPS) or TI type 2 (TI-2; TNP_{65}-Ficoll) antigens, and the serum levels of specific anti-TNP antibodies analyzed by ELISA. Regarding the TD response, shCD5EμTg mice showed significantly

higher IgG_1 titers at day 21 post-immunization (**Fig.IV.7a**). Regarding the TI-1 response, significantly higher antibody titers were observed at nearly all time points for all the Ig isotypes tested in shCD5EμTg mice compared with Non-Tg controls (**Fig.IV.7b**). By contrast, the antibody titers in mice immunized with TI-2 antigen did not differ between shCD5EμTg and Non-Tg mice at all time points, for all the different Ig isotypes analyzed (**Fig.IV.7c**). These results suggest that the B-cell antibody responses against TI-1 antigens and, to a lesser extent, against TD antigens are enhanced in shCD5EμTg mice compared with that of Non-Tg ones.

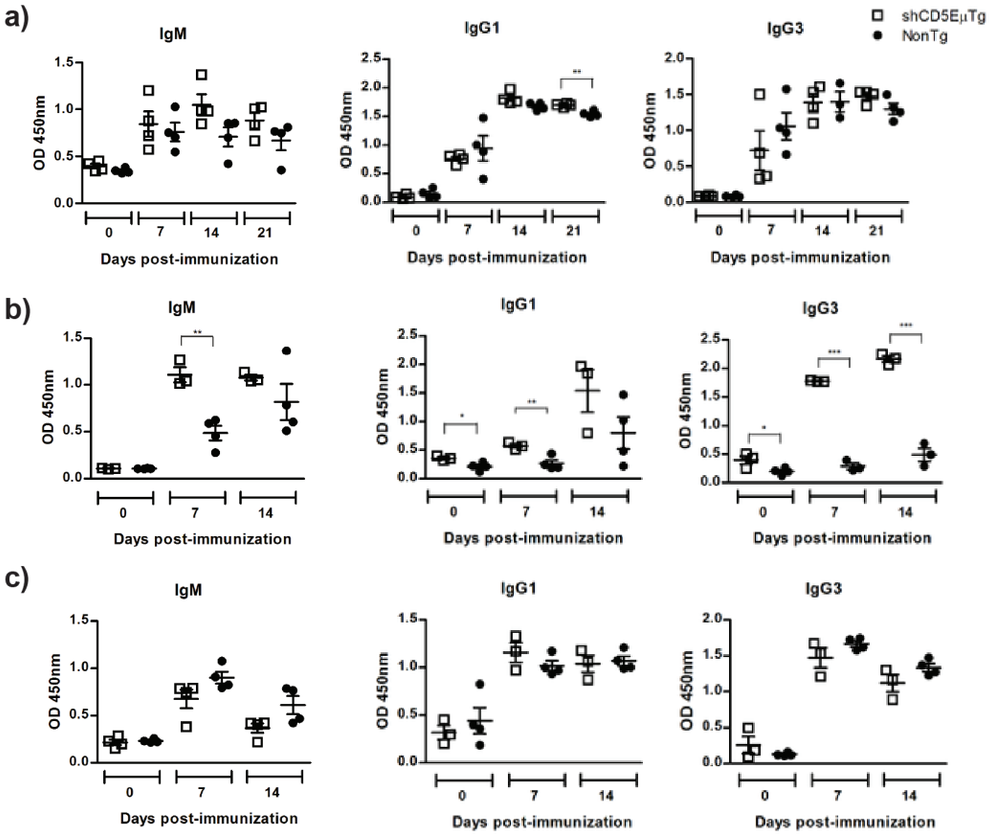

Fig.IV.7 – Analysis of humoral responses of shCD5EμTg and Non-Tg mice to TD and TI antigens. Mice were immunized *i.p.* with **a)** 50 μg TNP_5-KLH (TD) (n = 4 mice per group), **b)** $TNP_{0.3}$-LPS (TI-1) (n = 4 mice per group) or **c)** TNP_{65}-Ficoll (TI-2) (n = 4 mice per group), and their sera collected 0, 7, 14 or 21 days later for further quantitation of TNP-specific IgM, IgG_1 and IgG_3 antibody levels by ELISA. Values are expressed as OD 450 nm reads. The bars represent the average value for each group. *p<0.05; ** p<0.01; ***p<0.001 by unpaired *t*-test.

1.3.2. Autoimmune Disease Models

1.3.2.1. Collagen-Induced arthritis model

Next, to gain insight into the *in vivo* immune response of shCD5EμTg mice to auto-antigens, two different models of experimentally induced autoimmune disease were evaluated. First, we studied a collagen-induced arthritis model (CIA) in B6×DBA/1 F_1 mice, a well-established model of T-cell mediated autoimmune disease resembling human Rheumatoid Arthritis (RA). As shown in **Fig.IV.8a**, increased severity of arthritis symptoms (oedema, joint narrowing, marginal erosion, osteopenia) was observed in shCD5EμTg mice compared Non-Tg mice. Moreover, IL-6 levels were significantly increased in joint tissue from shCD5EμTg mice, while a trend towards increased levels of other pro-inflammatory cytokines (IFN-γ, IL-1β, IL-17 and TNF-α) was observed (**Fig. IV.8b**). Total anti-collagen II antibody levels were also increased in the sera of shCD5EμTg tce, mostly of the IgG_2 subtype, (**Fig.IV.8c**), characteristic of an enhanced T_H1 response.

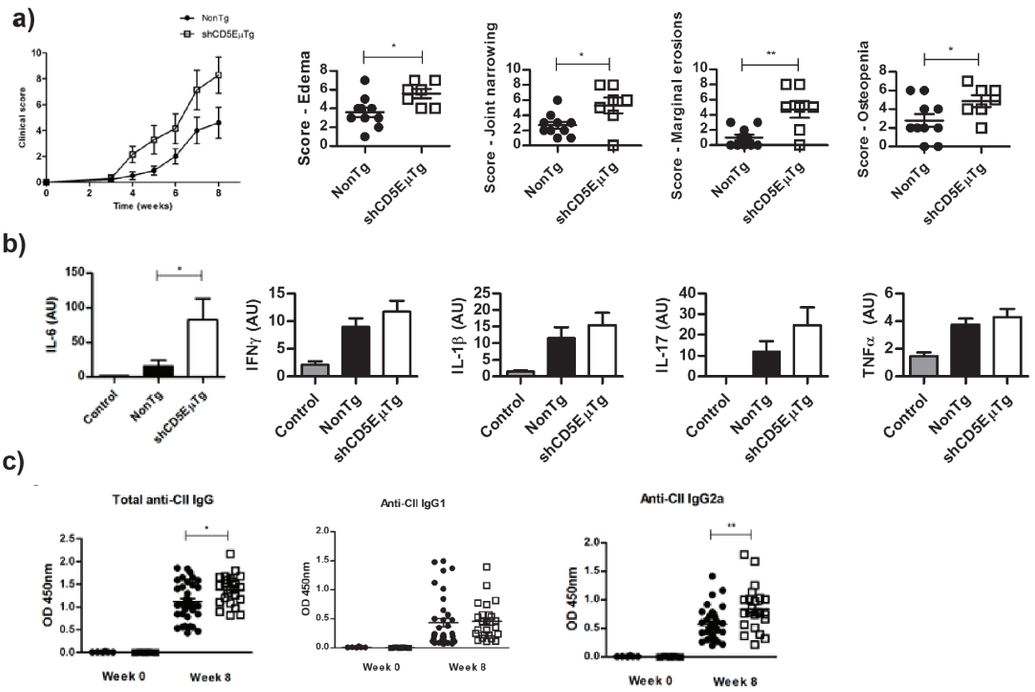

Fig.IV.8 - Exacerbated CIA disease in shCD5EμTg mice. **a)** CIA was induced in 7–8 week old (DBA_B6) F_1 × shCD5EμTg (n = 7) and Non-Tg mice (n = 10) by *s.c.* immunization near the base of the tail with type II bovine collagen emulsified in CFA plus Arthrogen-CIA adjuvant. Radiological signs were scored weekly for each mouse and results for each group averaged to determine overall clinical score. Radiological signs (oedema, joint narrowing, marginal erosions and osteopenia) were scored at week 8 for each mouse. **b)** Cytokine mRNA levels were determined by RT-qPCR in joint tissue, normalizing results to GAPDH expression levels. Results are expressed in arbitrary units (A.U.). **c)** Total IgG and IgG_1 and IgG_{2a} antibodies against type II collagen were measured by ELISA in sera from both groups of mice collected at weeks 0 and 8. Results are expressed as OD 450 nm. *p<0.05; ** p<0.01 by Student's *t*-test.

1.3.2.2. Experimental Autoimmune Encephalomyelitis model

The other model studied was the Myelin Oligodendrocyte Glycoprotein (MOG)-induced model of experimental autoimmune encephalomyelitis (EAE), a well-established model of T-cell mediated autoimmune disease resembling human Multiple Sclerosis (MS). As shown in **Fig.IV.9a**, the clinical score of the disease was significantly increased in shCD5EμTg mice compared with Non-Tg mice. Moreover, demyelination was also significantly increased in shCD5EμTg mice (**Fig.IV.9b**). Altogether, the data show that shCD5EμTg mice display more severe forms of experimentally induced autoimmune disease in models developed against different auto-antigens.

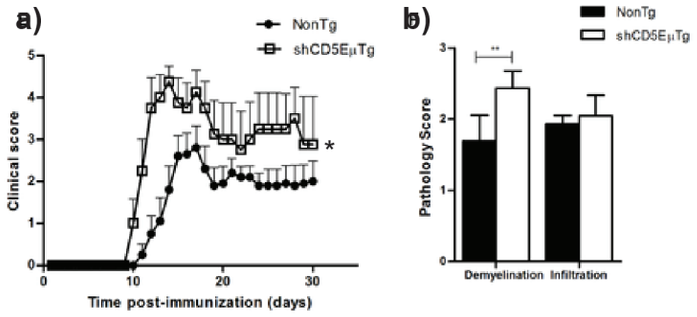

Fig.IV.9 - Exacerbated EAE disease in shCD5EμTg mice. **a)** EAE was induced in 8–10 week old shCD5EμTg mice by *s.c.* administration of MOG peptide emulsified in CFA. At the time of immunization and 48 h later, Pertussis toxin was also injected *i.p.* The graph shows the clinical score of shCD5EμTg (n = 5) and Non-Tg mice (n = 10). * p=0.05 by ANOVA test. **b)** Demyelination and infiltration scores, as detected by solochrome cyanin and hematoxylin and eosin staining, respectively. ** p<0.02, by Student's *t*-test.

1.3.3. Cancer Models

1.3.3.1. Characterization Of The Anti-Tumor Immune Response Of Heterozygous shCD5EμTg Mice

Since autoimmune and anti-tumoral immune responses are flip sides of the same coin, we decided to evaluate the *in vivo* response of shCD5EμTg mice to autologous tumor cells. A melanoma B16-F0 cell model (syngeneic with C57BL/6 mice) was chosen, and tumor growth was measured over time. As shown in **Fig.IV.10a**, B16-F0 tumors grew significantly more slowly in shCD5EμTg mice compared with their Non-Tg controls. Taking these data into account, a potentially improved response of shCD5EμTg mice to *i.v.* injected B16-F0 cells was also evaluated. Experimental metastasis assays revealed a decrease in the number of lung metastases observed in shCD5EμTg mice compared with Non-Tg ones (**Fig.IV.10b**), which was close to significance (p=0.09). Finally, to evaluate whether administration of exogenous rshCD5 protein to WT mice could also delay tumor growth, WT C57BL/6 mice *s.c.* implanted with B16-F0 cells were treated with vehicle (PBS + glycerol) or rshCD5 (1.25 mg/kg) every 48 h from the day of tumor cell injection.

A single dose of chemotherapy (0.5 mg/kg vincristine plus 3.3 mg/kg doxorubicin) was also administered at day 3 after tumor cell injection in both groups. As shown in **Fig. IV.10c**, tumor progression was slowed in mice treated with chemotherapy plus rshCD5, compared with mice treated with chemotherapy plus vehicle. Altogether, these results suggest that increased circulating levels of rshCD5 delay progression of melanoma cells in mouse tumor models.

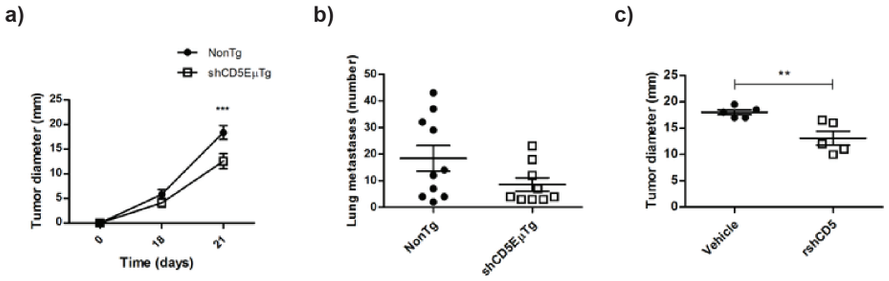

Fig.IV.10 – Enhanced anti-tumoral response to syngeneic melanoma cells in shCD5EμTg mice. **a)** shCD5EμTg (n = 16) and Non-Tg mice (n = 15) were injected *s.c.* with 5×10^4 B16-F0 melanoma cells and tumour growth recorded over time. **b)** Experimental metastasis assay. shCD5EμTg (n = 10) and Non-Tg mice (n = 9) mice were injected *i.v.* with B16-F0 melanoma cells (1×10^5) and 15 days later sacrificed and their lungs removed for counting of surface metastases. **c)** WT C57BL/6 mice (n = 5 for each group) were injected with 5×10^4 B16-F0 cells as before and then rshCD5 (25 μg) or vehicle was injected *i.p.* every 48 h for the whole duration of the experiment (20 days). A single dose of vincristine plus Doxorubicin was administered *i.p.* at day 3 after tumor cell injection. Values are represented as mean ± SEM. **p<0.01; ***p<0.001 by unpaired *t*-test.

1.3.3.2. Characterization Of The Anti-Tumor Immune Response Of Homozygous shCD5EμTg Mice

To better disclose the underlying mechanism of action of shCD5 in the anti-tumor response, we analyzed a new line of homozygous shCD5EμTg mice obtained by intercrossing the above described heterozygous animals. As observed with heterozygous mice, the growth of melanoma B16-F0 tumors was slower in homozygous shCD5EμTg mice compared with Non-Tg controls (**Fig.IV.11a**). To ensure that their anti-tumor response was not specific to B16-F0 cells, homozygous shCD5EμTg mice were challenged with several isogenic tumor cell lines of different origins, such as the EG7-OVA lymphoma cell line (a derivative from the murine thymoma EL-4 cell line genetically modified in order to express ovalbumin), the RMA-S lymphoma cell line, the sarcoma MCA-205 cell line, and the MC-38 cell line (which derives from a murine colon adenocarcinoma). As shown in **Fig.IV.11b**, EG7-OVA tumors also had a slower growth rate and reduced weight, while no differences were observed regarding growth of the other tumor cell lines tested (**Fig. IV.11c-e**). This would indicate that, though non-specific, the efficacy of the anti-tumor response of homozygous shCD5EμTg mice is influenced by the tumor cell type.

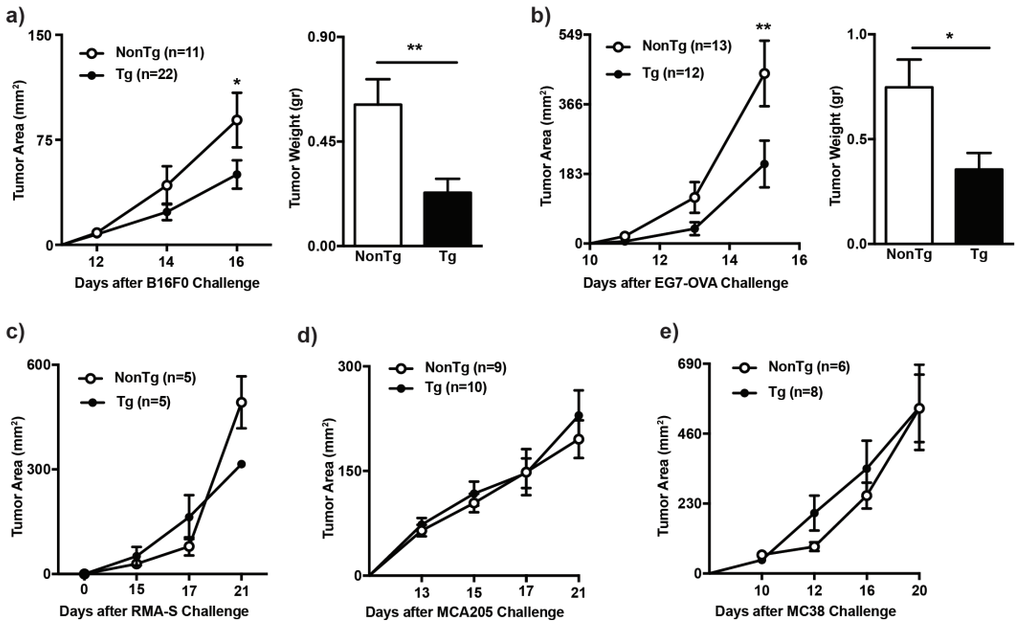

Fig.IV.11 – Comparative growth of different tumor cell types in shCD5EμTg and Non-Tg male mice. **a)** shCD5EμTg (n = 22) and Non-Tg (n = 11) mice were injected *s.c.* with 5 x 10^4 B16-F0 melanoma cells and monitored for tumor area (at different time points) and tumor weight (at final day 16). **b)** shCD5EμTg (n = 12) and Non-Tg (n = 13) mice were injected *s.c.* with 5 x 10^4 EG7-OVA cells and monitored for tumor area (at different time points) and tumor weight (at final day 15). **c)** shCD5EμTg (n = 5) and Non-Tg mice (n = 5) were injected *s.c.* with 5 x 10^4 RMA-S cells and monitored for tumor area (at different time points) and tumor weight (at final day 21). **d)** shCD5EμTg (n = 10) and Non-Tg (n = 9) mice were injected *s.c.* with 5 x 10^4 MCA-205 cells and monitored for tumor area (at different time points) and tumor weight (at final day 21). **e)** shCD5EμTg (n = 8) and Non-Tg (n = 6) mice were injected *s.c.* with 5 x 10^4 MC-38 cells and monitored for tumor area (at different time points) and tumor weight (at final day 20). Results are representative of 1 or 2 independent experiments in the conventional mice facility. Values are represented as mean ± SEM. *p<0.05; **p<0.01 by unpaired *t*-test.

Given the improved anti-tumor immune response observed in homozygous shCD5EμTg mice against B16-F0 and EG7-OVA cells, we decided to further characterize it at the local level by analyzing the composition of the tumor draining (TdLN) and contralateral (cLN) lymph nodes. As shown by **Fig.IV.12a** and **Fig.IV.14a**, the reduction in B16-F0 or EG7-OVA tumor size and weight was concurrent with a significant increase of total cell numbers in the TdLN from shCD5EμTg mice compared with that from Non-Tg controls. Further flow cytometry analyses showed higher total numbers of both $CD8^+$ and $CD4^+$ T cells in TdLN but not cLN of shCD5EμTg mice challenged with B16-F0 cells compared to Non-Tg controls (**Fig.IV.12b-c**). By contrast, no statistically significant changes were observed for other lymphocyte subpopulations such as NK, NKT or B cells (**Fig.IV.12d-f**). Likewise, non-statistically significant differences between shCD5EμTg

and Non-Tg mice were observed during the analysis of the cLN (**Fig.IV.12a-f**). Regarding changes in cell percentages, only that of $CD4^+$ T cells was significantly increased (**Fig. IV.12c**). As represented in **Fig.IV.12g** and **Fig.IV.12h**, the analysis of surface expression levels of the activation marker CD69 in $CD4^+$ and $CD8^+$ T cells did not reveal significant differences between shCD5EμTg and Non-Tg controls.

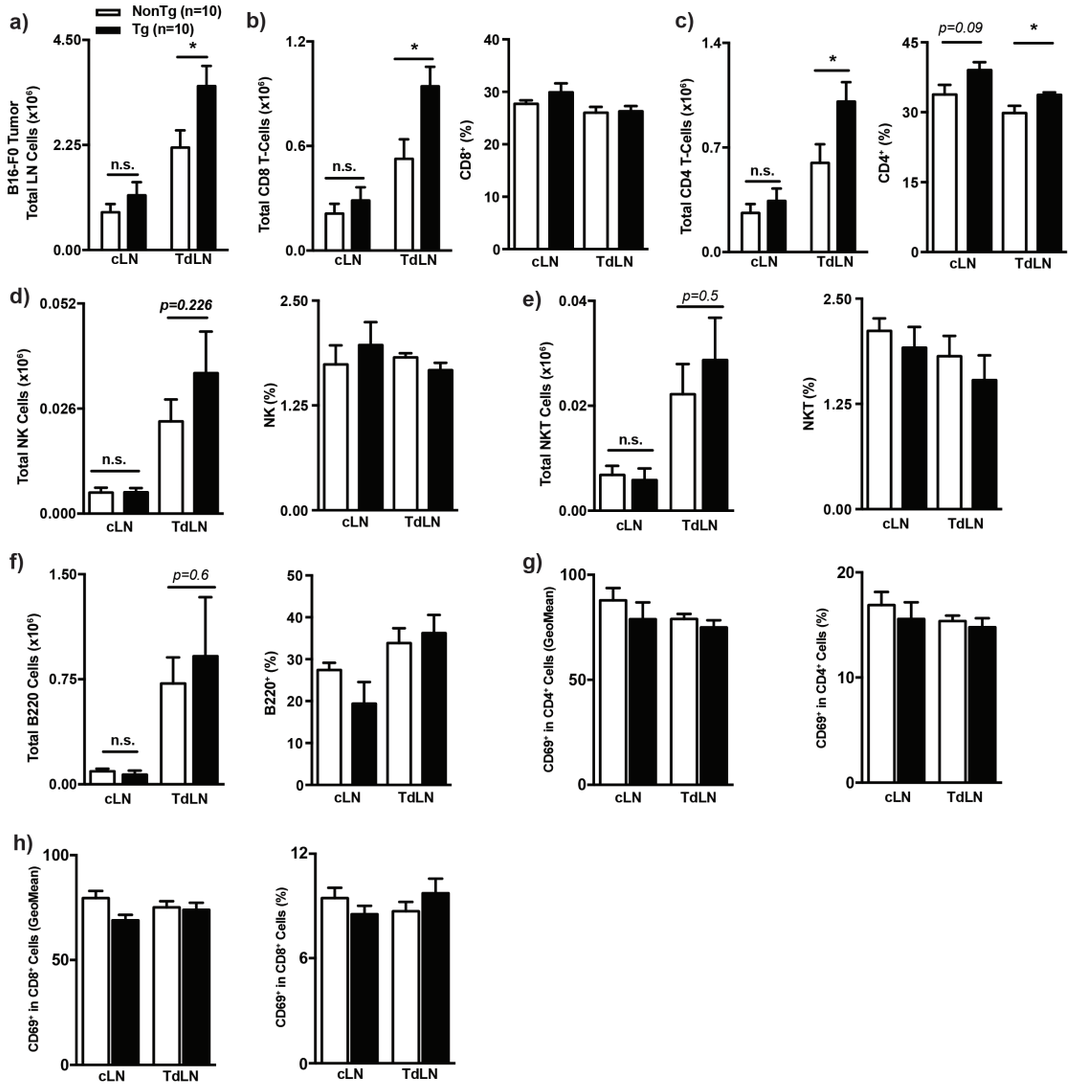

Fig.IV.12 – Comparative analysis of TdLN and cLN lymphocyte composition from shCD5EμTg and Non-Tg male mice challenged with B16-F0 tumor cells. cLN and TdLN of shCD5EμTg and Non-Tg mice (n = 10 per group) challenged with B16-F0 as in Fig.IV.11 were analyzed for **a)** total cell numbers; **b** and **c)** total number and percentage of $CD8^+$ and $CD4^+$ T cells, respectively; **d, e** and **f)** total number and percentage of NK, NKT and B cells, respectively; **g** and **h)** Mean fluorescence (GeoMean) (**left panel**) and percentage (**right panel**) of $CD69^+$ cells in $CD4^+$ and $CD8^+$ T cells, respectively. Values are represented as mean ± SEM in conventional mice facility. *p< 0.05 by unpaired *t*-test.

Worth noting was the fact that, although the number of total $CD4^+$ T cells was increased in the TdLN but not cLN of shCD5EμTg mice, the percentage of $CD4^+$ cells with regulatory phenotype ($CD25^+FoxP3^+$) was found significantly reduced in both TdLN and cLN compared to Non-Tg mice (**Fig.IV.13a left**). However, the intrinsic suppressive activity of T_{reg} did not differ between shCD5EμTg and Non-Tg controls (**Fig.IV.13a right**). Overall, the changes observed in the lymphocyte subset composition of TdLN from shCD5EμTg (increased $CD4^+$ and $CD8^+$ T cells and decreased T_{reg} cells) are compatible with a more efficient immune response to tumor challenge.

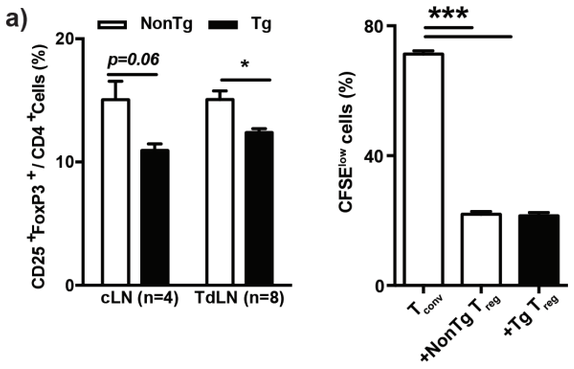

Fig.IV.13 – Comparative analysis of TdLN and cLN T_{reg} lymphocyte percentage and suppressor activity from shCD5EμTg and Non-Tg mice. **a, left)** Percentage of $CD25^+FoxP3^+$ $CD4^+$ cells in cLN and TdLN from shCD5EμTg and Non-Tg male mice challenged with B16-F0 cells as in Fig.IV.11. **a, right)** T_{reg} suppressor activity assay. CFSE-stained Tconv cells (1×10^5) from LN of Non-Tg mice were cultured in anti-CD3 mAb–coated plates plus soluble anti-CD28 mAb in the absence or presence of T_{reg} cells (5×10^4) from LN of Non-Tg or shCD5EμTg mice at 2:1 ratio. Shown is the percentage of $CFSE^{low}$ lymphocytes at day 3 of culture from one experiment of three performed (3 mice pools of each phenotype). Values are represented as mean ± SEM in conventional mice facility. *p< 0.05 ***, p <0.0001 by unpaired *t*-test.

To further analyze the enhanced anti-tumor immune response of shCD5EμTg mice, we took advantage of the OVA expression by EG7-OVA cells to analyze the specific response against these cells. To that end, lymphocyte suspensions from cLN and TdLN of shCD5EμTg and Non-Tg mice challenged with EG7-OVA tumor cells (harvested at day 18 post-tumor challenge) were cultured for 48 h in the presence or absence of OVA-specific peptide (SIINFEKL), native OVA antigen, and EG7-OVA irradiated cells. At 48 h post-stimulation, IFN-γ production in culture supernatants was assessed by ELISA. As shown by **Fig.IV.14b** statistically significantly higher levels of IFN-γ were detected in culture supernatants from TdLN cells of shCD5EμTg mice under all the stimulatory conditions tested, compared with those from Non-Tg mice. In cLN of both mice groups, IFN-γ levels were undetectable following stimuli (data not shown). Interestingly, similar IFN-γ results were obtained when the same lymphoid cell suspensions were challenged with

irradiated allogeneic YAC-1 cells, a mouse thymoma of A/Sn origin (H2a) commonly used for assaying NK-mediated cytotoxicity (**Fig.IV.14c**). These findings are suggestive of shCD5EμTg mice exhibiting enhanced specific ($CD8^+$T) and unspecific (NK) anti-tumor immune responses.

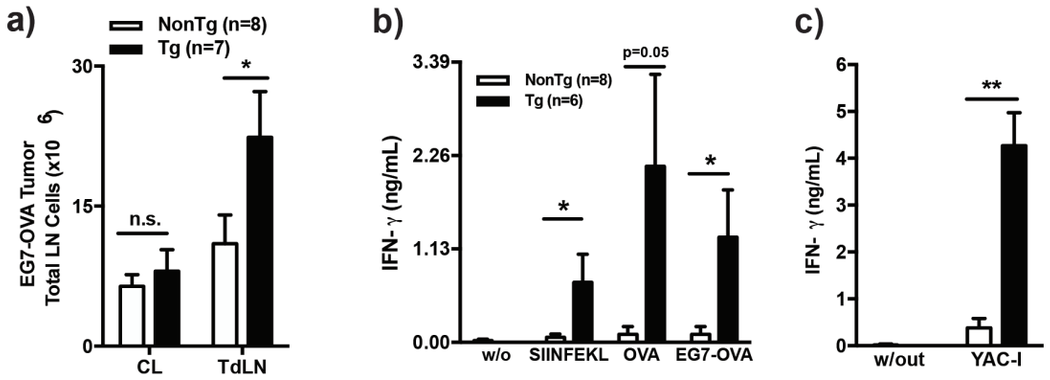

Fig.IV.14 - shCD5EμTg mice exhibit enhanced innate and adaptive anti-tumor responses. **a)** Total cell numbers from cLN and TdLN of Non-Tg (n = 8) and shCD5EμTg (n = 7) male mice challenged with EG7-OVA cells. **b)** TdLN cells from EG7-OVA-challenged Non-Tg (n = 8) and shCD5EμTg (n = 7) mice were cultured alone or in the presence of SIINFEKL peptide, OVA or irradiated EG7-OVA cells for 48 h and IFN-γ levels in culture supernatants assayed by ELISA. **c)** TdLN cells from EG7-OVA-challenged Non-Tg (n = 8) and shCD5EμTg (n = 6) mice were co-cultured with YAC-1 cells for 48 h and culture supernatants assayed by ELISA for IFN-γ levels. Results are representative of 2 independent experiments. Data are presented as mean ± SEM. *p< 0.05; **p<0.01 by unpaired *t*-test.

Further evidence on the later regard was obtained by performing lytic assays with whole spleen cell suspensions from shCD5EμTg and Non-Tg mice bearing B16-F0 tumors, using B16-F0 as target cells. As illustrated by **Fig.IV.15a**, splenocytes from shCD5EμTg mice were more efficient in inducing cell lysis than those from Non-Tg mice at high effector:target ratios. Similar results were obtained when spleen cell suspensions from shCD5EμTg and Non-Tg mice bearing EG7-OVA tumors were assayed against EG7-OVA cells or RMA-S as lysis targets (**Fig.IV.15b**), presenting more lysis at both high and low effector:target ratios to specific or unspecific target cells. These results further support that the enhanced anti-tumor activity of shCD5EμTg splenocytes very likely involves both specific ($CD8^+$ T) and unspecific (NK) cytotoxicity.

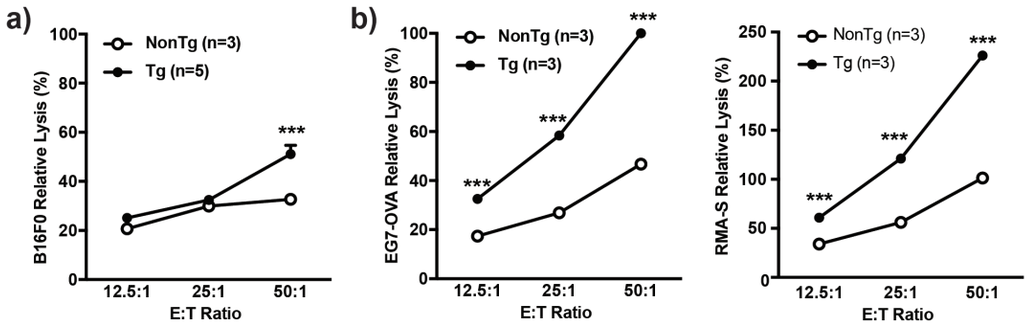

Fig.IV.15 - Relative lysis of B16-F0 and EG7-OVA cells by total splenocytes from tumor-bearing mice. **a)** B16-F0 cells (5 x 10^4) were co-cultured at different efector:target (E:T) ratios for 4 h with total splenocytes from male shCD5EμTg (n = 5) and Non-Tg (n = 3) mice previously challenged with B16-F0 tumor cells. **b)** Same as in a) but with EG7-OVA cells and total splenocytes from male shCD5EμTg (n = 3) and Non-Tg (n = 3) mice previously challenged with EG7-OVA tumor cells (**left panel**) or RMA-S (**right panel**). Results represent the average of two independent experiments for the B16-F0 model and one experiment for EG7-OVA model. Cell lysis was measured using the CytoTox-ONE™ Homogeneous Membrane Integrity Assay. Data are presented as mean ± SEM. *** p<0.0001 by unpaired *t*-test.

The evaluation of mRNA expression levels for some cytokine and immune regulators in the tumor microenvironment showed a statistically significant reduction of *il-6* in shCD5EμTg mice compared with Non-Tg animals. By contrast, non significant differences were observed between the two groups of mice regarding *il-10, foxp3, ifn-γ, il-15*, and *il-22* mRNA expression levels (**Fig.IV.16**).

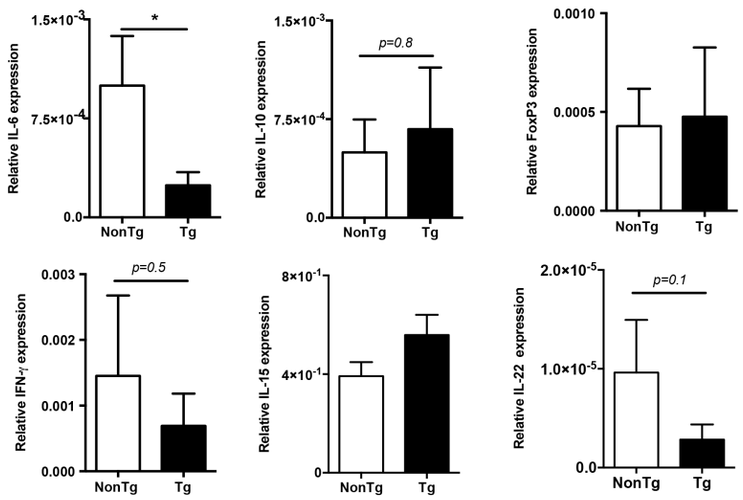

Fig.IV.16 – Intratumoral mRNA expression levels. Relative mRNA *il-6, il-10, foxp3, ifn-γ, il-15* and *il-22* gene expression levels in B16-F0 tumors at final day (day 16) from shCD5EμTg (n = 9) and NonTg male mice (n = 6) measured by qRT-PCR (relative to *gapdh* levels on the same samples). Data are presented as mean ± SEM. *p< 0.05 by unpaired *t*-test.

The results so far, together with the notion that IL-6 is a down-regulator of NK cell activity (Cifaldi et al., 2015)and impairment of natural killer (NK, led us to consider the possibility that NK cells could play a key role in the antitumor response mediated by shCD5. To confirm such an issue, shCD5EμTg and Non-Tg mice were subjected to mAb-induced NK-cell depletion before and after challenge with B16-F0 melanoma cells. As illustrated by **Fig.IV.17**, the enhanced antitumor response observed for shCD5EμTg mice was abrogated when they were subjected to NK cell depletion. This would support a relevant role for NK cells in potentiating the antitumor responses associated with transgenic shCD5 expression.

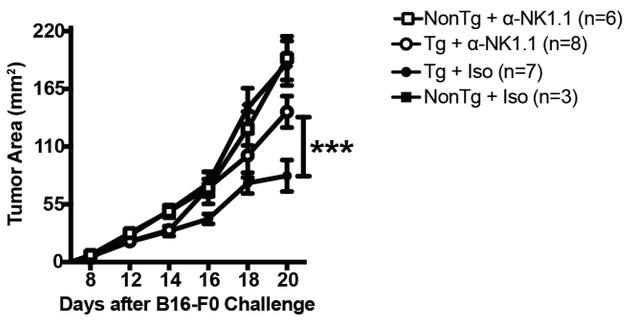

Fig.IV.17 – NK cell implication in the antitumor response of shCD5EμTg mice. 5 x 10^4 B16-F0 cells were *s.c.* injected. NK cell depletion was achieved by *i.p.* administration of three doses (days -2, -1, 0) of anti-NK1.1-PK136 mAb (male shCD5EμTg n = 8; male Non-Tg mice n = 6) and then every 48 h until the end of the experiment (day 20). As a control, mice from the two experimental groups were administered with the same doses of rat IgG_{2a} isotype control (shCD5EμTg n = 7; Non-Tg mice n = 3). Data are presented as mean ± SEM. ***p<0.0001 by ANOVA test.

1.3.3.3. Therapeutic Administration Of Exogenous Soluble Human CD5 Protein To Tumor-Challenged WT Mice

In order to exclude putative transgenesis artifacts and also to get closer to a clinical application, the effects of recombinant shCD5 (rshCD5) protein infusion to WT C56BL/6 mice bearing B16-F0 tumors was further explored. To this end, rshCD5 or human serum albumin (HSA) were administered every other day by two different routes (*i.p.* or *s.c.* peritumorally – *p.t.*) at two different doses (100 μg and 25 μg), starting when tumors were ≈9-12 mm^2 in size (≈day 7-8). As illustrated by **Fig.IV. 18**, no significant effects on tumor growth were observed when rshCD5 was administered *i.p.* even at high doses (100 μg) or *p.t.* at low doses (25 μg). On the contrary, *p.t.* administration of high rshCD5 doses (100 μg/mice) induced a statistically significant slower tumor growth and lower tumor weight compared with those from HSA-treated mice.

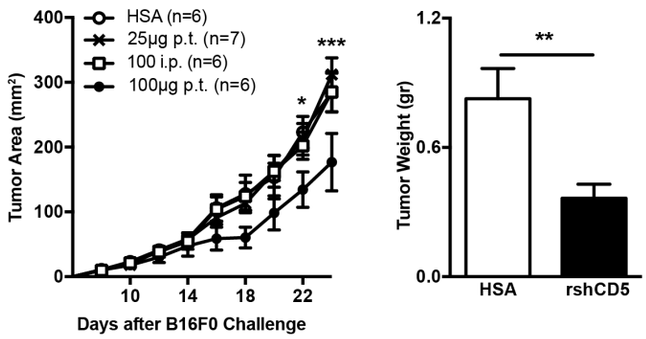

Fig.IV.18 - Exogenous administration of rshCD5 to WT mice challenged with B16-F0 cells. C57BL/6J male mice (n = 6-7/group) were injected *s.c.* with 5 x 10^4 B16-F0 cells. The treatment with HSA or rshCD5 (25 or 100 µg *s.c.* peritumoral; and 100 µg *i.p.*) every 48 h started when tumor size was ≈9-12 mm^2. Tumor weight was measured at day 23. Results are representative of 2 independent experiments. Data presented as mean ± SEM. * $p<0.05$, ** $p<0.01$, and *** $p<0.0001$ by unpaired *t*-test.

As happened with the shCD5EµTg mice, the analysis of total cell numbers in TdLN from rshCD5-treated mice (100 µg *p.t.*) showed statistically significantly higher total cell numbers with regard to those found in HSA-treated mice (**Fig.IV.19a**). No differences between the two groups of mice were found during the analysis of cLN (**Fig.IV.19a**). The observed increment in TdLN total cell numbers was likely at the expense of total $CD8^+$ and $CD4^+$ T cells as well as total NK and NKT cell numbers (**Fig.IV.19b-e**). Regarding cell percentages, $CD8^+$ T cells were reduced as well as $CD4^+$ (**Fig.IV.19b-c**), but NK and NK cells were significantly increased (**Fig.IV.19d-e**). No statistically significant differences were observed regarding total B cell numbers (**Fig.IV.19f**).

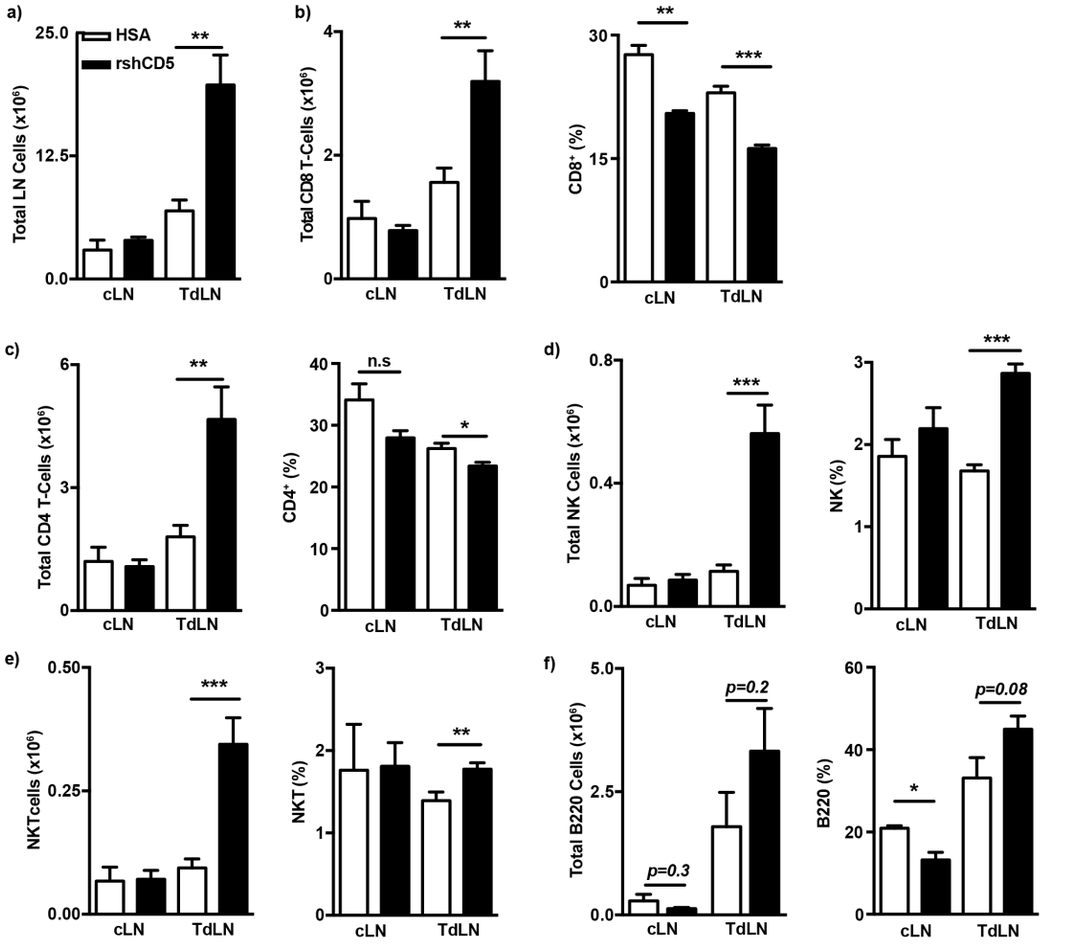

Fig.IV.19 – Characterization of lymphocyte subpopulations in TdLN and cLN from rshCD5-treated mice challenged with B16-F0 cells. WT C57BL/6 male mice were *s.c.* challenged with 5 x 10^4 B16-F0 cells as in Fig.IV.18, and then infused *p.t.* with rshCD5 or HSA (100 μg) every 48 h when tumor size reached ≈9-12 mm^2. **a)** Total cell number was analyzed in cLN and TdLN at the end of the follow-up period (day 24). **b)** Total cell number and percentage of $CD8^+$T cells of the same samples as in a). **c)** Idem for $CD4^+$T cells. **d)** Idem for NK cells. **e)** Idem for NKT cells. **f)** Idem for $B220^+$ cells. Results are representative of 2 independent experiments. Data presented as mean ± SEM. * $p<0.05$, ** $p<0.01$, and *** $p<0.0001$ by unpaired *t*-test.

The percentage of T_{reg} cells within the $CD4^+$ subset was significantly reduced in TdLN but not cLN from rshCD5-treated mice (**Fig.IV.20**) compared with HSA-treated ones. This finding was validated by the analysis of *foxp3* mRNA levels in TdLN of these mice (*p.t.* rshCD5-treated versus HSA-treated mice).

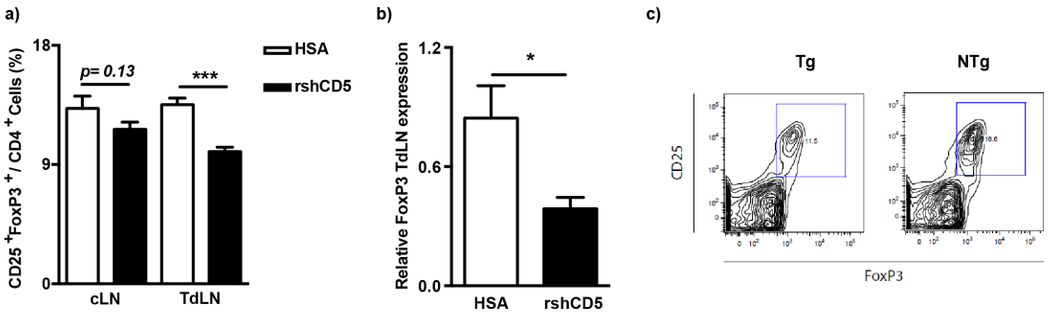

Fig.IV.20 – Analysis of T_{reg} from TdLN and cLN of rshCD5-treated mice challenged with B16-F0 cells. WT C57BL/6 male mice were *s.c.* challenged with 5 x 10^4 B16-F0 cells as in Fig.IV.18 and infused *p.t.* with rshCD5 or HSA (100 µg) every 48 h when tumor size reached ≈9-12 mm^2. **a)** Percentage of $CD25^+FoxP3^+$ cells in $CD4^+$ T cells. **b)** Relative *foxp3* mRNA expression level in TdLN cells from both groups of treated mice (*gapdh* as control gene). **c)** Dot plot representation of one representative mouse per group of $CD25^+FoxP3^+$ cells in $CD4^+$ T cell gate from viable cells. Data presented as mean ± SEM. * p<0.05, ***p<0.0001 by unpaired *t*-test.

The expression of the early lymphocyte activation marker CD69 was also analyzed in rshCD5-treated mice. In this case, both the surface expression level of C69 and the percentage of $CD69^+$ cells were increased in the $CD4^+$ T cell subset of TdLN from rshCD5-treated mice, although only reached statistical significance for the later (**Fig.IV.21a**). No differences were observed for the $CD8^+$ T cell subset (**Fig.IV.21b**).

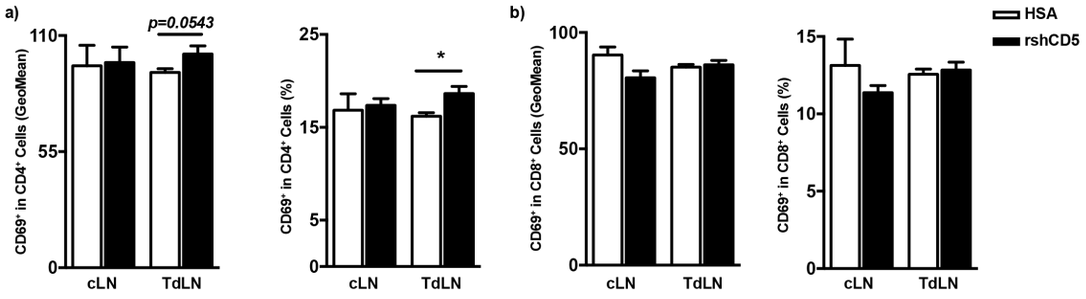

Fig.IV.21 – CD69 expression in TdLN from rshCD5-treated WT mice previously challenged with B16-F0 melanoma cells. **a)** CD69 mean fluorescence (GeoMean) (**left panel**) and percentage of $CD69^+$ (**right panel**) in $CD4^+$ T cells from day 24 cLN and TdLN of rshCD5-treated WT male mice previously challenged with 5 x 10^4 B16-F0 cells as in Fig.IV.18. **b)** Idem for $CD8^+$ T cells. Data presented as mean ± SEM. * p<0.05 by unpaired *t*-test.

The mRNA expression levels of different cytokines and transcription factors were next evaluated in B16-F0 tumors from rshCD5-treated WT mice. As shown by **Fig.IV.22**, a non-statistically significant reduction (p = 0.09) in the *il-6* mRNA levels was observed. By contrast, the differences did not reach statistical significance for *il-10*, *foxp3*, *ifn-γ*, *il-15*, and *il-22* mRNA levels.

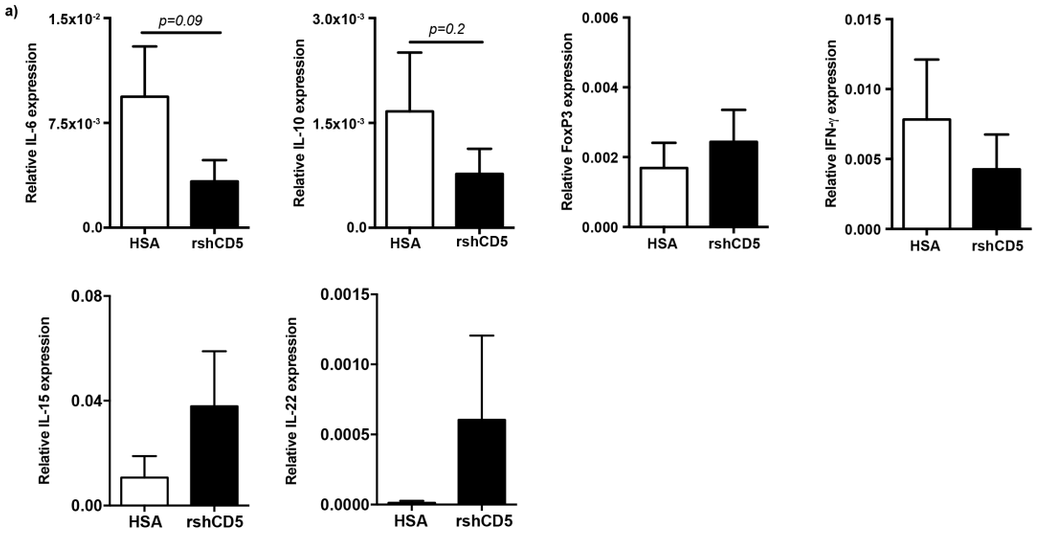

Fig.IV.22 – Intratumoral cytokine mRNA expression levels. **a)** Relative *il-6*, *il-10*, *foxp3*, *ifn-γ*, *il-15* and *il-22* gene mRNA expression at day 24 after 5 x 10^4 B16-F0 tumor cells challenge in rshCD5- (n = 8) or HSA- (n = 4) treated WT male mice. Data are presented as mean ± SEM. Analyzed with unpaired *t*-test.

As performed in the shCD5EμTg mice, NK cell depletion was also carried out in rshCD5-treated WT mice previously challenged with B16-F0 melanoma tumor cells. In this case, 2 days before the tumor reached approximately ≈9-12 mm^2, we started the depletion by treating the mice with anti-NK1.1 (PK136) mAb for 3 consecutive days, and on the last day of this schedule, we began local (*p.t.*) administration of rshCD5. Both the mAb and the protein were administered every 48 h until the end of the experiment. Results show that NK cell-depletion treatment also abrogated the enhanced anti-tumor effect of *p.t.* rshCD5 administration to tumor-bearing WT mice (**Fig.IV.23a**), thus confirming the relevant role played by NK cells in shCD5-mediated tumor outcome.

Next it was also evaluated the therapeutic effect of rshCD5 infusion in the EG7-OVA tumor model. In the same experiment, we added a group to find out whether these NK cells play an important role in the anti-tumor response against a T cell-dependent tumor response model. We found that the tumor growth rate was similar for the three groups (**Fig. IV.23b**). These results show that for this tumor model, the rshCD5 treatment schedule was not effective, and NK-depletion is not relevant for tumor progression.

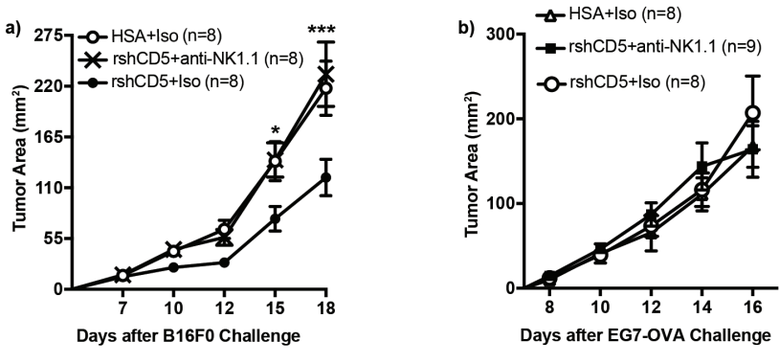

Fig.IV.23 – Effect of NK-depletion on the anti-tumor properties of rshCD5 treatment. **a)** WT C57BL/6 male mice (n = 8 per group) injected *s.c.* with B16-F0 (5 x 10^4) cells were depleted of NK cells by *i.p.* administration of 3 doses daily of anti-NK1.1 (PK136) mAb or rat IgG_{2a} isotype control just before starting proteins (rshCD5 or HSA) infusion, and then every 48 h until the end of the experiment. rshCD5/HSA treatment was performed as previously described (see Fig.IV.18). Results (mean ± SEM) are representative of 2 independent experiments. *p<0.05, ***p<0.0001 by unpaired *t*-test. **b)** C57BL/6 mice (n = 8/9 mice per group) were injected *s.c.* with EG7-OVA (5 x 10^4) cells. Depletion of NK cells and protein treatment was performed as in a). Data are presented as mean ± SEM.

Finally, the combined effect of rshCD5 and anti-CTLA-4 (the first immune checkpoint inhibitor receptor to be clinically targeted) mAb infusion in the B16-F0 model was also studied. With the schedule and doses studied, we found that both groups treated with anti-CTLA-4 showed slower tumor growth, but no differences between rshCD5 or HSA treatment were observed (**Fig.IV.24**).

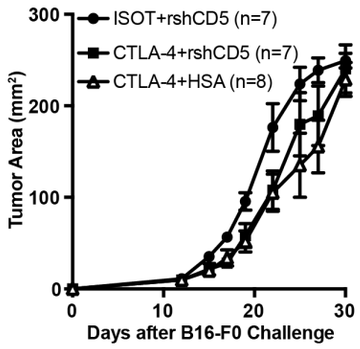

Fig.IV.24 – Combined effect of rshCD5 and anti-CTLA-4 on B16-F0 tumor growth. WT C57BL/6J male mice (n = 7/8 mice group) were injected *s.c.* with B16-F0 (5 x 10^4) cells. Two days later, a blocking anti-CTLA-4 mAb (clone 9H10, 75 µg per mice) or isotype control (IgG_1) were administrated *i.p.* and then three more doses each 72 h. When tumors reached ≈9-12 mm^2, rshCD5 or HSA (100 µg) were administered every 48 h (*p.t.*). Data are presented as mean ± SEM.

Taken together, these results indicate that *p.t.* infusion of rshCD5 reproduces some of the observations made in shCD5EμTg mice mainly regarding to slower tumor growth and cellularity changes in TdLN.

1.3.3.4. Housing Conditions And Anti-Tumor Response Of Mice Transgenic For Soluble Human CD5 Expression (shCD5EμTg)

During the development of this work, we noticed that the mouse facility environment influenced the anti-tumor response of the shCD5EμTg mice. The colony, as said before, was established in an SPF facility, but all of the tumor models were performed in a conventional facility, and it appeared that tumor growth in these two facilities had a different behavior. In **Fig.IV.25a** shCD5EμTg mice present the same B16-F0 tumor growth when kept at the SPF facility (**left panel**) as the Non-Tg mice, the reverse of the conventional facility (**right panel**). The same reverse result was observed with an EG7-OVA model in an SPF facility (**Fig.IV.25b left panel**).

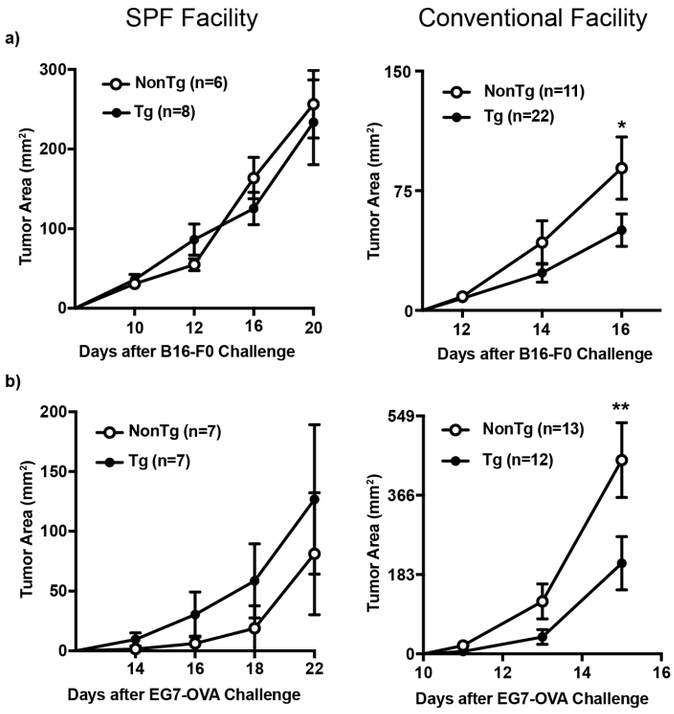

Fig.IV.25 – Influence of housing conditions on tumor growth in shCD5EμTg mice. **a)** Male shCD5EμTg and Non-Tg mice kept under SPF (**left panels**) or conventional (**right panels**) housing conditions were injected *s.c.* with B16-F0 (5 x 10^4) cells. **b)** Idem as in a) with mice challenged with EG7-OVA (5 x 10^4) cells. Values are represented as mean ± SEM. *p<0.05; **p<0.01 by unpaired *t*-test.

It was then speculated that environmental factors were at play, specifically concerning gut microbiota, and so preliminary microbiological studies were initiated in fecal samples (in collaboration with Dr. Jose González and Dr. Eduardo Huarte, South Dakota State University). When housed in the SPF facility, there were no genus differences

between shCD5EμTg and Non-Tg mice (**Fig.IV.26a**). When analyzed with more detail some differences could be detected in the Prevotellaceae and Rikenallaceae genus, Gram-negative bacteria (**Fig.IV.26b**).

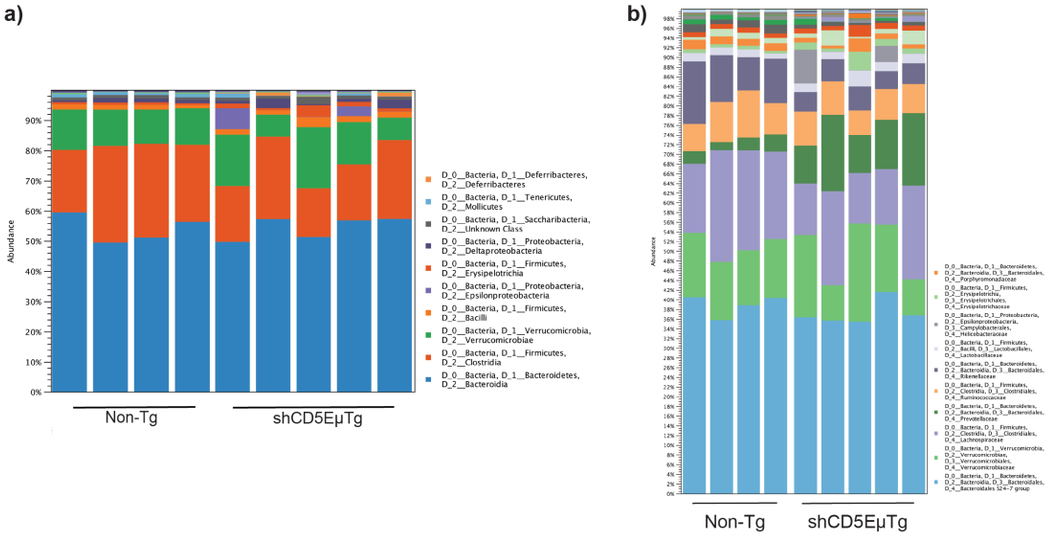

Fig.IV.26 – Influence of mice genetic background in the mice microbiota in a SPF facility. **a)** and **b)** shCD5EμTg (n = 5) and Non-Tg mice (n = 4) fecal samples were collected when housed in a SPF facility. Next-generation sequencing was performed to identify different bacteria genus present on the samples.

Next, we wanted to verify if the housing change could induce some microbiota modification. Samples were collected at different time points and as seen in **Fig.IV.27**, after more than 14 days in a conventional facility there were obvious changes in all mice. The Bacteroidaceae and Erysipelotrichaceae families expanded and the Lachnospiraceae, Rikenellaceae and Verrucomicrobiaceae families diminished.

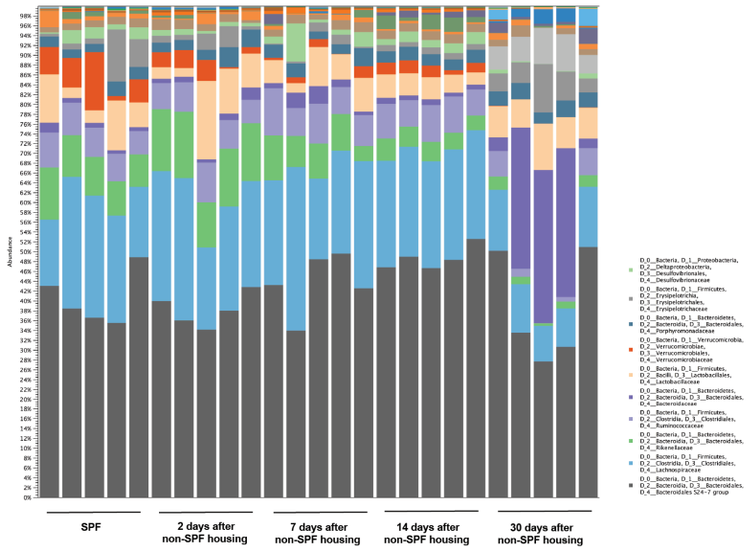

Fig.IV.27 – Influence of housing conditions in the shCD5EμTg mice microbiota in a SPF and conventional facility. shCD5EμTg (n = 5) fecal samples were collected when housed in a SPF facility and conventional consecutive housing. Next-generation sequencing was performed to identify different bacteria genus present on the samples.

Further analysis is currently being performed by two collaborator groups, in order to complete this analysis and improve the study.

1.4. PHENOTYPICAL AND FUNCTIONAL ANALYSIS OF A SECOND GENERATION CD5 TRANSGENIC MICE - shCD5LckEμTg MICE

Although we already have a mouse line for transgenic shCD5 expression (shCD5EμTg), we generated a new one - shCD5LckEμTg - hoping to express higher levels of shCD5 preferably in lymphoid organs with the intention of boosting the phenotypical changes observed previously. To this end, the cDNA sequence coding for the whole extracellular region of CD5 (shCD5) was synthesized from the initiation Methionine to Asp345 and subcloned into the BamHI site of the p1026x vector, just downstream the transcriptional control of the Lck proximal promoter and the immunoglobulin heavy chain (Eμ) enhancer (**Fig.IV.28a**). Thus, it would be preferentially expressed not only by B cells as in the previous mouse model, but also by T cells. Transgenic mice were generated by injecting the purified fragment into zygotes from superovulated C57BL/6N female mice mated to C57BL/6 breeder males. These mice showed no physical (weight, size, temperature), nor behavior (mobility, mating, cycles) abnormality. Both housing and experiments were performed in a SPF facility.

The first step in the characterization of this new transgenic mouse line was to confirm the integration of the transgene (**Fig.IV.28b**). To this end, genomic DNA was subjected to PCR by means of the same two primer pairs used in the analysis of shCD5EμTg mice: one specific for the shCD5 transgene and another specific for a housekeeping mouse gene (invariant Li chain of MHC class II). To be certain that the amplified segment corresponded to CD5, both positive as well as negative samples were sequenced (**Fig. IV.28c**). Only the shCD5LckEμTg mice had the correct and complete sequence of the extracellular region of CD5. In addition, we analyzed the levels of hCD5 expression in different organs (lymphoid and non-lymphoid) to confirm that the human CD5 transgene was expressed (**Fig.IV.28d**) in shCD5LckEμTg mice (**left panel**) and compared them to the levels of the previous shCD5EμTg mice (**right panel**). In the samples of Non-Tg mice, no hCD5 expression was detected. In the new transgenic mice line, we could increase the relative CD5 expression in thymus and spleen, previously at the same level or lower than in lung, and the overall CD5 expression.

Next, the serum levels of shCD5 (**Fig.IV.28e**) were assessed by ELISA and found that homozygous shCD5LckEμTg mice display levels of around 80 ng/mL, while the levels in heterozygous shCD5LckEμTg mice are around 60 ng/mL. Although the previous mouse colony presented values in the same order of magnitude, there was a much greater dispersion of values (10-100 ng/mL) which in this case is much more consistent. The unresponsiveness (tolerance) to immunization with purified recombinant shCD5

(rshCD5) emulsified in CFA was also evaluated. As expected, shCD5LckEμTg mice were specifically tolerant to rshCD5 but not to the highly homologous human protein CD6 (rshCD6) (**Fig.IV.28f**). Interestingly, shCD5LckEμTg mice showed significantly higher levels of serum anti-CD6 antibodies than their Non-Tg counterparts.

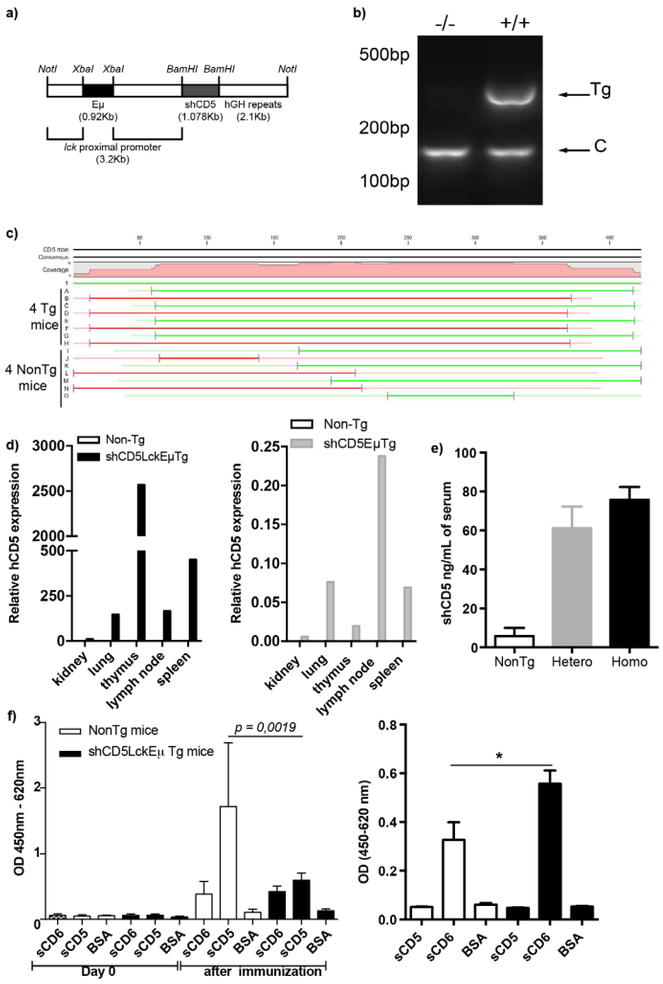

Fig.IV.28 – Generation of shCD5LckEμTg mice. **a)** Schematic representation of the transgene coding for shCD5 expression under the transcriptional control of the lymphocyte-specific Lck proximal promoter and the Igμ enhancer (Eμ). b) PCR screening of genomic DNA from homozygous (+/+) shCD5LckEμTg and Non-Tg (-/-) mice. Bands correspond to transgene (Tg) and internal PCR control (C). **b)** Sequencing of the previous PCR products (four mice each group) First green lane with number 1 represents the shCD5 sequence expressed by the transgenic mice. Lanes A, C, E and G in green represent the sequence of the shCD5 with a Forward primer from 4 shCD5LckEμTg mice, and lanes B, D, F and H in red the sequence with a Reverse primer of the same mice, respectively. The same for 4 Non-Tg mice in IJ, KL, MN, OP lanes. **c)** Relative human CD5 expression in kidney, lung, thymus, LN and spleen of one shCD5LckEμTg (**left panel**), three shCD5EμTg (**right panel**) and one Non-Tg mice. **d)** ELISA quantification of serum shCD5 levels from Non-Tg (n = 7), homozygous (n = 4) and heterozygous (n = 3) shCD5LckEμTg mice. Data expressed as mean ± SEM. **e)** Antibody response to immunization with purified rshCD5 (**left panel**, 6 shCD5LckEμTg mice and 5 Non-Tg mice) and rshCD6 (**right panel**, 4 shCD5LckEμTg mice and 5 Non-Tg

mice) (2 mg) emulsified in CFA. Mouse sera were collected 2 weeks after the second boost (1 mg emulsified in IFA) and tested by ELISA for specific IgG antibody levels to rshCD5, rshCD6 or BSA. Data represented as mean ± SEM of OD 450-620nm values. * p<0.05; ** p<0.01; two-tailed Student's *t*-test.

In the same line, the *in vivo* humoral response to TD and TI antigens conjugated to TNP was studied. As illustrated by **Fig.IV.29a-b**, shCD5LckEμTg mice exhibited increased levels of some anti-TNP specific Ig antibody subclasses, which reached statistically significant values for IgG_1 and IgG_{2c} when challenged with TNP_5-KLH (TD) and IgG_1 when challenged with TNP_{65}-Ficoll (TI type 2). On the contrary, lower levels of antibody were generated when mice were challenged with $TNP_{0,3}$-LPS (TI type 1), which reached statistically significant values for the IgG_3 subclass (**Fig.IV.29c**). This increment in IgG_1 levels and reduction in IgG_3 seems to indicate that shCD5LckEμTg mice is associated with a T_H2 response.

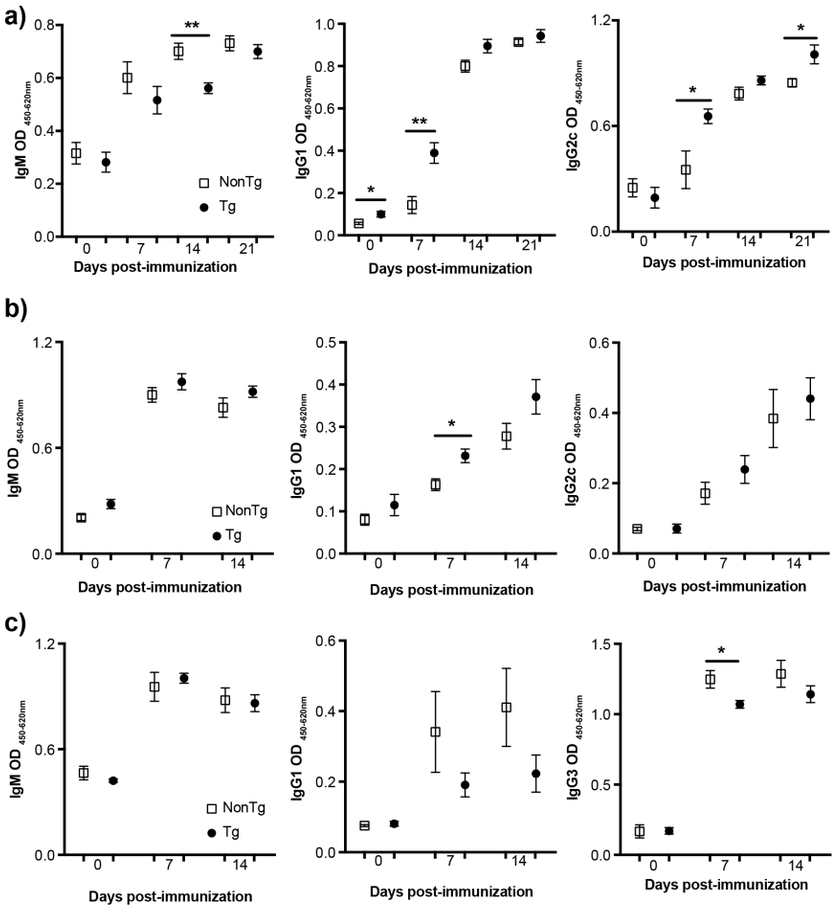

Fig.IV.29 – Characterization of shCD5LckEμTg mice humoral responses. Antibody response to *i.p.* immunization with **a)** TNP_5-KLH (TD); **b)** TNP_{65}-Ficoll (TI-2), and **c)** $TNP_{0,3}$-LPS (TI-1) antigens (50 μg in CFA or PBS). Sera (n = 4 mice per group) were collected at day 21 (TD) or 14 (TI) for ELISA determination of TNP-specific IgM and IgG subclass levels. Data are expressed as mean ± SEM of OD 450-620 nm values. *, p<0.05; **, p<0.01; (two-tailed Student's *t*-test).

A preliminary quantitative and qualitative analysis of major lymphocyte subpopulations from primary and secondary lymphoid organs was performed in shCD5LckEμTg mice (**Fig.IV.30**). No differences in total cell numbers from thymus, spleen and lymph node were detected (**Fig.IV.30a**), neither in the proportion of thymic T cell subtypes (**Fig.IV.30b**); spleen T subtypes, NK, NKT, and B cells (**Fig.IV.30c**); and lymph node T cells (**Fig.IV.30d**).

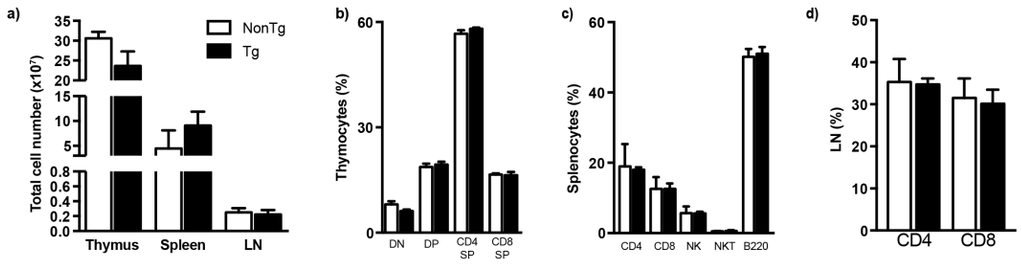

Fig.IV.30 – Immunophenotypical characterization of shCD5LckEμTg mice. **a)** Total lymphoid cell numbers in thymus, spleen, and LN from shCD5LckEμTg (n = 4) and Non-Tg (n = 4) mice. **b)** Percentage of $CD4^-CD8^-$ (DN), $CD4^+CD8^+$ (DP), $CD4^+CD8^-$ (CD4 SP) and $CD4^-CD8^+$ (CD8 SP) thymocytes from shCD5LckEμTg (n = 4) and Non-Tg (n = 6) mice. **c)** Percentage of spleen T ($CD4^+$ and $CD8^+$), NK, NKT, and B cells from shCD5LckEμTg (n = 4) and Non-Tg (n = 6) mice. **d)** Percentage of LN T ($CD4^+$ and $CD8^+$) cells from shCD5LckEμTg (n = 5) and Non-Tg (n = 5) mice.

Even knowing that we cannot control the amount of soluble CD5 expressed by the shCD5LckEμTg mice when working in *in vitro* conditions, we performed some activation and proliferation studies. When total splenocytes were activated using soluble anti-CD3 mAb alone or in combination with soluble anti-CD28 mAb, we did not find any gross differences regarding cell viability, activation (CD69 expression) or proliferation parameters between shCD5LckEμTg mice and Non-Tg controls (**Fig.IV.31a-b**).

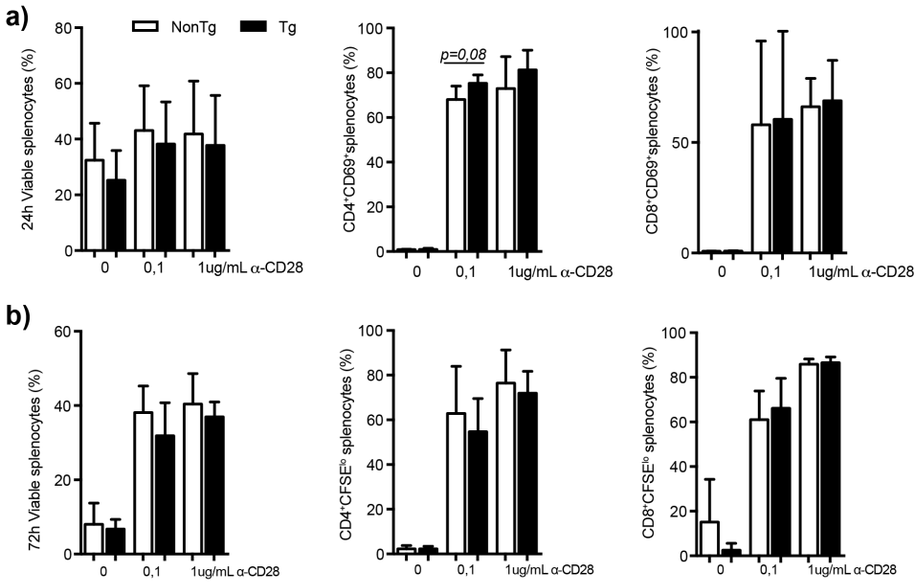

Fig.IV.31 – Ex vivo analysis of splenocytes from shCD5LckEμTg mice. Cell viability (as measured by forward and side scatter), activation (as determined by CD69 expression) and proliferation (as measured by CFSE dilution) of total and $CD4^+$ and $CD8^+$ T splenocytes from shCD5LckEμTg (n = 6) or Non-Tg (n = 11) stimulated for 24 **(a)** or 72 h **(b)** with soluble anti-CD3 mAb (0.1 μg/mL) alone or plus soluble anti-CD28 mAb (1 μg/mL). *, $p<0.05$; two-tailed Student's *t*-test.

Finally, we also tested the anti-tumor response in these mice using the B16-F0 and RMA-S models. First, we analyzed the anti-tumor response in a SPF facility and both shCD5LckEμTg and Non-Tg mice showed similar B16-F0 tumor growth rates (**Fig.IV.32a**). In the case of RMA-S, there was a trend for a slower tumor growth rate in shCD5LckEμTg mice but it was not statistically significant (**Fig.IV.32b**). As we saw a different anti-tumoral response depending on the mice facility for the previous transgenic mice analyzed, in this case we also evaluated this response moving the mice to a conventional facility. We moved males and females and challenged them with B16-F0 cells. When analyzing only males, as performed so far, we did not saw any differences (**Fig.IV.32c**). On the other hand, when analyzing females, the tumor growth was slower in shCD5LckEμTg mice compared to Non-Tg females (**Fig.IV.32d**). If we analyze both male and female together, we still saw a reduction in tumor growth in the shCD5LckEμTg mice compared to Non-Tg mice (**Fig. IV.32e**).

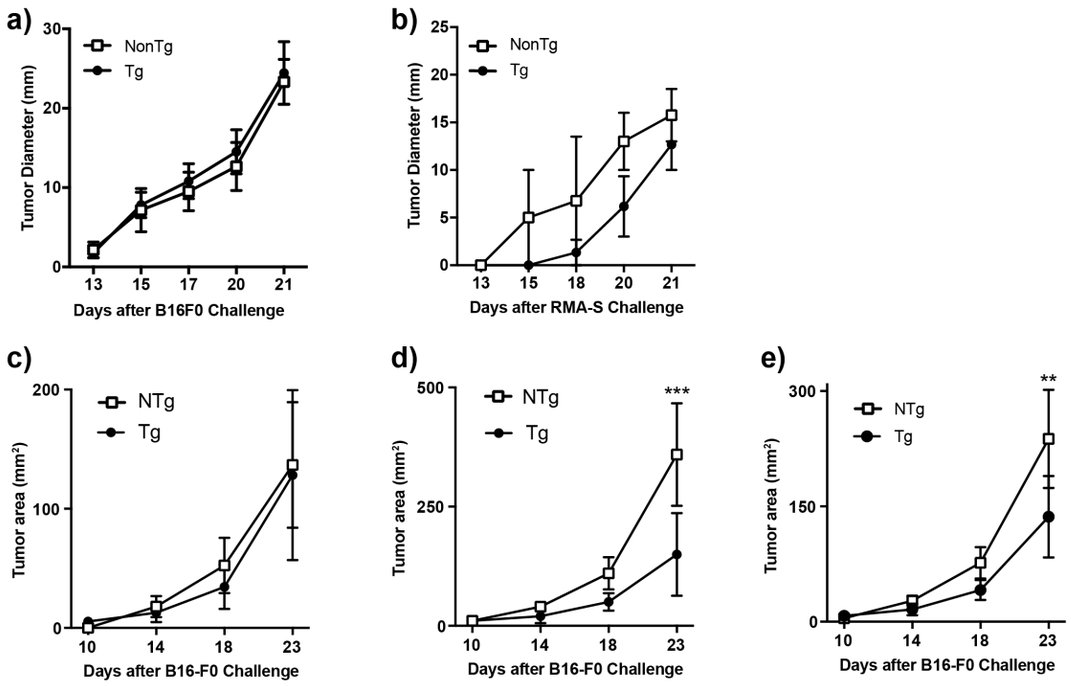

Fig.IV.32 – Tumor growth in shCD5LckEμTg and Non-Tg mice. **a**) Syngeneic B16-F0 (5 x 10^4) cells were injected *s.c.* into male shCD5LckEμTg (n = 8) and Non-Tg (n = 6) mice in a SPF facility. Tumor growth (diameter in mm) was measured every other day until sacrifice. **b)** Syngeneic RMA-S (5 x 10^4) cells were injected *s.c.* into male shCD5LckEμTg (n = 4) and Non-Tg (n = 5) mice in a SPF facility. Tumor growth was measured every other day until sacrifice. **c)** Syngeneic B16-F0 (5 x 10^4) cells were injected *s.c.* into male shCD5LckEμTg (n = 8) and Non-Tg (n = 7) mice in a conventional facility. Tumor growth (area in mm^2) was measured every other day until sacrifice. **d)** Syngeneic B16-F0 (5 x 10^4) cells were injected *s.c.* into female shCD5LckEμTg (n = 6) and Non-Tg (n = 5) mice in a conventional facility. Tumor growth (area in mm^2) was measured every other day until sacrifice. **e)** Syngeneic B16-F0 (5 x 10^4) cells were injected *s.c.* into male and female shCD5LckEμTg (n = 14) and Non-Tg (n = 12) mice in a conventional facility. Tumor growth (area in mm^2) was measured every other day until sacrifice. Two-way ANOVA test was used for statistical analysis of tumor growth. Data are presented as mean ± SEM. **p<0.01; ***p<0.001 by unpaired *t*-test.

2. ANALYSIS OF THE IMMUNOMODULATORY PROPERTIES OF SOLUBLE HUMAN CD6 EXPRESSION

2.1. PHENOTYPICAL CHARACTERIZATION OF MICE HOMOZYGOUS FOR TRANSGENIC EXPRESSION OF SOLUBLE HUMAN CD6 (shCD6LckEμTg)

To study the relevance of the immunomodulatory interactions mediated by human CD6 *in vivo*, our group generated a new mouse line (shCD6LckEμTg) in C57BL/6N background expressing a transgene coding for the extracellular region of human CD6 in soluble form (shCD6). To this end, cDNA sequence coding for the whole extracellular region of CD6 (shCD6) was synthesized from the initiation Methionine to Arg373 and

subcloned into the BamHI site of the p1026x vector, just downstream of the Lck proximal promoter and the immunoglobulin heavy chain enhancer (Eμ), driving its expression preferentially to B and T cells (**Fig.IV.33a**). Transgenic mice were generated by injecting the purified fragment into zygotes from superovulated C57BL/6 female mice mated to C57BL/6 breeder males. The shCD6LckEμTg mice were viable and fertile, and their lifespan and behavior were equivalent to those of their Non-Tg littermates. Mice housing and experimental procedures were performed in a SPF facility, unless otherwise stated.

Identification of transgenic mice was performed by PCR amplification of a 495 bp fragment (corresponding to the extracellular region of human CD6) from tail genomic DNA (**Fig.IV.33b**), and sandwich ELISA measurement of serum shCD6 levels, the latter being 79.2 ± 19.7 and 38.7 ± 6.3 ng/mL for homozygous and heterozygous mice, respectively (**Fig.IV.33c**). As expected, homozygous shCD6LckEμTg mice were poorly reactive (tolerant) to specific immunization with purified recombinant shCD6 protein (rshCD6), but not with a similar recombinant soluble form of the highly homologous human protein CD5 (rshCD5) (**Fig.IV.33d**). Interestingly, homozygous shCD6LckEμTg mice showed significantly higher levels of serum anti-CD5 antibodies than Non-Tg controls.

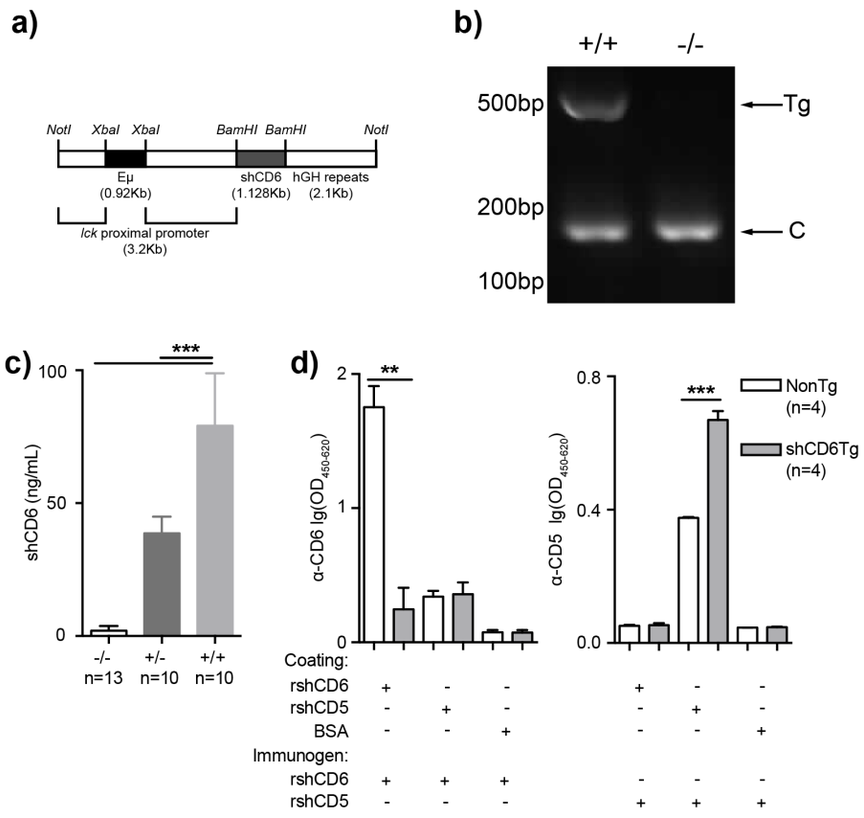

Fig.IV.33 – Generation of shCD6LckEμTg mice. **a)** Schematic representation of the transgene coding for shCD6 expression under the transcriptional control of the lymphocyte-specific Lck proximal promoter and the Igμ enhancer (Eμ). **b)** PCR screening of genomic DNA from homozygous (+/+) shCD6LckEμTg

and Non-Tg (-/-) mice. Bands corresponding to the transgene (Tg) and the internal PCR control (C) are indicated by arrows. **c)** ELISA quantification of serum shCD6 levels from Non-Tg (-/-, n = 13) as well as from homozygous (+/+, n = 10) and heterozygous (+/-, n = 10) shCD6LckEμTg mice. Data are cumulative of two independent experiments. Results are expressed as mean ± SEM. **d)** Antibody response to immunization with purified rshCD6 (**left panel**, 4 shCD6LckEμTg and 6 Non-Tg male mice) and rshCD5 (**right panel**, 4 shCD6LckEμTg and 4 Non-Tg male mice) (2 μg) emulsified in CFA. Mouse sera were collected 2 weeks after the second boost (1 μg emulsified in IFA) and tested by ELISA for specific IgG antibody levels to rshCD5, rshCD6 or BSA. Data represented as mean OD450-620nm values ± SEM. *, $p<0.05$; ***, $p<0.0001$ (two-tailed Student's *t*-test).

In order to identify putative quantitative and/or qualitative changes in major lymphocyte subpopulations from primary and secondary lymphoid organs of shCD6LckEμTg mice, immunophenotyping analyses were performed. Regarding the former, total cell numbers from thymus and BM of shCD6LckEμTg mice did not significantly differ from those of Non-Tg controls (**Fig.IV.34a**). Further BM analysis did not reveal significant differences between shCD6LckEμTg and Non-Tg mice regarding the proportion of different B-cell developmental subsets (**Fig.IV.34b**). By contrast, significantly higher proportions of quantitatively minor (DN and $CD8^+SP$), but not major (DP and $CD4^+SP$) thymocyte subsets were found in shCD6LckEμTg mice compared with Non-Tg ones (**Fig.IV.34c**). Proportion of T_{reg} cells was also equal between shCD6LckEμTg mice and Non-Tg mice (**Fig.IV.34c**). These results support a role of CD6-mediated interactions during T-cell but not B-cell development.

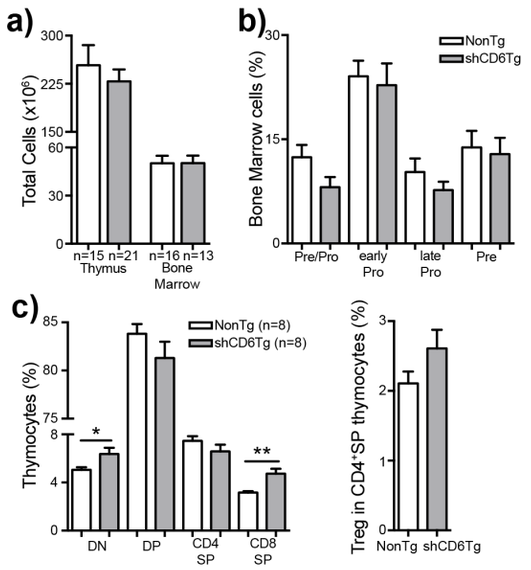

Fig.IV.34 – Immunophenotypical characterization of primary lymphoid organs from shCD6LckEμTg mice. **a)** Total lymphoid cell numbers from thymus and BM of shCD6LckEμTg (n = 21 and n = 13, respectively) and Non-Tg (n = 15 and n = 16, respectively) mice. **b)** Percentage of $CD24^{low}BP\text{-}1^-$ (Pre-Pro B cells), $CD24^+BP\text{-}1^-$ (early Pro B cells), $CD24^+BP\text{-}1^+$ (late Pro B cells) and $CD24^{high}BP\text{-}1^+$ (Pre B cells) within gated $CD43^+B220^+$

BM cells from shCD6LckEμTg (n = 15) and Non-Tg (n = 15) mice. **c) Left panel**, Percentage of $CD4^-CD8^-$ (DN), $CD4^+CD8^+$ (DP), $CD4^+CD8^-$ ($CD4^+$SP) and $CD4^-CD8^+$ ($CD8^+$SP) thymocytes from shCD6LckEμTg (n = 8) and Non-Tg (n = 8) mice. **Right panel**, Percentage of $CD25^+FoxP3^+$ within $CD4^+CD8^-$ gated cells from the same groups of mice as in left panel. Data are cumulative results from two or more different experiments, and are represented as mean ± SEM. *, $p<0.05$; **, $p<0.01$ (two-tailed Student's *t*-test).

Concerning peripheral tissues, total cell numbers from spleen and LN - but not peritoneal cavity - were significantly lower in shCD6LckEμTg mice compared with Non-Tg controls (**Fig.IV.35a**). Further lymphocyte subset analysis showed no significant differences regarding the percentage of spleen T ($CD4^+$), B ($CD19^+$), NK ($NK\text{-}1.1^+$,) and macrophage ($CD11c^+F4/80^+$MHC II^+) cells, with the only exception being a significantly lower frequency of $CD8^+$T cells in shCD6LckEμTg mice (**Fig.IV.35b**). Inconsistently, LN analyses showed no significant differences regarding the percentage of $CD8^+$T and NK cells, though a significantly higher frequency of $CD4^+$T and B cells and a lower frequency of macrophages was observed in shCD6LckEμTg mice (**Fig.IV.35c**). Interestingly, the percentage $CD25^+FoxP3^+$ cells within the $CD4^+$ subset was found to be significantly decreased in both spleen and LN samples from shCD6LckEμTg mice (**Fig.IV.35b-c, right**).

Assessment of the underlying causes of lower spleen and LN total cell numbers was carried out by analyzing the *in vivo* levels of apoptotic and proliferating cells. Apoptotic cell level detection by Annexin V and 7-AAD staining showed no significant differences between shCD6LckEμTg and Non-Tg mice (**Fig.IV.35d**). Investigation of *in vivo* BrdU-incorporation assays revealed a statistically significant lower percentage of $BrdU^+$ spleen cells and a trend for a lower percentage in LN cells among shCD6LckEμTg mice (**Fig. IV.35e** and **f**). A more detailed analysis showed that lower BrdU-incorporation affected both T and B cell compartments, although it only reached statistical significance for spleen B ($CD19^+$) cells, supporting lower (homeostatic) proliferation as the main putative cause of reduced lymphoid organ cellularity.

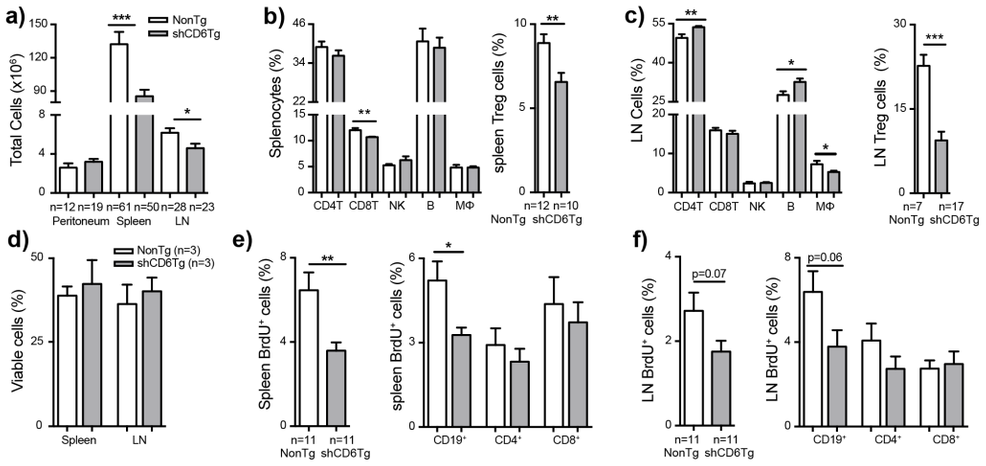

Fig.IV.35 – Immunophenotypical characterization of secondary lymphoid organs from shCD6LckEμTg mice. **a)** Total lymphoid cell numbers in peritoneal cavity, spleen, and LN from shCD6LckEμTg (n = 19, n = 50, and n = 23, respectively) and Non-Tg (n = 12, n = 61, and n = 28, respectively) mice. **b) Left panel**, Percentage of spleen T ($CD4^+$ and $CD8^+$), NK, B and MØ cells from shCD6LckEμTg (n = 15) and Non-Tg (n = 10) mice. **Right panel**, Percentage of $CD25^+FoxP3^+$ within $CD4^+$ gated T cells from shCD6LckEμTg (n = 10) mice and Non-Tg (n = 12) mice. **c) Left panel**, Percentage of LN T ($CD4^+$ and $CD8^+$), NK, B and MØ cells from shCD6LckEμTg (n = 15) and Non-Tg (n = 15) mice. **Right panel**, Percentage of $CD25^+FoxP3^+$ within $CD4^+$ gated T cells from LN of shCD6LckEμTg (n = 12) and Non-Tg (n = 10) mice. **d)** Percentage of viable cells ($7AAD^+Annexin\ V^+$) from spleen and LN of shCD6LckEμTg (n = 3) and Non-Tg (n = 3) mice. The results shown are from one representative experiment out of two independents performed. **e) Left panel**, Percentage of spleen $BrdU^+$ cells from shCD6LckEμTg (n = 11) and Non-Tg (n = 11) mice. **Right panel**, Percentage of spleen $BrdU^+$ cells within $CD19^+$, $CD4^+$ and $CD8^+$ from the same groups of mice as in the left panel. **f) Left panel**, Percentage of $BrdU^+$ cells from LN of shCD6LckEμTg (n = 11) and Non-Tg (n = 11) mice. **Right panel**, Percentage of $BrdU^+$ cells within $CD19^+$, $CD4^+$ and $CD8^+$ subsets from LN of the same groups of mice as in left panel. Data are cumulative results from at least two independent experiments, and are represented as mean ± SEM. *, $p<0.05$; **, $p<0.01$; ***, $p<0.0001$ (two-tailed Student's *t*-test).

Next, experiments were addressed to verify whether transgenic shCD6 could impair the function of the membrane-bound CD6 form by preventing its interaction with the CD6 ligand/s, and whether its effects were compatible with a negative/positive immunomodulatory role of CD6. Accordingly, the *in vitro* mAb-induced CD3-crosslinking of sorted $CD4^+$ and $CD8^+$ T cells from shCD6LckEμTg mice led to significantly increased proliferative responses compared with Non-Tg controls. However, these differences were lost under CD28 co-stimulation conditions (**Fig.IV.36a**). Regarding cytokine production, shCD6LckEμTg mice $CD4^+$ T cells - but not $CD8^+$ T cells - produced higher levels of IL-2 under both stimulatory conditions, (**Fig.IV.36c top/middle panels**). IFN-γ was found

elevated only following co-stimulation (anti-CD3 plus anti-CD28 mAb) of $CD4^+$ T cells from shCD6LckEμTg mice (**Fig.IV.36c top/middle panels**). As for TGF-β levels, there was high dispersion of values for both conditions, and so no significant differences were observed (**Fig. IV.36ctop/middle panels**).

Besides the decreased proportion of T_{reg} cells in spleen and LN we also wanted to assess whether their function was affected. As shown by **Fig.IV.36b**, sorted spleen $CD4^+CD25^+$ T cells from shCD6LckEμTg mice exhibited lower *in vitro* suppression activity than those from Non-Tg controls. No significant differences were observed regarding IL-2, IFN-γ, and TGF-β cytokine levels in supernatants from this T_{reg} suppression assay (**Fig. IV.36c, bottom panel**).

When whole splenocytes were assessed for *in vitro* proliferation studies, similar results to those above mentioned for sorted T cells were obtained. Thus, anti-CD3 stimulation induced significantly higher proliferative responses in $CD4^+$ and $CD8^+$ subsets from shCD6LckEμTg mice compared with Non-Tg controls (**Fig.IV.36d**). Again, the differences observed were lost in the presence of co-stimulation with anti-CD3 plus anti-CD28 (**Fig.IV.36d**). In cell supernatants following anti-CD3 stimulation, the IFN-γ levels were higher for the shCD6LckEμTg mice (**Fig.IV.36e**). Regarding the expression of the early cell activation marker CD69, no significant differences between both groups were observed (**Fig.IV.36f**).

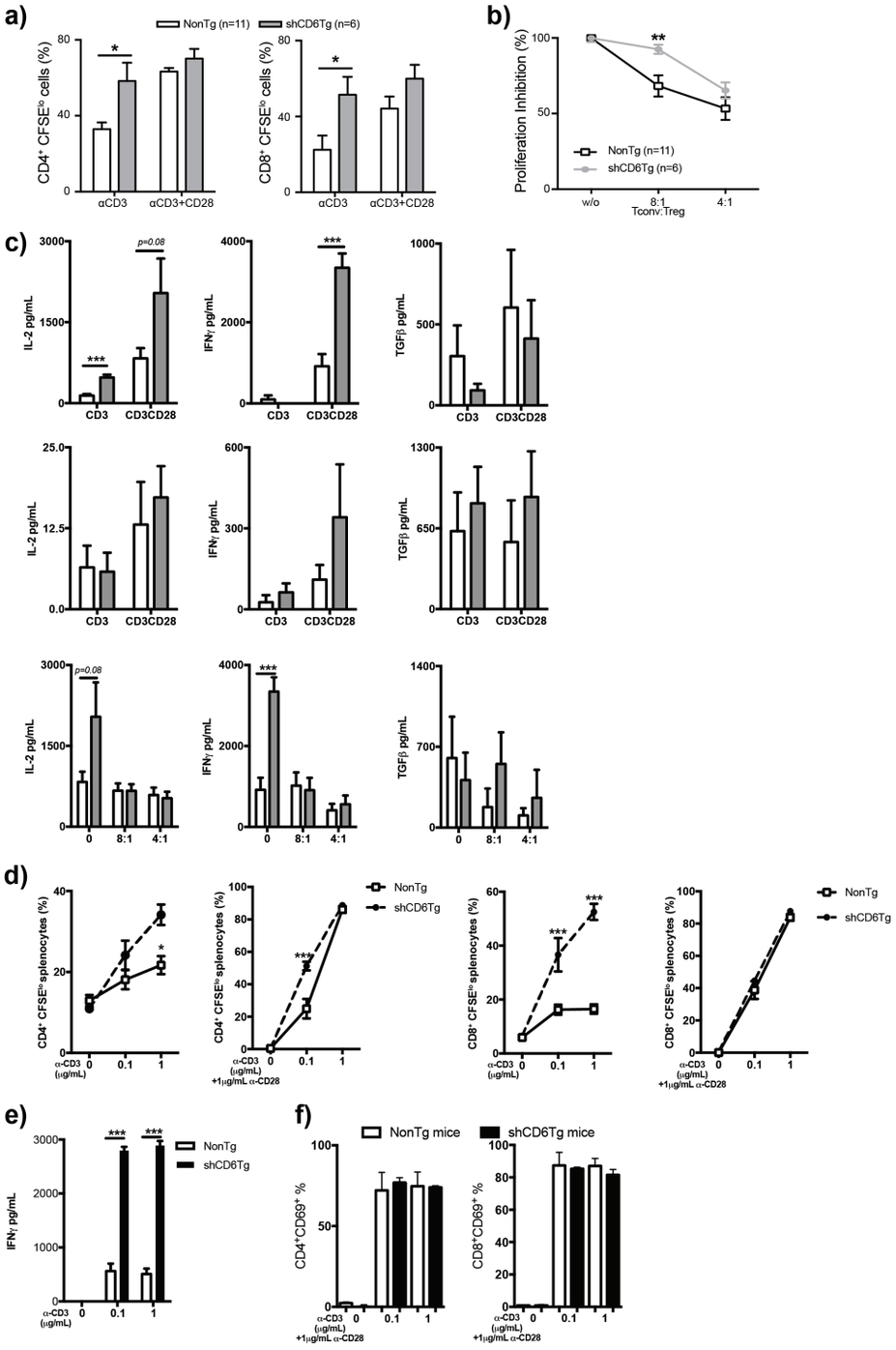

Fig.IV.36 – Ex vivo analysis of the T-cell proliferative and suppressive responses of shCD6LckEμTg mice. **a)** Proliferative responses of sorted CFSE-labeled $CD4^+$ (**left panel**) and $CD8^+$ (**right panel**) T cells from shCD6LckEμTg (n = 6) or Non-Tg (n = 11) spleens cultured for 72 h in the presence of plastic-bound anti-CD3 alone or plus soluble anti-CD28 mAb. **b)** Percentage of $CD4^+CD25^-$ (T_{conv}) cell proliferation inhibition from Non-Tg mice stimulated for 72 h with plastic-bound anti-CD3 mAb plus soluble anti-CD28 mAb in the absence (w/o) or presence of different ratios of $CD4^+CD25^+$ (T_{reg}) cells from shCD6LckEμTg (n = 6) or Non-Tg (n = 11) mice. **c)** Levels of IL-2, IFN-γ and TGF-β in the supernatants of sorted $CD4^+$ (**top panels**) and $CD8^+$ (**middle panels**) T cells from the same experiment as in a); same is also shown

(**bottom panels**) for supernatants from the experiment depicted in b). **d)** Proliferative responses of CD4⁺ (**left panel**) and CD8⁺ (**right panel**) T cells from whole spleen cell suspensions of shCD6LckEμTg (n = 9) or Non-Tg (n = 9) cultured for 72 h in the presence of anti-CD3 alone or plus soluble anti-CD28 (3 independent experiments with 3 mice pools each time in triplicate). **e)** IFN-γ levels in supernatants from whole splenocytes stimulated with anti-CD3 alone as in d). **f)** CD69⁺ expression in CD4⁺ and CD8⁺ T cells from whole spleen cell suspensions stimulated with anti-CD3 alone as in d) for 18 h. Data are represented as mean ± SEM. *, p<0.05; **, p<0.01; ***, p<0.0001 (two-tailed Student's *t*-test).

Next, the effect of rshCD6 on the *in vitro* proliferative responses of CD4⁺ T cells from WT mice was explored. To this end, sorted spleen CD4⁺ T cells were stimulated with anti-CD3 and anti-CD28 in the presence of different concentrations of rshCD6. As shown by **Fig.IV.37a**, low rshCD6 concentrations (1 μg/mL) induced a significant reduction of CD4⁺ T cell proliferation, while higher concentrations (10 μg/mL) induced a significant increase. By contrast, the presence of rshCD6 (at both low and high concentrations) did not induce any significant change on the suppressive activity of T_{reg} cells from WT mice (**Fig.IV.37b**). Regarding cytokine production, there were trends indicating higher levels of secretion of IL-2, IFN-γ and TGF-β; however, we found no significant differences due to value dispersion (**Fig.IV.37c**).

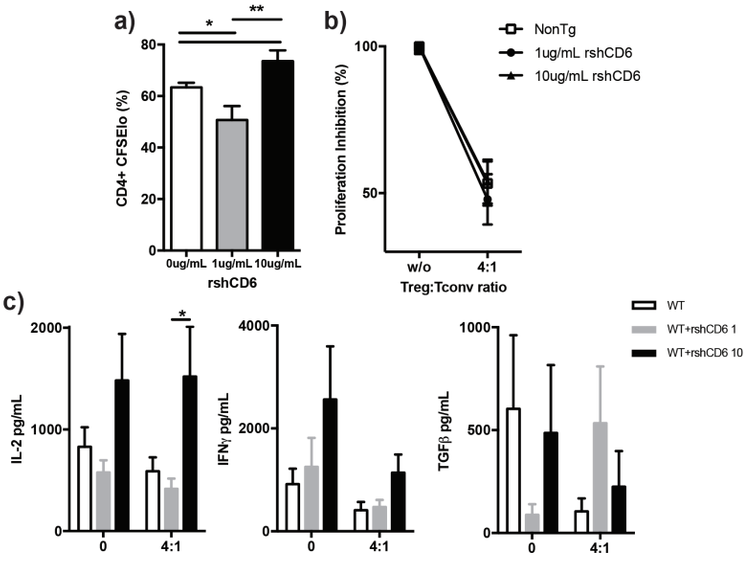

Fig.IV.37 – Ex vivo analysis of the proliferative and suppressive responses of CD4⁺ T cells from WT mice in the presence of exogenous rshCD6. **a)** Proliferative responses of sorted CFSE-labeled CD4⁺ T cells from WT mice (n = 11) spleens were stimulated for 72 h with plastic-bound anti-CD3 plus soluble anti-CD28 in the presence or absence of rshCD6 (1 or 10 μg/mL). **b)** Suppression assays of WT T_{conv} cells by WT T_{reg} cells in the presence of rshCD6. Sorted WT $CD4^+CD25^-$ (T_{conv}) cells stimulated for 72 h with plastic-bound anti-CD3 plus soluble anti-CD28 mAb in the absence (w/o) or the presence of sorted $CD4^+CD25^+$ (T_{reg}) cells from WT (n = 11) mice at a T_{reg}:T_{conv} ration of 4:1, in the presence of different amounts of rshCD6 (0, 1 or 10 μg/mL). **c)** Levels of IL-2, IFN-γ and TGF-β in the supernatants of the suppression assays performed in b). Data are represented as mean ± SEM. *, p<0.05; **, p<0.01; (two-tailed Student's *t*-test).

Given the decreased total cell numbers observed in shCD6LckEμTg spleens and the lower BrdU incorporation of splenocytes from the same mice (mainly at the expense of B cells), the *in vitro* response of spleen B cells to different stimuli was also analyzed. Under both BCR-dependent (IgM crosslinking alone or in the presence of anti-CD40 or IL-4) and BCR-independent (LPS alone or in the presence of IL-4) stimulatory conditions, a trend for decreased proliferative responses was observed compared with Non-Tg mice. These differences were statistically significant when B cells were co-stimulated with anti-IgM or LPS plus IL-4 (**Fig.IV.38a**). The analysis of IL-6 and IL-10 cytokine levels in supernatants from the previously mentioned stimulatory conditions did not result in any statistically significant differences (**Fig.IV.38b**).

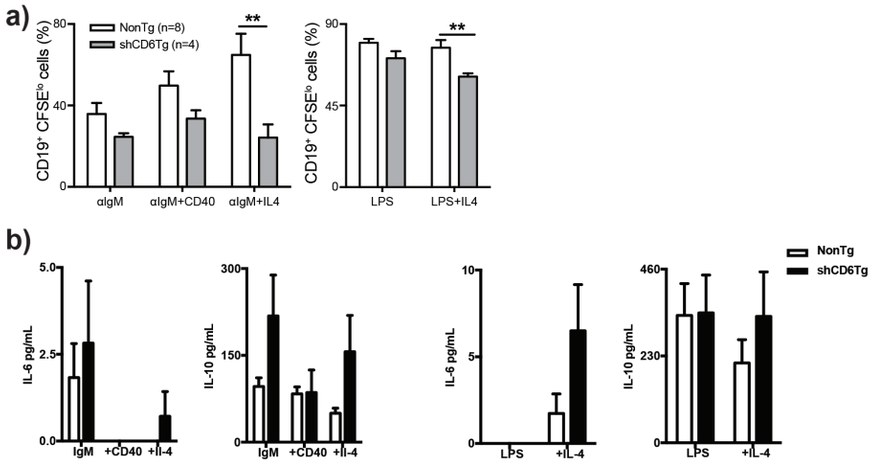

Fig.IV.38 – Ex vivo analysis of B-cell proliferative responses of shCD6LckEμTg mice. **a)** Proliferative responses of sorted CFSE-labeled CD19⁺ cells from shCD6LckEμTg (n = 4) or Non-Tg (n = 8) spleens cultured for 72 h with anti-IgM alone or in combination with anti-CD40 or IL-4 (**left panel**) or with LPS alone or plus IL-4 (**right panel**). **b)** Levels of IL-6 and IL-10 in culture supernatants from the same experimental conditions as in a). Data are represented as mean ± SEM. **, p<0.01; (two-tailed Student's *t*-test).

2.2. CHARACTERIZATION OF IMMUNOPHENOTYPICAL CHANGES INDUCED BY SUSTAINED INFUSION OF EXOGENOUS RSHCD6 PROTEIN TO WT MICE

To rule out the possibility that the immunophenotypical changes observed in shCD6LckEμTg mice were not due to increased serum shCD6 levels but to transgenesis-related artifacts, similar analyses were performed in WT C57BL/6 mice treated every-other-day for 14 days with *i.p.* infusions of purified recombinant shCD6 protein (rshCD6, 1.25 mg/kg) or vehicle (PBS plus 10 % glycerol). As illustrated by **Fig.IV.39a**, statistically significant reductions of total cell numbers was detected in spleen and LN but not thymus of rshCD6-treated mice. Intriguingly, total cell numbers were significantly higher in the peritoneal cavity of rshCD6-treated mice (**Fig.IV.39a**), a fact that could be attributed to local inflammatory effects of *i.p.* rshCD6 infusion or blockade of CD166/ALCAM-

mediated cell traffic across the peritoneal vessels or serous membrane. Regarding qualitative changes in spleen, no significant differences were observed in the percentages of B and NK cells, while those of CD4$^+$ and CD8$^+$ T cells were significantly decreased in rshCD6-treated mice (**Fig. IV.39b**). In LN samples, only a significant reduction in the percentage of CD8$^+$ T cells could be detected in rshCD6-treated mice (**Fig.IV.39c**). Interestingly, the percentage of CD25$^+$FoxP3$^+$ cells within the CD4$^+$ subset was also found to be significantly decreased in LN but not spleen samples from rshCD6-treated mice (**Fig.IV.39b** and **c, right**). The thymi of these mice were also analyzed and no differences were detected between the two groups regarding the main thymocyte developmental stages (DN, DP, CS4$^+$SP and CD8$^+$SP) (**Fig.IV.39d**). Altogether, these results show that administration of exogenous rshCD6 reproduces some of the lymphocyte subset changes found in transgenic (shCD6LckEμTg) mice.

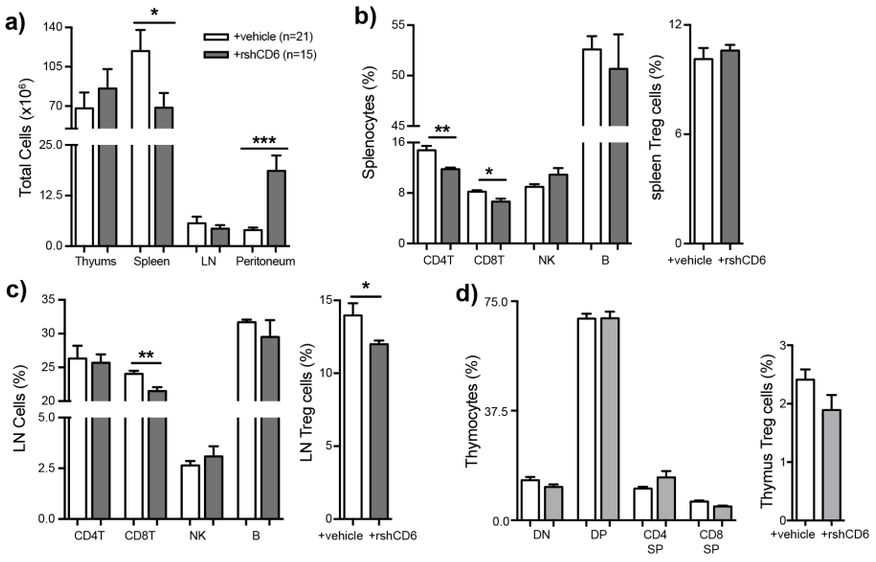

Fig.IV.39 – Immunophenotypical analyses of lymphoid organs from WT C57BL/6 mice treated with exogenous rshCD6. **a)** Total cell numbers from thymus, spleen, LN and peritoneum of C57BL/6 mice treated every 48 h for 14 days with 25 μg of rshCD6 (n = 15) or vehicle (PBS 10 % glycerol, n = 21). **b)** Percentage of spleen CD4$^+$ T, CD8$^+$ T, NK, and CD19$^+$ B cell populations (**left panel**), and CD25$^+$FoxP3$^+$ in CD4$^+$T cells (T_{reg}) (**right panel**) from the same group of mice as in a). **c)** Percentage of CD4$^+$ T, CD8$^+$ T, NK, CD19$^+$ B cells (**left panel**), and CD25$^+$FoxP3$^+$ in CD4$^+$T cells (T_{reg}) (**right panel**) from LN of the same group of mice as in a). **d)** Percentage of DN, DP, CD4$^+$SP and CD8$^+$SP cells (**left panel**), and CD25$^+$FoxP3$^+$ in CD4$^+$T cells (T_{reg}) (**right panel**) from thymus of the same group of mice as in a). Data are cumulative results from two different experiments and presented as mean ± SEM. * $p<0.05$, ** $p<0.01$, *** $p<0.0001$ two-tailed Student's *t*-test.

2.3. FUNCTIONAL CHARACTERIZATION OF HOMOZYGOUS shCD6LckEμTg MICE

In order to further explore the *in vivo* functional consequences of the immunophenotypical changes observed in shCD6LckEmTg) mice, they were immune challenged to different experimental models.

2.3.1. Humoral Response To TD And TI Antigens

Interestingly, homozygous shCD6LckEμTg mice showed significantly higher levels of serum anti-CD5 antibodies than Non-Tg controls. Concordantly to the increment in the serum anti-CD5 antibodies production by the shCD6LckEμTg mice, increased *in vivo* humoral responses were also observed when homozygous shCD6LckEμTg mice were challenged with both T-independent (TI; Ficoll or LPS) or T-dependent (TD; keyhole limpet hemocyanin, KLH) antigens conjugated to the trinitrophenol (TNP) hapten. As illustrated by **Fig.IV.40**, shCD6LckEμTg mice exhibited statistically significant increased levels of anti-TNP antibodies of IgG_1 and IgG_{2b} subclasses when challenged with TD (TNP_5-KLH) antigen, which is indicative of increased T_H2 and T_H1 responses, respectively. When challenged with TI type 2 (TNP_{65}-Ficoll) antigen statistically increased levels of TNP-specific IgG_{2c} and IgG_3 antibodies were observed. By contrast, when challenged with TI type 1 ($TNP_{0,3}$-LPS) antigen there were almost no differences in Ig levels, but a significant decrease of TNP-specific antibodies of IgG_3 subclass (**Fig.IV.40**). Overall, the antibody production seems higher in the shCD6LckEμTg mice to TD and TI type 2 antigens, but to TI type 1 antigen (LPS) the antibody production is the same to both groups. It was described that sCD6 recognize and aggregates LPS, which could be the reason to the lower response observed.

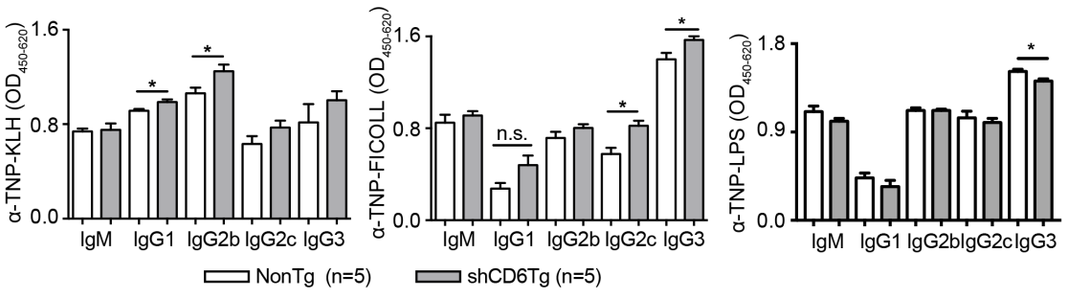

Fig.IV.40 – Analysis of humoral responses of shCD6LckEμTg and Non-Tg mice to TD and TI antigens. Antibody response to TD, TI-2 and TI-1 antigens. shCD6LckEμTg (n = 5) and Non-Tg (n = 5) mice were immunized (*i.p.*) with 50 μg of TNP_5-KLH (TD; **left panel**), TNP_{65}-Ficoll (TI-2; **middle panel**) and $TNP_{0,3}$-LPS (TI-1; **right panel**). Sera were collected at day 21 (TD) or 14 (TI-1/2) for ELISA determination of TNP-specific IgM and IgG subclass levels. Data are expressed as mean ± SEM of OD 450-620 nm values. *, $p < 0.05$; **, $p < 0.01$; ***, $p < 0.0001$ (two-tailed Student's *t*-test).

2.3.2. LPS-Induced Septic Shock

As previously reported by our group, shCD6 is capable of binding to bacterial PAMPs and, consequently, of protecting mice from LPS-induced septic shock when exogenously infused at high concentrations (1.25 mg/kg) (M.-R. Sarrias et al. 2007). Thereby, we decided to verify whether the shCD6LckEμTg mice would also be protected from an LPS-induced septic shock compared to Non-Tg mice. Both groups showed 100 % survival rate (**Fig.IV.41a**) following *i.p.* LPS administration at the relatively low concentration chosen (1 mg/Kg). The analysis of serum levels of several cytokines also did not show significant differences between shCD6LckEμTg and Non-Tg mice; however, there were some trends toward lower levels in all of the cytokines tested in shCD6LckEμTg mice sera, as represented in **Fig.IV.41b-e**.

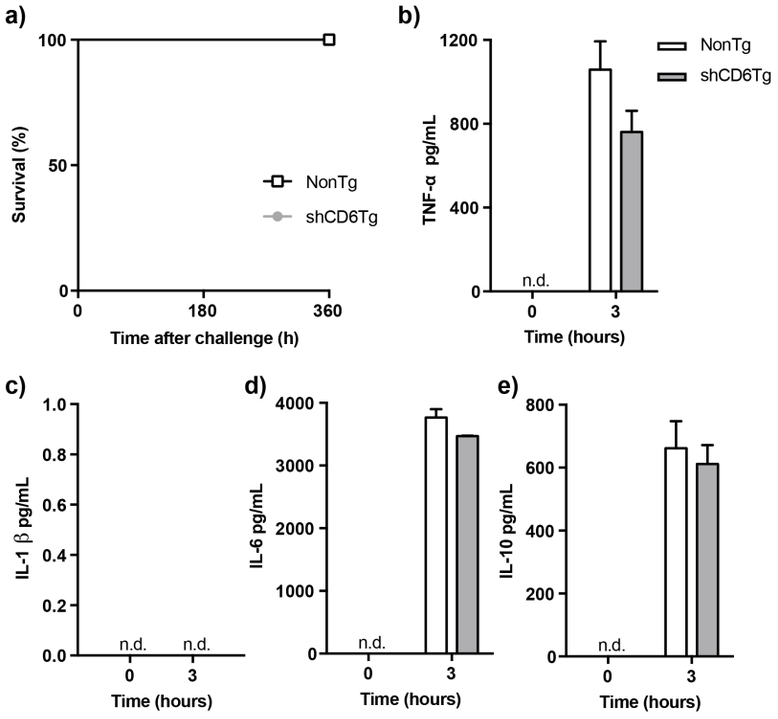

Fig.IV.41 – shCD6LckEμTg mice response to LPS-induced septic shock. **a)** Male mice were *i.p.* injected with LPS (1 mg/kg) and the survival rate was monitored up to 15 days. **b-e)** Plasma levels of pro- (TNF-α, IL-1β, IL-6) and anti- (IL-10) inflammatory cytokines were monitored by ELISA at the indicated time points (0h and +3h) post LPS-induced septic shock in shCD6LckEμTg (n = 3) and Non-Tg (n = 6) mice. Data are expressed as pg/mL (mean ± SD). Statistical comparisons made by using the two-tailed Student *t*-test. n.d., non-detected.

These results indicate that the serum shCD6 levels expressed by shCD6LckEμTg mice (in the ng/mL range) would be very likely insufficient to achieve the protective effects against LPS-induced septic shock previously observed by *i.p.* infusion of rshCD6 (in the μg/mL range). However, it would be interesting to further explore whether shCD6LckEμTg mice show significantly blunted inflammatory responses induced by

lower LPS concentrations than those here tested.

2.3.3. Cancer Models

To further elucidate the functional relevance of the *in vivo* and *in vitro* findings made in shCD6LckEμTg mice, their cellular immune responses were explored by challenging them with ectopically injected autologous cancer cells. As shown in **Fig.IV.42a** (**left panel**), growth of *s.c.* injected melanoma B16-F0 tumor cells, which constitutively express high CD166/ALCAM surface levels, was significantly slower in shCD6LckEμTg mice than in Non-Tg controls kept under SPF conditions (**Fig.IV.42a, left panel**). Tumor weight at the end of the follow-up period (day 20) was also reduced but the differences did not reach statistical significance (**Fig.IV.42a, right panel**). A similar analysis performed with autologous tumor cells from different lineage origins (sarcoma MCA-205 and lymphoma RMA-S cells) also showed significantly reduced tumor growth in shCD6LckEμTg mice (**Fig. IV.42b** and **c**). This would indicate that the enhanced anti-tumor response exhibited by shCD6LckEμTg mice is broad and not tumor cell-type specific.

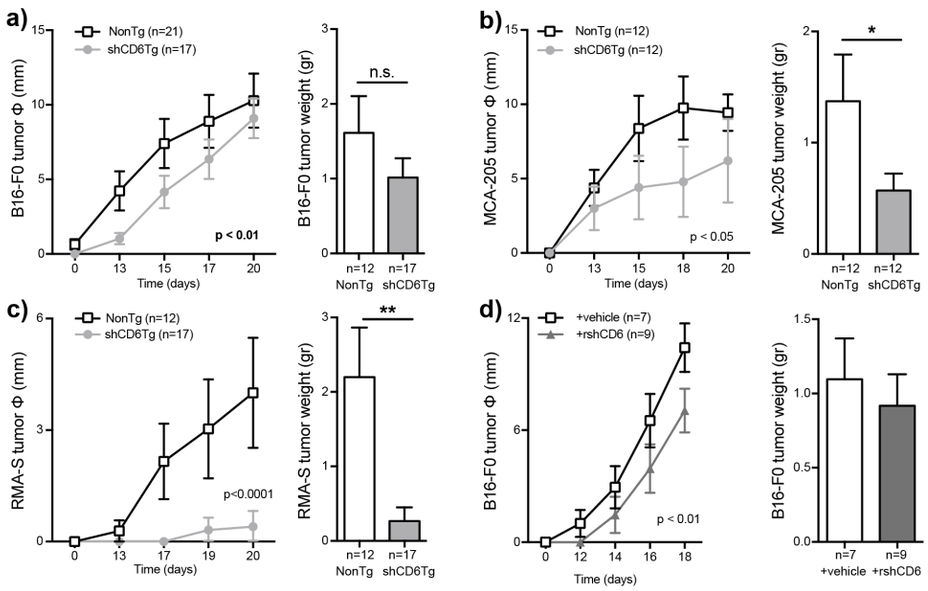

Fig.IV.42 – Enhanced antitumor response in shCD6LckEμTg mice and rshCD6-treated WT mice. **a).** Autologous B16-F0 (5 x 10^4) cells were injected *s.c.* into shCD6LckEμTg (n = 21) and Non-Tg (n = 17) mice. Tumor growth (Ø, diameter in mm) (**left panel**) and weight (gr) (**right panel**) were measured every other day and at sacrifice (day 20), respectively. Data are cumulative from three different experiments. **b)** Autologous MCA-205 (5 x 10^4) cells were *s.c.* injected into shCD6LckEμTg (n = 12) and Non-Tg (n = 12) mice. Tumor growth (**left panel**) and weight (**right panel**) were measured as in a). Data are cumulative from two different experiments. **c)** Autologous RMA-S (2.5 x 10^4) cells were injected *s.c.* into shCD6LckEμTg (n = 17) and Non-Tg (n = 12) mice. Tumor growth (**left panel**) and weight (**right panel**) were measured as in a). **d)** B16-F0 (5 x 10^4) cells were *s.c.* injected into C57BL/6 WT mice receiving *i.p.* injections of rshCD6 (1.25 mg/Kg; n = 9) or vehicle (PBS 10 % glycerol; n = 7) every other day from tumor implantation. Tumor growth

(**left panel**) and weight (**right panel**) were measured as in a). Two-way ANOVA and Mann Whitney tests were used for statistical analysis of tumor growth and weight, respectively. Data are presented as mean ± SEM. * $p<0.05$; ** $p<0.01$.

In order to further investigate whether infusion of exogenous rshCD6 protein could also delay tumor cell growth *in vivo*, WT C57BL/6 mice were implanted (*s.c.*) with B16-F0 cells and then infused (*i.p.*) with HSA in PBS plus 10 % glycerol (vehicle) or rshCD6 (1.25 mg/Kg) every other day from the day of tumor implantation. As illustrated by **Fig. IV.42d**, rshCD6-treated mice kept under SPF conditions showed a statistically significant reduction in B16-F0 tumor cell growth compared to mice treated with vehicle. This result supports circulating shCD6 as responsible for the enhanced anti-tumor response observed in shCD6LckEμTg mice, and also opens the possibility of modulating the anti-tumoral response *in vivo* through rshCD6 infusion.

Interestingly, with shCD6LckEμTg mice we were able to see differences in the tumor growth in a SPF facility, unlike with both CD5 transgenic mice. Despite it, we still performed a preliminary evaluation of the gut microbiota of these mice when housed in the SPF facility (in collaboration with Dr. Jose González and Dr. Eduardo Huarte, South Dakota State University). As illustrated by **Fig.IV.43a**, there were some genus differences between them, such as, reduction in Firmicutes – Clostridia and Verrucomicrobia phylum, and an expansion of Bacteroidetes phylum, Firmicutes – Bacilli and Erysipelotrichia class in the shCD6LckEμTg mice. More differences were detected among other lesser abundant bacteria. When analyzed in more detail (**Fig.IV.43b**), an increment in Prevotellaceae and Lactobacillaceae and a decrease in Rikenellaceae families was observed in the shCD6LckEμTg mice.

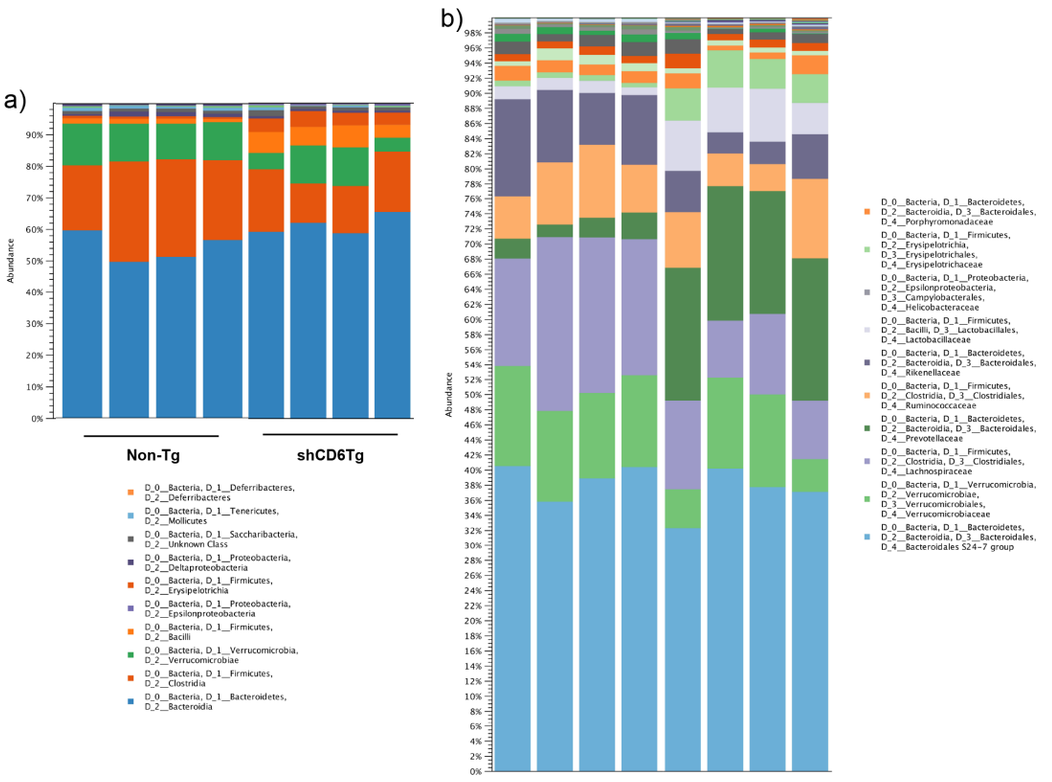

Fig.IV.43 – Influence of mice genetic background in the mice microbiota in a SPF facility. **a)** and **b)** shCD6LckEμTg (n = 4) and Non-Tg mice (n = 4) fecal samples were collected when housed in a SPF facility. Next-generation sequencing was performed to identify different bacteria genus present on the samples.

2.3.4. Autoimmune Disease Models

The drawback of dysregulated immune responses effective for tumor growth control is that they could also break self-tolerance and facilitate autoimmune disorders. Thus, the putative deleterious effects of circulating levels of shCD6 in mouse models of T-cell mediated autoimmune diseases were analyzed.

2.3.4.1. Experimental Autoimmune Encephalitis Model

First, the susceptibility of shCD6LckEμTg and Non-Tg mice to EAE, a well-established model of autoimmune disease resembling human Multiple Sclerosis, was explored. EAE shares many clinical and pathophysiological characteristics with Multiple Sclerosis. Actively-induced EAE with myelin peptides (myelin oligodendrocyte glycoprotein - MOG) in female C57BL/6 mice is easy and present replicable results. The low immunogenicity of these peptides, makes necessary the combination with adjuvants, such as complete Freund's adjuvant (CFA). The immunogenic epitope MOG_{35-55} is suspended in CFA prior to immunization and pertussis toxin is applied on the day of immunization and two days later. Mice develop a "classic" self-limited monophasic EAE with ascending flaccid paralysis within 9-14 days after immunization, disease maximum about 3-5 days

after disease onset and slow and partial symptom recovery over the next 10-20 days. CFA will activate the mononuclear phagocytes inducing the phagocytosis of these molecules and the secretion of cytokines. This results in the prolongation of the presence of antigens and a more efficient transport of these to the lymphatic system. Pertussis toxin has been suggested as a modulator of the blood-brain barrier and its immunological responsiveness.

As illustrated by **Fig.IV.44a**, shCD6LckEμTg mice kept under non-SPF (conventional) housing conditions showed a significantly lower clinical score than Non-Tg controls. The same EAE model was performed in WT female mice treated with rshCD6 or vehicle every other day for the duration of the experiment (from the induction day - day 0 - until day 30). Again, rshCD6-treated mice presented a significantly lower clinical score (**Fig. IV.44b**), thus confirming that the presence of circulating shCD6 attenuates EAE.

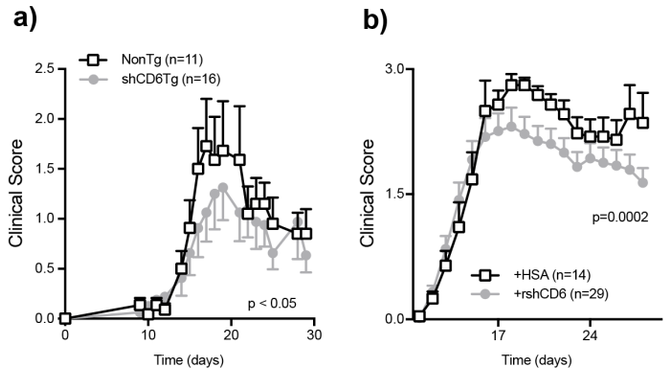

Fig.IV.44 – Attenuated EAE in shCD6LckEμTg mice and rshCD6-treated C57BL/6 WT mice. **a)** Clinical scores of 8–10 week old female shCD6LckEμTg (n = 16) and Non-Tg (n = 11) mice subjected to EAE. Graph shows cumulative data from two independent experiments. **b)** Clinical scores of 8-week-old C57BL/6 WT female mice subjected to EAE and treated *i.p.* with rshCD6 (1.25 mg/Kg; n = 29) or HSA (1.25 mg/Kg in PBS-10 % glycerol; n = 14) every 48 h, starting from day 0. Cumulative data from two independent experiments and presented as mean ± SEM. Two-way ANOVA test was used for statistical analysis.

2.3.4.2. Collagen-Induced Arthritis Model

To disclose the possibility that the attenuated autoimmune response was exclusive to EAE, CIA -a well-established model of autoimmune disease resembling human Rheumatoid Arthritis- was next explored (in collaboration with Dr. Merino, CSIC-UC-SODERCAN, Santander). The classical CIA model, as performed with shCD5EμTg mice, is based in type II collagen immunization in DBA/1 mice strain, since some mice strains are resistant to CIA (like C57BL/6 strain). The solution was to backcross the genetically modified strain onto the DBA/1 background. However, it is expensive and time consuming. An alternative CIA protocol was described, enabling CIA induction in C57BL/6 mice, immunizing the mice with chicken (instead of bovine) type II collagen plus CFA. It is worth mentioning, that variability in incidence and severity is expected in this model, and

that they are generally lower than in the DBA/1 mice model.

As shown by **Fig.IV.45a-b**, both the clinical score and the cumulative incidence were significantly lower for shCD6LckEμTg mice compared with Non-Tg controls, both kept under conventional housing conditions. No statistically significant differences were observed, however, regarding serum levels of IgG anti-collagen antibodies (**Fig.IV.45c**), or joint mRNA levels for different pro- and anti-inflammatory cytokines and transcription factors analyzed (*il-6*, *il-10*, *foxp3*, *tgf-β*, *ifn-γ*, *il-1β*, *tnf-α*, *il-2*, *il-17α*, and *t-bet*) (**Fig. IV.45d**).

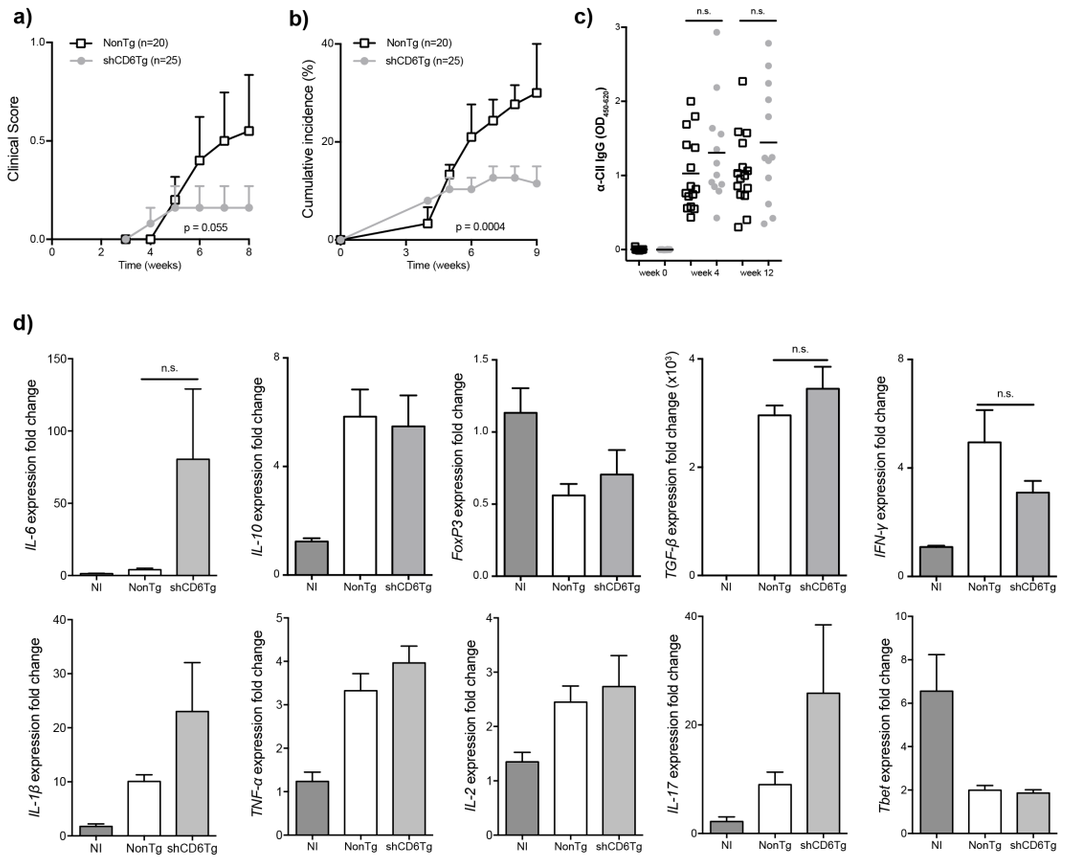

Fig. 45. Attenuated CIA in shCD6LckEμTg mice. **a)** 7–8 week old male shCD6LckEμTg (n = 25) and Non-Tg controls (n = 20) mice were immunized *s.c.* with type II chicken collagen emulsified in CFA plus M. tuberculosis. Radiological signs were scored weekly for each mouse and results for each group averaged to determine overall clinical score. **b)** Representation of cumulative incidence percentage in both groups. Data are cumulative results from three different experiments and presented as mean ± SEM. Two-way ANOVA test was used for statistical comparisons. **c)** Levels of serum IgG antibodies to type II collagen were measured by ELISA in the sera of both groups. Results are expressed as OD 450 nm - 620 nm. **d)** Quantitative RT-PCR analysis of joint mRNA levels (mean ± SD fold change of triplicates) of *il-6, il-10, foxp3, tgf-β, ifn-γ, il-1 β, tnf-α, il-2, il-17α*, and *tbet* relative to *gapdh* expression, before (NI, dark grey bars, n = 3) and 8 wk after CIA induction in shCD6LckEμTg (light grey bars, n = 8) and Non-Tg (white bars, n = 5) mice. Student's *t*-test were used for statistical comparisons of anti-collagen antibody and mRNA levels.

The drawback of dysregulated immune responses effective for tumor growth control is that they could also break self-tolerance and facilitate autoimmune disorders. Interestingly, with the two autoimmune disease models studied we observed a better outcome (lower clinical score) in the shCD6LckEμTg mice and rshCD6-treated mice. These results support that circulating shCD6 is also responsible for the attenuated autoimmune response, and raise the possibility of modulating autoimmune responses *in vivo* through rshCD6 infusion aside with improve the anti-tumor response as well. One hypothesis is that the shCD6 interferer with ALCAM-ALCAM, ALCAM-CD6, and CD318-CD6 interactions, interfering with lymphocyte infiltration and subsequent inflammation in autoimmune conditions.

3. RETROSPECTIVE ANALYSIS OF HUMAN SAMPLES FROM THE CANCER GENOME ATLAS DATABASE

During a short research stay abroad at the laboratory of Dr. Yvonne Saenger (Hematology/Oncology, New York-Presbyterian - Columbia University Medical Center, New York), we had the opportunity to analyze a pre-selected data set from "The Cancer Genome Atlas" database. The data set consisted of 409 melanoma tumor samples (biopsies) with gene expression data for 626 genes. Dividing the patient samples by alive/dead we observed that the "alive" group presented significantly higher expression levels of T (CD3, CD4, CD8) and B (CD19) cell markers, as well as of the CD5 and CD6 receptors (**Fig. IV.46a**). This would indicate that the samples from "alive" patients would have higher lymphocyte infiltration levels. Furthering the analysis with the "alive" group, we separated them into two new groups – with and without tumor in the last follow-up. The group with better survival and tumor regression (without tumor in the last follow-up) had lower CD3, CD4, CD8, CD19 expression but higher expression levels of CD5 and CD6 compared with the group with tumor (**Fig.IV.46b**). These results would suggest that the presence of lymphocyte infiltrates exhibiting higher CD5 and CD6 expression levels is associated with better prognosis in melanoma.

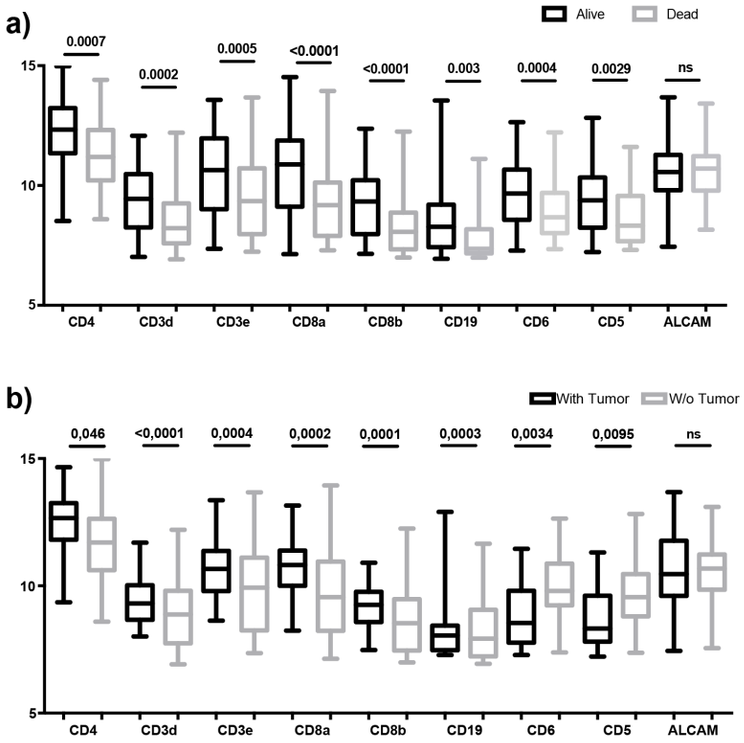

Fig.IV.46 – Retrospective analysis of gene expression in human melanoma samples. **a)** Melanoma tumor biopsies (n = 409) were divided into "alive" [being alive for more than 4 years (1460 days) from day of diagnosis; n = 74] or "dead" [being dead in less than 2 years (730 days) from diagnosis; n = 49)] groups. **b)** The alive group was subdivided into two other groups; with tumor (information of last follow-up; n = 16) and without tumor (information of last follow-up; n = 58). Gene expression values of CD3*d*, CD3*e*, CD4, CD8α, CD8β, CD19, CD6, CD5, and ALCAM are presented in both graphs. Mann-Whitney test was used for statistical comparisons between groups.

V. DISCUSION

This thesis had as its main aim to approach the *in vivo* characterization of the immunomodulatory properties of two highly homologous lymphocyte surface receptors – CD5 and CD6 - in health and disease. As a result from the duplication of a common ancestral gene, these two receptors share substantial structural and functional similarities, which make tackling their study in parallel inevitable. In spite of being two of the earliest lymphocyte receptors to be identified thanks to the mAb technology advent (more than 40 years ago), their *in vivo* functionality has not been fully unveiled yet. To date, their main functional features lie in that they both are: 1) physically associated to the antigen-specific clonotypic receptor present in all T cells and in the B1a cell subset (TCR and BCR, respectively), and 2) equipped with a cytoplasmic tail suitable for signaling transduction and, consequently, modulating (either positively or negatively) the activation/differentiation signals transduced by the TCR/BCR receptors. Despite the availability of mAbs for *in vitro* (and *in vivo*) studies, their signaling modulation characteristics could not be unequivocally disclosed until CD5-deficient (first) and CD6-deficient (more recently) mice were accessible.

In the case of CD5, studies with deficient mice definitively consolidated its role in the fine-tuning of antigen-mediated responses. However, some questions are still unanswered, such as the nature of its ligand/s, the biological role of its soluble form or the functional consequences of its ligation by PAMPs. More research is also needed to clarify the conflicting results concerning the role of $CD5^{+}$ cells in different autoimmune, infectious, and neoplastic disorders. Regarding the latter, recent evidence obtained with experimental tumor models suggests that CD5 function can be impaired in order to enhance the anti-tumor immune response, similar to other current immunotherapies for cancer. For all this, CD5 is an attractive target for developing novel immunotherapies aimed at potentiating or inhibiting ongoing immune responses, and also a candidate as a new immune-checkpoint molecule.

In contrast, until very recently there was no information available for CD6-deficency. It was only last year that the first CD6-deficient mice were described by our group (Orta-Mascaró et al., 2016), and at the beginning of this year a different group described a second CD6-deficient mouse line with a different background (Enyindah-Asonye et al., 2017b; Li et al., 2017). These two mouse models revealed new and interesting functions of CD6. Until 2012, CD6 was considered as a co-stimulatory molecule of the TCR and that year for the first time it was demonstrated that it could act as a negative regulator (Oliveira et al., 2012). This hypothesis was confirmed for thymocytes in one of the studies with CD6-deficient mice mentioned earlier (Orta-Mascaró et al., 2016). However, contradictory results obtained from CD6-deficient mice in different experimental models of disease (Consuegra-Fernandez et al., 2017; Enyindah-Asonye, Li, Xin, et al., 2017b; Li et al., 2017; Orta-Mascaró et al., 2016), makes CD6 function in peripheral T cells still a matter of

further study.

In any case, the information obtained from these CD5/6-deficient mouse models is very useful but, unfortunately, cannot be directly translated into humans mainly because of ethical constraints related to gene expression manipulation. To overcome this problem, some studies have tested the effects of mAbs against both proteins in different immune disorders (M. Consuegra-Fernández et al., 2015; Hernández, Moreno, Aira, & Rodríguez, 2016), but in this thesis, we have tried to demonstrate the usefulness of a different strategy – the potential applications of the CD5/6 soluble proteins as "decoy" receptors. Our hypothesis was that decoy shCD5/6 receptors could interfere with the heterophilic and/or homophilic interactions played by the CD5/6 ligand/s resulting in a "functional" knockdown effect. To test this, we generated different transgenic mouse lines (shCD5EμTg, shCD5LckEμTg and shCD6LckEμTg) that express shCD6 under the control of T and B lymphocyte-specific transcriptional regulatory elements (Ig heavy chain enhancer, Eμ; and Lck proximal promoter). This kind of strategy has been successfully used in the past to understand whether soluble forms could be exploited to manipulate *in vivo* immune responses (Bao et al., 2002; Hunger, Carnaud, Garcia, Vassalli, & Mueller, 1997; Mäkinen et al., 2001; Peters et al., 1996; Ronchese, Hausmann, Hubele, & Lane, 1994; Tamura et al., 1999). Indeed, a great advantage of this strategy is that the results can be easily translated to clinical practice by means of already existing exogenous or endogenous protein delivery systems.

1. CHARACTERIZATION OF THE IMMUNOMODULATORY PROPERTIES OF SOLUBLE CD5 IN BOTH TRANSGENIC AND EXOGENOUSLY INFUSED FORMS

Recent available evidence supports the involvement of CD5 in the regulation of immune responses in general and of antitumor responses in particular (Marta Consuegra-Fernández et al., 2015; Soldevila, Raman, & Lozano, 2011; Tabbekh, Mokrani-Hammani, Bismuth, & Mami-Chouaib, 2013). The results obtained in this thesis would help set the basis for listing CD5 as an immune checkpoint inhibitor candidate and, consequently, targeting CD5 to improve the efficacy of current immunotherapeutic approaches against cancer.

Our study has confirmed the importance of the functional blockade of CD5 in the anti-tumor immune response; CD5 acts in a similar way to other immune checkpoints, and as such, its blockade results in an enhanced immune response. In this work, we studied the effect of functional blockade of membrane-bound CD5 by increasing the levels of the soluble receptor form which would work as a decoy-receptor. In order to avoid repeated infusions of purified protein (for economic reasons) and to maintain the levels of protein stable during the desired time (from early embryonic developmental stages), we designed shCD5-expressing transgenic mouse lines. As mentioned above, a similar

strategy has been successfully used in the functional study of relevant components of the immune system (e.g., CTLA-4, TNF-α, CD14, IL-6, etc.) (Bao et al., 2002; Hunger et al., 1997; Mäkinen et al., 2001; Peters et al., 1996; Ronchese et al., 1994; Tamura et al., 1999). One of the main advantages of such experimental models is that they generate information easily translatable to the clinical practice by infusion of soluble recombinant forms in the subject receptor. To this, we took advantage of the inter-species recognition of the receptor-ligand interactions between mouse and human CD5. To rule out that the observed results were CD5-dependent and not from random transgene insertions, we reproduced in WT C57BL/6 mice the results obtained with the shCD5-expressing transgenic mice by repeated administration of exogenous rshCD5 protein.

1.1. shCD5EμTg MICE

The first set of results was obtained with heterozygous transgenic mice in collaboration with another PhD student from the laboratory (Fenutría et al., 2014). The function of shCD5 is still unknown but one hypothesis was that it could compete with membrane-bound CD5 for interaction with its ligand/s, thus interfering with homeostatic lymphocyte responses. As presented in the Results section, the serum levels of shCD5 in transgenic mice were modest but sustainable from early stages of development, tolerizing the mice to immunization with the human protein.

The phenotypical analysis of shCD5EμTg mice did not reveal any gross alterations in major lymphocyte subpopulations. However, a decrease in T and B cell subsets with regulatory function, as well as an increase in NKT cells were observed. It has been reported that generation of thymus-derived T regulatory cells (nT_{regs}) – which express high levels of membrane-bound CD5 - appears to be regulated by CD5 expression (Dasu et al., 2008; Ordoñez-Rueda et al., 2009). However, T_{reg} cells were decreased in the periphery but not in the thymus of shCD5EμTg mice. This could be explained by the fact that shCD5 expression is under the control of the Eμ enhancer (being expressed preferentially by B cells) and local expression in the thymus would be very low and might not be enough to alter the development or maintenance of nT_{reg} cells. This suggests that the observed decrease in this population is at the expense of inducible T_{reg} (iT_{regs}) cells. Another possibility is that cross-linking of membrane-bound CD5 is not necessary for T cell development in the thymus, as it has been reported that the cytoplasmic region alone might be sufficient for intrathymic selection (Brown et al., 2002). This is consistent with the authors mentioning the lack of CD5L expression in the thymus. However, the authors also point out that CD5-CD5L interactions would indeed be important in the periphery, which is in agreement with our results.

A decrease in B regulatory (B_{reg}) cells was also observed, and this can be explained by the fact that CD5 expression is required for IL-10 production by these cells, acting as

a survival factor (Gary-Gouy et al., 2002). In a similar way, intact CD5 function might be required for other CD5-expressing cell types, such as NKT cells. It is also possible that NKT cell number and/or activity could be influenced indirectly by regulatory T and/or B cells, as has been speculated previously (Mauri, 2010) (Fig. V.1).

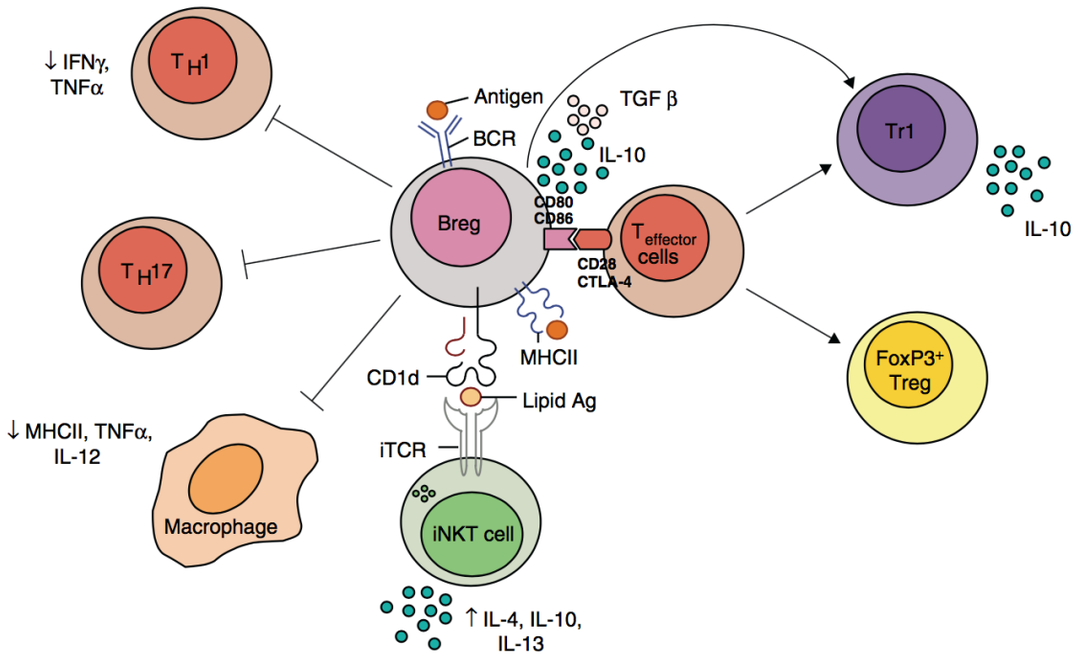

Fig. V.1 – Effector mechanisms of B_{reg} cells. Adopted from (Mauri, 2010).

Importantly, the observed changes in regulatory lymphocyte subpopulations were reproduced in WT C57BL/6 mice by repeated administration of exogenous rshCD5 protein. These results indicate that there is a causal relationship between the presence of increased circulating levels of shCD5 and changes in cell subpopulation dynamics, particularly in those cell types with high membrane-bound CD5 expression.

It was expected that shCD5EμTg mice would have a lower threshold for antigen-specific receptor-mediated activation and subsequently, an enhanced immune response, since the function of membrane-CD5 was "blocked". To verify this, shCD5EμTg mice were first challenged with TD and TI antigens. An enhanced *in vivo* antibody response was observed. Then, induction of two different experimental autoimmune disease models (CIA and EAE) resulted in a more severe outcome for shCD5EμTg mice compared with Non-Tg controls. The increase in disease severity was measured not only by clinical score, but also through determination of pro-inflammatory cytokine levels and autoantibody responses. Although no CIA studies have been carried out in CD5KO mice, it has been shown that CD5KO and CD5ΔCKIIBD mice (mice expressing a truncated and functionally defective form of CD5) immunized with relatively high doses of MOG show more severe forms of EAE than WT mice (Sestero et al., 2012). Thus, physical deletion or functional

knock-down of CD5 both appear to lead to a similar outcome with regard to autoimmune responses.

After autoimmune response evaluation, we thought it would be interesting to analyze the anti-tumor response which is directed mainly towards autologous antigens. Indeed, syngeneic B16-F0 melanoma tumors grew at a slower rate in shCD5EμTg mice than in Non-Tg mice. shCD5EμTg mice also showed a trend towards a decreased number of lung metastases following *i.v.* injection of B16-F0 cells. These results are also in agreement with previous studies carried out in CD5KO mice, in which B16-F10 tumors grew more slowly compared to those in WT mice (Tabbekh et al., 2011).

The results obtained in autoimmune and tumor models could also be explained by the decrease in lymphocyte subpopulations with regulatory/suppressor function observed in shCD5EμTg mice. Regulatory cells have been shown to suppress activation of the immune system, and a decrease in these cells would then be expected to enhance the immune response to self and non-self antigens, particularly when coupled with an increment in NKT cells. These cells can produce large quantities of cytokines that can quickly modulate and polarize the immune response. In addition, a decrease in T_{reg} cells by itself has been reported to slow down tumor growth (Oleinika, Nibbs, Graham, & Fraser, 2013).

Once the enhancement of the anti-tumor response in transgenic mice was established, we further these studies in an attempt to unravel the mechanism by which shCD5EμTg mice showed slower B16-F0 tumor growth compared to Non-Tg mice. In this second study, we used homozygous shCD5EμTg mice, identified through backcrossing transgenic mice, in an attempt of obtain higher levels of soluble protein and more similar mouse groups. We found that the TdLNs from homozygous shCD5EμTg mice had higher total cell numbers after B16-F0 tumor challenge. This included larger numbers of effector subpopulations ($CD4^+$ and $CD8^+$ T lymphocytes), but a decreased T_{reg} subpopulation. In addition to the higher cell numbers, we also observed that spleen cells from shCD5EμTg mice had higher lytic ability against tumor cells *in vitro*, although only at high effector:target ratios. This could be due to B16-F0 cells expressing very low levels of class I MHC, although it could also mean that lysis of tumor cells is carried out mainly by NK cells. As these assays were performed with whole splenocytes, we hypothesize that the observed response can be attributed to NK/NKT cells as well as $CD8^+$ cytotoxic T cells.

The observed anti-tumor effect was not limited to one specific cell type, as similar results were obtained using the EG7-OVA cell line. Unlike the B16-F0 cells, this cell line is highly immunogenic due to the expression of the human OVA (ovalbumin) antigen. Once again the lytic ability of shCD5EμTg splenocytes was shown to be increased, even in lower ratios of effector:target cells, both towards specific (the EG7-OVA cells) as well as

unspecific stimuli (RMA-S). It is worth mentioning that RMA-S cells express low levels of MHC class I molecules, being mainly lysed through NK cells as in the case of B16-F0. Regarding the TdLN total cell numbers, in the EG7-OVA model they were also higher in shCD5EμTg mice than in Non-Tg mice, and cells from TdLN of shCD5EμTg mice were more responsive than cells from Non-Tg mice to *in vitro* re-stimulation with SIINFEKL (a specific $CD8^+$ T cell OVA-derived peptide), OVA protein, or irradiated EG7-OVA and YAC-I cells, as shown by IFN-γ release. Once again this may lead to speculate that besides NK cells, $CD8^+$ cells can play an important role in the anti-tumor response of shCD5EμTg mice. Nevertheless, the levels of IFN-γ obtained after SIINFEKL stimulation were the lowest of all the stimuli tried, suggesting that either the stimulus is suboptimal or the $CD8^+$ cells are only a minor source of IFN-γ. The high levels of IFN-γ observed following stimulation with YAC-1 cells are probably due to an unspecific response, unrelated to the tumor that mice are bearing, and thus mediated mostly by NK cells. It should also be noted that TdLN cells were pre-activated, since stimulation of the contra-lateral lymph node cells showed undetectable IFN-γ levels.

The central proof of the implication of NK cells in the antitumor effect of shCD5 was confirmed when mice were depleted of NK cells and the antitumor effect was lost. The tumor growth rate of NK-depleted shCD5EμTg mice was equal to that of the NK-depleted Non-Tg mice. The depletion, as expected, enhanced tumor growth, but more importantly, without NK cells rshCD5 also lost its beneficial effect. In addition, it was also reported that IL-6 can negatively modulate the NK cytotoxic activity (Cifaldi et al., 2015), so we evaluated the expression levels of this cytokine in B16-F0 tumors of shCD5EμTg mice and found that the IL-6 levels were diminished. This could explain the higher NK cell activity observed. Other cytokine levels were analyzed, such as IL-10, IL-15 (which induces expansion of NK, NKT and cytotoxic lymphocytes), IL-22 and IFN-γ, but no differences were observed.

To assess the therapeutic effect of rshCD5 infusion in the B16-F0 melanoma model, we treated WT mice with rshCD5, both locally and systemically. Local (i.e. peritumoral) treatment proved to be the most effective route, lowering tumor growth rate and weight in a dose-dependent manner. The presence of rshCD5 in the tumor environment was able to mimic the effect observed in shCD5EμTg mice of increasing the total cell numbers in TdLNs. We also observed a decrease in the proportion of T_{reg} cells, coupled with an increment in CD69-expressing $CD4^+$ T, NK and NKT cells, which are likely to promote the anti-tumor response (Borrego, Robertson, Ritz, Peña, & Solana, 1999). Indeed, it is known that T_{reg} cells can suppress NK cell activity (Pedroza-Pacheco, Madrigal, & Saudemont, 2013).

We also evaluated the effect of the presence of rshCD5 in the microenvironment

of a T-cell dependent tumor model (EG7-OVA) and found that, unlike the beneficial effect observed in the shCD5EμTg mice, the therapeutical effect of rshCD5 was lost in the studied conditions. We hypothesize that, unlike what happens in the shCD5EμTg mice, in which the immune cells are always in contact with CD5 and have been immunomodulated from the start, with the exogenous protein administration the cells did not undergo immunomodulation in time to control tumor growth. It is likely then that cells need to be exposed to high levels of shCD5 for a certain amount of time in order to enhance their response against this tumor type.

The first days following tumor implantation are essential to control growth, and at these stages the innate immune response is heavily implicated. Once again, intratumoral IL-6 was diminished following administration of rshCD5 as had been observed in shCD5EμTg mice. In an attempt to analyze the role of NK cells in the anti-tumor response in the presence of rshCD5, as previously performed in shCD5EμTg mice, we depleted NK cells concurrently with rshCD5 treatment in our melanoma model. NK cell depletion completely abolished the beneficial effects of rshCD5, once again suggesting that NK cells are essential for rshCD5-mediated anti-tumor effect. This does not imply that $CD8^+$ cells do not play a role here, but as this tumor model is very aggressive, once the cells are implanted it is hard to see differences in growth rates. At an early stage, when the anti-tumor response is assembling and NK cells are the main line of defense, it is possible to see this effect more easily. This early key role of NK cells could also explain why we did not observe a beneficial effect of rshCD5 in the EG7-OVA model, since it is a T-dependent model. It is also important to mention that the presence of rshCD5 in the tumor microenvironment also induced a reduction of T_{reg} cells that is known to slow down tumor growth (Oleinika et al., 2013). We can therefore hypothesize that the presence of rshCD5 in the tumor environment induces cell activation and also cell proliferation or cell recruitment to LNs, either by direct contact with its ligand/s or indirectly by other signals such as cytokines, or by a decrease in regulatory cells, and as a result an increment in cell numbers is observed.

Another important factor worth discussing is the “feed-forward loop” between CD5 expression and STAT3 activation induced by IL-6 interaction with membrane CD5 expressed by intratumoral B cells (Zhang et al., 2016). The presence of rshCD5 in the tumor microenvironment could block the interaction of membrane CD5 with IL-6, thus inhibiting STAT3 activation and consequently tumor progression.

In this work we were able to demonstrate that besides having a prophylactic effect on tumor growth and improving the efficacy of chemotherapy, repeated exogenous administration of rshCD5 shows significant anti-tumor effect, likely through improving the anti-tumor response as previously reported (Fenutría et al., 2014). These results

show that CD5 can have an important clinical application in tumor treatment as a novel checkpoint inhibitor-type target. This fact does not exclude the importance of combining CD5 targeting with other therapies (either conventional or immunotherapies) in order to prevent immune evasion and thus allowing CD5 to immunomodulate the anti-tumor response. Unfortunately, when we combined rshCD5 infusion with anti-CTLA-4 we did not observe a combined (synergic/additive) effect. However, we believe this is a result of unoptimized schedule and/or doses, rather than a lack of synergy/addition between the two therapies. Further work needs to be carried out in this respect.

Another important finding of this work was the unveiling of a new implication of CD5 in the antitumor response which is dependent on the microbiota environment. In the course of our studies with shCD5EμTg mice we found that the mouse facility used influenced the results obtained. When the B16-F0 or EG7-OVA tumor models were performed in the conventional mouse facility, we observed a better antitumor response in the shCD5EμTg mice. However, when the same models were performed in the SPF mice facility, the tumor growth rates were reversed, and the beneficial effect observed in the shCD5EμTg mice was lost. Given these results, we hypothesized that the cause of this change would be the changes in food, water, and cage conditions, which would be reflected in gut microbiota alterations. Preliminary microbiological studies demonstrated that indeed the housing conditions had a direct effect in the gut microbiota. When collecting samples from shCD5EμTg mice housed in an SPF facility and then when moved to a conventional facility, we could observe changes in microbiota composition over the time. Moreover, even between the shCD5EμTg and Non-Tg mice, at basal normal conditions and under the same housing there were already differences in the gut microbiota. Increasingly studies are demonstrating an association between gut microbiota composition and antitumor response (Roy & Trinchieri, 2017; Zitvogel, Daillère, Roberti, Routy, & Kroemer, 2017). Currently, our group is performing more studies in this sense to understand the relation between CD5, the gut microbiota and the immune response.

1.2. shCD5LckEμTg MICE

Another goal of this thesis was to characterize the new shCD5 transgenic mouse line - shCD5LckEμTg. This line expresses shCD5 under the control of lymphoid-specific transcriptional elements (T and B). The lymphoid-specific Lck promoter and Eμ enhancer are active from early T and B developmental stages (Wildin et al., 1991), so in this case we hypothesized that we mainly would obtain higher levels of shCD5 in primary and secondary lymphoid organs in contrast with the previous mouse line. Similar to the other transgenic line, we hypothesized that soluble CD5 would behave as a "decoy receptor", impairing the interactions of membrane-bound CD5 with its ligand/s.

It is worth mentioning that all the results were obtained with mice housed in an SPF

facility since at that point we still did not know about the possible association between CD5 function and the environment/microbiota. All the performed characterization is now being performed in a conventional facility for comparative purposes.

With these mice, we could obtain a modest, but with less dispersion, increment in the serum levels of shCD5. Another observation was that the relative expression of shCD5 mRNA levels in this new shCD5LckEμTg line was much higher than in the previous one (shCD5EμTg), a finding that could correspond to a higher copy number of integrated transgenes rather than superiority of the Lck vs. SV40 promoter. More importantly, the relative expression of shCD5 in lymphoid tissues (thymus, spleen and lymph node) from shCD5LckEμTg mice was indeed qualitatively higher than in non-lymphoid ones (kidney, lung). For the Non-Tg mice, no shCD5 expression was detected. As observed in the previous transgenic model, they were also tolerant to immunization with the shCD5 protein. Regarding the response to TD and TI antigens, shCD5LckEμTg mice showed higher levels of IgG_1 for TD and TI-2 antigens and lower IgG_3 for TI-1, a pattern compatible with enhanced T_H2 responses.

There were no statistically significant differences between shCD5LckEμTg and Non-Tg mice regarding the total cell numbers in thymus, spleen and LNs, as well as the main lymphocyte subtypes analyzed (CD4, CD8, NK, NKT and B cells). When splenocytes were stimulated *in vitro* with anti-CD3 plus anti-CD28 mAbs, no differences in cell activation (as measured by expression of CD69 marker) or cell proliferation of CD4 and CD8 cell subsets was observed. Again, we did not observe significant differences regarding the tumor responses of shCD5LckEμTg and Non-Tg mice: however, as explained above, the lack of immunomodulatory effects of shCD5 expression in shCD5LckEμTg mice could be conditioned by the SPF environment where all the experiments were performed. Indeed, when shCD5LckEμTg mice were challenged with B16-F0 cells under conventional (non-SPF) housing conditions, an improved antitumor response was observed compared with Non-Tg mice. Therefore, further extensive studies under non-SPF conditions are needed to fully and better characterize this mouse line and improve our knowledge on shCD5-induced immunomodulation.

2. CHARACTERIZATION OF THE IMMUNOMODULATORY PROPERTIES OF SOLUBLE CD6 IN BOTH TRANSGENIC AND EXOGENOUSLY INFUSED FORMS

Recently available pre-clinical and clinical information, though still limited, is attracting new interest in targeting the CD6 lymphocyte surface receptor for therapeutic purposes. Genetic studies have shown association of CD6 single nucleotide polymorphisms with Multiple Sclerosis susceptibility and with treatment response to TNF-α blockers in Rheumatoid Arthritis (Kofler, Farkas, von Bergwelt-Baildon, & Hafler, 2016). A humanized anti-CD6 IgG_1 mAb (Itolizumab) has been tested in different autoimmune

diseases (Hernández et al., 2016) and is currently under phase III clinical trials for moderate-to-severe Psoriasis (Krupashankar et al., 2014). So, a better understanding of the immunomodulatory properties of CD6 *in vivo* will help with the implementation of CD6-based therapies.

Since no human CD6 deficiencies have been reported, the availability of genetically modified mouse models would greatly contribute to increase our knowledge of the *in vivo* role of CD6. Accordingly, recently published data from already available CD6 knockout mice is beginning to bring us new and unsuspected information on the role of CD6 in health and disease (Consuegra-Fernandez et al., 2017; Enyindah-Asonye, Li, Xin, et al., 2017b; Li et al., 2017; Orta-Mascaró et al., 2016). However, knocking down gene expression for human therapeutic purposes is not a straightforward approach for both technical and bioethical reasons. Moreover, gene knockdown results cannot always be taken as a surrogate of the blockade of the receptor-ligand interactions mediated by the knocked-out receptor in study. This is well illustrated by a recent report on the role of ALCAM in neuroinflammation (Lécuyer et al., 2017b), where ALCAM-KO mice behaved in an opposite way to mice treated with anti-ALCAM blocking mAbs when subjected to EAE-inducing conditions. The unexpected increase in neuroinflammation observed in ALCAM-KO mice was attributed to concomitant dysregulation of tight and adherent junction molecules in the blood–brain barrier.

Here, we have taken the same approach as for CD5, to understand the *in vivo* consequences of blocking the homophilic and/or heterophilic interaction/s mediated by CD6 and its ligand/s. We generated a transgenic mouse line (shCD6LckEμTg) that expresses a soluble form of human CD6 (shCD6) under the control of lymphoid-specific transcriptional elements (Lck promoter and Eμ enhancer). As for the previous model, we hypothesized that soluble CD6 would behave as a "decoy receptor", impairing the heterotypic and homotypic interactions of the CD6 ligand/s (CD166/ALCAM and CD318).

The phenotypical analysis of primary lymphoid organs from shCD6LckEμTg mice and of WT mice infused with rshCD6 protein under disease-free conditions did not reveal any gross alterations. The only noteworthy finding was an increased frequency of DN and $CD8^+$SP thymocytes in conjunction with non-significant reductions in DP and $CD4^+$SP thymocytes compared with Non-Tg mice. This would indicate that effective interactions between CD6 and CD166/ALCAM expressed on the surface of developing thymocytes and thymic epithelial cells, respectively, are favoring progression from the DN to the DP developmental stage, and limiting that of DP to $CD8^+$SP. Interestingly this thymic phenotype is not overlapping with our results in $CD6^{-/-}$ mice (Orta-Mascaró et al., 2016), where we observed an increased frequency of DP undergoing selection concomitantly with a reduction in recently selected $CD4^+$SP and $CD8^+$SP thymocytes. This disparity

between shCD6LckEμTg and CD6$^{-/-}$ mice could relate to the fact that the latter are not only unable to interact with CD166/ALCAM but also to transduce subsequent intracellular signals. By contrast, shCD6LckEμTg mice do express surface CD6 molecules still available for ligation-independent signal transduction during selective interactions between thymocytes and thymic stromal cells in a similar way to that previously reported for CD5 (Brown et al., 2002). Information on thymocyte developmental processes from CD166/ALCAM-deficient mice would be of great interest to clarify this issue.

The phenotypical analysis of secondary lymphoid organs from shCD6LckEμTg mice revealed decreased total cell numbers in spleen and LN concomitantly with reduced *in vivo* homeostatic proliferative capability of B cells but not T cells. We did not observe any differences in the percentages of apoptotic cells in shCD6LckEμTg mice, but BrdU labeling indicated a significant decrease in the percentage of cycling cells in spleen and LN, mostly in the B cell compartment. Interestingly, WT mice receiving recombinant shCD6 infusion also showed significantly reduced total cell numbers in spleen, indicating a clear role for shCD6 in reducing cell proliferation.

In vitro studies with shCD6LckEμTg splenocytes showed increased CD4^{+} and CD8^{+} T cell proliferative responses via TCR/CD3-crosslinking compared to splenocytes from Non Tg mice, a fact that was abrogated under co-stimulatory conditions (CD28 co-crosslinking). Regarding B cells, stimulation under BCR-dependent conditions (IgM crosslinking) showed reduced proliferative responses in transgenic cells that reached statistical significance in the presence of IL-4 co-stimulation. This contrasts with similar analyses performed with CD6$^{-/-}$ mice, which revealed no reductions in total cell numbers from spleen and LN (Orta-Mascaró et al., 2016), as well no defects in B cell proliferative responses *in vitro* (Consuegra-Fernandez et al., 2017). As previously mentioned shCD6LckEμTg mice had smaller spleens and their B splenocytes incorporated less BrdU than the Non-Tg mice, which seems to indicate that the cells proliferated less (since the apoptotic levels were the same). We could hypothesize that shCD6LckEμTg B cells are less responsive to stimulation, which could help explaining some of the findings made in autoimmune disease models. In any way, further studies are needed to clarify these effects of shCD6 on B and T cell activation and proliferation.

A second consistent finding in peripheral lymphoid organs from shCD6LckEμTg mice was a reduced frequency of CD4^{+} T_{reg} cells in both spleen and LN. These cells also showed decreased suppressive activity *in vitro* compared to those of Non-Tg mice. Importantly, repeated infusion of recombinant shCD6 in WT mice also induced a significant reduction of T_{reg} frequency in LN. These data contrast with those from CD6$^{-/-}$ mice, which showed an increased frequency of peripheral T_{reg}, though they were dysfunctional and also had lower suppressive activity than those from WT mice (Orta-Mascaró et al., 2016). The reduced

T_{reg} cell functionality could be explained by the lack of strong interactions during thymic cell development or the lack of strong cell-cell contacts due to disruption of CD6-ALCAM interactions during immune synapse formation and maturation.

To improve our understanding of cell functionality in the presence of shCD6, we performed *in vitro* experiments with WT $CD4^+$ T cells treated with TCR/CD3- plus CD28-co-crosslinking in the presence or absence of shCD6 (two different concentrations). We observed that, as seen with the shCD6LckEμTg mice, in the presence of the higher concentration the WT $CD4^+$ T cells proliferated more than in the absence of shCD6. Surprisingly, with the lower concentration of shCD6 we observed lower proliferation levels than in its absence. These results suggest that the role of shCD6 could be determined by its relative abundance in the environment. The T_{reg} suppressive activity was also analyzed *in vitro* in the presence or absence of shCD6 and no differences were observed, which could indicate that the impairment in T_{reg} activity observed in the shCD6LckEμTg mice may be caused by thymic developmental problems and not by disruption of cell-cell contacts.

As seen in the $CD6^{-/-}$ model, shCD6LckEμTg mice also showed an increased humoral response against TD and TI antigens. Besides the presence of dysfunctional T_{reg} cells, this could result from a lowered threshold for antigen-specific receptor-mediated activation. Indeed, recent evidence supports a role for CD6 as a negative modulator of antigen-receptor signaling (Li et al., 2017; Oliveira et al., 2012; Orta-Mascaró et al., 2016), and the presence of shCD6 may reduce such a modulatory effect by precluding proper CD6 ligation by CD166/ALCAM.

The functional relevance of the above mentioned phenotypical changes in peripheral T and B cell populations was addressed by subjecting shCD6LckEμTg mice to different experimental models of disease. First, the anti-tumoral response of shCD6LckEμTg mice was explored by challenging them with syngeneic tumor cell lines of three different origins (B16-F0 melanoma, MCA-205 fibrosarcoma, and RMA-S lymphoma). In all three cases, tumor growth was significantly slower in the shCD6LckEμTg mice compared with Non-Tg controls. A similar significant reduction in tumor growth was observed when WT mice were infused every other day with recombinant shCD6 from day 0 of B16-F0 melanoma cell injection. The enhanced anti-tumor response in both experimental settings may relate to the observation of lower levels of peripheral T_{reg} cells with reduced suppressive activity. However, $CD6^{-/-}$ mice, which present an increased frequency of dysfunctional T_{reg} cells (Orta-Mascaró et al. 2016), do not significantly differ from WT mice regarding anti-tumor responses. Once again, this discrepancy might be explained by the presence of intact ligand-independent CD6 signaling in shCD6LckEμTg mice, on which the beneficial effect of circulating shCD6 depends.

Preliminary gut microbiota analyses also showed differences between the

shCD6LckEμTg mice and Non-Tg mice that could influence the antitumor response of these mice. It should be noted on this regard that natural IgM titers have been found reduced in $CD6^{-/-}$ mice in association with a significantly decreased B1a cell population (Enyindah-Asonye et al., 2017b). It would be interesting to explore whether these changes are also observed in our shCD6LckEμTg mice, since natural IgM are actively transported from intestinal mucosa to the intestinal lumen thus likely influencing microbiota composition.

A general concern with therapeutic approaches that potentiate immune responses is the development of autoimmune responses as an adverse effect (Ciccarese et al., 2016). To test whether expression of shCD6 made our shCD6LckEμTg mice more prone to autoimmunity, we tested their responses in two different models of induced autoimmune disease (CIA and EAE). In contrast to our expectations, shCD6LckEμTg mice presented a less severe outcome in both models compared with Non-Tg controls. Importantly, a similarly attenuated EAE autoimmune disease was observed when WT mice were infused every other day with rshCD6 from day 0 of disease induction. These results differed from those anticipated by the anti-tumoral response of shCD6LckEμTg mice and from previous CIA results reported in $CD6^{-/-}$ C57BL/6 mice (Orta-Mascaró et al. 2016). Intriguingly, recent published data show that $CD6^{-/-}$ DBA-1 mice present attenuated EAE disease severity (Li et al., 2017), though information on their anti-tumoral responses is still due.

In summary, analysis of our new shCD6LckEμTg model revealed novel therapeutic potential that was not apparent from the previous analysis of $CD6^{-/-}$ and $ALCAM^{-/-}$ C57BL/6 mice (Orta-Mascaró et al. 2016; Lécuyer et al. 2017). Importantly, the reduced tumor growth rate and severity of autoimmune disorders observed in shCD6LckEμTg mice were well reproduced by recombinant shCD6 infusion. Similar enhancement of antitumor responses and attenuation of autoimmune responses has also been reported by CD166/ALCAM blockade with scFv fragments (Thune et al., 2010) or whole antibodies (Cayrol et al., 2008). The CD166/ALCAM blockade has been reported to disturb cell-to-cell and cell-extracellular matrix interactions important for primary tumor growth (Thune et al., 2010) and/or leukocyte trafficking through blood barriers (Cayrol et al., 2008), including that of T_{reg} cells (Nummer et al., 2007). Alternative to these mechanisms likely behind the therapeutic effects here reported for shCD6 could also be the very recently reported interaction of CD6 with CD318 (Enyindah-Asonye, Li, Ruth, et al., 2017a). CD318 (also named CDCP1 or Trask for CUB domain-containing protein 1 or Transmembrane and associated with src kinases, respectively) is a cell surface glycoprotein broadly present on normal epithelial cells and many tumor cells, and with a role in negative regulation of cell adhesion (Wortmann, He, Deryugina, Quigley, & Hooper, 2009). Overexpression of CD318 increases the tumorigenic and metastatic abilities of tumor cell lines in model systems, and targeting CD318 or CD318-mediated signaling pathways has been proposed

to inhibit cancer dissemination. Whatever the case, in light of the present proof-of-concept data, future studies are warranted to fully understand the immunomodulatory role/s of shCD6 and their immunotherapeutic applications in relevant human disorders such as cancer and autoimmunity.

3. RETROSPECTIVE ANALYSIS OF TUMOR HUMAN SAMPLES

While most of our work on CD5 and CD6 was performed in experimental mouse models, we were also interested in getting further evidence on the putative immunomodulatory role of both receptors from the analysis of human clinical samples (e.g., patient blood and biopsies). On this regard our group has reported the influence of CD5 polymorphisms on cancer (Delgado et al., 2016; Potrony et al., 2016) and autoimmune diseases (Cenit et al., 2014), and is currently investigating similar kinds of influences by CD6 gene variants. Regarding the role of CD5 in human cancer, work by Fathia Mami-Chouaib's group has shown that TILs from human tumors (e.g., lung carcinoma and melanoma) undergo CD5 downregulation as a matter of adaptation to tumor environment and of optimization of their cytotoxic antitumor responses (Tabbekh et al., 2013). Intratumor CD5 downregulation potentiates tumor-specific T-cell reactivity and would be a strategy to overcome evasion by tumor cells expressing low levels of peptide-MHC complexes. By contrast, CD5 overexpression also protects tumor-specific T lymphocytes from overactivation and further AICD, thus potentiating tumor growth reduction (Tabbekh et al., 2013).

Based on this evidence, a preliminary analysis of the TCGA database was performed in order to evaluate the gene expression of T and B cell receptors in human melanoma biopsies. The TCGA database is composed of more than two petabytes of genomic data, which are available to everyone with the aim of helping improve cancer research by finding new genes with a potential role in cancer prevention, diagnosis and treatment. With this analysis, we have once again proof of CD5 and CD6 implication in the anti-tumor response. Overexpression of CD5 and CD6 seems to be a good prognostic feature since the group with better prognosis and also better survival presented the highest expression levels of these genes. This is likely due to the increased presence of tumor-infiltrating immune cells (namely TILs) within the sample, although it may also reflect idiosyncratic differences in immune receptor expression levels among patients. One hypothesis could be that lymphocytes with higher CD5 expression have a more effective and efficient response than those with low CD5 expression. Moreover, those cells after activation are less sensitive to apoptosis (by AICD) because of the CD5 pro-survival signaling (Fulton et al., 2015). Further studies should be made to properly evaluate the clinical relevance of intratumor CD5 and CD6 expression as prognosis markers.

4. CONCLUDING REMARKS

Altogether, the results obtained in this thesis support the relevance of CD5 and CD6 in maintaining the homeostasis of lymphocyte populations that depend on the signaling generated by the interaction of these receptors with their ligands. These interactions between CD5/CD6 and their ligands are key to lymphocyte activation, differentiation, and modulation, either directly or indirectly, as discussed previously in the case of CD5 which can modulate the B_{reg} population and this in turn the others (Mauri, 2010).

Briefly, we found that the impairment of membrane-bound CD5 function with shCD5 led to an increment in the NKT population and decreases of T_{reg}, B_{reg} and B1a populations (**Fig. V.2**). These lymphocytic changes in turn led to an enhanced autoimmune and also antitumor response. Local/systemic shCD5 would then favor accumulation of innate and adaptive immune effector cells (by increasing cell proliferation and/or cell recruitment) into TdLN, while limiting that of cells with regulatory function. This would be likely achieved by interfering (decoy receptor effect) with the interactions between membrane CD5 and its still ill-defined membrane-bound and/or soluble ligand/s.

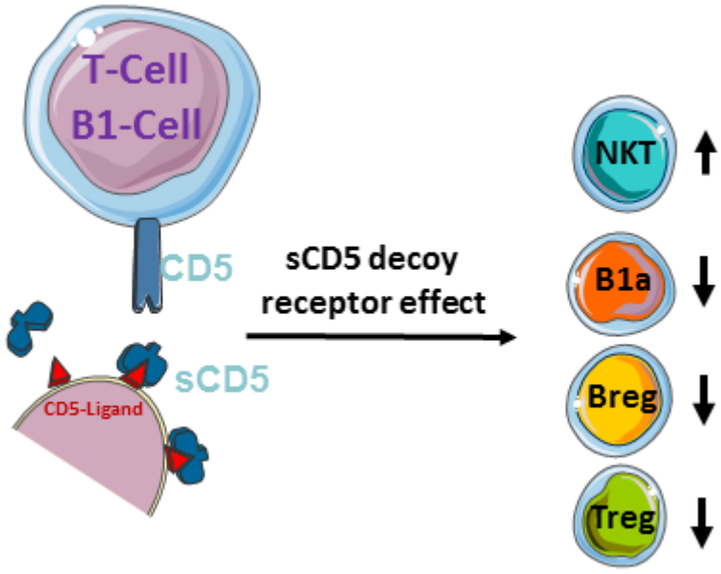

Fig. V.2 –Influence of shCD5 on lymphocyte physiology. The impairment of CD5 function in lymphocytes by the presence of shCD5 protein working as a decoy receptor modulates lymphocyte subpopulations and consequently potentiates autoimmune and anti-tumor activity. Adapted from (Vasquez et al., 2017).

Regarding CD6, the results obtained indicate a similar scenario. Analysis of our new shCD6LckEμTg model revealed novel therapeutic potential that was not apparent from the previous analyses of $CD6^{-/-}$ and $ALCAM^{-/-}$ C57BL/6 mice (Lécuyer et al., 2017; Orta-Mascaró et al., 2016). Membrane-bound CD6 functional impairment with shCD6 led to an increment in DN and $CD8^{+}$SP thymocytes coupled with a decrease in total

cell numbers in spleen and LN; these findings were concomitant with reduced *in vivo* proliferative capability of B cells but not T cells, and also reduction of T_{reg} population and function (**Fig. V.3**). These changes led to reductions in tumor growth and severity of autoimmune disorders. A general concern with therapeutic approaches that potentiate immune responses is the development of autoimmune responses as a secondary effect, which was not the case with the sCD6 approach. Clinical trials using CD6 mAbs are under development with favorable results in rheumatoid arthritis and psoriasis but failed in multiple sclerosis (Itolizumab, IOR-T1, anti-T12 respectively). The use of shCD6 could be a feasible alternative, not only by inhibiting the function of membrane-bound CD6 (immune checkpoint inhibitors blockade) but also by modulating lymphocyte homeostasis.

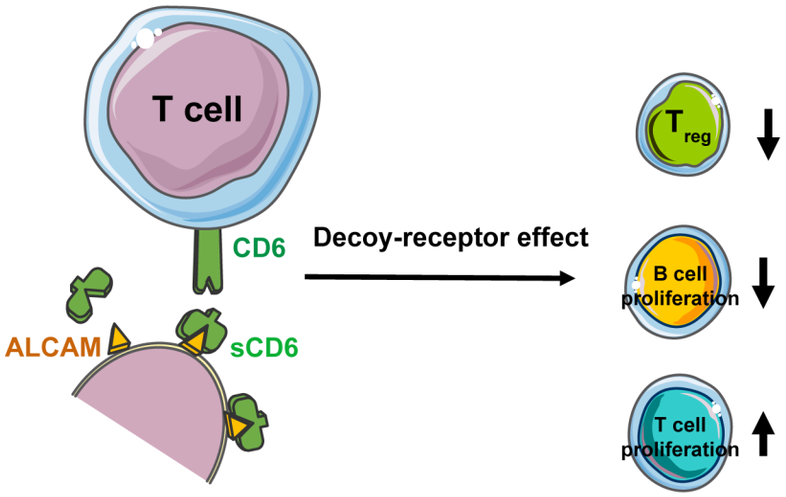

Fig. V.3 –Influence of shCD6 on lymphocyte physiology. The impairment of the membrane-bound CD6 function in lymphocytes by the presence of shCD6 protein as a decoy receptor modulates lymphocyte physiology and consequently potentiates antitumor activity without worsening the autoimmune response.

It is well established that cancer immunity can be boosted by blockade of immune checkpoint inhibitors, and with this work we set the basis for the recognition of CD5 and CD6 as new immune checkpoint inhibitors. Counteracting the function of membrane-bound CD5/CD6 with sCD5/CD6 may enhance current immunotherapies for cancer, as well as be used in other possible applications such as in acute or chronic infections (CD5 recognizes fungal and viral components, and CD6 bacterial components) and vaccines.

VI. CONCLUSIONS

1. The blockade of homophilic and/or heterophilic interaction/s of membrane CD5 by shCD5 (either transgenically expressed or exogenously infused):

   - dysregulates the normal immune cell homeostasis by decreasing the frequency of cells with regulatory function (T_{reg} and B_{reg} cells) and increasing that of cells with effector function (NKT cells);
   - improves the immune response to some experimental tumor models (B16-F0 and EG7-OVA), by increasing the number and function of TdLN cells, in a NK cell-dependent manner.

2. The blockade of homophilic and/or heterophilic interaction/s of the CD6 ligand/s (CD166/ALCAM and CD318) by shCD6 (transgenically expressed or exogenously infused):

   - dysregulates the normal immune cell homeostasis by decreasing cell numbers in different organs, as well as their proliferative and suppressive function;
   - improves the immune response to all the experimental tumor models analyzed (B16-F0, EG7-OVA, MCA-205, and RMA-S);
   - improves the outcome of different experimental autoimmune diseases (CIA and EAE).

3. The immunomodulatory effects of shCD5 and shCD6 in mouse models are likely influenced by environmental factors including gut microbiota composition.

4. The results of the present thesis provide new evidence supporting CD5 and CD6 lymphocyte receptors as immune checkpoints, being two potential therapeutic targets for the development of new drugs for cancer and autoimmune diseases.

VII. REFERENCES

Adams, E. L., P. J. Rice, B. Graves, H. E. Ensley, H. Yu, G. D. Brown, S. Gordon, M. A. Monteiro, E. Papp-Szabo, D. W. Lowman, T. D. Power, M. F. Wempe, and D. L. Williams. 2008. Differential high-affinity interaction of dectin-1 with natural or synthetic glucans is dependent upon primary structure and is influenced by polymer chain length and side-chain branching. Journal of Pharmacology and Experimental Therapeutics 325:115–123.

Aibar, J., M. Martínez-Florensa, P. Castro, E. Carrasco, C. Escoda-Ferran, S. Fernández, M. Butjosa, C. Hernández, M. Rinaudo, F. Lozano, and J. M. Nicolás. 2015. Pattern of soluble CD5 and CD6 lymphocyte receptors in critically ill patients with septic syndromes. Journal of critical care 30:914–9.

Alberola-Ila, J., L. Places, D. A. Cantrell, J. Vives, and F. Lozano. 1992. Intracellular events involved in CD5-induced human T cell activation and proliferation. Journal of immunology (Baltimore, Md. : 1950) 148:1287–93.

Antin, J. H., K. A. Ault, J. M. Rappeport, and B. R. Smith. 1987. B lymphocyte reconstitution after human bone marrow transplantation. Leu-1 antigen defines a distinct population of B lymphocytes. The Journal of clinical investigation 80:325–32.

Aparicio-Siegmund, S., M. Deseke, A. Lickert, and C. Garbers. 2017. Trans-signaling of interleukin-6 (IL-6) is mediated by the soluble IL-6 receptor, but not by soluble CD5. Biochemical and Biophysical Research Communications 6:1–5.

Arman, M., N. Aguilera-Montilla, V. Mas, A. Puig-Kröger, M. Pignatelli, R. Guigó, A.-L. Corbí, and F. Lozano. 2009. The human CD6 gene is transcriptionally regulated by RUNX and Ets transcription factors in T cells. Molecular Immunology 46:2226–2235.

Aruffo, A., M. B. Melnick, P. S. Linsley, and B. Seed. 1991. The lymphocyte glycoprotein CD6 contains a repeated domain structure characteristic of a new family of cell surface and secreted proteins. The Journal of experimental medicine 174:949–52.

Axtell, R. C., M. S. Webb, S. R. Barnum, and C. Raman. 2004. Cutting edge: critical role for CD5 in experimental autoimmune encephalomyelitis: inhibition of engagement reverses disease in mice. Journal of immunology (Baltimore, Md. : 1950) 173:2928–32.

Axtell, R. C., L. Xu, S. R. Barnum, and C. Raman. 2006. CD5-CK2 binding/activation-deficient mice are resistant to experimental autoimmune encephalomyelitis: protection is associated with diminished populations of IL-17-expressing T cells in the central nervous system. Journal of immunology (Baltimore, Md. : 1950) 177:8542–9.

Azzam, H. S., J. B. DeJarnette, K. Huang, R. Emmons, C. S. Park, C. L. Sommers, D. El-Khoury, E. W. Shores, and P. E. Love. 2001. Fine tuning of TCR signaling by CD5.

Journal of immunology 166:5464–5472.

Azzam, H. S., A. Grinberg, K. Lui, H. Shen, E. W. Shores, and P. E. Love. 1998. CD5 expression is developmentally regulated by T cell receptor (TCR) signals and TCR avidity. The Journal of experimental medicine 188:2301–11.

Bao, L., M. Haas, S. A. Boackle, D. M. Kraus, P. N. Cunningham, P. Park, J. J. Alexander, R. K. Anderson, K. Culhane, V. M. Holers, and R. J. Quigg. 2002. Transgenic expression of a soluble complement inhibitor protects against renal disease and promotes survival in MRL/lpr mice. Journal of immunology (Baltimore, Md. : 1950) 168:3601–3607.

Bassi, N., S. Zampieri, A. Ghirardello, M. Tonon, M. Zen, F. Cozzi, and A. Doria. 2009. Pentraxins, anti-pentraxin antibodies, and atherosclerosis. Clinical Reviews in Allergy and Immunology 37:36–43.

Begum-Haque, S., M. Christy, J. Ochoa-Reparaz, E. C. Nowak, D. Mielcarz, A. Haque, and L. H. Kasper. 2011. Augmentation of regulatory B cell activity in experimental allergic encephalomyelitis by glatiramer acetate. Journal of Neuroimmunology 232:136–144.

Berland, R., and H. H. Wortis. 2002. Origins and functions of B-1 cells with notes on the role of CD5. Annual Review of Immunology 20:253–300.

De Bernardis, F., R. Lucciarini, M. Boccanera, C. Amantini, S. Arancia, S. Morrone, M. Mosca, A. Cassone, and G. Santoni. 2006. Phenotypic and functional characterization of vaginal dendritic cells in a rat model of Candida albicans vaginitis. Infection and Immunity 74:4282–4294.

Beyers, A. D., L. L. Spruyt, and A. F. Williams. 1992. Multimolecular associations of the T-cell antigen receptor. Trends in cell biology 2:253–5.

Biancone, L., M. A. Bowen, A. Lim, A. Aruffo, G. Andres, and I. Stamenkovic. 1996. Identification of a novel inducible cell-surface ligand of CD5 on activated lymphocytes. The Journal of experimental medicine 184.

Bikah, G., J. Carey, J. R. Ciallella, A. Tarakhovsky, and S. Bondada. 1996. CD5-Mediated Negative Regulation of Antigen Receptor-Induced Growth Signals in B-1 B Cells. Science 274:1906–1909.

Bikah, G., F. M. Lynd, A. A. Aruffo, J. A. Ledbetter, and S. Bondada. 1998. A role for CD5 in cognate interactions between T cells and B cells, and identification of a novel ligand for CD5. International Immunology 10:(8):1185-96.

Böhm, I. 2004. Increased peripheral blood B-cells expressing the CD5 molecules in association to autoantibodies in patients with lupus erythematosus and evidence to

selectively down-modulate them. Biomedicine and Pharmacotherapy 58:338–343.

Bonet, L., M. Farnós, M. Martínez-Florensa, V. G. Martínez, and F. Lozano. 2013. Identification of functionally relevant phoshorylatable serine clusters in the cytoplasmic region of the human CD6 lymphocyte surface receptor. FEBS Letters 587:2205–2213.

Bongioanni, P., C. Fioretti, R. Vanacore, F. Bianchi, F. Lombardo, F. Ambrogi, and G. Meucci. 1996. Lymphocyte subsets in multiple sclerosis A study with two-colour fluorescence analysis. Journal of the Neurological Sciences 139:71–77.

Boomer, J. S., and J. M. Green. 2010, August. An enigmatic tail of CD28 signaling. Cold Spring Harbor Laboratory Press.

Borrego, F., M. J. Robertson, J. Ritz, J. Peña, and R. Solana. 1999. CD69 is a stimulatory receptor for natural killer cell and its cytotoxic effect is blocked by CD94 inhibitory receptor. Immunology 97:159–165.

Borrello, M. A., J. Palis, and R. P. Phipps. 2001. The relationship of $CD5^+$ B lymphocytes to macrophages: insights from normal biphenotypic B/macrophage cells. International reviews of immunology 20:137–155.

Bott, C. M., J. B. Doshi, L. L. Li, S. A. McMurtry, J. L. Sanders, and D. A. Fox. 1994. Transcriptional regulation of CD6 expression on human T lymphocytes by phorbol ester. Journal of immunology (Baltimore, Md. : 1950) 153:1–9.

Bowen, M. A., D. D. Patel, X. Li, B. Modreu, A. R. Malacko, W.-C. Wang, H. Marquardt, M. Neubauer, J. M. Pesando, U. Francke, B. F. Haynes, and A. Aruffo. 1995. Cloning, Mapping, and Characterization of Activated Leukocyte-Cell Adhesion Molecule (ALCAM), a CD6 Ligand. Journal of experimental medicine 181:2213–20.

Bowen, M. A., G. S. Whitney, M. Neubauer, G. C. Starling, D. Palmer, J. Zhang, N. J. Nowak, T. B. Shows, and A. Aruffo. 1997. Structure and chromosomal location of the human CD6 gene: detection of five human CD6 isoforms. The Journal of Immunology 158.

Braun, M., B. Müller, D. ter Meer, S. Raffegerst, B. Simm, S. Wilde, S. Spranger, J. Ellwart, B. Mosetter, L. Umansky, T. Lerchl, D. J. Schendel, and C. S. Falk. 2011. The CD6 scavenger receptor is differentially expressed on a CD56 natural killer cell subpopulation and contributes to natural killer-derived cytokine and chemokine secretion. Journal of innate immunity 3:420–34.

Breuning, J., and M. H. Brown. 2017. T cell costimulation by CD6 is dependent on bivalent binding of a GADS/SLP-76 complex. Molecular and Cellular Biology 16;37(11).

Brossard, C., M. Semichon, A. Trautmann, and G. Bismuth. 2003. CD5 inhibits signaling at the immunological synapse without impairing its formation. Journal of immunology (Baltimore, Md. : 1950) 170:4623–4629.

Brown, J. A., R. J. Greenwald, S. Scott, A. N. Schweitzer, A. R. Satoskar, C. Chung, L. R. Schopf, D. Van Der Woude, J. P. Sypek, and A. H. Sharpe. 2002. CD5-mediated inhibition of TCR signaling during intrathymic selection and development does not require the CD5 extracellular domain. European Journal of Immunology 32:1811–1817.

Brown, M. H., and E. Lacey. 2010. A ligand for CD5 is CD5. Journal of immunology (Baltimore, Md. : 1950) 185:6068–74.

Brown, M. S., and J. L. Goldstein. 1979a. Receptor-mediated endocytosis: insights from the lipoprotein receptor system. Proceedings of the National Academy of Sciences of the United States of America 76:3330–7.

Brown, M. S., J. L. Goldstein, M. Krieger, Y. K. Ho, and R. G. Anderson. 1979b. Reversible accumulation of cholesteryl esters in macrophages incubated with acetylated lipoproteins. Journal of Cell Biology 82:597–613.

Burastero, S. E., M. Cutolo, V. Dessi, and F. Celada. 1990. Monoreactive and Polyreactive Rheumatoid Factors Produced by *in Vitro* Epstein-Barr Virus-Transformed Peripheral Blood and Synovial B Lymphocytes from Rheumatoid Arthritis Patients. Scandinavian Journal of Immunology 32:347–357.

Burastero, S. E., G. Lo Pinto, D. Goletti, M. Cutolo, L. Burlando, and P. Falagiani. 1993. Rheumatoid arthritis with monoclonal IgE rheumatoid factor. Journal of Rheumatology 20:489–494.

Caì, Y., E. N. Postnikova, J. G. Bernbaum, S. Yú, S. Mazur, N. M. Deiuliis, S. R. Radoshitzky, M. G. Lackemeyer, A. McCluskey, P. J. Robinson, V. Haucke, V. Wahl-Jensen, A. L. Bailey, M. Lauck, T. C. Friedrich, D. H. O'Connor, T. L. Goldberg, P. B. Jahrling, and J. H. Kuhn. 2015. Simian hemorrhagic fever virus cell entry is dependent on CD163 and uses a clathrin-mediated endocytosis-like pathway. Journal of Virology 89:844–856.

Caligaris-Cappio, F., M. Gobbi, M. Bofill, and G. Janossy. 1982. Infrequent normal B lymphocytes express features of B-Chronic Lymphocitic Leukemia. Journal of Experimental Medicine 623:623–628.

Calvo, J., L. Places, G. Espinosa, O. Padilla, J. M. Vilà, N. Villamor, M. Ingelmo, T. Gallart, J. Vives, J. Font, and F. Lozano. 1999a. Identification of a natural soluble form of human CD5. Tissue antigens 54:128–37.

Calvo, J., L. Places, O. Padilla, J. M. Vilà, J. Vives, M. A. Bowen, and F. Lozano. 1999b. Interaction of recombinant and natural soluble CD5 forms with an alternative cell surface ligand. European Journal of Immunology 29:2119–2129.

Cannon, G. W., D. A. Marble, M. M. Griffiths, B. C. Cole, S. McCall, S. F. Schulman, and V. Strand. 1995. Immunologic assessment during treatment of rheumatoid arthritis with anti-CD5 immunoconjugate. Journal of Rheumatology 22:207–213.

Cantaert, T., M. E. Doorenspleet, G. Francosalinas, J. E. Paramarta, P. L. Klarenbeek, Y. Tiersma, C. M. Van Der Loos, N. De Vries, P. P. Tak, and D. L. Baeten. 2012. Increased numbers of $CD5^{+}$ B lymphocytes with a regulatory phenotype in spondylarthritis. Arthritis and Rheumatism 64:1859–1868.

Caramalho, I., T. Lopes-Carvalho, D. Ostler, S. Zelenay, M. Haury, and J. Demengeot. 2003. Regulatory T Cells Selectively Express Toll-like Receptors and Are Activated by Lipopolysaccharide. The Journal of Experimental Medicine 197:403–411.

Carnero-Montoro, E., L. Bonet, J. Engelken, T. Bielig, M. Martínez-Florensa, F. Lozano, and E. Bosch. 2012. Evolutionary and functional evidence for positive selection at the human CD5 immune receptor gene. Molecular biology and evolution 29:811–23.

Carrasco, E., C. Escoda-Ferran, N. Climent, C. Miró-Julià, I. T. Simões, M. Martínez-Florensa, A. Sarukhan, E. Carreras, and F. Lozano. 2017. Human CD6 Down-Modulation following T-Cell Activation Compromises Lymphocyte Survival and Proliferative Responses. Frontiers in Immunology 8:769.

Castro, M. A. A., R. J. Nunes, M. I. Oliveira, P. A. Tavares, C. Simões, J. R. Parnes, A. Moreira, and A. M. Carmo. 2003. OX52 is the rat homologue of CD6: evidence for an effector function in the regulation of CD5 phosphorylation. Journal of leukocyte biology 73:183–90.

Castro, M. A. A., M. I. Oliveira, R. J. Nunes, S. Fabre, R. Barbosa, A. Peixoto, M. H. Brown, J. R. Parnes, G. Bismuth, A. Moreira, B. Rocha, and A. M. Carmo. 2007. Extracellular isoforms of CD6 generated by alternative splicing regulate targeting of CD6 to the immunological synapse. Journal of immunology (Baltimore, Md. : 1950) 178:4351–61.

Cayrol, R., K. Wosik, J. L. Berard, A. Dodelet-Devillers, I. Ifergan, H. Kebir, A. S. Haqqani, K. Kreymborg, S. Krug, R. Moumdjian, A. Bouthillier, B. Becher, N. Arbour, S. David, D. Stanimirovic, and A. Prat. 2008. Activated leukocyte cell adhesion molecule promotes leukocyte trafficking into the central nervous system. Nature immunology 9:137–45.

Cenit, M. C., M. Martínez-Florensa, M. Consuegra, L. Bonet, E. Carnero-Montoro, N. Armiger, M. Caballero-Baños, M. T. Arias, D. Benitez, N. Ortego-Centeno, E. de

Ramón, J. M. Sabio, F. J. García-Hernández, C. Tolosa, A. Suárez, M. A. González-Gay, E. Bosch, J. Martín, and F. Lozano. 2014. Analysis of Ancestral and Functionally Relevant CD5 Variants in Systemic Lupus Erythematosus Patients. PloS one 9:e113090.

Ceuppens, J. L., and M. L. Baroja. 1986. Monoclonal antibodies to the CD5 antigen can provide the necessary second signal for activation of isolated resting T cells by solid-phase-bound OKT3. Journal of immunology (Baltimore, Md. : 1950) 137:1816–21.

Chappell, P. E., L. I. Garner, J. Yan, C. Metcalfe, D. Hatherley, S. Johnson, C. V. Robinson, S. M. Lea, and M. H. Brown. 2015. Structures of CD6 and Its Ligand CD166 Give Insight into Their Interaction. Structure (London, England : 1993) 23:1426–36.

Chopra, A., S. Chandrashekara, R. Iyer, L. Rajasekhar, N. Shetty, S. M. Veeravalli, A. Ghosh, M. Merchant, J. Oak, V. Londhey, A. Barve, M. S. Ramakrishnan, and E. Montero. 2016. Itolizumab in combination with methotrexate modulates active rheumatoid arthritis: Safety and efficacy from a phase 2, randomized, open-label, parallel-group, dose-ranging study. Clinical Rheumatology 35:1059–1064.

Ciccarese, C., S. Alfieri, M. Santoni, D. Santini, M. Brunelli, C. Bergamini, L. Licitra, R. Montironi, G. Tortora, and F. Massari. 2016. New toxicity profile for novel immunotherapy agents: focus on immune-checkpoint inhibitors. Expert opinion on drug metabolism & toxicology 12:57–75.

Cifaldi, L., G. Prencipe, I. Caiello, C. Bracaglia, F. Locatelli, F. De Benedetti, and R. Strippoli. 2015. Inhibition of natural killer cell cytotoxicity by interleukin-6: implications for the pathogenesis of macrophage activation syndrome. Arthritis & rheumatology (Hoboken, N.J.) 67:3037–46.

Consuegra-Fernández, M., F. Aranda, I. Simões, M. Orta, A. Sarukhan, and F. Lozano. 2015. CD5 as a target for immune-based therapies. Critical Reviews in Immunology 35.

Consuegra-Fernandez, M., M. Martinez-Florensa, F. Aranda, J. de Salort, N. Armiger-Borras, T. Lozano, N. Casares, J. J. Lasarte, P. Engel, and F. Lozano. 2017. Relevance of CD6-Mediated Interactions in the Regulation of Peripheral T-Cell Responses and Tolerance. Frontiers in Immunology 8.

Cooper, M. D. 2015. The early history of B cells. Nature reviews. Immunology 15:191–7.

Cooper, M. D., R. D. Peterson, and R. A. Good. 1965. Delineation of the thymic and bursal lymphoid systems in the chicken. Nature 205:143–146.

Correale, J., E. Mix, T. Olsson, V. Kostulas, S. Fredrikson, B. Höjeberg, and H. Link. 1991. $CD5^+$ B cells and $CD4^-8^-$ T cells in neuroimmunological diseases. Journal of

Neuroimmunology 32:123–132.

Cortés, F., F. Deschaseaux, N. Uchida, M. C. Labastie, A. M. Friera, D. He, P. Charbord, and B. Péault. 1999. HCA, an immunoglobulin-like adhesion molecule present on the earliest human hematopoietic precursor cells, is also expressed by stromal cells in blood-forming tissues. Blood 93:826–37.

Croft, M., T. So, W. Duan, and P. Soroosh. 2009, May. The significance of OX40 and OX40L to T-cell biology and immune disease.

Cui, D., L. Zhang, J. Chen, M. Zhu, L. Hou, B. Chen, and B. Shen. 2014. Changes in regulatory B cells and their relationship with rheumatoid arthritis disease activity. Clinical and Experimental Medicine 15:285–292.

Daien, C. I., S. Gailhac, T. Mura, R. Audo, B. Combe, M. Hahne, and J. Morel. 2014. Regulatory B10 cells are decreased in patients with rheumatoid arthritis and are inversely correlated with disease activity. Arthritis and Rheumatology 66:2037–2046.

Dambuza, I. M., and G. D. Brown. 2015. C-type lectins in immunity: recent developments. Current Opinion in Immunology 32:21–27.

Le Dantec, C., R. Alonso, T. Fali, E. Montero, V. Devauchelle, A. Saraux, J. O. Pers, and Y. Renaudineau. 2013. Rationale for treating primary Sjögren's syndrome patients with an anti-CD6 monoclonal antibody (Itolizumab). Immunologic Research 56:341–347.

Dasu, T., J. E. Qualls, H. Tuna, C. Raman, D. A. Cohen, and S. Bondada. 2008. CD5 plays an inhibitory role in the suppressive function of murine $CD4^+$ $CD25^+$ T_{reg} cells. Immunology Letters 119:103–113.

Dauphinée, M., Z. Tovar, and N. Talal. 1988. B cells expressing cd5 are increased in sjögren's syndrome. Arthritis & Rheumatism 31:642–647.

Delgado, J., T. Bielig, L. Bonet, E. Carnero-Montoro, X. S. Puente, D. Colomer, E. Bosch, E. Campo, and F. Lozano. 2016. Impact of the functional CD5 polymorphism A471V on the response of chronic lymphocytic leukaemia to conventional chemotherapy regimens. British journal of haematology. 177(1):147-150

Dillman, R. O., D. L. Shawler, J. B. Dillman, and I. Royston. 1984. Therapy of chronic lymphocytic leukemia and cutaneous T-cell lymphoma with T101 monoclonal antibody. Journal of clinical oncology : official journal of the American Society of Clinical Oncology 2:881–91.

Dorothée, G., I. Vergnon, F. El Hage, B. Le Maux Chansac, V. Ferrand, Y. Lécluse, P. Opolon, S. Chouaib, G. Bismuth, and F. Mami-Chouaib. 2005. In situ sensory adaptation

of tumor-infiltrating T lymphocytes to peptide-MHC levels elicits strong antitumor reactivity. Journal of immunology (Baltimore, Md. : 1950) 174:6888–97.

Engelmann, R., N. Wang, C. Kneitz, and B. Müller-Hilke. 2014. Bone resorption correlates with the frequency of $CD5^+$ B cells in the blood of patients with rheumatoid arthritis. Rheumatology (Oxford, England) 54:1–9.

Enyindah-Asonye, G., Y. Li, J. H. Ruth, D. S. Spassov, K. E. Hebron, A. Zijlstra, M. M. Moasser, B. Wang, N. G. Singer, H. Cui, R. A. Ohara, S. M. Rasmussen, D. A. Fox, and F. Lin. 2017a. CD318 is a ligand for CD6. Proceedings of the National Academy of Sciences:201704008.

Enyindah-Asonye, G., Y. Li, W. Xin, N. G. Singer, N. Gupta, J. Fung, and F. Lin. 2017b. CD6 Receptor Regulates Intestinal Ischemia/Reperfusion-induced Injury by Modulating Natural IgM-producing B1a Cell Self-renewal. Journal of Biological Chemistry 292:661–671.

Escoda-Ferran, C., E. Carrasco, M. Caballero-Baños, C. Miró-Julià, M. Martínez-Florensa, M. Consuegra-Fernández, V. G. Martínez, F.-T. Liu, and F. Lozano. 2014. Modulation of CD6 function through interaction with Galectin-1 and -3. FEBS letters 588:2805–13.

Eyre, S., J. Bowes, D. Diogo, A. Lee, A. Barton, P. Martin, A. Zhernakova, E. Stahl, S. Viatte, K. McAllister, C. I. Amos, L. Padyukov, R. E. M. Toes, T. W. J. Huizinga, C. Wijmenga, G. Trynka, L. Franke, H.-J. Westra, L. Alfredsson, X. Hu, C. Sandor, P. I. W. de Bakker, S. Davila, C. C. Khor, K. K. Heng, R. Andrews, S. Edkins, S. E. Hunt, C. Langford, D. Symmons, P. Concannon, S. Onengut-Gumuscu, S. S. Rich, P. Deloukas, M. A. Gonzalez-Gay, L. Rodriguez-Rodriguez, L. Ärlsetig, J. Martin, S. Rantapää-Dahlqvist, R. M. Plenge, S. Raychaudhuri, L. Klareskog, P. K. Gregersen, and J. Worthington. 2012. High-density genetic mapping identifies new susceptibility loci for rheumatoid arthritis. Nature genetics 44:1336–40.

Fenutría, R., V. G. Martinez, I. Simões, J. Postigo, V. Gil, M. Martínez-Florensa, J. Sintes, R. Naves, K. S. Cashman, J. Alberola-Ila, M. Ramos-Casals, G. Soldevila, C. Raman, J. Merino, R. Merino, P. Engel, and F. Lozano. 2014. Transgenic expression of soluble human CD5 enhances experimentally-induced autoimmune and anti-tumoral immune responses. PLoS ONE 9:e84895.

Fishwild, D. M., and V. Strand. 1994. Administration of an anti-CD5 immunoconjugate to patients with rheumatoid arthritis: effect on peripheral blood mononuclear cells and *in vitro* immune function. The Journal of rheumatology 21:596–604.

Foss, F. M., A. Raubitscheck, J. L. Mulshine, T. A. Fleisher, J. C. Reynolds, C. H. Paik, R. D. Neumann, C. Boland, P. Perentesis, M. R. Brown, J. M. Frincke, C. P. Lollo, S.

M. Larson, and J. A. Carrasquillo. 1998. Phase I study of the pharmacokinetics of a radioimmunoconjugate, 90Y-T101, in patients with CD5-expressing leukemia and lymphoma. Clinical cancer research : an official journal of the American Association for Cancer Research 4:2691–700.

Friedlein, G., F. El Hage, I. Vergnon, C. Richon, P. Saulnier, Y. Lécluse, A. Caignard, L. Boumsell, G. Bismuth, S. Chouaib, F. Mami-Chouaib. 2007. Human CD5 protects circulating tumor antigen-specific CTL from tumor-mediated activation-induced cell death. The Journal of Immunology 178:6821–7.

Fulton, R. B., S. E. Hamilton, Y. Xing, J. A. Best, A. W. Goldrath, K. A. Hogquist, and S. C. Jameson. 2015. The TCR's sensitivity to self peptide-MHC dictates the ability of naive CD8(+) T cells to respond to foreign antigens. Nature immunology 16:107–17.

Gangemi, R. M., J. A. Swack, D. M. Gaviria, and P. L. Romain. 1989. Anti-T12, an anti-CD6 monoclonal antibody, can activate human T lymphocytes. Journal of immunology (Baltimore, Md. : 1950) 143:2439–47.

Garaud, S., C. Le Dantec, C. Berthou, P. M. Lydyard, P. Youinou, and Y. Renaudineau. 2008. Selection of the Alternative Exon 1 from the cd5 Gene Down-Regulates Membrane Level of the Protein in B Lymphocytes. J. Immunol. 181:2010–2018.

Garaud, S., C. Le Dantec, S. Jousse-Joulin, C. Hanrotel-Saliou, A. Saraux, R. A. Mageed, P. Youinou, and Y. Renaudineau. 2009. IL-6 modulates CD5 expression in B cells from patients with lupus by regulating DNA methylation. Journal of immunology 182:5623–5632.

Garcia Santana, C. A., J. W. Tung, and S. Gulnik. 2014. Human T_{reg} cells are characterized by low/negative CD6 expression. Cytometry. Part A : the journal of the International Society for Analytical Cytology 85:901–8.

Gary-Gouy, H., J. Harriague, G. Bismuth, C. Platzer, C. Schmitt, and A. H. Dalloul. 2002. Human CD5 promotes B-cell survival through stimulation of autocrine IL-10 production. Blood 100:4537–4543.

Germain, R. N. 2002. T-cell development and the CD4-CD8 lineage decision. Nature reviews. Immunology 2:309–322.

Gimferrer, I., M. Calvo, M. Mittelbrunn, M. Farnós, M. R. Sarrias, C. Enrich, J. Vives, F. Sánchez-Madrid, and F. Lozano. 2004. Relevance of CD6-mediated interactions in T cell activation and proliferation. Journal of immunology (Baltimore, Md. : 1950) 173:2262–70.

Gimferrer, I., M. Farnós, M. Calvo, M. Mittelbrunn, C. Enrich, F. Sánchez-Madrid, J. Vives, and F. Lozano. 2003. The accessory molecules CD5 and CD6 associate on the membrane of lymphoid T cells. The Journal of biological chemistry 278:8564–71.

Gimferrer, I., A. Ibáñez, M. Farnós, M.-R. Sarrias, R. Fenutría, S. Roselló, P. Zimmermann, G. David, J. Vives, C. Serra-Pagès, and F. Lozano. 2005. The lymphocyte receptor CD6 interacts with syntenin-1, a scaffolding protein containing PDZ domains. Journal of immunology (Baltimore, Md. : 1950) 175:1406–14.

Glick, B., T. S. Chang, and J. G. 1956. The bursa of Fabricius and antibody production. Poultry Science 35:224–225.

Gogolin-Ewens, K., E. Meeusen, C. S. Lee, and M. Brandon. 1989. Expression of CD5, a lymphocyte surface antigen on the endothelium of blood vessels. European journal of immunology 19:935–8.

Gorp, H. Van, W. Van Breedam, J. Van Doorsselaere, P. L. Delputte, and H. J. Nauwynck 1#. 2010. Identification of the CD163 Protein Domains Involved in Infection of the Porcine Reproductive and Respiratory Syndrome Virus. Journal of Virology 84:3101–3105.

Haas, K. M., and D. M. Estes. 2001. The identification and characterization of a ligand for bovine CD5. Journal of immunology (Baltimore, Md. : 1950) 166:3158–66.

Hafler, D. A., R. J. Fallis, D. M. Dawson, S. F. Schlossman, E. L. Reinherz, and H. L. Weiner. 1986. Immunologic responses of progressive multiple sclerosis patients treated with an anti-T-cell monoclonal antibody, anti-T12. Neurology 36:777–84.

Hagn, M., V. Ebel, K. Sontheimer, E. Schwesinger, O. Lunov, T. Beyer, D. Fabricius, T. F. E. Barth, A. Viardot, S. Stilgenbauer, J. Hepp, K. Scharffetter-Kochanek, T. Simmet, and B. Jahrsdörfer. 2010. $CD5^+$ B cells from individuals with systemic lupus erythematosus express granzyme B. European Journal of Immunology 40:2060–2069.

Hara, M., A. Kitani, T. Hirose, K. Norioka, M. Harigai, K. Suzuki, H. Tabata, M. Kawakami, M. Kawagoe, and H. Nakamura. 1988. Stimulatory effect of CD5 antibody on B cells from patients with rheumatoid arthritis. Clinical immunology and immunopathology 49:223–30.

Hardy, R. R., and K. Hayakawa. 2001. B cell development pathways. Annual review of immunology 19:595–621.

Hardy, R. R., Y. S. Li, D. Allman, M. Asano, M. Gui, and K. Hayakawa. 2000. B-cell commitment, development and selection. Immunological reviews 175:23–32.

Hassan, N. J., S. J. Simmonds, N. G. Clarkson, S. Hanrahan, M. J. Puklavec, M. Bomb, A. N. Barclay, and M. H. Brown. 2006. CD6 regulates T-cell responses through activation-dependent recruitment of the positive regulator SLP-76. Molecular and cellular biology 26:6727–38.

Hawiger, D., R. F. Masilamani, E. Bettelli, V. K. Kuchroo, and M. C. Nussenzweig. 2004. Immunological Unresponsiveness Characterized by Increased Expression of CD5 on Peripheral T Cells Induced by Dendritic Cells *In Vivo.* Immunity 20:695–705.

Hayakawa, K., and R. R. Hardy. 2000, June. Development and function of B-1 cells. Curr Opin Immunol 12(3):346-53

Hem, C. D., M. Ekornhol, S. Granum, V. Sundvold-Gjerstad, and A. Spurkland. 2017. CD6 and Linker of Activated T Cells are Potential Interaction Partners for T Cell-Specific Adaptor Protein. Scandinavian Journal of Immunology 85:104–112.

Henderson, J. G., and D. Hawiger. 2015. Regulation of extrathymic T_{reg} cell conversion by CD5. Oncotarget 6:26554–5.

Henderson, J. G., A. Opejin, A. Jones, C. Gross, and D. Hawiger. 2015. CD5 instructs extrathymic regulatory T cell development in response to self and tolerizing antigens. Immunity 42:471–83.

Hendriks, J., L. a Gravestein, K. Tesselaar, R. A. van Lier, T. N. Schumacher, and J. Borst. 2000. CD27 is required for generation and long-term maintenance of T cell immunity. Nature immunology 1:433–40.

Hernández, P., E. Moreno, L. E. Aira, and P. C. Rodríguez. 2016. Therapeutic Targeting of CD6 in Autoimmune Diseases: A Review of Cuban Clinical Studies with the Antibodies IOR-T1 and Itolizumab. Current drug targets 17:666–77.

Hillion, S., S. Garaud, V. Devauchelle, A. Bordron, C. Berthou, P. Youinou, and C. Jamin. 2007. Interleukin-6 is responsible for aberrant B-cell receptor-mediated regulation of RAG expression in systemic lupus erythematosus. Immunology 122:371–380.

Hippen, K. L., L. E. Tze, and T. W. Behrens. 2000. CD5 maintains tolerance in anergic B cells. The Journal of experimental medicine 191:883–90.

Hollander, N. 1985. The immunotherapeutic effect of anti Lyt-1 antibodies on local and metastatic tumor growth. Advances in experimental medicine and biology 186:819–826.

Hollander, N., E. Pillemer, and I. L. Weissman. 1981. Effects of Lyt antibodies on T-cell functions: augmentation by anti-Lyt-1 as opposed to inhibition by anti-Lyt-2.

Proceedings of the National Academy of Sciences of the United States of America 78:1148–51.

Huang, X. R., P. G. Tipping, J. Apostolopoulos, C. Oettinger, M. D'Souza, G. Milton, and S. R. Holdsworth. 1997. Mechanisms of T cell-induced glomerular injury in anti-glomerular basement membrane (GBM) glomerulonephritis in rats. Clinical and experimental immunology 109:134–42.

Hunger, R. E., C. Carnaud, I. Garcia, P. Vassalli, and C. Mueller. 1997. Prevention of autoimmune diabetes mellitus in NOD mice by transgenic expression of soluble tumor necrosis factor receptor p55. European journal of immunology 27:255–61.

Huppa, J. B., and M. M. Davis. 2003. T-cell-antigen recognition and the immunological synapse. Nature Reviews Immunology 3:973–983.

Ibáñez, A., M.-R. Sarrias, M. Farnós, I. Gimferrer, C. Serra-Pagès, J. Vives, and F. Lozano. 2006. Mitogen-activated protein kinase pathway activation by the CD6 lymphocyte surface receptor. Journal of immunology (Baltimore, Md. : 1950) 177:1152–9.

Ikezumi, Y., K. Kanno, T. Karasawa, G. I. Dong Han, Y. Ito, H. Koike, S. Toyabe, M. Uchiyama, F. Shimizu, and H. Kawachi. 2004. The role of lymphocytes in the experimental progressive glomerulonephritis. Kidney International 66:1036–1048.

Ikezumi, Y., H. Kawachi, S. Toyabe, M. Uchiyama, and F. Shimizu. 2000. An anti-CD5 monoclonal antibody ameliorates proteinuria and glomerular lesions in rat mesangioproliferative glomerulonephritis. Kidney International 58:100–114.

Illei, G. G., Y. Shirota, C. H. Yarboro, J. Daruwalla, E. Tackey, K. Takada, T. Fleisher, J. E. Balow, and P. E. Lipsky. 2010. Tocilizumab in systemic lupus erythematosus: Data on safety, preliminary efficacy, and impact on circulating plasma cells from an open-label phase I dosage-escalation study. Arthritis and Rheumatism 62:542–552.

Imboden, J. B., C. H. June, M. A. McCutcheon, and J. A. Ledbetter. 1990. Stimulation of CD5 enhances signal transduction by the T cell antigen receptor. The Journal of clinical investigation 85:130–4.

Iritani, B. M., K. A. Forbush, M. A. Farrar, and R. M. Perlmutter. 1997. Control of B cell development by Ras-mediated activation of Raf. The EMBO journal 16:7019–7031.

Izquierdo Cano, L. M., E. E. Espinosa Estrada, C. H. Padrón, L. G. Ramón Rodríguez, O. M. Ávila Cabrera, P. H. Ramírez, J. E. Montero Casimiro, and P. H. Casaña. 2014. Anticuerpo monoclonal humanizado itolizumab (anti-CD6) en sindromes linfoproliferativos $CD6^{+}$. Experiencia preliminar. Revista Cubana de Hematologia,

Inmunologia y Hemoterapia 30:0–0.

De Jager, P. L., X. Jia, J. Wang, P. I. W. de Bakker, L. Ottoboni, N. T. Aggarwal, L. Piccio, S. Raychaudhuri, D. Tran, C. Aubin, R. Briskin, S. Romano, International MS Genetics Consortium, S. E. Baranzini, J. L. McCauley, M. A. Pericak-Vance, J. L. Haines, R. A. Gibson, Y. Naeglin, B. Uitdehaag, P. M. Matthews, L. Kappos, C. Polman, W. L. McArdle, D. P. Strachan, D. Evans, A. H. Cross, M. J. Daly, A. Compston, S. J. Sawcer, H. L. Weiner, S. L. Hauser, D. A. Hafler, and J. R. Oksenberg. 2009. Meta-analysis of genome scans and replication identify CD6, IRF8 and TNFRSF1A as new multiple sclerosis susceptibility loci. Nature genetics 41:776–82.

Jameson, S. C., and M. J. Bevan. 1995. T cell receptor antagonists and partial agonists. Immunity 2(1):1-11.

Janeway, C. A., and R. Medzhitov. 2002. Innate Immune Recognition. Annual Review of Immunology 20:197–216.

Jeannin, D., C. David, H. Gascan, G. Caron, D. Duluc, I. Frémaux, P. Jeannin, and Y. Delneste. 2005. Direct Stimulation of Human T Cells via TLR5 and TLR7/8: Flagellin and R-848 Up-Regulate Proliferation and IFN-gamma Production by Memory $CD4^+$ T Cells. The Journal of Immunology 175:1551–1557.

Jiang, S., X. Li, N. J. Hess, Y. Guan, and R. I. Tapping. 2016. TLR10 Is a Negative Regulator of Both MyD88-Dependent and -Independent TLR Signaling. The Journal of Immunology 196:3834–3841.

Kamoun, M., M. E. Kadin, P. J. Martin, J. Nettleton, and J. A. Hansen. 1981. A novel human T cell antigen preferentially expressed on mature T cells and shared by both well and poorly differentiated B cell leukemias and lymphomas. Journal of immunology (Baltimore, Md. : 1950) 127:987–91.

Kim, H. S., A.-R. Kim, D. K. Kim, H. W. Kim, Y. H. Park, G. H. Jang, B. Kim, Y. M. Park, J. S. You, H. S. Kim, M. A. Beaven, Y. M. Kim, and W. S. Choi. 2015. Interleukin-10-producing $CD5^+$ B cells inhibit mast cells during immunoglobulin E-mediated allergic responses. Science signaling 8:ra28.

Kim, Y. L., S. J. Gong, Y. H. Hwang, J. E. Joo, Y. U. Cho, J. A. Lee, S. A. Sung, S. Y. Lee, and N. Y. Kim. 2011. Waldenstrom macroglobulinemia with $CD5^+$ expression presented as cryoglobulinemic glomerulonephropathy: A case report. Journal of Korean Medical Science 26:824–828.

Kirkman, R. L., J. L. Araujo, G. J. Busch, C. B. Carpenter, E. L. Milford, E. L. Reinherz, S. F. Schlossman, T. B. Strom, and N. L. Tilney. 1983. Treatment of acute renal allograft

rejection with monoclonal anti-T12 antibody. Transplantation 36:620–6.

Kobarg, J., G. S. Whitney, D. Palmer, A. Aruffo, and M. A. Bowen. 1997. Analysis of the tyrosine phosphorylation and calcium fluxing of human CD6 isoforms with different cytoplasmatic domains. European Journal of Immunology 27:2971–2980.

Kofler, D. M., A. Farkas, M. von Bergwelt-Baildon, and D. A. Hafler. 2016. The Link Between CD6 and Autoimmunity : Genetic and Cellular Associations. Current drug targets 17:651–665.

Kofler, D. M., C. A. Severson, N. Mousissian, P. L. De Jager, and D. A. Hafler. 2011. The CD6 multiple sclerosis susceptibility allele is associated with alterations in $CD4^+$ T cell proliferation. Journal of immunology (Baltimore, Md. : 1950) 187:3286–91.

Konno, A., J. S. Ahn, H. Kitamura, M. J. Hamilton, J. A. Gebe, A. Aruffo, and W. C. Davis. 2001. Tissue distribution of CD6 and CD6 ligand in cattle: expression of the CD6 ligand (CD166) in the autonomic nervous system of cattle and the human. Journal of leukocyte biology 69:944–50.

Krintel, S. B., L. Essioux, A. Wool, J. S. Johansen, E. Schreiber, T. Zekharya, P. Akiva, M. Østergaard, and M. L. Hetland. 2012. CD6 and syntaxin binding protein 6 variants and response to tumor necrosis factor alpha inhibitors in danish patients with rheumatoid arthritis. PLoS ONE 7:1–8.

Krupashankar, D. S., S. Dogra, M. Kura, A. Saraswat, L. Budamakuntla, T. K. Sumathy, R. Shah, M. G. Gopal, T. Narayana Rao, C. R. Srinivas, R. Bhat, N. Shetty, G. Manmohan, K. Sai Krishna, D. Padmaja, D. V. S. Pratap, V. Garg, S. Gupta, N. Pandey, U. Khopkar, E. Montero, M. S. Ramakrishnan, P. Nair, and P. C. Ganapathi. 2014. Efficacy and safety of itolizumab, a novel anti-CD6 monoclonal antibody, in patients with moderate to severe chronic plaque psoriasis: Results of a double-blind, randomized, placebo-controlled, phase-III study. Journal of the American Academy of Dermatology 71:484–492.

Krupnick, A. S., A. E. Gelman, W. Barchet, S. Richardson, F. H. Kreisel, L. A. Turka, M. Colonna, G. A. Patterson, and D. Kreisel. 2005. Murine vascular endothelium activates and induces the generation of allogeneic $CD4^+25^+FoxP3^+$ regulatory T cells. Journal of Immunology 175:6265–6270.

Kumar, H., T. Kawai, and S. Akira. 2011. Pathogen recognition by the innate immune system. International reviews of immunology 30:16–34.

Lanier, L. L., N. L. Warner, J. A. Ledbetter, and L. A. Herzenberg. 1981. Expression of Lyt-1 antigen on certain murine B cell lymphomas. Journal of Experimental Medicine

153:998–1003.

Lecomte, O., J. B. Bock, B. W. Birren, D. Vollrath, and J. R. Parnes. 1996. Molecular linkage of the mouseCD5 andCD6 genes. Immunogenetics 44:385–390.

Lécuyer, M.-A., O. Saint-Laurent, L. Bourbonnière, S. Larouche, C. Larochelle, L. Michel, M. Charabati, M. Abadier, S. Zandee, N. Haghayegh Jahromi, E. Gowing, C. Pittet, R. Lyck, B. Engelhardt, and A. Prat. 2017. Dual role of ALCAM in neuroinflammation and blood–brain barrier homeostasis. Proceedings of the National Academy of Sciences 114.

Ledbetter, J. A., R. L. Evans, M. Lipinski, C. Cunningham-Rundles, R. A. Good, and L. A. Herzenberg. 1981. Evolutionary conservation of surface molecules that distinguish T lymphocyte helper/inducer and cytotoxic/suppressor subpopulations in mouse and man. The Journal of experimental medicine 153:310–23.

Ledbetter, J. A., R. V Rouse, H. Spedding Micklem, and L. A. Herzenberg. 1980. T cell subsets defined by expression of Lyt-1,2,3 and Thy-1 antigens. Journal of Experimental Medicine 152:280–295.

Lee, C. C., A. M. Avalos, and H. L. Ploegh. 2012. Accessory molecules for Toll-like receptors and their function. Nature Reviews Immunology 12:168–79.

Lee, S. Y., D. K. Jung, J. E. Choi, C. C. Jin, M. J. Hong, S. K. Do, H.-G. Kang, W. K. Lee, Y. Seok, E. B. Lee, J. Y. Jeong, K. M. Shin, S. S. Yoo, J. Lee, S. I. Cha, C. H. Kim, and J. Y. Park. 2016. PD-L1 polymorphism can predict clinical outcomes of non-small cell lung cancer patients treated with first-line paclitaxel-cisplatin chemotherapy. Scientific reports 6:25952.

Lemaitre, B., E. Nicolas, L. Michaut, J. M. Reichhart, and J. A. Hoffmann. 1996. The dorsoventral regulatory gene cassette spatzle/Toll/Cactus controls the potent antifungal response in Drosophila adults. Cell 86:973–983.

Lenz, L. L. 2009. CD5 sweetens lymphocyte responses. Proceedings of the National Academy of Sciences of the United States of America 106:1303–4.

Li, Y., N. G. Singer, J. Whitbred, M. A. Bowen, D. A. Fox, and F. Lin. 2017. CD6 as a potential target for treating multiple sclerosis. Proceedings of the National Academy of Sciences of the United States of America:201615253.

Liu, H., M. Komai-Koma, D. Xu, and F. Y. Liew. 2006. Toll-like receptor 2 signaling modulates the functions of $CD4^+$ $CD25^+$ regulatory T cells. Proceedings of the National Academy of Sciences of the United States of America 103:7048–53.

Loo, Y. M., and M. Gale. 2011, May 27. Immune Signaling by RIG-I-like Receptors. Immunity 27;34(5):680-92.

López-Hoyos, M., R. Marquina, E. Tamayo, J. González-Rojas, S. Izui, R. Merino, and J. Merino. 2003. Defects in the regulation of B cell apoptosis are required for the production of citrullinated peptide autoantibodies in mice. Arthritis and Rheumatism 48:2353–2361.

Lorenz, H. M., and J. R. Kalden. 1998. Biological agents in rheumatoid arthritis: Which ones could be used in combination? BioDrugs: Clinical Immunotherapeutics, Biopharmaceuticals and Gene Therapy 9(4):303-324

Lorini, R., M. Massa, G. D'Annunzio, L. Cortona, F. De Benedetti, A. Martini, and F. Severi. 1993. CD5-Positive B cells in type 1 (insulin-dependent) diabetic children. Diabetes Research and Clinical Practice 19:17–22.

Lozano, F., M. Simarro, J. Calvo, J. Vila, O. Padilla, M. Bowen, K. S. Campbell, V. A, ` J M, O. Padilla, J. Bowen, K. S. Campbell, and Cd5. 2000. CD5 signal transduction: positive or negative modulation of antigen receptor signaling. Critical reviews in immunology 20:347.

Ma, L., B. Liu, Z. Jiang, and Y. Jiang. 2014. Reduced numbers of regulatory B cells are negatively correlated with disease activity in patients with new-onset rheumatoid arthritis. Clinical Rheumatology 33:187–195.

Mäkinen, T., L. Jussila, T. Veikkola, T. Karpanen, M. I. Kettunen, K. J. Pulkkanen, R. Kauppinen, D. G. Jackson, H. Kubo, S.-I. Nishikawa, S. Ylä-Herttuala, and K. Alitalo. 2001. Inhibition of lymphangiogenesis with resulting lymphedema in transgenic mice expressing soluble VEGF receptor-3. Nature Medicine 7:199–205.

Markeljevic, J., D. Batinic, B. Uzarevic, J. Bozikov, N. Cikes, D. Babic-Naglic, Z. Horvat, and M. Marusic. 1994. Peripheral blood $CD5^+$ B cell subset in the remission phase of systemic connective tissue diseases. Journal of Rheumatology 21:2225–2230.

Martínez-Florensa, M., M. Consuegra-Fernández, F. Aranda, N. Armiger-Borràs, M. Di Scala, E. Carrasco, J. Pachón, J. Vila, G. González-Aseguinolaza, and F. Lozano. 2017. Protective Effects of Human and Mouse Soluble Scavenger-Like CD6 Lymphocyte Receptor in a Lethal Model of Polymicrobial Sepsis. Antimicrobial Agents and Chemotherapy 61:e01391-16.

Martínez-Florensa, M., M. Consuegra-Fernández, V. G. Martínez, O. Cañadas, N. Armiger-Borràs, L. Bonet-Roselló, A. Farrán, J. Vila, C. Casals, and F. Lozano. 2014. Targeting of key pathogenic factors from gram-positive bacteria by the soluble ectodomain of

the scavenger-like lymphocyte receptor CD6. Journal of Infectious Diseases 209:1077–1086.

Martinez-Pasamar, S., E. Abad, B. Moreno, N. Velez de Mendizabal, I. Martinez-Forero, J. Garcia-Ojalvo, and P. Villoslada. 2013. Dynamic cross-regulation of antigen-specific effector and regulatory T cell subpopulations and microglia in brain autoimmunity. BMC systems biology 7:34.

Martinez, V. G., S. K. Moestrup, U. Holmskov, J. Mollenhauer, and F. Lozano. 2011. The Conserved Scavenger Receptor Cysteine-Rich Superfamily in Therapy and Diagnosis. Pharmacological Reviews 63:967–1000.

Masuda, K., and T. Kishimoto. 2016, April 19. CD5: A New Partner for IL-6.

Matalka, K. Z., M. F. Tutunji, M. Abu-Baker, and Y. Abu Baker. 2005. Measurement of protein cytokines in tissue extracts by enzyme-linked immunosorbent assays: Application to lipopolysaccharide-induced differential milieu of cytokines. Neuroendocrinology Letters 26:231–236.

Matsushita, T., K. Yanaba, J.-D. Bouaziz, M. Fujimoto, and T. F. Tedder. 2008. Regulatory B cells inhibit EAE initiation in mice while other B cells promote disease progression. The Journal of clinical investigation 118:3420–30.

Mauri, C. 2010, December. Regulation of immunity and autoimmunity by B cells.

Mayer, B., I. Funke, B. Seed, G. Riethmüller, and E. Weiss. 1990. Expression of the CD6 T lymphocyte differentiation antigen in normal human brain. Journal of neuroimmunology 29:193–202.

Mier-Aguilar, C. A., B. Vega-Baray, E. Burgueño-Bucio, F. Lozano, E. A. García-Zepeda, C. Raman, and G. Soldevila. 2015. Functional requirement of tyrosine residue 429 within CD5 cytoplasmic domain for regulation of T cell activation and survival. Biochemical and Biophysical Research Communications 466:381–387.

Miller, J. F. A. P. 1962. Immunological Significance of the Thymus of the Adult Mouse. Nature 195:1318–1319.

Miller, J. F. A. P. 2002. The discovery of thymus function and of thymus-derived lymphocytes. Immunological Reviews 185:7–14.

Mittrücker, H.-W., A. Visekruna, and M. Huber. 2014. Heterogeneity in the Differentiation and Function of $CD8^+$ T Cells. Archivum Immunologiae et Therapiae Experimentalis 62:449–458.

Mix, E., T. Olsson, J. Correale, S. Baig, V. Kostulas, O. Olsson, and H. Link. 1990. B cells expressing CD5 are increased in cerebrospinal fluid of patients with multiple sclerosis. Clinical and experimental immunology 79:21–7.

Mogensen, T. H. 2009, April. Pathogen recognition and inflammatory signaling in innate immune defenses. American Society for Microbiology (ASM).

Morbach, H., S. K. Singh, C. Faber, P. E. Lipsky, and H. J. Girschick. 2006. Analysis of RAG expression by peripheral blood $CD5^+$ and $CD5^-$ B cells of patients with childhood systemic lupus erythematosus. Annals of the rheumatic diseases 65:482–7.

Moreau, M. F., J. L. Thibaud, L. Ben Miled, M. Chaussepied, M. Baumgartner, W. C. Davis, P. Minoprio, and G. Langsley. 1999. Theileria annulata in $CD5^+$ macrophages and B1 B cells. Infection and Immunity 67:6678–6682.

Muñoz, A., T. Gallart, O. Viñas, and R. Gomis. 1991. Increased CD5-positive B lymphocytes in type I diabetes. Clinical and experimental immunology 83:304–308.

Nagatani, K., R. Yamaoka, Y. Tezuka, and M. Hayashi. 2013. Involvement of $CD5^+CD19^+$Cell in steroid-dependent nephrotic syndrome treated with B-cell targeting therapy. Pediatrics International 55:99–101.

Niino, M., T. Fukazawa, N. Minami, I. Amino, J. Tashiro, N. Fujiki, S. Doi, and S. Kikuchi. 2012. CD5-positive B cell subsets in secondary progressive multiple sclerosis. Neuroscience Letters 523:56–61.

Nishimura, Y., B. E. Bierer, and S. J. Burakoff. 1988. Expression of CD5 regulates responsiveness to IL-1. Journal of immunology (Baltimore, Md : 1950) 141:3438–3444.

Nummer, D., E. Suri-Payer, H. Schmitz-Winnenthal, A. Bonertz, L. Galindo, D. Antolovich, M. Koch, M. Büchler, J. Weitz, V. Schirrmacher, and P. Beckhove. 2007. Role of tumor endothelium in $CD4^+$ $CD25^+$ regulatory T cell infiltration of human pancreatic carcinoma. Journal of the National Cancer Institute 99:1188–1199.

Ochoa-Repáraz, J., D. W. Mielcarz, S. Haque-Begum, and L. H. Kasper. 2010. Induction of a regulatory B cell population in experimental allergic encephalomyelitis by alteration of the gut commensal microflora. Gut Microbes 1:103–108.

Oleinika, K., R. J. Nibbs, G. J. Graham, and A. R. Fraser. 2013. Suppression, subversion and escape: the role of regulatory T cells in cancer progression. Clinical and experimental immunology 171:36–45.

Oliveira, M. I., C. M. Gonçalves, M. Pinto, S. Fabre, A. M. Santos, S. F. Lee, M. A. A. Castro, R. J. Nunes, R. R. Barbosa, J. R. Parnes, C. Yu, S. J. Davis, A. Moreira, G. Bismuth, and

A. M. Carmo. 2012. CD6 attenuates early and late signaling events, setting thresholds for T-cell activation. European journal of immunology 42:195–205.

Olsen, N. J., R. H. Brooks, J. J. Cush, P. E. Lipsky, E. W. St Clair, E. L. Matteson, K. N. Gold, G. W. Cannon, C. G. Jackson, W. J. McCune, D. A. Fox, B. Nelson, T. Lorenz, and V. Strand. 1996. A double-blind, placebo-controlled study of anti-CD5 immunoconjugate in patients with rheumatoid arthritis. The Xoma RA Investigator Group. Arthritis and rheumatism 39:1102–1108.

Olsen, N. J., G. P. Teal, and V. Strand. 1993. *In vivo* T cell depletion in rheumatoid arthritis is associated with increased *in vitro* IgM-rheumatoid factor synthesis. Clinical immunology and immunopathology 67:124–129.

Ordoñez-Rueda, D., F. Lozano, A. Sarukhan, C. Raman, E. A. Garcia-Zepeda, and G. Soldevila. 2009. Increased numbers of thymic and peripheral $CD4^+$ $CD25^+FoxP3^+$ cells in the absence of CD5 signaling. European Journal of Immunology 39:2233–47.

Orta-Mascaró, M., M. Consuegra-Fernández, E. Carreras, R. Roncagalli, A. Carreras-Sureda, P. Alvarez, L. Girard, I. Simões, M. Martínez-Florensa, F. Aranda, R. Merino, V.-G. G. Martínez, R. Vicente, J. Merino, A. Sarukhan, M. Malissen, B. Malissen, and F. Lozano. 2016. CD6 modulates thymocyte selection and peripheral T cell homeostasis. The Journal of Experimental Medicine 214:1–12.

Osorio, L. M., C. A. Garcia, M. Jondal, and S. C. Chow. 1994. The anti-CD6 mAb, IOR-T1, defined a new epitope on the human CD6 molecule that induces greater responsiveness in T cell receptor/CD3-mediated T cell proliferation. Cellular immunology 154:123–33.

Osorio, L. M., M. Rottenberg, M. Jondal, and S. C. Chow. 1998. Simultaneous cross-linking of CD6 and CD28 induces cell proliferation in resting T cells. Immunology 93:358–65.

Osorio, L. M., A. De Santiago, M. Aguilar-Santelises, H. Mellstedt, and M. Jondal. 1997. CD6 ligation modulates the Bcl-2/Bax ratio and protects chronic lymphocytic leukemia B cells from apoptosis induced by anti-IgM. Blood 89:2833–2841.

Padilla, O., J. Calvo, J. M. Vila, M. Arman, I. Gimferrer, L. Places, M. T. Arias, M. A. Pujana, J. Vives, and F. Lozano. 2000. Genomic organization of the human CD5 gene. Immunogenetics 51:993–1001.

Patel, D. D., S. F. Wee, L. P. Whichard, M. A. Bowen, J. M. Pesando, A. Aruffo, and B. F. Haynes. 1995. Identification and characterization of a 100-kD ligand for CD6 on human thymic epithelial cells. The Journal of experimental medicine 181:1563–8.

Pedroza-Pacheco, I., A. Madrigal, and A. Saudemont. 2013. Interaction between natural

killer cells and regulatory T cells: perspectives for immunotherapy. Cellular & molecular immunology 10:222–9.

Peña-Rossi, C., and L. Zuckerman. 1999. Negative regulation of CD4 lineage development and responses by CD5. The Journal of Immunology 163:6494–6501.

Perillo, N. L., C. H. Uittenbogaart, J. T. Nguyen, and L. G. Baum. 1997. Galectin-1, an endogenous lectin produced by thymic epithelial cells, induces apoptosis of human thymocytes. The Journal of experimental medicine 185:1851–8.

Peters, M., S. Jacobs, M. Ehlers, P. Vollmer, J. Müllberg, E. Wolf, G. Brem, K. H. Meyer zum Büschenfelde, and S. Rose-John. 1996. The function of the soluble interleukin 6 (IL-6) receptor *in vivo*: sensitization of human soluble IL-6 receptor transgenic mice towards IL-6 and prolongation of the plasma half-life of IL-6. The Journal of experimental medicine 183:1399–406.

Pieper, K., B. Grimbacher, and H. Eibel. 2013, April. B-cell biology and development.

Plater-Zyberk, C., P. C. Taylor, M. G. Blaylock, and R. N. Maini. 1994. Anti-CD5 therapy decreases severity of established disease in collagen type. Clinical and experimental immunology 98:442–447.

Pospisil, R., G. J. Silverman, G. E. Marti, A. Aruffo, M. A. Bowen, and R. G. Mage. 2000. CD5 is A potential selecting ligand for B-cell surface immunoglobulin: a possible role in maintenance and selective expansion of normal and malignant B cells. Leukemia & lymphoma 36:353–65.

Postigo, J., F. Genre, M. Iglesias, M. Fernández-Rey, L. Buelta, J. Carlos Rodríguez-Rey, J. Merino, and R. Merino. 2011. Exacerbation of type II collagen-induced arthritis in apolipoprotein E-deficient mice in association with the expansion of T_h1 and T_h17 cells. Arthritis and rheumatism 63:971–80.

Potrony, M., E. Carreras, F. Aranda, L. Zimmer, J.-A. Puig-Butille, G. Tell-Martí, N. Armiger, A. Sucker, P. Giménez-Xavier, M. Martínez-Florensa, C. Carrera, J. Malvehy, D. Schadendorf, S. Puig, and F. Lozano. 2016. Inherited functional variants of the lymphocyte receptor CD5 influence melanoma survival. International journal of cancer.

PrabhuDas, M., D. Bowdish, K. Drickamer, M. Febbraio, J. Herz, L. Kobzik, M. Krieger, J. Loike, T. K. Means, S. K. Moestrup, S. Post, T. Sawamura, S. Silverstein, X.-Y. Wang, and J. El Khoury. 2014. Standardizing scavenger receptor nomenclature. Journal of immunology (Baltimore, Md. : 1950) 192:1997–2006.

PrabhuDas, M. R., C. L. Baldwin, P. L. Bollyky, D. M. E. Bowdish, K. Drickamer, M. Febbraio, J. Herz, L. Kobzik, M. Krieger, J. Loike, B. McVicker, T. K. Means, S. K. Moestrup, S. R. Post, T. Sawamura, S. Silverstein, R. C. Speth, J. C. Telfer, G. M. Thiele, X.-Y. Wang, S. D. Wright, and J. El Khoury. 2017. A Consensus Definitive Classification of Scavenger Receptors and Their Roles in Health and Disease. The Journal of Immunology 198:3775–3789.

Ramos-Casals, M., J. Font, M. Garcı, J. Calvo, L. Places, O. Padilla, R. Cervera, M. a Bowen, F. Lozano, and M. Ingelmo. 2001. High circulating levels of soluble scavenger receptors (sCD5 and sCD6) in patients with primary Sjogren's syndrome. Arthritis & Rheumatism:1056–1059.

Rasmussen, R. A., S. L. Counts, J. F. Daley, and S. F. Schlossman. 1994. Isolation and characterization of $CD6^-$ T cells from peripheral blood. Journal of immunology (Baltimore, Md. : 1950) 152:527–36.

Reinherz, E. L., R. Geha, J. M. Rappeport, M. Wilson, A. C. Penta, R. E. Hussey, K. A. Fitzgerald, J. F. Daley, H. Levine, F. S. Rosen, and S. F. Schlossman. 1982. Reconstitution after transplantation with T-lymphocyte-depleted HLA haplotype-mismatched bone marrow for severe combined immunodeficiency. Proceedings of the National Academy of Sciences of the United States of America 79:6047–51.

Reinherz, E. L., P. C. Kung, G. Goldstein, and S. F. Schlossman. 1979. A Monoclonal Antibody with Selective Reactivity with Functionally Mature Human Thymocytes and All Peripheral Human T Cells. The Journal of Immunology 123.

Renaudineau, Y., S. Hillion, A. Saraux, R. A. Mageed, and P. Youinou. 2005. An alternative exon 1 of the CD5 gene regulates CD5 expression in human B lymphocytes. Blood 106:2781–2789.

Robinson, W. H., H. E. N. de Vegvar, S. S. Prohaska, J. W. Rhee, and J. R. Parnes. 1995. Human CD6 possesses a large, alternatively spliced cytoplasmic domain. European Journal of Immunology 25:2765–2769.

Rodriguez, P. C., R. Torres-Moya, G. Reyes, C. Molinero, D. Prada, A. M. Lopez, I. M. Hernandez, M. V. Hernandez, J. P. Martinez, X. Hernandez, A. Casaco, M. Ramos, Y. Avila, Y. Barrese, E. Montero, and P. Hernandez. 2012. A clinical exploratory study with itolizumab, an anti-CD6 monoclonal antibody, in patients with rheumatoid arthritis. Results in Immunology 2:204–211.

Roncagalli, R., S. Hauri, F. Fiore, Y. Liang, Z. Chen, A. Sansoni, K. Kanduri, R. Joly, A. Malzac, H. Lähdesmäki, R. Lahesmaa, S. Yamasaki, T. Saito, M. Malissen, R. Aebersold, M. Gstaiger, and B. Malissen. 2014. Quantitative proteomics analysis of signalosome

dynamics in primary T cells identifies the surface receptor CD6 as a Lat adaptor-independent TCR signaling hub. Nature immunology 15:384–92.

Ronchese, F., B. Hausmann, S. Hubele, and P. Lane. 1994. Mice transgenic for a soluble form of murine CTLA-4 show enhanced expansion of antigen-specific $CD4^+$ T cells and defective antibody production *in vivo*. The Journal of experimental medicine 179:809–17.

Roy, S., and G. Trinchieri. 2017. Microbiota: a key orchestrator of cancer therapy. Nature Reviews Cancer 17:271–285.

Saifullah, M. K., D. a Fox, S. Sarkar, S. M. a Abidi, J. Endres, J. Piktel, T. M. Haqqi, and N. G. Singer. 2004. Expression and characterization of a novel CD6 ligand in cells derived from joint and epithelial tissues. Journal of immunology (Baltimore, Md. : 1950) 173:6125–33.

Sakaguchi, S., K. Fukuma, K. Kuribayashi, and T. Masuda. 1985. Organ-specific autoimmune diseases induced in mice by elimination of T cell subset. I. Evidence for the active participation of T cells in natural self-tolerance; deficit of a T cell subset as a possible cause of autoimmune disease. The Journal of experimental medicine 161:72–87.

Salin, H., M. Ricoul, L. Morat, and L. Sabatier. 2009. Increased genomic alteration complexity and telomere shortening in B-CLL cells resistant to radiation-induced apoptosis. Cytogenetic and Genome Research 122:343–349.

Sarhan, M. A., T. N. Pham, A. Y. Chen, and T. I. Michalak. 2012. Hepatitis C virus infection of human T lymphocytes is mediated by CD5. J Virol 86:3723–3735.

Sarrias, M.-R., M. Farnós, R. Mota, F. Sánchez-Barbero, A. Ibáñez, I. Gimferrer, J. Vera, R. Fenutría, C. Casals, J. Yélamos, and F. Lozano. 2007. CD6 binds to pathogen-associated molecular patterns and protects from LPS-induced septic shock. Proceedings of the National Academy of Sciences of the United States of America 104:11724–9.

Sarrias, M. R., J. Grønlund, O. Padilla, J. Madsen, U. Holmskov, and F. Lozano. 2004a. The Scavenger Receptor Cysteine-Rich (SRCR) domain: an ancient and highly conserved protein module of the innate immune system. Critical reviews in immunology 24:1–37.

Sarrias, M. R., O. Padilla, Y. Monreal, M. Carrascal, J. Abian, J. Vives, J. Yélamos, and F. Lozano. 2004b. Biochemical characterization of recombinant and circulating human Spalpha. Tissue antigens 63:335–44.

Sarukhan, A., M. Martinez-Florensa, C. Escoda-Ferran, E. Carrasco, E. Carreras, and F.

Lozano. 2016. Pattern Recognition by CD6: A Scavenger-Like Lymphocyte Receptor. Current drug targets 17:640–50.

Scott, T. F., J. McKolanis, W. Rothfus, and E. Cottington. 1994. Lymphocyte subsets in relapsing-remitting multiple sclerosis: a longitudinal study of B lymphocytes and T lymphocytes. Neurological research 16:385–8.

Seidi, O. A., Y. K. Semra, and M. K. Sharief. 2002. Expression of CD5 on B lymphocytes correlates with disease activity in patients with multiple sclerosis. Journal of Neuroimmunology 133:205–210.

Sellebjerg, F., J. Jensen, C. V Jensen, and A. Wiik. 2002. Expansion of CD5- B cells in multiple sclerosis correlates with CD80 (B7-1) expression. Scandinavian Journal of Immunology 56:101–107.

Sellick, G. S., R. Wade, S. Richards, D. G. Oscier, D. Catovsky, and R. S. Houlston. 2008. Scan of 977 nonsynonymous SNPs in CLL4 trial patients for the identification of genetic variants influencing prognosis. Blood 111:1625–1633.

Sembries, S., H. Pahl, S. Stilgenbauer, H. Döhner, and F. Schriever. 1999. Reduced expression of adhesion molecules and cell signaling receptors by chronic lymphocytic leukemia cells with 11q deletion. Blood 93:624–31.

Sestero, C. M., D. J. McGuire, P. De Sarno, E. C. Brantley, G. Soldevila, R. C. Axtell, and C. Raman. 2012. CD5-dependent CK2 activation pathway regulates threshold for T cell anergy. Journal of immunology (Baltimore, Md. : 1950) 189:2918–30.

Shirota, Y., C. Yarboro, R. Fischer, T.-H. Pham, P. Lipsky, and G. G. Illei. 2013. Impact of anti-interleukin-6 receptor blockade on circulating T and B cell subsets in patients with systemic lupus erythematosus. Annals of the rheumatic diseases 72:118–28.

Shishido, S. N., S. Varahan, K. Yuan, X. Li, and S. D. Fleming. 2012. Humoral innate immune response and disease. Clinical immunology (Orlando, Fla.) 144:142–158.

Singer, N. G., D. A. Fox, T. M. Haqqi, L. Beretta, J. S. Endres, S. Prohaska, J. R. Parnes, J. Bromberg, and R. M. Sramkoski. 2002. CD6: expression during development, apoptosis and selection of human and mouse thymocytes. International immunology 14:585–597.

Singer, N. G., B. C. Richardson, D. Powers, F. Hooper, F. Lialios, J. Endres, C. M. Bott, and D. A. Fox. 1996. Role of the CD6 glycoprotein in antigen-specific and autoreactive responses of cloned human T lymphocytes. Immunology 88:537–43.

Skyler, J. S., T. J. Lorenz, S. Schwartz, G. S. Eisenbarth, D. Einhorn, J. P. Palmer, J. B. Marks,

C. Greenbaum, E. A. Saria, and V. Byers. 1993. Effects of an anti-CD5 immunoconjugate (CD5-plus) in recent onset type I diabetes mellitus: a preliminary investigation. The CD5 Diabetes Project Team. Journal of diabetes and its complications 7:224–32.

Smith, H. R., and R. R. Olson. 1990. $CD5^+$ B lymphocytes in systemic lupus erythematosus and rheumatoid arthritis. The Journal of rheumatology 17:833–5.

Soiffer, R. J., C. Murray, P. Mauch, K. C. Anderson, A. S. Freedman, S. N. Rabinowe, T. Takvorian, M. J. Robertson, N. Spector, and R. Gonin. 1992. Prevention of graft-versus-host disease by selective depletion of CD6-positive T lymphocytes from donor bone marrow. Journal of Clinical Oncology 10:1191–1200.

Soldevila, G., C. Raman, and F. Lozano. 2011. The immunomodulatory properties of the CD5 lymphocyte receptor in health and disease. Current opinion in immunology 23:310–8.

Sowden, J. A., P. J. Roberts-Thomson, and H. Zola. 1987. Evaluation of CD5-positive B cells in blood and synovial fluid of patients with rheumatic diseases. Rheumatology international 7:255–9.

Stafford, F. J., T. A. Fleisher, G. Lee, M. Brown, V. Strand, H. A. Austin, J. E. Balow, and J. H. Klippel. 1994. A pilot study of anti-CD5 ricin A chain immunoconjugate in systemic lupus erythematosus. Journal of Rheumatology 21:2068–2070.

Stahl, E. A., S. Raychaudhuri, E. F. Remmers, G. Xie, S. Eyre, B. P. Thomson, Y. Li, F. A. Kurreeman, A. Zhernakova, A. Hinks, C. Guiducci, R. Chen, L. Alfredsson, C. I. Amos, K. G. Ardlie, A. Barton, J. Bowes, E. Brouwer, N. P. Burtt, J. J. Catanese, J. Coblyn, M. J. Coenen, K. H. Costenbader, L. A. Criswell, J. B. Crusius, J. Cui, P. I. de Bakker, P. L. De Jager, B. Ding, P. Emery, E. Flynn, P. Harrison, L. J. Hocking, T. W. Huizinga, D. L. Kastner, X. Ke, A. T. Lee, X. Liu, P. Martin, A. W. Morgan, L. Padyukov, M. D. Posthumus, T. R. Radstake, D. M. Reid, M. Seielstad, M. F. Seldin, N. A. Shadick, S. Steer, P. P. Tak, W. Thomson, A. H. van der Helm-van Mil, I. E. van der Horst-Bruinsma, C. E. van der Schoot, P. L. van Riel, M. E. Weinblatt, A. G. Wilson, G. J. Wolbink, B. P. Wordsworth, C. Wijmenga, E. W. Karlson, R. E. Toes, N. de Vries, A. B. Begovich, J. Worthington, K. A. Siminovitch, P. K. Gregersen, L. Klareskog, and R. M. Plenge. 2010. Genome-wide association study meta-analysis identifies seven new rheumatoid arthritis risk loci. Nature genetics 42:508–514.

Stamou, P., J. de Jersey, D. Carmignac, C. Mamalaki, D. Kioussis, and B. Stockinger. 2003. Chronic exposure to low levels of antigen in the periphery causes reversible functional impairment correlating with changes in CD5 levels in monoclonal CD8 T cells. Journal of immunology (Baltimore, Md : 1950) 171:1278–1284.

Strand, V., P. E. Lipsky, G. W. Cannon, L. H. Calabrese, C. Wiesenhutter, S. B. Cohen, N. J. Olsen, M. L. Lee, T. J. Lorenz, and B. Nelson. 1993. Effects of administration of an anti-CD5 plus immunoconjugate in rheumatoid arthritis. Results of two phase II studies. The CD5 Plus Rheumatoid Arthritis Investigators Group. Arthritis and rheumatism 36:620–630.

Strigård, K., T. Olsson, P. Larsson, R. Holmdahl, and L. Klareskog. 1988. Modulation of experimental allergic neuritis in rats by *in vivo* treatment with monoclonal anti T cell antibodies. Journal of the Neurological Sciences 83:283–291.

Sutmuller, R. P. M., M. H. M. G. M. Den Brok, M. Kramer, E. J. Bennink, L. W. J. Toonen, B. J. Kullberg, L. A. Joosten, S. Akira, M. G. Netea, and G. J. Adema. 2006. Toll-like receptor 2 controls expansion and function of regulatory T cells. Journal of Clinical Investigation 116:485–494.

Suzuki, H., Y. Shinkai, L. G. Granger, F. W. Alt, P. E. Love, and A. Singer. 1997. Commitment of immature $CD4^{+}8^{+}$ thymocytes to the CD4 lineage requires CD3 signaling but does not require expression of clonotypic T cell receptor (TCR) chains. The Journal of experimental medicine 186:17–23.

Swaminathan, B., A. Cuapio, I. Alloza, F. Matesanz, A. Alcina, M. García-Barcina, M. Fedetz, O. Fernández, M. Lucas, T. Orpez, M. J. Pinto-Medel, D. Otaegui, J. Olascoaga, E. Urcelay, M. A. Ortiz, R. Arroyo, J. R. Oksenberg, A. Antigüedad, E. Tolosa, K. Vandenbroeck, Ó. Fernández, M. Lucas, T. Órpez, M. J. Pinto-Medel, D. Otaegui, J. Olascoaga, E. Urcelay, M. A. Ortiz, R. Arroyo, J. R. Oksenberg, A. Antigüedad, E. Tolosa, and K. Vandenbroeck. 2013. Fine Mapping and Functional Analysis of the Multiple Sclerosis Risk Gene CD6. PLoS ONE 8:e62376.

Tabbekh, M., K. Franciszkiewicz, H. Haouas, Y. Lécluse, K. Benihoud, C. Raman, F. Mami-Chouaib, Y. Lecluse, K. Benihoud, C. Raman, and F. Mami-Chouaib. 2011. Rescue of tumor-infiltrating lymphocytes from activation-induced cell death enhances the antitumor CTL response in CD5-deficient mice. Journal of immunology (Baltimore, Md. : 1950) 187:102–9.

Tabbekh, M., M. Mokrani-Hammani, G. Bismuth, and F. Mami-Chouaib. 2013. T-cell modulatory properties of CD5 and its role in antitumor immune responses. Oncoimmunology 2:e22841.

Takeuchi, O., S. Akira. 2010. Pattern recognition receptors and inflammation. Cell 140:805–20.

Tamura, Y., Y. Higuchi, M. Kataoka, S. Akizuki, K. Matsuura, and S. Yamamoto. 1999. CD14 transgenic mice expressing membrane and soluble forms: comparisons of levels

of cytokines and lethalities in response to lipopolysaccharide between transgenic and non-transgenic mice. International immunology 11:333–339.

Tarakhovsky, A., S. Kanner, J. Hombach, J. Ledbetter, W. Muller, N. Killeen, and K. Rajewsky. 1995. A role for CD5 in TCR-mediated signal transduction and thymocyte selection. Science 269:535–537.

Thune, M., Wiiger, H. B. Gehrken, Ø. Fodstad, Gunhild, M. Maelandsmo, and Y. Andersson. 2010. A novel human recombinant single-chain antibody targeting CD166/ALCAM inhibits cancer cell invasion *in vitro* and *in vivo* tumour growth. Cancer Immunology Immunotherapy 59:1665–1674.

Tipping, P. G., X. R. Huang, M. C. Berndt, and S. R. Holdsworth. 1996. P-selectin directs T lymphocyte-mediated injury in delayed-type hypersensitivity responses: Studies in glomerulonephritis and cutaneous delayed-type hypersensitivity. European Journal of Immunology 26:454–460.

Vallera, D. A., S. F. Carroll, S. Brief, and B. R. Blazar. 1992. Anti-CD3 immunotoxin prevents low-dose STZ/interferon-induced autoimmune diabetes in mouse. Diabetes 41:457–464.

Vasquez, M., I. Simões, M. Consuegra-Fernández, F. Aranda, F. Lozano, and P. Berraondo. 2017. Exploiting scavenger receptors in cancer immunotherapy: Lessons from CD5 and SR-B1. European Journal of Immunology 47.

Van de Velde, H., I. von Hoegen, W. Luo, J. R. Parnes, and K. Thielemans. 1991. The B-cell surface protein CD72/Lyb-2 is the ligand for CD5. Nature 351:662–5.

Vera, J., R. Fenutría, O. Cañadas, M. Figueras, R. Mota, M.-R. Sarrias, D. L. Williams, C. Casals, J. Yelamos, and F. Lozano. 2009. The CD5 ectodomain interacts with conserved fungal cell wall components and protects from zymosan-induced septic shock-like syndrome. Proceedings of the National Academy of Sciences of the United States of America 106:1506–11.

Verwilghen, J., G. H. Kingsley, J. L. Ceuppens, and G. S. Panayi. 1992. Inhibition of synovial fluid T cell proliferation by anti-CD5 monoclonal antibodies. A potential mechanism for their immunotherapeutic action *in vivo*. Arthritis & Rheumatism 35:1445–1451.

Verwilghen, J., P. Vandenberghe, G. Wallays, M. de Boer, N. Anthony, G. S. Panayi, and J. L. Ceuppens. 1993. Simultaneous ligation of CD5 and CD28 on resting T lymphocytes induces T cell activation in the absence of T cell receptor/CD3 occupancy. Journal of immunology (Baltimore, Md. : 1950) 150:835–46.

Villa-Verde, D. M. S., E. Silva-Monteiro, M. G. Jasiulionis, D. A. Farias-De-Oliveira, R. R. Brentani, W. Savino, and R. Chammas. 2002. Galectin-3 modulates carbohydrate-dependent thymocyte interactions with the thymic microenvironment. European Journal of Immunology 32:1434–1444.

Villar, L. M., M. Espiño, E. Roldán, N. Marín, L. Costa-Frossard, A. Muriel, and J. C. Alvarez-Cermeño. 2011. Increased peripheral blood $CD5^{+}$ B cells predict earlier conversion to MS in high-risk clinically isolated syndromes. Multiple sclerosis (Houndmills, Basingstoke, England) 17:690–694.

Vollger, L. W., D. T. Tuck, T. A. Springer, B. F. Haynes, and K. H. Singer. 1987. Thymocyte binding to human thymic epithelial cells is inhibited by monoclonal antibodies to CD-2 and LFA-3 antigens. Journal of Immunology 138:358–363.

Wacholtz, M. C., and P. E. Lipsky. 1992. Treatment of lupus nephritis with cd5 plus, an immunoconjugate of an anti-cd5 monoclonal antibody and ricin a chain. Arthritis & Rheumatism 35:837–839.

Wagner, M., M. Bilinska, A. Pokryszko-Dragan, M. Sobczynski, M. Cyrul, P. Kusnierczyk, and M. Jasek. 2014. ALCAM and CD6 - multiple sclerosis risk factors. Journal of Neuroimmunology 276:98–103.

Wang, C. Y., R. A. Good, P. Ammirati, G. Dymbort, and R. L. Evans. 1980. Identification of a p69,71 complex expressed on human T cells sharing determinants with B-type chronic lymphatic leukemic cells. The Journal of experimental medicine 151:1539–44.

Wang, Y.-Y., L. Zhang, P.-W. Zhao, L. Ma, C. Li, H.-B. Zou, and Y.-F. Jiang. 2014. Functional implications of regulatory B cells in human IgA nephropathy. Scandinavian journal of immunology79:51–60.

Wee, S., G. L. Schieven, J. M. Kirihara, T. T. Tsu, J. A. Ledbetter, and A. Aruffo. 1993. Tyrosine phosphorylation of CD6 by stimulation of CD3: augmentation by the CD4 and CD2 coreceptors. The Journal of experimental medicine 177:219–23.

Wee, S., W. C. Wang, A. G. Farr, A. J. Nelson, D. D. Patel, B. F. Haynes, P. S. Linsley, and A. Aruffo. 1994. Characterization of a CD6 ligand(s) expressed on human- and murine-derived cell lines and murine lymphoid tissues. Cellular immunology 158:353–64.

White, M., E. Crouch, M. van Eijk, M. Hartshorn, L. Pemberton, I. Tornoe, U. Holmskov, and K. Hartshorn. 2005. Cooperative anti-influenza activities of respiratory innate immune proteins and neuraminidase inhibitor. American Journal Of Physiology 288:L831-40.

Whitney, G. S., G. C. Starling, M. A. Bowen, B. Modrell, A. W. Siadak, and A. Aruffo. 1995. The membrane-proximal scavenger receptor cysteine-rich domain of CD6 contains the activated leukocyte cell adhesion molecule binding site. Journal of Biological Chemistry 270:18187–18190.

Wildin, R. S., A. M. Garvin, S. Pawar, D. B. Lewis, K. M. Abraham, K. A. Forbush, S. F. Ziegler, J. M. Allen, and R. M. Perlmutter. 1991. Developmental regulation of lck gene expression in T lymphocytes. Journal of Experimental Medicine 173:383–393.

Wood, G. S., and P. S. Freudenthal. 1992. CD5 monoclonal antibodies react with human peripheral blood dendritic cells. The American Journal of Pathology 141:789–795.

Wortmann, A., Y. He, E. I. Deryugina, J. P. Quigley, and J. D. Hooper. 2009, July. The cell surface glycoprotein CDCP1 in cancer - Insights, opportunities, and challenges.

Wu, G., Y. M. Peng, H. Liu, Q. Di Hou, F. Y. Liu, N. L. Chen, and H. X. Bi. 2011. Expression of CD19(+)CD5(+)B cells and IgA1-positive cells in tonsillar tissues of IgA nephropathy patients. Renal failure 33:159–63.

Wu, Z., S. Lee, W. Abrams, D. Weissman, and D. Malamud. 2006. The N-Terminal SRCR-SID Domain of gp-340 Interacts with HIV Type 1 gp120 Sequences and Inhibits Viral Infection. AIDS RESEARCH AND HUMAN RETROVIRUSES 22:508–515.

Yanaba, K., J.-D. D. Bouaziz, K. M. Haas, J. C. Poe, M. Fujimoto, and T. F. Tedder. 2008. A Regulatory B Cell Subset with a Unique $CD1d^{hi}CD5^{+}$ Phenotype Controls T Cell-Dependent Inflammatory Responses. Immunity 28:639–50.

Yanaba, K., A. Yoshizaki, Y. Asano, T. Kadono, T. F. Tedder, and S. Sato. 2011. IL-10-producing regulatory B10 cells inhibit intestinal injury in a mouse model. American Journal of Pathology 178:735–743.

Yoon, S., B. W. Kang, S. Y. Park, H. J. Kim, J. S. Park, G. S. Choi, and J. G. Kim. 2016. Prognostic relevance of genetic variants involved in immune checkpoints in patients with colorectal cancer. Journal of cancer research and clinical oncology 142:1775–80.

Zani, I., S. Stephen, N. Mughal, D. Russell, S. Homer-Vanniasinkam, S. Wheatcroft, and S. Ponnambalam. 2015. Scavenger Receptor Structure and Function in Health and Disease. Cells 4:178–201.

Zhang, C., H. Xin, W. Zhang, P. J. Yazaki, Z. Zhang, K. Le, W. Li, H. Lee, L. Kwak, S. Forman, R. Jove, and H. Yu. 2016. CD5 Binds to Interleukin-6 and Induces a Feed-Forward Loop with the Transcription Factor STAT3 in B Cells to Promote Cancer. Immunity 44:913–23.

Zhou, X. Y., Y. Yashiro-Ohtani, K. Toyo-Oka, C. S. Park, X. G. Tai, T. Hamaoka, and H. Fujiwara. 2000. CD5 costimulation up-regulates the signaling to extracellular signal-regulated kinase activation in $CD4^+CD8^+$ thymocytes and supports their differentiation to the CD4 lineage. Journal of immunology (Baltimore, Md. : 1950) 164:1260–8.

Zimmerman, A. W., B. Joosten, R. Torensma, J. R. Parnes, F. N. van Leeuwen, and C. G. Figdor. 2006. Long-term engagement of CD6 and ALCAM is essential for T-cell proliferation induced by dendritic cells. Blood 107:3212–20.

Zitvogel, L., R. Daillère, M. P. Roberti, B. Routy, and G. Kroemer. 2017. Anticancer effects of the microbiome and its products. Nature reviews. Microbiology 15:465–478.

Zúñiga-Pflücker, J. C. 2004. T-cell development made simple. Nature reviews. Immunology 4:67–72.

VIII. PUBLICATIONS AND CONFERENCE PRESENTATIONS

The following papers were submitted or are in preparation to submit:

Inês Simões, Vanesa G. Martinez, Marta Consuegra-Fernández, Pilar Alvarez, Marc Orta-Mascaró, María Velasco, Sergi Casadó-Llombart, Fernando Aranda, Ramón Merino, Jesús Merino, Esther Carreras, José Alberola-Ila, Francisco Lozano. (2017) "Immunomodulatory effects of human soluble CD6 in experimental mouse models of cancer and autoimmunity". (in preparation)

Inês Simões, Fernando Aranda, Esther Carreras, Maria Velasco, Sergi Casadó, Vanesa G. Martinez, Francisco Lozano. (2017) "Immunomodulatory effects of soluble CD5 on experimental tumor models". (in revision)

Marcos Vasquez*, **Inês Simões***, Marta Consuegra-Fernandez, Fernando Aranda, Francisco Lozano¥, Pedro Berraondo¥. (2017) "Exploiting Scavenger Receptors in Cancer Immunotherapy: Lessons from CD5 and SR-B1". European Journal of Immunology; doi:10.1002/eji.201646903.

Marc Orta-Mascaró, Marta Consuegra-Fernández, Esther Carreras, Romain Roncagalli, Amado Carreras-Sureda, Pilar Alvarez, Laura Girard, **Inês Simões**, Mario Martínez-Florensa, Fernando Aranda, Ramón Merino, Vanesa-Gabriela Martínez, Rubén Vicente, Jesús Merino, Adelaida Sarukhan, Marie Malissen, Bernard Malissen, and Francisco Lozano. (2016). "CD6 modulates thymocyte selection and peripheral T cell homeostasis". The Journal of Experimental Medicine; 213(8):1387-97.

Marta Consuegra-Fernández, Fernando Aranda, **Inês Simões**, Marc Orta, Adelaida Sarukhan, Francisco Lozano. (2015). "CD5 as a Target for Immune-Based Therapies". Critical Reviews in Immunology; 35(2):85-115.

Fenutría R, Martinez VG, **Simões I**, Postigo J, Gil V, Martínez-Florensa M, Sintes J, Naves R, Cashman KS, Alberola-Ila J, Ramos-Casals M, Soldevila G, Raman C, Merino J, Merino R, Engel P, Lozano F. (2014). "Transgenic expression of soluble human CD5 enhances experimentally-induced autoimmune and anti-tumoral immune responses". PLoS One; 9(1):e84895.

Participation in other publications submitted or in preparation unrelated to the present Thesis:

Carreras E., Orta-Mascaró M., Velasco M., **Simões I.**, Zaragoza O., Lozano F. (2017). Differential inflammatory response of inbred C57Bl/6 and outbred CD1 mice to Zymosan Induced Generalized Inflammation model (ZIGI). (in preparation).

Esther Carrasco, Cristina Escoda-Ferrán, Núria Climent, Cristina Miró-Julià, **Inês T. Simões**, Mario Martínez-Florensa, Adelaida Sarukhan, Esther Carreras, Francisco Lozano. (2017). "Human CD6 down-modulation following T-cell activation compromises lymphocyte survival and proliferative responses." Frontiers in Immunology; doi: 10.3389/fimmu.2017.00769.

Martinez, V. G., Escoda-Ferran C., **Tadeu Simões, I.**, Arai, S., Orta-Mascarò, M., Carreras, E., Martínez-Florensa, M., Yélamos, J., Miyazaki, T., Lozano, F. (2014). "The macrophage soluble receptor AIM/Api6/CD5L displays a broad pathogen recognition spectrum and is involved in early response to microbial aggression." Cellular & Molecular Immunology; 11(4):343-54.

With the development of this work the following conference presentations were performed:

AUTHORS: **I. T. Simões**, F. Aranda, E. Carreras, V. G. Martinez, F. Lozano

TITLE: Anti-tumoral effects of soluble CD5 in a melanoma mouse model

Poster Presentation

CONGRESS: X Congrés de la Societat Catalana d'Immunologia, Barcelona, Spain, 2016

AUTHORS: I. T. Simões, F. Aranda, E. Carreras, V.G. Martinez, F. Lozano

TITLE: Soluble human CD5 improves the anti-tumoral response in a heterotopic melanoma mouse model

Poster Presentation

CONGRESS: 39 Congreso de la Sociedad Española de Inmunología, Alicante, Spain, 2016

AUTHORS: **I. T. Simões**, F. Aranda, E. Carreras, V.G. Martinez, F. Lozano

TITLE: Anti-tumoral effects of soluble CD5 in a melanoma mouse model

Poster Presentation

CONGRESS: IX Congrés de la Societat Catalana d'Immunologia, Barcelona, Spain, 2015

AUTHORS: **I. T. Simões**, V. G. Martinez, E. Carreras, M. Orta, M. Mané, R. Fenutría J., Alberola- Ila, F. Lozano

TITLE: Molecular and phenotypical analysis of soluble human CD6 transgenic mice

Poster Presentation

CONGRESS: 4th European Congress of Immunology, Vienna, Austria, 2015

AUTHORS: **Inês Simões**; Vanesa G. Martínez; Esther Carreras; Marc Orta; Marina Mané; Rafael Fenutría; José Alberola-Ila; Francisco Lozano

TITLE: Molecular and phenotypical analysis of transgenic mice for soluble human CD6 expression

Oral Communication

CONGRESS: VIII Congrés de la Societat Catalana d'Immunologia, Barcelona, Spain, 2014

AUTHORS: **Inês Simões**; Vanesa G. Martínez; Rafael Fenutría; José Alberola-Ila; Francisco Lozano

TITLE: Phenotypical analysis of transgenic mice expressing soluble human CD6 supports an immunomodulatory role for this protein

Poster Presentation

CONGRESS: 15th International Congress of Immunology, Milan, Italy, 2013

AUTHORS: Fenutría R, Martinez VG, Gil V, Sintes J, Simões I, Merino J, Merino R, Postigo J, Ramos-Casals M, Raman C, Engel P, Lozano F.

TITLE: Role of CD5/CD5L interactions in the homeostasis of regulatory lymphocyte subpopulations and the control of autoimmune disorders

Oral Communication

CONGRESS: 6th European Workshop on Immune-Mediated Inflammatory Diseases, Nice, France, 2011